UNIVERSITA' DEGLI STUDI DI FIRENZE
&
CRANFIELD UNIVERSITY

ALESSANDRA BINI

# APTAMERS FOR BIOSENSORS

**PhD THESIS**

UNIVERSITA' DEGLI STUDI DI FIRENZE
&
CRANFIELD UNIVERSITY

CRANFIELD HEALTH

DOTTORATO DI RICERCA IN SCIENZE CHIMICHE
XXI CYCLE

**PhD THESIS**

Academic years 2006-2008

ALESSANDRA BINI

# APTAMERS FOR BIOSENSORS

Supervisors:

Professor Marco Mascini

Professor Anthony P.F. Turner

This thesis is submitted in partial fulfilment of the requirements for the degree of Doctor of Philosophy in co-tutela between University of Firenze and University of Cranfield.

# ABSTRACT

Aptamers are single-stranded DNA or RNA molecules isolated *in vitro* by a selection and amplification method. Aptamers bind with high specificity and affinity to a wide range of target molecules, with dissociation constant comparable to antibodies.

In this work aptamers were employed as a new kind of bio-recognition element in affinity biosensors for the detection of clinically relevant proteins in heterogeneous assay, using Piezoelectric Quartz Crystal Microbalance and Surface Plasmon Resonance as transducers. The work was focused on two case studies, i.e. the Thrombin-binding aptamer and the aptamer against C-Reactive Protein. From an analytical point of view, the work was devoted to the optimisation of the analytical performance of a piezoelectric and an optical aptasensor for Thrombin and C-Reactive Protein detection, respectively. Efforts towards the application of these aptasensors in complex matrices, such as human plasma and serum, were also undertaken, in order to demonstrate the wide applicability of aptamers, as an alternative to antibodies.

In this work, the possibility of introducing a computationally-assisted method to study aptamer-protein interaction and aptamer selection was also evaluated. For this purpose, the Thrombin-binding aptamer was chosen as a model and a retrospective docking study was performed by comparing the affinity of mutated sequences for thrombin with that of the Thrombin-binding aptamer, on the basis of a computationally-derived binding score. Finally, the reliability of computational results was tested by experimental measurements. For this purpose, the Thrombin-binding aptamer and other mutated sequences, selected on the basis of their binding score, were employed for the development of optical biosensors and the resulting analytical performances were compared. Even if further studies should be carried out in order to validate the proposed computational approach to aptamer selection, this work can have a significant impact on future aptamers selection for sensors and diagnostics.

# ACKNOWLEDGMENTS

I would like to thank Professor Marco Mascini and Professor Anthony Turner for their advices and guidance and for offering me the opportunity to undertake this project, enriched by a nice period spent in Silsoe (UK).

I wish to thank Dr. Manuela Minunni and Dr. Sara Tombelli, for their contribution to this project. I also thank Dr. Marcello Mascini and Dr. Kal Karim for their help in modeling experiments.

I would especially like to thank all the staff of the laboratory of Prof. Mascini, for their help and support.

.

# Table of Contents

## ABBREVIATIONS

| | |
|---|---|
| A | Adenine |
| AC | Affinity Chromatography |
| BAW | Bulk Acoustic Wave |
| bFGF | Basic Fibroblast Growth Factor |
| bpy | 2,2'-bipyridine |
| C | Cytosine |
| CM | carboxymethyl |
| cCRP | cardiac C-Reactive Protein |
| CRP | C-Reactive Protein |
| CVD | Cardiovascular disease |
| DEPC | diethylpyrocarbonate |
| DL | Detection Limit |
| DNA | Deoxyribonucleotide acid |
| E-AB | electrochemical aptamer-beacon sensor |
| ECL | Electrogenerated Chemiluminescent |
| EDAC | 1-ethyl-3-(3-dimethylaminopropyl)carbodiimide |
| EDTA | Ethylenediaminotetracetic acid |
| ELISA | Enzyme Linked Immunosorbent Assay |
| ELONA | enzyme linked oligonucleotide assay |
| bFGF | fibroblast growth factor |
| G | Guanine |
| HEPES | 4-(2-hydroxyethyl)piperazine-1-ethanesulonic acid |
| HSA | Human serum albumin |
| hIgG | human immunoglobulin G |
| hsCRP | high sensitivity CRP assay |
| IMPDH | Inosine Monophosphate Dehydrogenase |
| KD | Dissociation constant |
| MB | Methylene Blue |
| MCH | 6-mercapto-1-hexanol |

| | |
|---|---|
| mCRP | monomeric C-Reactive Protein |
| MES | 2-(N-morpholino)ethanesulfonic acid |
| Molecular Weight | MW |
| NHS | N-Hydroxysuccinimide |
| NECEEM | Non-equlibrium capillary electrophoresis of equilibrium mixtures |
| NMR | Nuclear Magnetic Resonance |
| NP | nanoparticle |
| PCR | Polymerase Chain Reaction |
| pCRP | pentameric C-Reactive Protein |
| PDB | Protein Data Bank |
| PDGF | Platelet Derived Growth Factor |
| PlGF | Placental growth factor |
| QCM | Quartz Crystal Microbalance |
| RNA | Ribonucleic acid |
| RPM | rounds per minutes |
| RT-PCR | Reverse Transcriptase Polymerase Chain Reaction |
| RU | Resonant Units |
| SAM | self assembled monolayer |
| SAW | Surface Acoustic Wave |
| SELEX | Systematic Evolution of Ligands by Exponential enrichment |
| ss | single stranded |
| SP | Surface Plasmon |
| SPR | Surface Plasmon Resonance |
| SPRI | Surface Plasmon Resonance Imaging |
| T | thymine |
| TEG | triethylene glycol |
| TBA | Thrombin Binding Aptamer |
| Tris-HCl | tris-(hydroxymethyl)aminomethane |
| TSM | Thickness Shear Mode |
| Tween 20 | polyoxyethylene-sorbitan monolaurate |
| VEGF | Vascular Endothelial Growth Factor |

# LIST OF FIGURES

# LIST OF TABLES

TBA.

# GENERAL INTRODUCTION

## 1.1. Aim of the thesis

The aim of this work was to study a new kind of receptor for affinity biosensor development. Aptamers are single-stranded DNA or RNA molecules isolated *in vitro* by a selection and amplification method called SELEX (Systematic Evolution of Ligands by EXponential enrichment) [1,2]. The SELEX process is a powerful combinatorial methodology for identifying high affinity oligonucleotide ligands to any desired target, by screening nucleic acids libraries using iterative rounds of affinity-based enrichment alternating with oligonucleotide amplification using the Polymerase Chain Reaction (PCR).

A biosensor is an analytical device in which a biological element is coupled with a transducer, which converts the recognition event with the target into a measurable signal [3]. The aim of this work was the analytical characterisation of affinity biosensors in which aptamers are used as novel bio-recognition elements. Nowadays, antibodies are the most used receptors in affinity biosensor development [4], however novel non-natural approaches that challenge traditional methods are being discovered [5]. Employing the techniques of modern biotechnology, it is now possible to construct new receptors at will, such as aptamers [6], bio-mimetic peptides [7], molecular imprinted polymers [8], thus opening new paths for generation of biosensor recognition elements.

In this work, aptamer-based affinity biosensors (aptasensors) for the detection of clinically relevant proteins were developed using both mass and optical transduction principles, i.e. piezoelectric Quartz Crystal Microbalance (QCM) and Surface Plasmon Resonance (SPR) sensing. The work was focused on two case studies, i.e. Thrombin-Binding Aptamer (TBA) and an aptamer against C-Reactive Protein (CRP). These were immobilised on the gold surface of a piezoelectric quartz crystal or of a Biacore chip. Since aptamers targeted towards any kind of compounds can be isolated by SELEX and can be coupled to different transduction principles; this work aims to demonstrate the endless range of application of aptamers in biosensors. From an analytical point of view, the work was devoted to the optimisation of the analytical performances of a piezoelectric and an optical aptasensor for thrombin and C-Reactive Protein detection, respectively. Efforts towards the application of these aptasensors in complex matrices, such as human plasma and serum, were also undertaken.

The last part of the thesis describes a first attempt to introduce a computationally-assisted method to study aptamer-protein interaction and aptamer selection. Computational methods allow exploration of an induced fit between protein and a library of ligands to be screened. As a result, molecules most likely to bind the receptor are ranked on the basis of a binding score [9]. On the basis of this work there is the idea that the validation of a computational approach could reduce the amount of experimental time involved in the selection technique currently used for aptamer development: if a computationally-assisted screen of large libraries was able to identify a small number of sequences potentially able to bind, only a small number of sequences would have to be synthesised and assayed.

The aptamer-thrombin complex was chosen as a model in the computational approach. Starting from the oligonucleotide sequence selected by SELEX [1], a retrospective docking study for the selection of a thrombin aptamer was performed. For this purpose a modelling software was used to generate and screen libraries of oligonucleotide mutated sequences and to study the ligand-thrombin interaction by docking experiments. Docking experiments were carried out in order to verify if the sequences with the best score correspond to the high-affinity binding sequences identified using SELEX.

## 1.2. Biosensors: definition, function and applications

According to the modern definition, a biosensor is a compact analytical device in which a biological sensing element (biochemical receptor) is integrated within, or intimately associated with, a physiochemical transducer, which transforms the chemical recognition information into an analytically useful signal (Figure 1) [3].

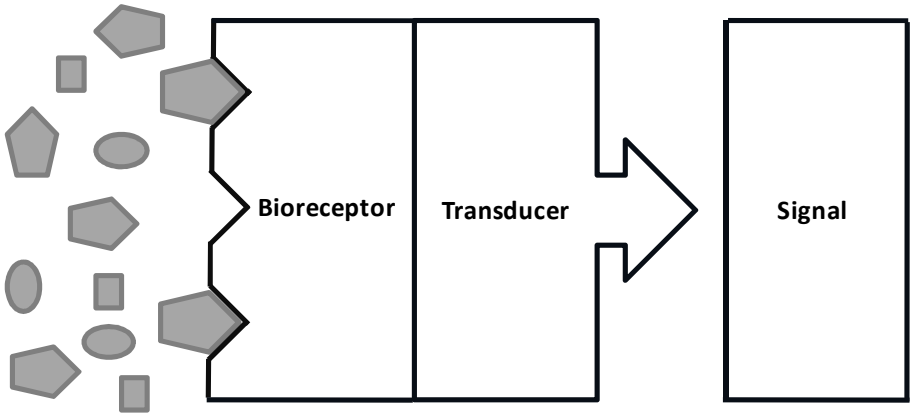


**Figure 1: Biosensor configuration, showing bioreceptor, transducer and signal detection.**

Biological elements specifically coupled to transducer can be grouped into two broad classes: catalytic (enzymes, microorganisms, biomimetic catalysts) and affinity-based (antibodies, nucleic acids, receptor proteins and systematic receptors) [10,11]. The biological element is immobilised on the sensor surface using a variety of methods such as chemical or physical adsorption, physical entrapment cross-linking or covalent binding. The receptor immobilisation is a critical aspect, because of the stoichiometric nature of the analyte binding and because of the finite sensor surface area. Receptor durability and availability determine whether the device has potential for commercialisation.

The key point in the development of a biosensor system is to generate a measurable signal from the receptor-target interaction. Transduction elements can be optical, electrochemical, calorimetric, magnetic or mass sensitive [12]. In the two last decades biosensors have gained considerable success and are now employed in a wide range of fields, such as food, environmental and clinical analysis [13]. The success of biosensors is due to low costs, small sizes, fast response times, minimum sample processing and to very high selectivity, sensitivity and reproducibility of the measurements. The main properties of biosensors are specificity and sensitivity towards the target analyte and rapidity of the analysis. The biological elements are highly selective and sensitive probes, which react with the analyte yielding a specific recognition signal. The transducer transforms the recognition signal into an electronic, optical or similar signal, which may be readily quantified [14]. Thus, the biological element determines the selectivity, the sensitivity and the stability, whereas the transducer effects the sensitivity and rapidity of the analysis.

These unique features make biosensors very attractive alternatives to conventional biological sensing devices. Compared with a conventional enzyme-linked immunosorbent assay (ELISA), which is characterised by one-use only, the immobilised biological recognition element of biosensors can often be reused or regenerated [15]. A wide range of biosensors have already been developed with numerous applications.

### 1.2.1. Affinity Biosensors

Biosensors are grouped into two broad classes: catalytic and affinity-based. Catalytic biosensors involve a catalytic event in which a substrate is converted into a product. Catalysis occurs at the transducer interface and depletion of the substrate or formation of the product is monitored by a transducer. When the biological element is an enzyme,

the main advantage is the very high specificity of the catalytic reaction, which helps avoid collateral reactions [16].

Affinity biosensors involve a reversible binding process between an immobilised biological receptor molecule and its target in solution. The affinity biosensor allows the kinetics governing the binding mechanism and detecting the reactants concentrations to be followed. The main advantage of affinity biosensors is the possibility of performing kinetic studies without requiring radioactive or fluorescent tags and recording the signals in real-time. The receptor-ligand interaction is detected with a high differential selectivity and high stability mode [17].

In the construction of a bioanalytical assay, the most used bio-recognition elements are antibodies and nucleic acids involved in an affinity reaction leading to the formation of bio-complexes, such as antigen-antibody, protein-nucleic acid or complementary strands of ssDNA [18]. If an antibody or an antigen are the biological elements immobilised onto the surface transducer, the sensor is an immunosensors; if the bioreceptor is a nucleic acid, the sensor is an RNA or DNA biosensor and the biorecognition mechanism may be based on a hybridisation reaction, which relies on the complementarity of Cytosine-Guanine (C-G) and Adenine-Thymine (A-T) pairing of two single sequences of DNA. Potential applications areas for affinity-based biosensors techniques reported over the past decade include clinical/diagnostic, food processing, military/antiterrorism and environmental monitoring.

Antibodies are the most widely reported biological recognition elements used in affinity biosensors, because of their high affinity, versatility and commercial availability [19]. However, the use of antibodies in multi-analyte detection methods and in very complex samples could encounter some limitations, mainly deriving from the nature and synthesis of these protein receptors. In order to circumvent some of these drawbacks, other recognition molecules are being explored as alternatives. In particular, recognition elements that do not occur naturally have been synthesised in the laboratory by employing modern biotechnology techniques, thus opening up new paths for affinity biosensor development.

# 1.3. Aptamers

## 1.3.1. Introduction

Aptamers are single stranded nucleic acids able to bind with high affinity and specificity to their target molecules and therefore they are considered to be the nucleic acid version of antibodies. Aptamers are generated *in vitro* by a selection and amplification technique called SELEX (Systematic Evolution of Ligands by EXponential enrichment) [1]. The length of aptamers is tens of nucleotides and the molecular weight is in the range 5-25 KDa [20]. The aptamer selection process, first reported in 1990 [2], starts from a large library of molecules containing randomly created sequences. This *in vitro* procedure satisfies the need to generate ligands exhibiting high affinity and specificity towards any defined recognition target.

In contrast to DNA or RNA sequences, which bind through base-base complementarities, these new oligonucleotides bind the ligand as a result of three-dimensional conformation changes [21]. Predominantly unstructured in solution, aptamers fold their flexible, single-stranded chains into well-defined three-dimensional structures upon binding to the target. In fact, the name aptamer originates from the Latin word “aptus”, which means “to fit” and the Greek suffix “-mer”. This folding involves the formation of stable stem-loop and internal loop structures, as a consequence of complementary Watson-Crick base-pairing [2]. In particular, RNA molecules are able to fold into a wide variety of conformations, while DNAs are known to fold *in vitro* into complex structures, even if less stable than the corresponding RNA structures [22].

Aptamers show a very high affinity for their targets, with dissociation constants typically from the micromolar to low picomolar range, which are comparable to those of some monoclonal antibodies, sometimes even better [23]. As a result of nearly 20 years’ endeavour, SELEX has been applied to a variety of molecular targets, which includes proteins, organic and inorganic small molecules, nucleic acids, peptides,

antibiotics, vitamins, drugs, metal ions and even whole cells or microorganism [24]. Aptamers have been extensively used in many analytical applications, such as chromatography, electrophoresis, mass spectrometry, molecular beacons, sensors and biosensors. In particular, aptamers have become increasingly important molecular tools for diagnostic and therapeutic [25].

### 1.3.2. Systematic Evolution of Ligands by EXponential enrichment

The SELEX procedure (Figure 2) is a powerful tool for screening large libraries of randomised nucleic acids (generally $10^{13}$- $10^{15}$ different structures), generated by combinatorial chemistry.

Each member in a library is a linear oligomer with a unique sequence, in which a central region of randomised sequence is flanked on either side by fixed regions, containing primer sequences for Polymerase Chain Reaction (PCR) and/or reverse transcriptase RT-PCR amplification, a promoter sequence for T7 RNA polymerase and perhaps restriction endonuclease sites for cloning. Randomisation is achieved simply by using a mixture (usually not equimolar) of the four standard nucleotides during solid-phase synthesis. In theory, a library containing a 40-nucleotide random region is represented by $4^{40}$ (= 1.24 x $10^{24}$) individual sequences available for partitioning. Although any length of randomised region may be used to provide $4^n$ theoretical random sequences, most libraries contain less than $10^{16}$ random sequences due to synthetic limitations. Therefore randomised regions of 30-60 nt are most common [26]. Generally, a library contains ten copies of the same random sequence. The single-stranded DNA pool is amplified by PCR in order to generate a double stranded DNA pool. This is then either transcribed (for RNA selection) or strand separated (for single-stranded DNA selection). As a result of Watson-Crick base-pairing and non-canonical intramolecular interactions, each of these sequences will adopt different three-dimensional structures, containing stem-loop, internal loops, etc.

After an incubation step with the target, the few sequences that reveal variable affinity towards the target are separated from the non-binding molecules by filtration through nitrocellulose (for protein targets) or by affinity chromatography (AC) (normally for small molecule targets). After elution and amplification by RT-PCR (for RNA libraries) or PCR (for DNA libraries), a new lower complexity pool enriched in target-binding species is achieved, and will be used for the next selection/amplification cycle (after *in vitro* transcription in the case of RNA libraries). Iterative rounds of selection and amplification are performed until the target-interacting sequences dominate the population: at the end of each cycle, under increasingly stringent conditions, the nucleotide pool is enriched in high-affinity binders, at the expense of the low-affinity binders.

The required number of cycles depends upon the stringency imposed on each cycle and upon the affinity of interaction between the target and the aptamers. In general, about 8-15 cycles of affinity selection and amplification are needed before selecting the ‘‘winning’’ aptamers, i.e. an oligonucleotide population dominated by those sequences which bind the target best. After cloning and sequencing, selected aptamers can be chemically synthesised and their binding activity confirmed to validate their affinity and specificity for the target [27].

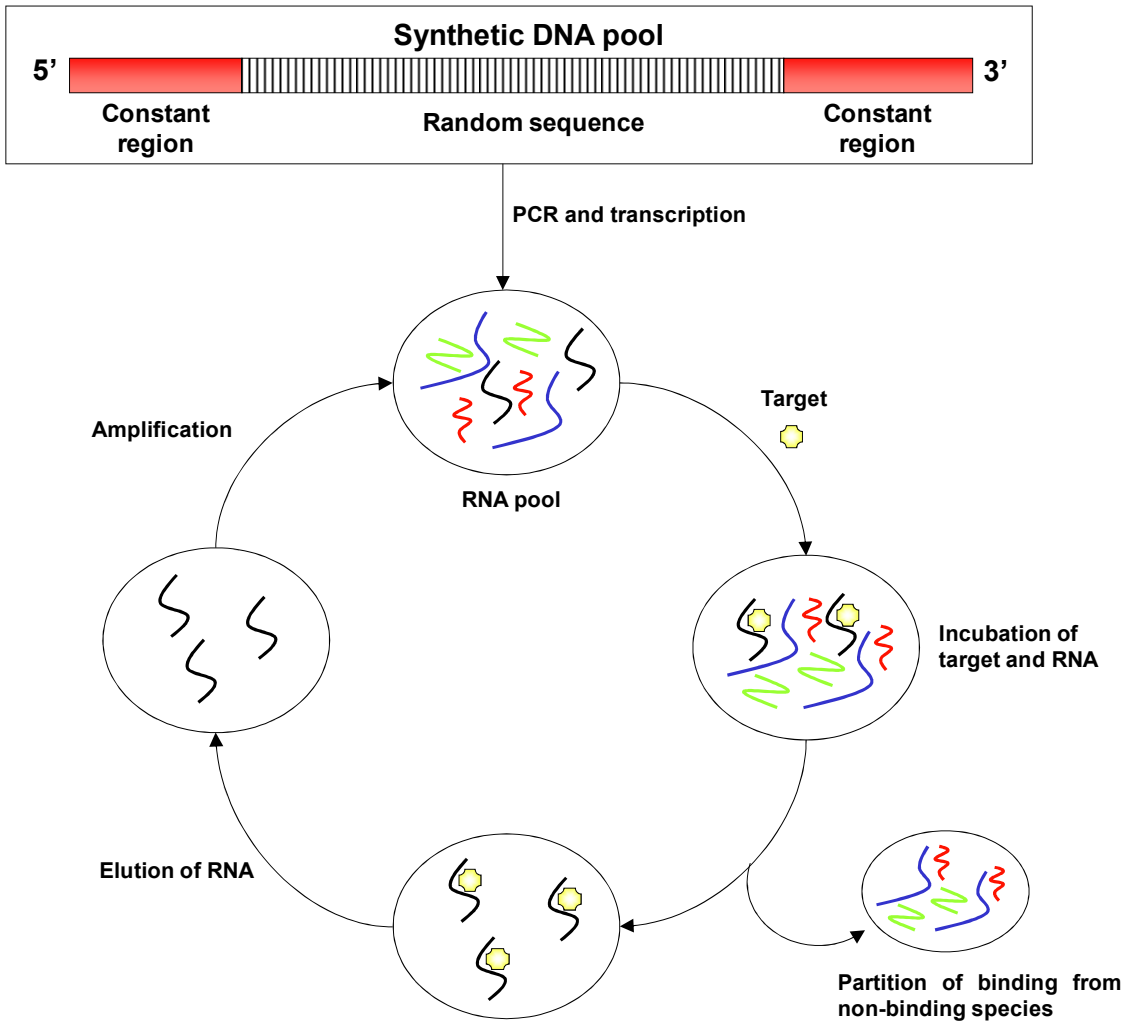


**Figure 2. Scheme of the in vitro selection of an RNA aptamer (SELEX) (adapted from [25]).**

Since these experiments take from weeks to months to be completed manually, the SELEX process has been automated [28]. Furthermore, several SELEX techniques have been developed using modified randomised ssRNA or ssDNA libraries. In particular, photocrosslinking procedure (PhotoSELEX) uses ssDNA libraries substituted with fluorophore-modified nucleotides, such as 5'-iodo or 5'-bromo uridine triphosphate (UTP) or deoxyUTP. Upon UV irradiation with a laser, these nucleotides facilitate cross-linking of an aptamer to the target [29].

### 1.3.3 Comparison of aptamers and antibodies

Until recently, molecules capable of molecular recognition, and therefore useful in sensing, have generally been limited to antibodies. Antibodies are excellent recognition elements, although they present certain limitations [19]. Antibody production relies on induction of an animal immune system, and is therefore subject to animal to animal variations. Some target molecules are poorly immunogenic or toxic, making it difficult or impossible to raise an antibody. Due to the *in vivo* generation, antibodies can recognise their targets only under physiological conditions, limiting the extent to which antibodies can be functionalised and applied in, for example, organic media. The large size (average 150 KDa) and complexity of a typical antibody can make it difficult to modify the antibodies with enzyme or other labels, and sometimes such modification reduces the affinity of the antibody. Antibodies are sensitive to temperature, undergoing irreversible denaturation and have a limited shelf life. The large size of antibodies can also negatively impact the performances of an assay.

Recently, many detection methods developed for antibodies have been successfully adapted to aptamer-based detections [30]. The widespread application of aptamers in analytical and diagnostic applications is mainly due to the advantages that they offer when used in place of antibodies. High specificity and affinity aptamers can, in principle, be selected *in vitro* for any target, ranging from small molecules to large proteins and whole cells. The *in vitro* generation process enables the selection of aptamers for non-immunogenic and even toxic compounds. Unlike antibodies, the aptamer selection process can be modified to produce aptamers which bind to a specific region of a target, with specific binding properties under different binding conditions. Once selected, aptamers are chemically synthesised and purified, eliminating the batch to batch variations encountered when using antibodies. Moreover, aptamers are usually highly chemically and thermally stable, but modifications can be introduced with the aim of enhancing the stability, affinity and specificity [22].

Aptamers undergo ligand-dependent conformational changes, and this aspect offers great flexibility in design of novel biosensors with high detection sensitivity and selectivity [21]. Aptamers show high selectivity and affinity toward their targets, with dissociation constants ($K_D$) ranging from picomolar to nanomolar, comparable to those of some monoclonal antibodies, or even better [23]. Interactions between aptamers and their targets are usually so specific that small variations in the target molecule may disrupt aptamer binding. For example, the aptamers for theophylline and L-arginine can discriminate closely related chemical structures (caffeine and D-arginine, respectively) by factors as high as 4 orders of magnitude [31].

Aptamer-based biosensors offer the advantage of reusability over antibody-based devices. Aptamer-based sensor layers can be regenerated more easily, undergo reversible denaturation and show a much longer shelf life [30]. Furthermore, their smaller size and versatility allows efficient immobilisation at high density, which is very important in miniaturised systems such as bioarrays and biochips. Commercial synthesis of aptamers by large scale manufacturing is fairly uncomplicated and cost effective. In addition, aptamers are more easily labelled with signal moieties, such as fluorophores or chemically reactive groups, even during their synthesis [19]. These functional groups permit aptamers to serve as conjugates of enzyme or beads. Finally, for *in vivo* applications aptamers are less likely to cause immune reaction than antibodies [32]. Consequently, aptamers offer a useful alternative to antibodies as sensing molecules, especially in the development of biosensors.

Despite their advantages among antibodies, aptamers shows some drawbacks, primarily regarding their generation through the SELEX process and their use as recognition elements in bioassays.

Even if to date almost all aptamers have been selected by SELEX, this process presents some disadvantages for aptamer generation. First of all, the starting random library generated by combinatorial chemistry must possess a sufficient number of different sequences, to ensure that the target-binding sequence exists in the pool. Random pools are anyway always incomplete, given the astronomical number of possible different

sequences that must be contained them [33]. Moreover, due to the large number of molecules in the initial library, selection strategies can be time consuming and expensive, and may not always result in the selection of the best aptamer for the desired application. The *in vitro* selection of aptamers is governed by the same principle as natural selection, which favours abundant targets. Rare targets, even those with high aptamer affinity, are often under-represented in final aptamer pools [34].

SELEX is applicable mostly to amplifiable libraries, i.e. DNA/RNA molecules. Because of the intermediate steps of PCR amplification and strand separation, the aptamer generation takes a long-time and is a complex process. Hence, the efficient screening of large nucleotide libraries generated by combinatorial chemistry is hard to realise [35]. However, an automated protocol for the *in vitro* selection of nucleic acids was developed [36] and then modified to be applied to the selection of anti-proteins aptamers on a robotic workstation, which allowed completing approximately 12 rounds of selection in few days [28]. Since then, other automatic approaches have been proposed or improved [37], in order to reduce times and reagents in the selection process.

A first experimental attempt at non-SELEX selection of aptamers, which avoided the PCR amplification step, has also been reported [38]. This method involved repetitive steps of partitioning by non-equilibrium capillary electrophoresis of equilibrium mixtures (NECEEM) and allowed the determination of the abundance of aptamers in the starting library up to a minimum of $5 \times 10^{-10}$ sequences, limited only by currently available commercial instrumentation.

The primary limitation on the use of aptamers as recognition elements is due to RNA nuclease sensitivity, which restricts *in vivo* and *ex vivo* applications [39]. An unmodified oligonucleotide has a half-life in serum of less than 1 minute. Therefore for applications requiring increased aptamer stability and ease of handling (such as biosensing, diagnostic and therapy) DNA aptamers are particularly useful. However, the chemical modification of the ribose ring at the 2'-position of pyrimidines with either an amino or fluoro functional group, increases the stability of RNA molecules by several

orders of magnitude [40]. Recently, it has been shown that nuclease-resistant aptamers can be generated substituting the 2'-hydroxyl position of purines with 2'-O-methyl [41].

An elegant methodology for increasing aptamer stability has been through the use of enantiomeric (L-nucleic acid) forms known as Spiegelmers. Because naturally occurring nucleic acids are composed of D-nucleotides, corresponding mirror-image L-oligonucleotides escape enzymatic recognition and subsequent degradation and consequently display dramatically enhanced nuclease resistance [42].

Finally, when labeled-probes are used as receptors, the labeling position has to be carefully selected so as not to interfere with the recognition event. To ensure the perfect binding of the aptamer to the analyte upon folding, the SELEX process is carried out using labelled oligonucleotide libraries [43].

### 1.3.4 Computational approach to aptamer selection

Some of the drawbacks encountered for the generation of aptamers by SELEX process could be tricked by the help of a computationally-assisted method: in particular, the introduction of a rationalized approach which makes use of a prediction model could overcome or minimize experimental problems currently met in SELEX process (such as reagent stability and separation procedures).

An important goal of computationally-assisted library screening would be to maximise the number of sequences without synthesising all possible sequences. If a computationally-assisted screening of large libraries identified only a few potentially binding sequences, only a few sequences would have to be synthesised and assayed, decreasing the effort required for the development of biosensors. In contrast, after

selection experiments, numerous different sequences typically have to be selected, characterised and screened for their ability to bind a target.

*In silico* screening of large libraries of compounds can be realised employing computational methods and, in the case of nucleic acids, algorithms for the prediction of secondary structures. Computational methods are routinely applied in the drug discovery process, with the purpose of predicting the binding mode of a known active ligand in a protein binding site, identifying new ligands using virtual screening and predicting the binding affinities of related compounds from a library of known active ligands [44]. In particular, the challenge of docking identifies the best candidate ligands, i.e. those compounds in a database of compounds showing the highest binding affinity towards the target, as a consequence of favourable steric, electrostatic, hydrophobic, van der Waals and hydrogen bonding interactions. The rigorous evaluation of the $\Delta G$ of binding, and hence the binding affinity of a ligand, is theoretically possible using molecular dynamics or Monte Carlo simulations. However these methods are too time-consuming to be used for the screening of large databases [45].

Scoring functions are algorithms that use simplified approximation of $\Delta G$ to calculate the binding affinity between a receptor and a ligand and predict the docked position of the ligand inside a binding pocket, through a virtual screening that allows the identification of high-affinity binders from low-affinity binders [46]. Docking methods employ scoring functions to assign a binding score to each docked compound, with the aim of identifying as quickly and accurately as possible the most likely candidate for the target. Therefore each molecule in the library must be docked into the protein to predict a "pose" of the ligand in the active site [47]. Scoring functions serve as an objective function to differentiate between diverse poses of a single ligand in the receptor binding site and to estimate and rank binding affinities of different ligands in a database, on the basis of a binding score. The best scoring pose of each molecule in the database is ranked to arrive at a top-ranking "hit-list": the general assumption is that molecules that bind tightly to the receptor should be given a higher score. Due to their crucial role, several scoring functions and docking programs have been developed [48,49].

The computational time required to dock and score a compound depends on the number of degrees of freedom as well as the complexity of the hypersurface. The degrees of freedom are the six degrees of translational and rotational freedom of one body relative to another and the conformational degrees of freedom of the ligand and the protein [44]. The hypersurface is generally very complex with many locally optimal values, due to the large number of atoms involved and the number of factors often accounted for (i.e. steric fitting, hydrogen bonding, electrostatics, torsional strain etc.). While the first docking algorithms treated both ligand and protein as rigid bodies, taking into account only translation and orientation, today's docking programs treat the ligand as flexible and the receptor as completely rigid, thanks to improvement in computer performance. Therefore, the degrees of freedom are 3 rotations and 3 translations for the rigid ligand with respect to the protein, plus N torsional degrees of freedom for the ligands rotatable bonds. However, the simulations are often time-consuming and treating some protein side chains as flexible may be computationally prohibited [33].

Algorithms for the prediction of oligonucleotide secondary structures starting from the nucleic acid sequence calculate the free energy of RNA or DNA secondary structures upon folding, predicting the base paired regions in the sequence. Examples are the Vienna RNA Package (Mfold) (http://www.bioinfo.φi.edu/applications/mfold/old/dna/), RNAfold (http://rna.tbi.univie.ac.at/cgi-bin/RNAfold.cgi), GeneBee (http://www.genebee.msu.su/services/rna2_full.html), RNAsoft (www.rnasoft.ca) and others. These software have been used to computationally generate non-random libraries containing 1000 oligonucleotides of potentially active aptamers for IgG, transferrin and α-1-anti-trypsin protein, with the aim of reducing the complexity of the starting library and increasing the fraction of binders with respect to non binders [50]. Starting from a template sequence containing a central random region flanked between two fixed regions able to form a stable double stranded stem, a binding potential, i.e. a value generated using data from structural and thermodynamic calculations, is calculated for each selected oligonucleotide. Sequences showing thermodynamic parameters at the upper end of the free energy range for a specific secondary structure, i.e. the most unstable secondary structures, correlate with the sequences most likely to bind the target. The binding event decreases the free energy of the system; the more the

free energy decreases upon binding, the greater the binding strength. Thus, starting with a single stranded region as high in free energy as possible means that there are many chemical groups available for interaction with a target. This increases the likelihood of the oligonucleotide being a functional aptamer with high affinity.

Using the Vienna RNA Package, the development of an algorithm for predicting the conformational change of an anti-flavin aptazyme and anti endothelial growth factor aptamer beacon upon binding has been shown [51]. Both the aptazyme and the aptamer beacon undergo small target-dependent displacement in the structure, assuming a different conformation referred to a "slip structure". Starting from a pool of sequences containing a central random region, for each sequence the free energy of folding was calculated along a series of "register" generated simply shifting a strand respect to the other. The changes in free energy that the sequences undergo as they slip from one register to another, allowing the slip structure model to be assessed and identifying the most stable structure. This method allows computing structures and free energies of millions of different sequences to be assessed in hours on a typical desktop computer.

## 1.4. Aptamer-based biosensors for clinical applications

### 1.4.1. Aptamers as biorecognition elements for clinical applications

The detection and quantification of proteins in their native environments has always been a critical and challenging task and plays an essential role in basic discovery research as well as in clinical practice. Assays that allow rapid, simple, sensitive, selective and cost-effective detection of proteins are of significant importance for the understanding, diagnosis, treatment, and prevention of many diseases. Diagnostic systems able to early and accurately detect protein biomarkers, such as cytokines or

growth factors, have a particular emphasis in clinical and medical research. Despite current techniques for protein detection, such as electrophoresis, affinity chromatography, ELISA, the development of sensitive methods for real time protein analysis is still a difficult task [52]. For this purpose, a highly selective molecular recognition element and a novel signal transduction mechanism have to be engineered together for successful assay development. Among many molecular recognition elements, aptamers have gained increasing interest in protein sensing and the use of aptamers for diagnostic applications has been extensively explored [53]. Several strategies for transducing aptamer-protein interactions into the changes in colorimetric, electrochemical, mechanical, piezoelectric or fluorescent signals, and in electrophoretic mobility have been reported.

### 1.4.2. Aptamers for Thrombin

The first aptamer selected *in vitro* towards a protein with no known nucleic acids binding properties is the 15-mer thrombin binding aptamer (TBA, 5'-GGTTGGTGTGGTTGG-3') [54]. The 15-mer TBA binds to the fibrinogen-recognition exosite of human α-thrombin (namely exosite I), with a $K_D$ of 26 nM . A 29-mer thrombin binding aptamer has also been selected (5'-CAGTCCGTGGTAGGGCAGGTTGGGGTGACTTCGTGGAA-3'), with a $K_D$ of 0.5 nM for the protein [55]. This aptamer binds to the heparin-binding exosite of thrombin (namely exosite II).

Two-dimensional NMR studies demonstrated that TBA folds into a unimolecular quadruplex structure, containing two G-quartets linked by two TT loops at one end and a TGT loop at the other end, usually referred to as a "chair structure" and stabilised by $K^+$ ions [56]. The thymines in the TT loops are potentially base-paired across the top of one G-quartet. The two G-quartets are connected by two TT loops that span the narrow

grooves at one end and a TGT loop that spans one of the wide grooves at the other end of the quadruplex, as shown in Figure 3. An interesting feature of TBA is the formation of a T4•T13 base-pair across the G-quartet.

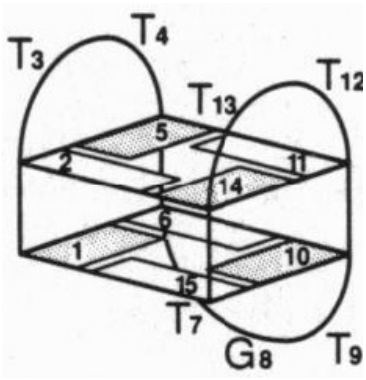


**Figure 3: Schematic model for TBA determined by analysis of NMR spectra (from [56]).**

The 29-mer anti-thrombin aptamer was found to adopt the same G-quartets structure when bound to thrombin (Figure 4).

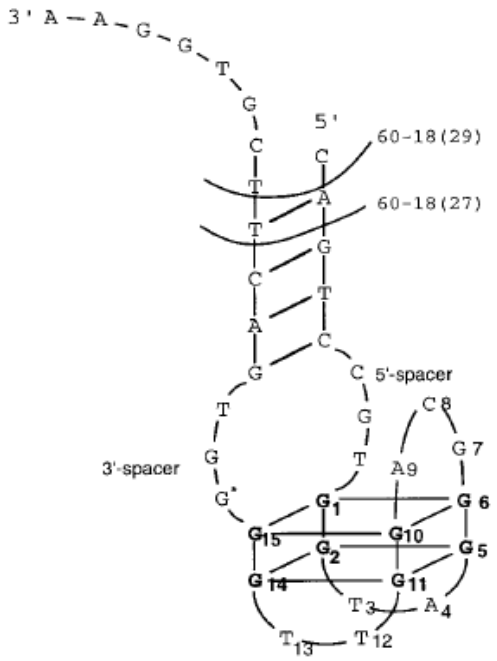


**Figure 4: Secondary structure of the 29-mer thrombin binding aptamer. The 15 nucleotides of the G-quartets core sequence are numbered (from [55])**

### 1.4.2.1. Thrombin

The coagulation cascade is a complex series of biochemical reactions that results in the polymerisation of fibrin and formation of platelet/fibrin haemostatic plugs (Figure 5). In normal vasculature, it serves as the primary mechanism to control bleeding. However, with vascular pathology, activation of coagulation pathway can result in thrombosis and life-threatening vascular occlusion. The primary approach to the development of novel anticoagulant/antithrombotic drugs has been the inhibition of specific biochemical targets in the coagulation cascade, in which the two central target are thrombin and Factor Xa. Thrombin (Factor IIa) is the last enzyme protease involved in the coagulation cascade: it converts fibrinogen to insoluble fibrin, which forms the fibrin gel, either in physiological conditions or in pathological thrombus [57]. Thrombin has also hormone-like properties and it is involved in thrombosis and platelet activation. Therefore, thrombin plays a central role in inflammation and tissue repair at the vessel wall [58]. Currently, the most commonly used antithrombotic agent is heparin, but other thrombin inhibitors are clinically available, such as hirudin.

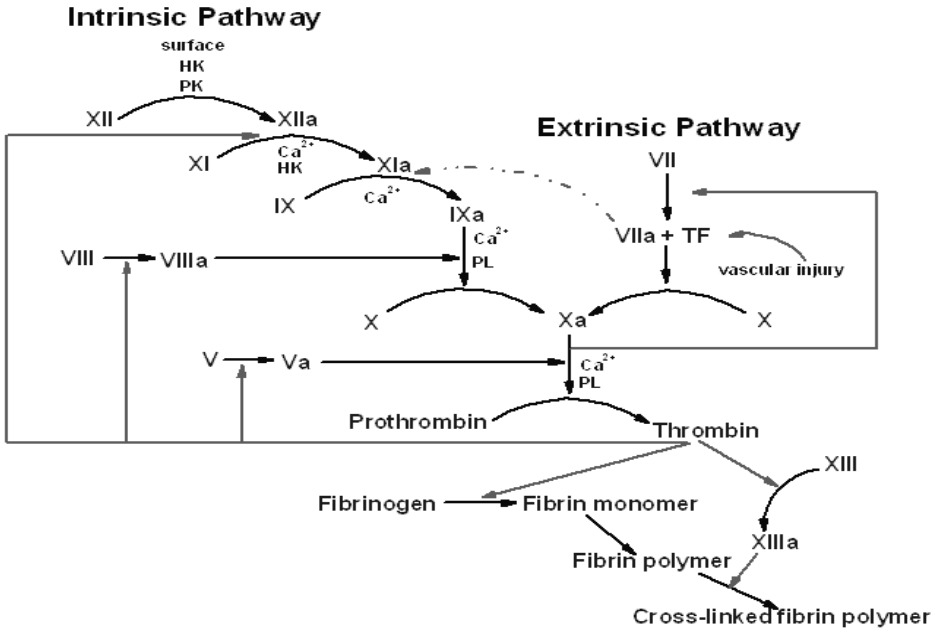


**Figure 5. The blood coagulation cascade. (from Website http://themedicalbiochemistrypage.org/blood-coagulation.html, copyright 1996 M. W. King))**

The concentration of thrombin in blood can vary considerably: thrombin, not present in blood under normal conditions, can reach low μM concentrations during the coagulation cascade, but low levels (low nM) of thrombin generated early in hemostasis are also important to the overall process [59]. Out of the hemostatic process, circulating thrombin has been detected at high pM range in blood of patients suffering from disease known to be associated with coagulation abnormalities [60]. This makes the determination of thrombin concentration in real time an excellent tool for obtaining accurate coagulability status. The measure of coagulation time forms the basis of clinical analysis of coagulation efficiency currently available on the diagnostic market [61] (Prothrombin Time (PT), activated Partial Thromboplastin Time (aPTT), Thrombin Time (TT) , activated Clotting Time (ACT), Thrombogram$^{TM}$ and inhibitors screening tests [62]).

Thrombin is a 308-amino acids serine protease (MW 36 KDa) containing two chains. The A chain is composed of 36 residues and is not essential for proteolytic activities. The B chain is composed of 259 amino acids and contains the three active sites residues (Hys57, Asp102, Ser195). Thrombin has four distinct binding sites for substrates, inhibitors, cofactors and $Na^+$ ions, and other three recognition sites (exosite I, exosite II and active site) for the molecules which take part in its different functions [63].

### 1.4.2.2. The aptamer-thrombin complex

The crystal structure of the complex thrombin-TBA was solved by X-Ray crystallography [64]. As in solution, in the crystal complex the single stranded DNA folds into a structure with two G-quartets, where a T7G8T9 loop is on one side of the quartets and the T3T4 and T12T13 loops are on the other hand.

Study for the identification of the binding pocket with which TBA interacts suggest that TBA is located in the thrombin fibrinogen-recognition exosite (the anion binding exosite) and overlaps the thrombin platelet receptor and thrombomodulin binding sites [65]. The Nuclear Magnetic Resonance (NMR) model of aptamer-thrombin complex (Protein Data Bank 1HAO) indicates that the dominant interactions in the fibrinogen exosite involve the TT loops (Figure 6), while the TGT loop interacts with the heparin-binding site of the neighbouring thrombin [66]. In the NMR model, the major binding interactions in the fibrinogen-binding site appears to be hydrophobic, involving T12 (Ile24, His71, Ile 29, Tyr117) and T3 (Tyr76, Ile82), while in the heparin exosite of a symmetry related thrombin molecule four residues are involved in ion pair interactions with the DNA [67]. The residues involved in the main aptamer-thrombin interactions are listed in Table 1.

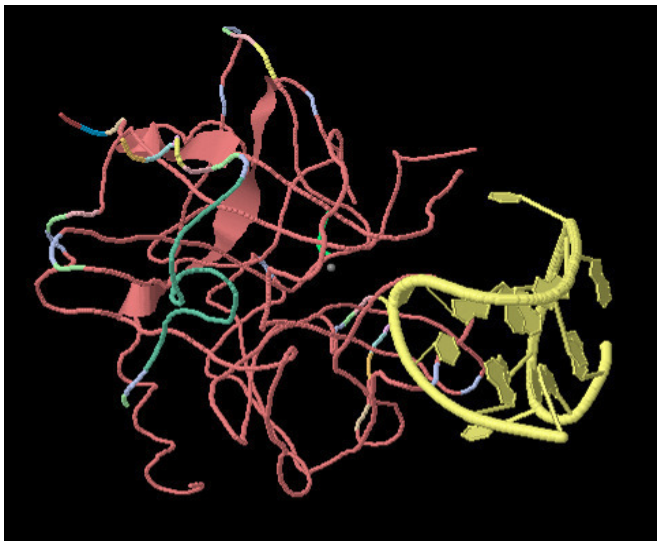

**Figure 6: The aptamer-thrombin complex (PDB 1HAO) [67].**

| NMR Model | | |
|---|---|---|
| Fibrinogen-recognition exosite | | |
| T3 | Tyr76, Ile82 | Hydrophobic |
| T12 | Ile24, His71, Ile79, Tyr117 | Hydrophobic |
| Heparin-binding site | | |
| G2 O2P | Arg233’ | Ion pair |
| G2 O2P | Arg233’ | Ion pair |
| G5 O1P | Lys236’ | Ion pair |
| G5 O2P | Lys236’ | Ion pair |
| T7 O1P | Lys240’ | Ion pair |
| T9 O1P | Arg93’ | Hydrogen bond, ion pair |

**Table 1. Interactions between thrombin and the DNA 15-mer (from [64]).**

### 1.4.2.3. Aptamer-based biosensors for thrombin detection

TBA has been coupled with different transduction principles to demonstrate the wide applicability of aptamers as bioreceptors in biosensors. In particular, the majority of the reported aptamer-based biosensors, sensors and assays for the detection of proteins with a certain importance in clinical chemistry, make use of the thrombin-binding aptamer. Many assays, mainly biosensors, based on the thrombin-binding aptamer for the detection of thrombin have been developed in the last 10 years, but only few of them have been really used as analytical method for the detection of thrombin in real samples.

*a) Biosensors employing labeled-thrombin*

First examples of aptasensor development for thrombin detection employed the analyte thrombin labeled with a fluorescein tag. In particular, a fiber-optic aptasensor for the measurement of thrombin was described [68]. An amino-derived TBA was immobilized on the surface of silica microspheres and incubated with fluorescein-labeled thrombin. Non-labeled thrombin was detected (DL 1 nM) using a competitive binding assay. Coupling the 15-mer thrombin aptamer on the sensor surface, a Love-wave biosensor was designed for detection of thrombin labeled with a fluorescent dye [69], with a DL of 72 pg/cm$^2$.

*b) Biosensors employing functionalized anti-thrombin aptamers*

Since aptamers are easy to label with different tags (such as fluorescent or electrochemical dyes), generally it is desirable to employ modified receptors rather than modified analytes when monitoring real-time interactions. The function of proteins in biological system is highly dependent on their tertiary structure and therefore labeling proteins may cause reduction or even loss of activity, by either blocking the binding site or affecting the three dimensional folding of the proteins [70].

Since one of the requirements for a biosensor is immobilisation of the receptor on the sensor surface, several 3' or 5' chemical modification of the aptamer were engineered to incorporate functional groups or molecules that facilitate the linkage to the surface. Therefore, different strategies for the development of thrombin biosensors using functionalized anti-thrombin aptamers were reported employing different transduction principles, which were mainly optical or electrochemical.

An anti-thrombin fluorescein-aptamer was covalently immobilized on a microscope cover slip, and protein binding was detected by fluorescent anisotropy method, with a Detection Limit (DL) of 5 nM [71].

A single-walled carbon nanotube field-effect transistor was used for the immobilisation of the amino-derived 15-mer thrombin aptamer. The following protein bonding caused a measurable decrease in conductance, and the DL was 0.1 nM [72].

Using methylene blue (MB) as electrochemical indicator, an electrochemical aptasensor for thrombin detection was developed by immobilising the biotinylated aptamer on the avidin-derived electrode gold surface and detecting the binding of thrombin to the aptamer with a DL of 10 nM [73]. A direct thrombin detection with 1 nM DL was also realised by immobilising the aptamer on the gold surface of a quartz crystal microbalance.

A signaling aptamer for thrombin was created by replacing the nucleotide T7, located close to the protein binding site, with a fluorescent analogue, which causes an increase in fluorescence upon thrombin binding at nanomolar concentrations, measured by a fluorescence microscope imaging [74].

*c) Aptamer beacons*

One of the more promising aptasensor approaches is aptamer beacons, optical sensors based on the binding-induced folding of unfolded or partially folded aptamers. In the absence of target, the fluorophore attached to the DNA aptamer is quenched by a complementary DNA fragment carrying a quencher dye. When the system is exposed to the target, the aptamer binds to it and the quencher-labelled DNA is released, generating a fluorescent signal. Because aptamer beacon couples signal generation to a binding-specific change in the aptamers rather than to adsorption to the sensor surfaces, they are relatively immune to false positives arising from non-specific interactions with contaminants.

An electronic sensor was developed by immobilising the thrombin binding aptamer labeled with methylene blue onto a gold electrode [75]. In the absence of the target the aptamer could maintain its unfolded structure and methylene blue could reach the electrode surface generating an electrochemical signal. Upon addition of thrombin, the aptamer folded its characteristic secondary structure when binding to the target, preventing the contact of methylene blue with the electrode. As a consequence, a decrease in signal was observed in the presence of thrombin. Thrombin was detected in the nanomolar range in buffer solutions and also in 50% diluted human serum spiked

with thrombin, to demonstrate the applicability of the sensor to the analysis of complex matrices. This "signal-off" sensor, in which the presence of the target reduces the signal, was further modified in a "signal-on" architecture [76] introducing a short methylene blue-oligonucleotide that hybridised with the immobilised aptamer. In the absence of target, the formation of the double strand prevented the methylene blue from approaching the electrode, while thrombin binding disrupted the hybrid, allowing the methylene-blue to reach the surface and produce a faradic current. The detection limit of this "signal-on" approach was 3 nM.

On the basis of the same principle, the development of an electrochemical molecular aptamer beacon was developed [77] by immobilising a thiolated ferrocene-labelled thrombin aptamer on a gold electrode surface and measuring the ferrocene-enhanced electron transfer upon target binding, resulting in a nanomolar detection limit.

*d) Sandwich formats*

Since thrombin presents two different non-overlapping binding sites for aptamer interactions, aptamer-based biosensors with sandwich formats for thrombin detection were recently reported, in which the protein is sandwiched between two identical aptamers or the protein binds two different nucleotide sequences. This highlights the importance of identifying multiple aptamers for a single molecular target.

In the first reported approach [78], the 15-mer aptamer was immobilised onto a gold electrode and, after thrombin bound, a sandwich assay was realised with a glucose dehydrogenase-labeled 29-mer aptamer. As the substrate glucose was added, an electric current proportional to thrombin concentration was measured, with a DL of 10 nM. Using a similar sandwich format, an electrochemical aptasensor for thrombin detection was developed by immobilising a thiolated aptamer on a gold electrode, incubating with thrombin and using a biotinylated 15-mer as secondary aptamer [79]. After the added of the streptavidin-peroxidase conjugated and further of the substrate, the enzymatic product was electrochemically detected. The detection limit in standard solution was 80 nM.

Another strategy employed gold nanoparticles (Au-NP) to functionalise the 15-mer TBA, covalently immobilised on the sensor surface [80]. After the thrombin bound, the same Au-NP functionalised 15-mer used as secondary aptamer associated to the other protein binding site. Following an amplification step with $HAuCl_4$, the absorbance spectra was recorded, with a detection limit of 2 nM. The same format was also realised using QCM measurements.

An interesting approach based on the use of aptamer-functionalised Pt nanoparticles has been optimized [81]. In this work, the metallic nanoparticles were used not as mere labels for an electrochemical detection, but as catalytic molecules, with the aim of overcoming some of the drawbacks associated with the thermal and environmental instability of traditional biological redox catalytic labels such as enzymes. The assay was conducted by immobilising the thiolated thrombin aptamer onto a gold electrode and using, after the interaction with thrombin, the same aptamer fixed onto Pt nanoparticles as secondary ligand. The Pt nanoparticles were then used to perform the electrocatalytic reduction of added $H_2O_2$ detected by linear sweep voltammetry. A detection limit of 1 nM for thrombin was achieved with this method.

The detection limit for thrombin using the specific aptamer was further improved down to 0.02 nM by using another sandwich assay based on gold nanoparticles and impedimetric detection [82]. The protein was sandwiched between the aptamer immobilised onto a gold substrate and the aptamer-functionalised gold nanoparticles, which were used to amplify the impedimetric signal.

An original electrochemical sandwich-type nanoparticle-based assay was developed using the specific anti-thrombin antibody immobilised onto microtitre plates to capture thrombin [83]. The bound thrombin was then linked to aptamer-functionalised gold nanoparticles. The adenine nucleobases were finally released from the nanoparticles by acid or nuclease treatment and electrochemically detected using a pyrolytic graphite electrode. The method has several advantages such as the direct detection of the redox activity of the adenine nucleobases of the aptamer avoiding, in this label-free format, the time-consuming and complicated labelling of the oligonucleotides. Moreover, the

aptamer-modified nanoparticles served not only as a target recognition elements, but also as amplification tool.

An aptamer-based sandwich assay based on electrochemical detection for thrombin analysis in complex matrices was developed by coupling the advantages of magnetic beads with those of aptamers [84]. The protein captured by the first aptamer, functionalised with magnetic beads, was detected after the addition of the second biotinylated aptamer and of streptavidin labelled with alkaline-phosphatase. The detection of the product generated by the enzymatic reaction was achieved by Differential Pulse Voltammetry (DPV) on screen-printed electrodes. Good sensitivity and selectivity were demonstrated by the sensor with a detection limit of 0.45 nM in buffer and negligible signal generated by negative control proteins. The system was also demonstrated to recognise the target analyte in protein rich media, such as thrombin spiked serum and plasma samples. Moreover, mimicking the physiological clogging event, thrombin was generated *in situ* by the conversion of its precursor prothrombin present in plasma and its concentration was measured at different incubation times. The results correlated well with thrombogram-mimicking software.

The best sensitivity for the detection of thrombin, with a detection limit of about 8 aM, was reached by using an electrochemical assay coupled to a novel amplification strategy [85]. This ultrasensitive aptamer-based bioanalytical method was based on a sandwich format with the target protein captured by the first aptamer-functionalised magnetic nanoparticles. A second aptamer was attached to gold nanoparticles, which facilitated the electrochemical transduction. The innovative amplification strategy was achieved by forming network-like thiocyanuric acid/gold nanoparticles whose aggregation greatly enhanced the transduction of the aptamer-protein recognition event.

A summary of the different methods with the corresponding detection limit is reported in Table 2.

| Method | Analyte label | Aptamer label | Secondary aptamer label / amplification | DL | Ref | Year |
|---|---|---|---|---|---|---|
| Optical | fluorescent | | | 1 nM | [68] | 2000 |
| Optical | fluorescent | | | 72 pg/cm$^2$ | [69] | 2004 |
| Optical | | fluorescent | | 5 nM | [71] | 1998 |
| Filed effect transistor | | | | 0.1 nM | [72] | 2005 |
| Electrochemical | | MB | | 10 nM | [73] | 2005 |
| Acoustic | | | | 1 nM | [73] | 2005 |
| Optical | | fluorescent | | nM | [74] | 2006 |
| Electronic | | MB | | nM | [75] | 2005 |
| Electronic | | MB | | 3 nM | [76] | 2005 |
| Electrochemical | | ferrocene | | nM | [77] | 2005 |
| Electrochemical | | | Enzyme | 10 nM | [78] | 2005 |
| Electrochemical | | | Biotin / streptavidin-enzyme conjugated | 80 nM | [79] | 2006 |
| Electrochemical / acoustic | | Au NP | Au NP / $HAuCl_4$ | 2 nM | [80] | 2004 |
| Electrochemical | | | Pt NP / $H_2O_2$ | 1 nM | [81] | 2006 |
| Electronic | | | Au NP | 0.02 nM | [82] | 2008 |
| Electrochemical | | | Au NP | 3 pM | [83] | 2007 |
| Electrochemical | | Magnetic beads | Biotin / streptavidin-enzyme conjugated | 0.45 nM | [84] | 2007 |
| Electrochemical | | Magnetic beads | Au NP | 8 aM | [85] | 2007 |

**Table 2. Overview of different aptamer-based biosensors developed for the detection of thrombin. Limit of detection of the assay is reported with the relative amplification strategies.**

*e) Aptamer-based biosensor arrays*

Since the value of any single marker is significantly enhanced by combination with other markers, the most relevant application of proteomics to disease is the analysis of multiple protein targets simultaneously, a task that has proved challenging in recent years. The main characteristic of a large multiplexed protein array is its ability to retain the specificity and sensitivity of detection without compromising the quality of individual reagents. The rapid detection and profiling of multiple protein biomarkers in blood and serum samples are a potentially powerful method for the diagnosis of diseases and the monitoring of subsequent therapeutic treatments. Microarrays of RNA aptamers are emerging as an attractive alternative to antibody arrays for the multiplexed bioaffinity detection and identification of protein biomarkers.

The development of an aptamer chip-based biosensor with fluorescence detection that is capable of specifically quantifying levels of several proteins with relevance to cancer, in particular thrombin, inosine monophosphate dehydrogenase (IMPDH), vascular endothelial growth factor (VEGF) and basic fibroblast growth factor (bFGF), has been described [86]. 5' biotinylated aptamers attached to a 12-carbon linker were immobilised on a streptavidin-derivatised glass substrate. The protein targets were spiked in complex biological solution, such as bacterial cell lysate diluted 1:10, and the target binding event was monitored using fluorescence polarisation anisotropy technique.

Another technique recently employed for the detection of protein on aptamer microarrays is Surface Plasmon Resonance Imaging (SPRI) [87]. Enzymatically amplified SPRI measurements of RNA aptamer microarrays were used to detect protein biomarkers (VEGF and Thrombin) down to subpicomolar concentrations. A surface-immobilised aptamer is used to capture the proteins onto the RNA microarray, and then the antibody conjugated with Horse Radish Peroxidase (HRP) is bound to the array element via the formation of an RNA aptamer/protein/antibody-HRP sandwich structure. On the addition of the substrate TMB (3,3',5,5'-tetramethylbenzidine), HRP catalyses localised formation of a dark blue precipitate, that is detected using SPRI measurements.

## 1.4.3. Aptamer for C-Reactive Protein

An RNA aptamer against C-Reactive Protein (CRP) was selected by SELEX [88] starting from a oligonucleotide library in which each sequence contained a central 43-mer random region flanked by constant regions. The constant regions included targets for PCR primers and cloning sites and a T7 promoter. After 10 rounds of SELEX, the resulting aptamer sequence was a 44-mer showing a $K_D$ of 125 nM:
(5'-GCCUGUAAGGUGGUCGGUGUGGCGAGUGUGUUAGGAGAGAUUGC-3').

### 1.4.3.1. C- Reactive Protein

C-Reactive Protein, so named for its capacity to precipitate the somatic C-polysaccharide of *Streptococcus pneumonia*, is a critical component of the immune system discovered nearly 70 years ago by scientists exploring the human inflammatory response. CRP is one of the cytokine-induced "acute-phase" proteins whose blood levels rise during a general, unspecific response to infections and non-infections inflammatory processes. Because of its lack of specificity, for about 30 years CRP has been considered not to provide clinically useful information [89].
CRP is a serum soluble protein synthesised in the liver by hepatocytes and its production is stimulated by proinflammatory cytokines, particularly interleukin (IL)-6 and tumor necrosis factor-α (TNF)- α [90]. Several recent studies have shown that CRP can be produced by non-hepatic tissues, such as epithelial cells of the respiratory tract, renal epithelium and neuronal cells [91].

*a) CRP structure*

CRP (MW 115.135) belongs to the pentraxin family of calcium-dependent ligand-binding plasma proteins having five identical, non-covalently associate subunits that form a symmetrical ring. Each nonglycosylated polypeptide subunit (MW 23 kDa)

contains 206 aminoacid residues and has the characteristic “lectin fold”, composed of a two antiparallel β sheet, with an α helix on the other protein face [92]. The ligand binding site for phosphocholine is composed of loops with two calcium ions next to a hydrophobic pocket (Figure 7). Phosphocholine binds to CRP in a calcium dependent manner, which then begins the complement pathway [89].

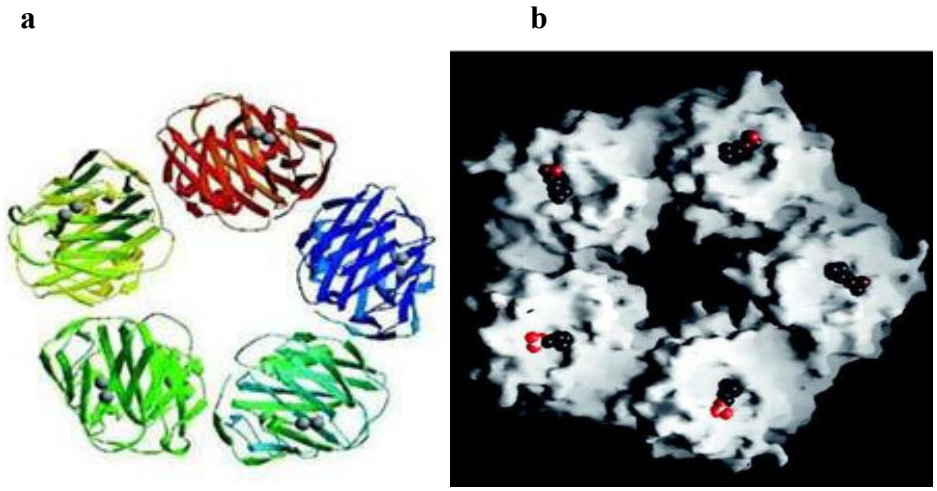


**Figure 7. Molecular structure of human CRP. (a) Ribbon diagram of the crystal structure, showing the lectin fold and the two calcium ions in the ligand-binding site of each protomer. (b) Space-filling model of the CRP molecule, showing a single phosphocoline molecule located in the ligand-binding site of each subunit. (from [89])**

*In vitro* studies [93,94,95] have shown that after binding to plasma membrane or in denaturing or oxidative environment, native CRP loses its pentameric symmetry (pCRP), resulting in a modified or monomeric CRP (mCRP), which may be the major CRP promoter of the proinflammatory response in the coronary arteries. Khreiss *et al.* [94] suggested that the bioactivity of CRP is expressed when the pentameric structure dissociates and undergoes a conformational rearrangement, resulting in formation of mCRP; in fact, mCRP was able to induce endothelial activation within 4 hours, whereas native CRP showed a proinflammatory effect in 24 hours.

Even though it is currently not known how mCRP is generated *in vivo*, acid-EDTA or urea-EDTA treatment of CRP, as well as surface adsorption and immobilisation on plastic surface, might cause the native CRP to irreversibly dissociate in monomers [93]. It has also been demonstrated [95,96] that in the absence of calcium ions, in neutral or mildly acid environments, the pentameric CRP slowly but continuously dissociated. The dissociation rate increased with the storage time. For this reason commercial high-purity (> 99%) human native CRP is stored in $NaN_3$-free buffer containing $CaCl_2$ to prevent spontaneous formation of mCRP from the pentamer.

*b) CRP levels*

CRP is normally present in healthy adults at concentrations < 10 ppm. In healthy young people the average concentration of CRP is 0.8 ppm, but serum levels increase in response to a variety of inflammatory stimuli, such as trauma, tissue necrosis, infection, surgery or myocardial infarction. Following an acute phase stimulus, values may rapidly increase over 1000 fold, from less than 50 ppb to more than 500 ppm, resulting in the release of elevated quantities into the circulation. When the stimulus for increased production completely ceases, the circulating CRP concentration falls rapidly [89]. The amount of CRP depends however on a variety of factors, including genetics and lifestyle habits. On average, smoking, high blood pressure, being overweight, sleep disturbances, depression, chronic fatigue, aging and physical inactivity are associated with high levels of CRP [97].

The recent attention focused on CRP reflects the discovery of its role in the prediction of future cardiovascular diseases (CVD) in apparently healthy people. It has been shown that an increased CRP production can be associated with a risk of atherothrombotic events, including coronary events, ischemic stroke, myocardial infarction [98,99]. Furthermore, CRP is detectable in the early stages of atherosclerotic plaque evolution, and can be used to predict the development of type 2 diabetes mellitus [100].

Although other inflammation markers show predictive associations with coronary events, the interest in CRP arises from its high stability in serum or plasma and the

availability of robust, well standardised and reproducible CRP immunoassays [89]. Furthermore CRP has a long half-life in serum, its levels remain stable over time without exhibiting circadian variability and fasting blood sample are not required [101].

*c) CRP commercial assays*

Different methods for CRP detection are commercially available. Conventional CRP assays include qualitative, semi-quantitative and quantitative assays (for example latex agglutination), used for evaluation of infections, tissue injury and inflammatory disorders [90]. These assays provide information for the diagnosis, therapy and monitoring of inflammatory diseases. For conventional CRP assays, test values are considered to be clinically significant at levels above 10 mg/L [102].

A lower limit of quantitation (LOQ), intended as the lowest concentration at which bias and precision are within acceptance criteria (i.e.% Coefficient of Variation ≤ 20% [102]) is achieved with high sensitivity CRP assays (hsCRP), which comprise immunonephelometric, immunoturbidimetric, immunoluminometric, microparticle enzyme immunoassay and sandwich immunoassay (such as ELISA) technologies [103]. These assays are used to evaluate conditions thought to be associated with inflammation in otherwise healthy people. Manufacturers of different hsCRP tests based on immunoturbidimetry or immunonephelometry claims detection limits between 0.005 and 0.08 ppm, intended as the minimum detectable concentration of the assay as measured by 2SD (standard deviation) from the mean of a zero standard [90]. The detection limit for commercial hsCRP assays based on ELISA tests is 0.1 ppm or even less. hsCRP assays are referred to as cardiac CRP assays (cCRP) when they are used for prediction of future cardiovascular diseases in conjunction with traditional clinical laboratory evaluation of acute coronary syndromes. Therefore, hsCRP represents the inflammatory marker to assess cardiovascular risk; its clinical cut-off points have been set in low (< 1.0 ppm), moderate (1.0 – 3.0 ppm) and high risk (3.0 – 10 ppm) [104] (Figure 8).

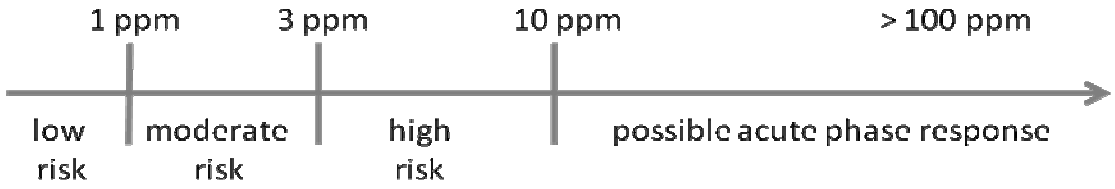


**Figure 8: CRP cut-off points to assess cardiovascular risk (adapted from[97]).**

Despite the commercial availability of automated hsCRP assays, there is still a need for a high sensitive CRP assay showing high precision at levels between 0.15 and 10 ppm to evaluate primary CVD prevention for patients at intermediate risk. Therefore, new generations of CRP assays are under development.

### 1.4.3.2. Immuno- Sensors and Biosensors for C-Reactive Protein detection

Immunochemical approaches for CRP detection as an alternative to commercially available immunoassays have been reported. Among these, a liposome-based immunosorbent assay (LISA) to detect human CRP in standard solution was described [105]. Liposomes containing $Ru(bpy)_3^{2+}$ (bpy = 2,2'-bipyridine) were prepared as an electrogenerated chemiluminescent (ECL) tag and polyclonal antiCRP antibodies were introduced onto liposomes via a streptavidin/biotin linkage. A sandwich assay was realised by using magnetic beads modified with polyclonal antiCRP antibodies, in order to magnetically separate the antigen-antibody conjugates from unreacted species. The addition of NaCl and TritonX caused liberation of $Ru(bpy)_3^{2+}$ from reacted liposomes and its detection was performed by luminescence and electrochemical techniques, with an experimental Detection Limit of 0.1 ppm, intended as the lowest concentration reliably detected.

Alternative new approaches for CRP detection in complex matrices such as whole blood, serum and plasma have been studied. In particular, a magnetic permeability

detection based immunoassay to detect CRP in venous and capillary whole blood samples was developed [106]. Monoclonal anti-CRP antibodies were immobilised on the dextran polymer shell of superparamagnetic nanoparticles and polyclonal anti-CRP antibodies were immobilised on silica microparticles. After the addition of CRP, the sandwich silica-microparticles/CRP/superparamagnetic nanoparticles formed and precipitated. The enrichment of superparamagnetic nanoparticles in the pellet was measured with a Detection Limit (LOD) of 0.2 ppm, intended as the lowest CRP concentration giving a signal higher than the signal of the zero standard plus 3 standard deviations.

A high-throughput multi-antigen microfluidic fluorescence immunoassay to detect simultaneously CRP, prostate specific antigen PSA, ferritin and vascular endothelial growth factor (VEGF) in spiked blood sample was also described [107]. After immobilisation of monoclonal antibodies on epoxide microchambers, ELISA tests were performed using biotinylated antibodies and fluorescently-labelled streptavidin, with an experimental Detection Limit of 1 ppb for CRP.

A few immune-biosensors for CRP detection in buffer solution or real matrices have been described, using transduction principles such as optical. In particular, an immunological optical biosensor capable to detect and recognise pCRP and mCRP in buffer solution was developed [108]. Since pCRP and mCRP exhibit different bioactivities for antibodies, three different monoclonal antibodies were immobilised on a gold sensor surface covered with a protein G layer and the analyte binding was monitored using surface plasmon resonance, yielding an experimental detection limit of 1 ppm. Other SPR-based biosensors for CRP detection have been recently reported, in which the covalent immobilisation of the analyte CRP on the gold sensor surface is achieved by using amide-linked N-hydroxysuccinimmide (NHS) – dextran [109], or the covalent immobilisation of an anti-CRP antibody is realised by forming a self-assembled monolayer (SAM) of poly(thiophene) containing NHS ester groups [110].

A label-free dual-polarisation interferometric biosensor for CRP was also developed by immobilising a monoclonal antibody, anti-CRP, on a glutaraldehyde-functionalised

sensor chip. Changes in the refractive index were monitored upon injection of 0.01 ppm CRP [111].

Electrochemical impedance was employed for the development of a label-free immunosensor for CRP, using a three-dimensional ordered macroporous gold film-modified electrode [112]. After antibody anti-CRP immobilisation on the electrode, the increase of impedance upon CRP binding was measured, yielding an experimental detection limit of 0.1 ppm.

The detection of CRP in blood, serum and urine-spiked samples was performed using a magnetic biosensor exploiting the frequency-mixing technique [113]. A two-frequency magnetic field excitation was used and the magnetic response was detected at a third frequency, which was a linear combination of the applied frequencies. Commercial columns containing polyethylene were modified by immobilisation of monoclonal anti-CRP antibody. After the CRP binding, a different biotinylated monoclonal anti-CRP antibody linked to magnetic-beads modified by streptavidin was added, giving an experimental detection limit of 25 ppb.

An acoustic biosensor for label-free CRP detection in diluted spiked serum was developed [114] by immobilising an anti-CRP chip on a piezoelectric quartz crystal and recording the oscillation frequency shifts upon the analyte binding and the consequent binding of the secondary anti-CRP antibody, to realise a sandwich assay. The detection of the lower spiked CRP concentration (0.1 ppm) in serum correlated well with a commercial hsCRP ELISA.

Finally, two different assay types, binding inhibition and sandwich assay, were used to measure CRP in human spiked serum, using fluorescence as transduction principle [115]. For the sandwich assay, an anti-CRP capture antibody was immobilised on the aminodextran-modified sensor surface, followed by diluted serum sample and further secondary fluorescent-labelled antibody injections. For the binding inhibition assay, the analyte CRP was covalently bound to the surface, then a mixture of diluted spiked

serum and fluorescent-labelled anti-CRP antibody was injected. The experimental limits of detection were respectively 0.13 ppm and 0.055 ppm.

## 1.5. Transduction Systems: Theory

Piezoelectric and Surface Plasmon Resonance (SPR) transduction methods have been widely used in biosensor development, mainly because they allow the detection of label-free targets and the kinetic measurement of molecular interactions in real-time. Moreover, piezoelectric crystals and SPR chips can be regenerated, allowing a multi-use of the sensor.

### 1.5.1. Piezoelectric Biosensors: theory and applications of piezoelectric effect

Piezoelectric crystals are acoustic transducers generally utilised as microbalance or microviscosimeters. In particular, piezoelectric quartz crystals are the basic elements of quartz crystal microbalance (QCM) device. The term “piezoelectric” is derived from the Greek word *piezen* meaning “to press”. The first investigation on the piezoelectricity was performed in 1880 by Jacques and Pierre Curie [116], who observed that a mechanical stress applied to the surfaces of various kinds of crystal caused a corresponding electrical potential across the crystal, whose magnitude was proportional to the applied stress. The charges generated in a piezoelectric crystal are due to the formation of dipoles that result from the displacement of atoms in an acentric crystalline material. The Curies also verified the converse piezoelectric effect, in which application of a voltage across these crystals caused a corresponding mechanical strain. This causes a vibrational, or oscillatory, motion in the crystal, resulting in the generation of acoustic

standing waves at a characteristic resonant frequency. The wave is called bulk acoustic wave (BAW) or surface acoustic wave (SAW) in the case of propagation through the substrate or on the surface, respectively.

A few naturally abundant crystals (i.e. quartz, tourmaline and Rochelle salt) are piezoelectric, but many other materials exhibit this effect, including quartz analogue crystals, such as berlinite ($AlPO_4$), gallium orthophosphate ($GaPO_4$), ceramics with perovskite or tungsten-bronze structures ($BaTiO_3$, $KNbO_3$, $LiNbO_3$, $LiTaO_3$, $BiFeO_3$, $Na_xWO_3$, $Ba_2NaNb_5O_5$, $Pb_2KNb_5O_{15}$). However, only quartz provides the unique combination of mechanical, electrical, chemical and thermal properties, which allowed its commercial success.

Direct and converse piezoelectricity has a wide range of applications. Piezoelectric quartz crystals are used in quartz watches, computers and in many high-performance devices (such as Atomic Force Microscopy) to apply tiny mechanical displacements on the scale of nanometers. Furthermore, such crystals are employed as quartz crystal microbalance for thickness monitoring.

The quartz crystal microbalance is a bulk acoustic wave device based on the converse piezoelectric effect, in which a quartz crystal is sandwiched between two electrodes. The resonant frequency of the quartz crystal depends on several parameters, such as size, density and cut [117]. The most used devices employ AT-cut quartz crystals, sliced with an angle of 35°10’ with respect to the optical z-axis (Figure 9). AT-cut quartz crystals show a high frequency stability and a temperature coefficient close to zero between 0 and 50 °C [118]. AT-cut crystals oscillate in the thickness shear mode (TSM) [119].

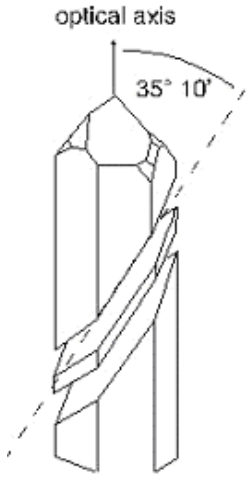


**Figure 9. AT-cut quartz crystals with a cut angle of 35° 10' with respect to the optical z-axis perform shear displacements perpendicular to the resonator surface (from Website http://www.tau.ac.il/~phchlab/experiments/QCM/QCM.html).**

The application of a voltage between the two electrodes causes a shear deformation of the crystal, which is maximised at the crystal faces, making the device sensitive to surface interactions. The resonant condition with the acoustic wave is satisfied by including the crystal into an oscillation circuit, where the frequency of the alternating potential difference applied to the electrodes matches the fundamental frequency of the crystal. The fundamental frequency depends upon the thickness of the wafer, its chemical structure, its shape and its mass [120].

Since the oscillation frequency depends on the crystal mass, deposition of thin films on the crystal surface increases the resonator thickness and decreases the frequency in proportion to the film mass. Measurements of the crystal frequency allow the detection of the film mass, therefore the device operates like a 'microbalance'.

The first quantitative investigation of the piezoelectric effect was performed by Sauerbrey [121], who derived the relationship for the change in frequency $\Delta F$ (in Hz) caused by the added mass $\Delta m$ (in g) in vacuum or in air:

$$\Delta F = -\frac{2F_0^2}{A\sqrt{\mu_Q \rho_Q}} \cdot \Delta m \qquad \text{(equation 1.1)}$$

where $F_0$ is the fundamental resonant frequency of unloaded quartz, $\mu_Q$ is the shear modulus of AT-cut quartz (2.947 x $10^{11}$ $gcm^{-1}s^{-2}$), $\rho_Q$ is the density of the quartz (2.648 $gcm^{-3}$) and A is the surface area in $cm^2$. The Sauerbrey equation assumes a uniform distribution of mass on the entire electrode portion of an AT-cut quartz crystal. Mass sensitivity decreases monotonically with the radius, in a Gaussian manner becoming negligible at and beyond the electrode boundary [122]. Another assumption of this equation is that the mass added or lost at the crystal surface does not experience any deformation during the oscillation; this is true for thin, rigid layers in vacuum or in air. For thicker, less rigid layers as happens for quartz crystals operating in liquid, a more complex theory is necessary. Many factors such as density, viscosity, conductivity and dielectric constant of the liquid may influence the oscillating behaviour. When a quartz crystal oscillates in contact with a liquid, a shear motion on the surface generates motion in the liquid near the interface. The resonant frequency change of a quartz crystal having one face in contact with liquid is described by the Kanazawa and Gordon equation [123] :

$$\Delta F = -F_0^{3/2}\left(\rho_L \eta_L / \pi\ \mu_Q \rho_Q\right)^{1/2} \qquad \text{(equation 1.2)}$$

where $\rho_L$ is the density of the liquid and $\eta_L$ is the viscosity of the liquid.

Piezoelectric crystals have been used as microbalances and as a microviscometer owing to their small size, high sensitivity, simplicity of construction and operation, low cost, light weight and the low power required [124].

The quartz-crystal microbalance has traditionally been used in many applications such as thin film deposition control, etching studies, aerosol mass measurements and space system contamination studies [120]. Recently however, the interest in the application of piezoelectric devices in the field of analysis has increased, since it was realised that

many opportunities for molecular sensing can be opened up once a suitable recognition layer or molecule is coated on the crystal [125]. Therefore by immobilising an affinity ligand on the surface of a quartz crystal covered with gold or silver, an affinity mass sensor is realised. When the affinity reaction with the target in solution take place, the binding ligates can be determined at nanogram levels from the piezoelectric frequency shift. Such piezoelectric biosensors have found a wide range of applications in food [126,127], environmental and clinical [128,129] analysis.

### 1.5.2. Optical Biosensors: theory of Surface Plasmon Resonance phenomenon

Surface Plasmon Resonance (SPR) is an optical technique that uses evanescent waves as a valuable tool to investigate chemical and biological interactions occurring at the surface of a thin sensing layer. Surface Plasmons (SPs) are electromagnetic waves that propagate along the boundary between a dielectric and a metal (gold or silver), because of their interaction with the free electrons of the conductor. In this interaction, the free electrons respond collectively by oscillating in resonance with the light wave. The most common method to excite surface plasmons is the Krestchmann prism configuration, which operates under condition of total internal reflection [130].

In general, total internal reflection occurs at a boundary interface between two media of different refractive indices when incoming light entering from the side having higher refractive index is partly reflected and partly refracted. Above a certain angle of incidence no light is refracted across the interface and total internal reflection is observed. As a consequence, an electromagnetic field called “evanescent wave” is generated and penetrates into the medium having a lower refractive index. In the Kretschmann prism configuration one face of the prism is coated with a thin metal film acting as the sensor surface and the incident light beam is totally reflected at the prism-

metal interface, generating an evanescent wave that penetrates into the metal layer (Figure 10). At the resonant angle, the propagation constant of the evanescent wave matches that of surface plasmons. The evanescent field exponentially decays from the sensor surface into the bulk solution, with a characteristic decay length of a few tens to a few hundreds of nanometers. Therefore, the system is sensitive to refractive index changes within the decay length [131].

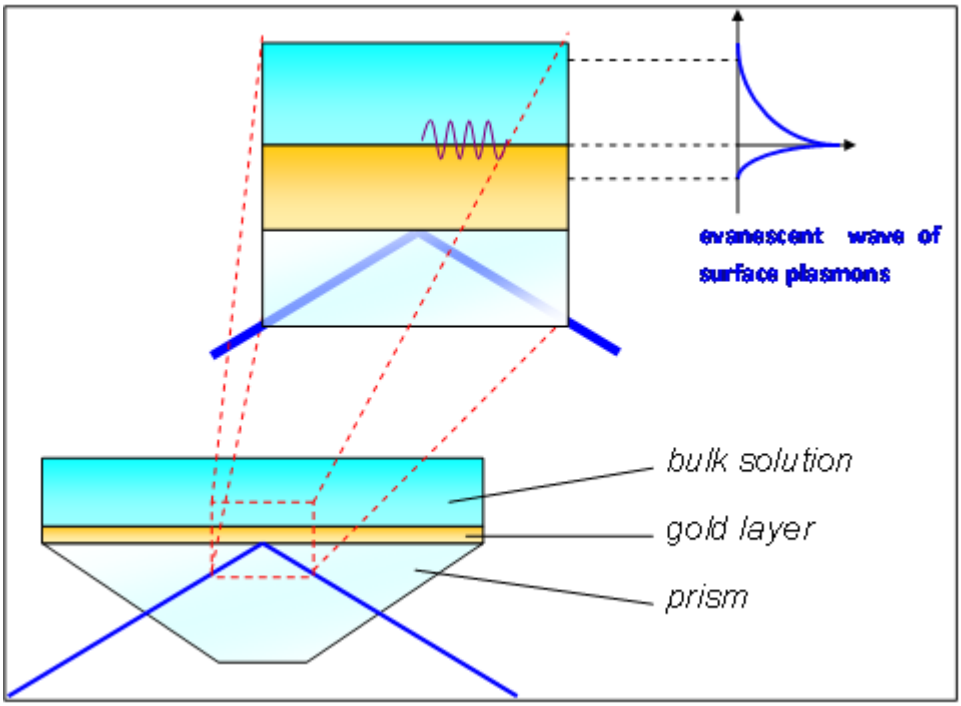


**Figure 10. Surface plasmon excitation in the Kretschmann configuration: the incoming light is reflected at the glass/gold interface. Changes of the refractive index in the dielectric medium are sensed up to 100 nm from the interface (adapted from [132] and [130]).**

Only p-polarized light, with its electric field vector oscillating perpendicular to the plane of the thin film, can be coupled into the plasmon mode. The s-polarised light, with its electric field vector oriented parallel to the metal film, cannot excite palsmons but can be used as a reference beam, since it is reflected at the metal surface.

The surface plasmon wave is affected by changes in refractive index near the metal surface and the coupling efficiency of the incident light into the plasmon mode can be monitored by scanning the incident beam angle throughout a range of values. The

incident beam angle giving maximum surface plasmon coupling ($\theta_{sp}$) is reached when a minimum in reflectivity is observed. At this particular angle of incidence, light is most efficiently coupled into the plasmon mode, therefore the reflection from the metal film is most attenuated as well as the intensity of the reflected light measured by a detector (Figure 11).

(a)

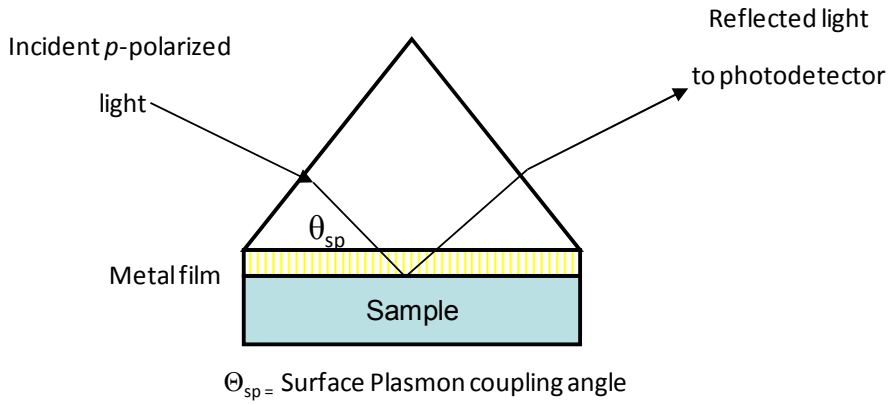


(b)

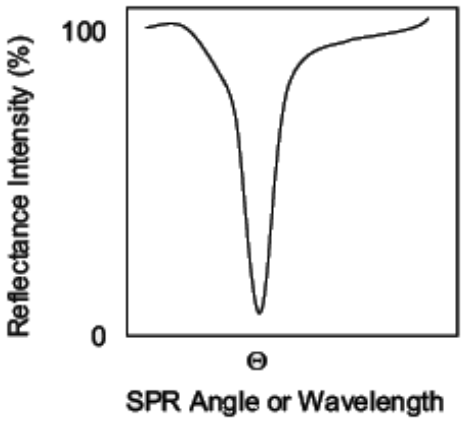


**Figure 11. (a) Surface Plasmon coupling angle, θsp (adapted from [130]); (b) The position of the strong minimum that occurs at the SPR resonance condition depends sensitively on the refractive index of the material above and near the gold surface, as it is sampled by the evanescent light intensity, which decays exponentially with distance above the gold surface (adapted from [133]).**

The SPR principle is used to develop biosensors which rely on the refractive index change induced by molecular interactions occurring at the sensor surface and related to the sample concentration or surface density. After the biorecognition molecule is immobilised on the metal sensor surface, the affinity reaction with the target is realised, resulting in a refractive index change near the sensor surface, which can be detect optically as the sensing transduction signal. Sensing is performed by relating $\theta_{sp}$ to small changes in the refractive index at the external surface of the metal film (Figure 12).

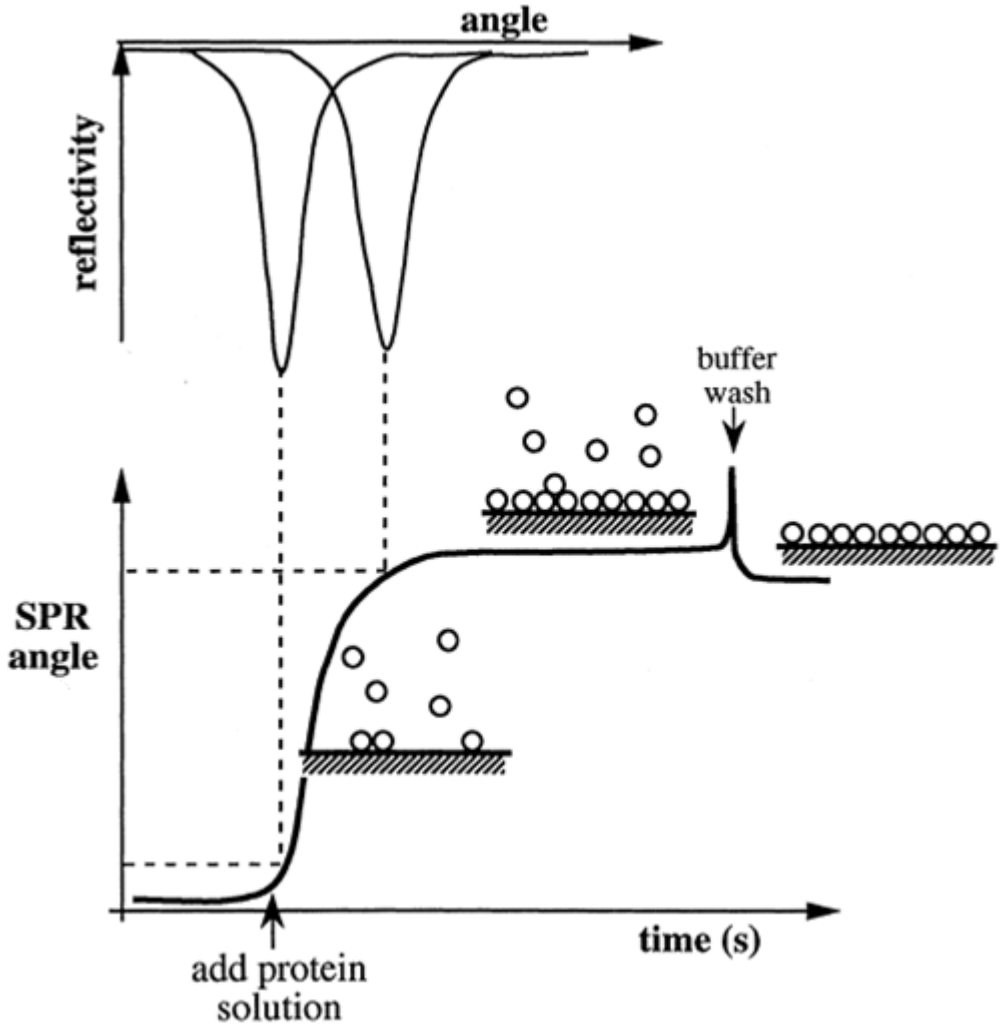


**Figure 12. The θ shift when the refractive index of the surface layer is changed, for example through the binding of biomolecules to the surface (adapted from [134]).**

The most used metals for plasmon generation are gold and silver, because of their optical qualities and the ease with which they can be deposited onto a substrate with accurate thickness. The optimal metal thickness lie in the range 40 - 60 nm.

The Biacore was the first commercial SPR biosensor, launched by Pharmacia Biosensor in 1990. The Biacore instrument is based on SPR technology using a modified Kretschmann prism arrangement, in which a multiwavelengh excitation and a cylindrical glass prism are employed with the aim of eliminating moving components and beam spreading on the gold sensor surface. The surface plasmon resonance angle is followed in real time to monitor biointeractions and is expressed in arbitrary units, called resonance units (RU). A detactable refractive index change is produced by analytes having MW > 1500.

Different types of chip consisting of glass coated with a bare or modified gold layer are available from Biacore. The most commonly used chips are CM5, where carboxymethylated dextran is covalently attached to the gold surface. Ligands immobilisation on CM5 can be performed via amine coupling, thiol-sulphide exchange or aldehyde coupling. The commercial success of Biacore is due to the sensor chip technology, which allows simple inter-exchanging at the sensor surface, and the use of microfluidic handling systems, which facilitate working with small sample volumes to be transported to the chip in a continuous flow, while ensuring a constant analyte concentration on the sensor surface all along the injection. Because of its high sensitivity, Biacore SPR has been applied in biosensors development for the detection of proteins, with a detection limit ranging from picomolecule to nanomolecule concentrations, but also for detection of DNA molecules, cancer biomarkers and bacterial cells [135].

# MATERIALS AND METHODS

This chapter describes the methods and protocols used to perform the experiments, and the materials and reagents purchased for this purpose. All reagents used were obtained from Merck (Darmstadt, Germany) unless otherwise specified.

## 2.1. Transduction systems: experimental apparatus

### 2.1.1. Piezoelectric biosensor for Thrombin detection

A piezoelectric system was employed for the development of an aptasensor for thrombin detection. The resonators used in this work were AT-cut quartz crystals having a circular shape, with a diameter of 14 mm and thickness 165 μm (International Crystal Manufacturing, USA). Gold electrodes (42.6 $mm^2$, Ø 7.4 mm) were evaporated on both sides (Figure 13): a 90 nm layer of gold (999.99 % pure) was deposited under vacuum evaporation on a 10 nm layer of Ni-Cr alloy, which assured good adhesion of the gold to the crystal surface. The fundamental resonant frequency of the resonators was 9.5 MHz and, according to the Sauerbrey equation (Equation 1.1), a frequency shift of 1 Hz is equivalent to 2.2 $ng/cm^2$ increase of the crystal mass (452 Hz/μg). Steel contacts allowed the resonator to be housed in a measurement cell for measurements in liquids.

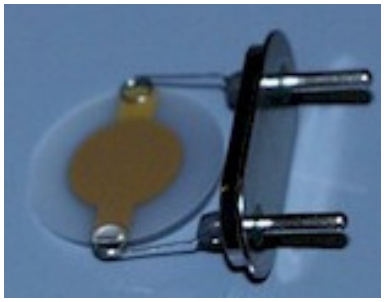

**Figure 13. Piezoelectric quartz crystal.**

The quartz crystal was housed inside the measurement cell, such that only one side of the resonator was in contact with the solution in the cell well; in this way, two measurements could be performed with the same resonator, one on each side.

The cell was made of methacrylate (Figure 14a), which is resistant and inert to the chemicals used in the experiments. In addition, this material is transparent, so that it is possible to observe any anomalies (e.g. air bubbles) that could be present in the well. The cell consisted of two blocks of methacrylate, which were held together by two screws. The crystal was housed between these two blocks, sandwiched between two Viton® o-rings, which assured that the crystal was held in the cell and prevented the wetting of the electrical contacts by the solution - both prerequisites for proper functioning of the system.

This kind of cell was used for batch measurements and the solution of the reagents was inserted into the cell by pipetting it directly in the upper cell well. The volume of the well was about 1 ml, but the typical volumes for the measurements were 100 or 200 µl.

The resonator frequency shifts were continuously recorded using a quartz crystal analyzer (*QCMagic*, Elbatech, Marciana, LI, Italy), configured as a multi-array system (Figure 14b).

(a)

(b)

**Figure 14. (a) QCM measurement cell; (b) QCMagic (Elbatech, Marciana, LI, Italy).**

The QCMagic was interfaced to the driving computer by means of a digital counter board, which could drive up to 4 oscillator units, thus allowing operation with up to 4 independent quartz crystals (or with two pairs of working/reference crystals). The *QCMagic* can be equipped with low-volume static or flow-through reaction chambers, where the oscillating crystal is housed.

*QCMagic* makes use of a precision internal reference crystal, used as a timebase comparator. Depending on the frequency of this internal timebase, each unit can be tuned to work with a specific working crystal, chosen between 1 and 10 MHz. A computer connected to the QCMagic system interface reads directly the data, displayed as resonance frequency *vs.* acquisition number, by means of the specific software, running under MS-Windows™. The resonant frequency can be measured with an accuracy of 0.1 Hz.

## 2.1.2. Optical biosensor: experimental set-up for Biacore

For the SPR experiments, the Biacore™ X analytical device (Biacore; Uppsala, Sweden) was used (Figure 15). The monitoring and analysis of the data was performed using the manufacturer's software Biaevaluation Version 3.1. The bare Biacore sensor chip (Biacore; Uppsala, Sweden) consists of a glass slide (1 $cm^2$) coated with gold (50 nm) on one side and embedded in a plastic support platform. The gold layer is often covered with a linking layer to facilitate binding of biomolecules, in particular carboxylated dextran-coated chips CM5 (Biacore; Uppsala, Sweden) were employed for the immobilisation of biotinylated aptamers. A shift of 1000 RU represents an increase in surface protein concentration of approximately 1 $ng/mm^{2.}$ The Biacore resolution is approximately 1.0 RU.

**Figure 15. Biacore X device.**

### 2.1.2.1. Special precautions for C-Reactive Protein detection

In the case of CRP detection with the specific anti-CRP RNA aptamer, special precautions had to be adopted with the aim of preventing aptamer degradation by RNase. Since the Biacore instrument provides a closed environment, SPR experiments were performed under virtually nuclease-free conditions. Before use, the

instrumentation (the fluidic cartridge and the tubing) was treated with cleaning solutions by running a specific Biacore cleaning procedures (Biacore Desorb and Sanitaze methods). Moreover, all the external instrumental components (the needle and the tubing) were treated with a specific RNase inhibiting solution (RNaseZap™; Sigma, Milan, Italy). Before chip docking, the RNase inhibiting solution was injected (20 µl at 20 µl/min) followed by ten subsequent injections of diethylpyrocarbonate (DEPC; Sigma, Milan, Italy) treated water, with which all solutions and buffers were also prepared. DEPC-treated water was prepared adding 1 ml of DEPC to 1 liter of MilliQ water and stirred overnight. The solution was then autoclaved at 1 atm for 20 min and filtered with 0.22 µm pore size filters (Nalgene; Milan, Italy). RNase free tips (Sarstedt, Numbrecht, Germany) and vials (Abgene; UK) were used for all the experiments.

These precautions were not necessary when using the anti-CRP RNA aptamer modified with 2'-fluoropyrimidines, since it is resistant to RNase degradation for up to 15 hours in biological fluids.

## 2.2. Linking a biological recognition element with the transduction system: immobilisation procedures

A key step in biosensor development is the immobilisation of the biological recognition element onto the transducer. In this thesis two immobilisation procedures were used to link aptamers to gold surfaces:

- Covalent immobilisation on gold surface of thiol-modified aptamers by creation of a self assembled monolayer (SAM)
- Immobilisation of biotin-modified aptamers by affinity reaction with streptavidin-gold modified surface.

With the aim of studying these two different immobilisation procedures, aptamers were purchased carrying different functionalisations (biotin or thiol dye). In addition, different spacers were tested, with the aim of conferring some flexibility to the immobilised molecule, without interfering with the binding to protein. In particular, a polyT tail formed by 20 thymines and a TEG (triethylene glycol) tail ($C_2H_{14}O_4$) were tested as spacer arms.

The 15-mer thrombin aptamers (MWG Biotech; Milan, Italy) had the following sequences:

- Biotinylated 15-mer aptamer: 5'-biotin-GGT TGG TGT GGT TGG-3' (Molecular Weight 5175 g/mol)
- Biotinylated 15-mer aptamer with polyT (20) tail: 5'-biotin-TT TTT TTT TTT TTT TTT TTT GGT TGG TGT GGT TGG-3' (Molecular Weight 11258 g/mol)
- Thiolated 15-mer aptamer: HS-$(CH_2)_6$-GGT TGG TGT GGT TGG-3' (Molecular Weight 4921 g/mol)
- BiotinTEG 15-mer aptamer: 5'-BiotinTEG-GGT TGG TGT GGT TGG-3' (Molecular Weight 5296 g/mol)
- BiotinTEG 15-mer sequence mutated in positions 5 and 14: 5'-BiotinTEG-GGT TTG TGT GGT TAG-3' (Molecular Weight 5255 g/mol)
- BiotinTEG 15-mer sequence mutated in positions 4 and 15: 5'-BiotinTEG-GGT AGG TGT GGT TGC-3' (Molecular Weight 5265 g/mol)
- BiotinTEG 15-mer sequence mutated in positions 3 and 11: 5'-BiotinTEG-GGC TGG TGT GAT TGG-3' (Molecular Weight 5265 g/mol)

The aptamers were received lyophilised and then diluted in MilliQ water and stored at -20 °C.

The 44-mer CRP aptamers (IBA Gmbh; Göttingen, Germany) had the following sequences:

- Biotinylated aptamer with polyT (20) tail: 5'-TT TTT TTT TTT TTT TTT TTT GCC UGU AAG GUG GUC GGU GUG GCG AGU GUG UUA GGA GAG AUU GC-3' (Molecular Weight 20132 g/mol)

- BiotinTEG aptamer: 5'-biotinTEG GCC UGU AAG GUG GUC GGU GUG GCG AGU GUG UUA GGA GAG AUU GC-3' (Molecular Weight 14110 g/mol). The same aptamer sequence biotinylated in 5' was also purchased modified with 2'-fluoropirymidines (Molecular Weight 13643 g/mol).

The aptamers were received lyophilized and then diluted in MilliQ water and stored at -20 °C.

### 2.2.1. Immobilisation of biotinylated aptamers on piezoelectric and optical devices

The procedure for the immobilisation of a biotinylated probe on a gold sensor surface was developed by Löfas [136] for surface plasmon resonance and further adapted to piezoelectric sensing [137]. According to this procedure, a gold sensor surface was modified with a carboxylated dextran layer on a self assembled monolayer (SAM) of alkanethiols; after the covalently linkage of streptavidin on the dextran layer, the biotinylated probe immobilisation was realised exploiting the high affinity and selectivity of the streptavidin-biotin interaction.

A detailed explanation of the multi-step immobilisation protocol followed for the piezoelectric measurements is described below. For the SPR measurements, since dextran modified chips (Biacore CM5) were employed, only the final steps of the procedure were employed.

*a) QCM device*

Before the immobilisation step, the quartz crystal surface was cleaned with a boiling solution of $H_2O_2$, $NH_3$ (30%) and MilliQ water in a ratio 1:1:5. The crystal was dipped in this solution for 10 minutes, then washed with MilliQ water and air dried. The

formation of the SAM was realised by coating the crystal with an unstirred 1 mM ethanolic solution of 11-mercapto-1-undecanol, $HS(CH_2)_{11}OH$ (Sigma; Milan, Italy), at room temperature for 48 hours, in the dark. The solution of 11-mercapto-1-undecanol was freshly prepared before use (2 mg of the thiol in 10 ml of ethanol). After washing with ethanol and MilliQ water, the crystal was sonicated in ethanol (10 minutes) to remove excess thiols, then rinsed with ethanol and MilliQ water. The hydroxylic surface was then treated with a 600 mM solution of epichlorohydrine in a 1:1 mixture of 400 mM NaOH and bis-2-methoxyethyl ether (diglyme) for 4 hours. This step allowed the introduction of epoxy groups on the surface, as electrophilic coupling sites for further binding of dextran. After washing with water, the crystal was immersed for 20 hours in a basic dextran solution (3 g of Dextran 500 (Amersham Biosciences, UK) in 10 ml of NaOH 100 mM). Due to the high concentration of hydroxyl groups in the dextran molecule, chemical modifications of this polymer was possible without significantly affecting its hydrophilicity. Therefore, the surface was further functionalised with carboxymethyl groups using 1M bromoacetic acid (Sigma, Milan, Italy) in 2 M NaOH for 16 hours. All the reactions were performed at room temperature out of the piezoelectric cell. Finally, the crystal was washed with MilliQ water and stored at 4 °C for several days.

For the surface activation of the carboxylic groups on the dextran for amino-coupling, the crystal was housed in the cell. The negatively charged crystal surface was activated with 200 µl of a solution of 50 mM N-Hydroxysuccinimide (NHS; Sigma, Milan, Italy) and 200 mM 1-ethyl-3-(3-dimethylaminopropyl)carbodiimide (EDAC; Sigma, Milan, Italy) in water. This reaction converted a fraction of carboxylic groups into active esters. The NHS/EDAC solution was prepared immediately before use to avoid loss of activity. After 5 minutes, the activating solution was replaced by a 200 µg/ml streptavidin (Sigma; Milan, Italy) solution in acetate buffer 10 mM, pH 5. Due to its neutral pI, at this pH streptavidin is positively charged and the electrostatic attraction of the protein molecules to the activated and partially negatively charged dextran considerably enhances the coupling yield. A much higher local concentration of the protein in the still partly negatively charged dextran layer compared to the bulk concentration is thus obtained and favours the reaction of the nucleophilic groups in the protein over

hydrolysis of the esters. After 20 minutes, the free residual reacting sites were blocked with 200 µl of a solution of ethanolamine hydrochloride (pH 8.6, 1 M water solution). This step was performed for 20 minutes. The quartz crystal modified surface was then washed with the immobilisation buffer (150 mM NaCl, 20 mM $Na_2HPO_4$, 0.1 mM EDTA, pH 7.4). Finally, the biotinylated aptamer was added (200 µl of a solution 1.0 µM in immobilisation buffer) and the reaction was allowed to proceed for 20 minutes, via streptavidin-biotin interaction. At this final stage the crystal was ready for the first cycle of binding, performed in binding buffer. The immobilisation protocol is shown schematically in Figure 16.

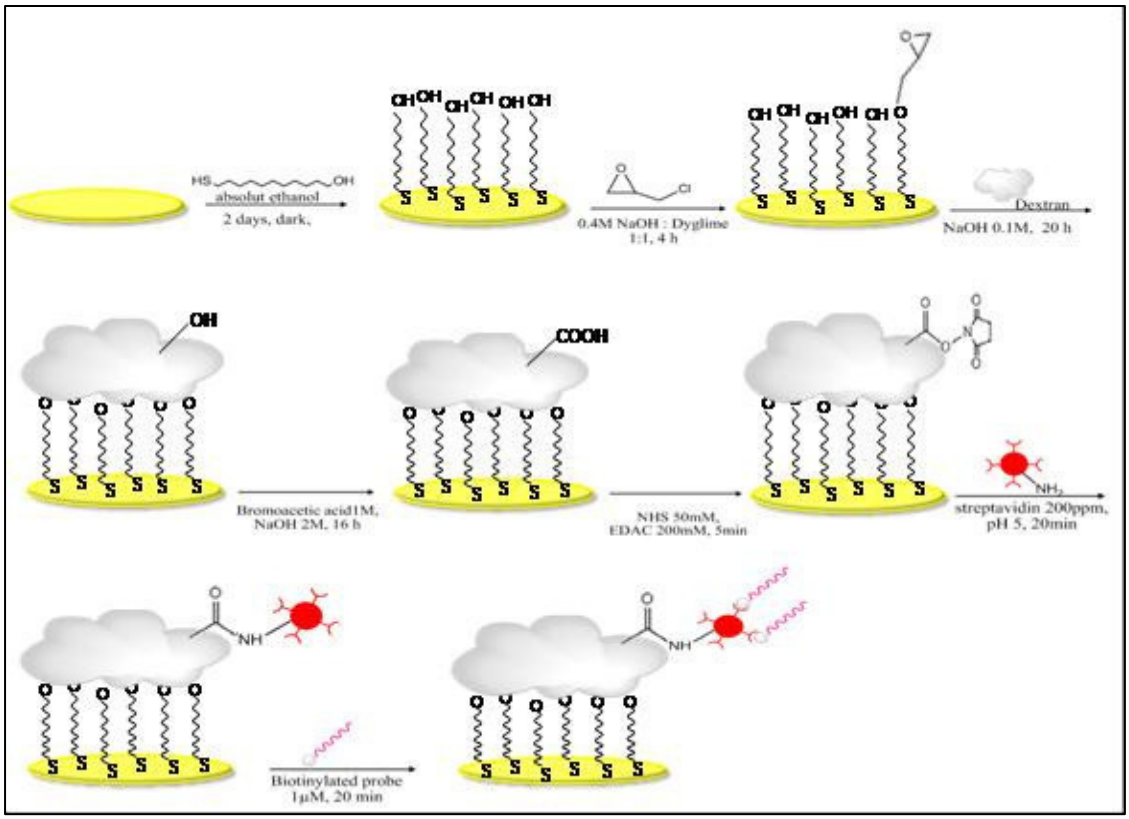


**Figure 16. Immobilisation of biotinylated probes on quartz crystal microbalance. The scheme also shows the functional groups involved.**

*b) SPR device*

For the SPR measurements, the biotinylated aptamer immobilisation was realised on dextran-modified CM5 Biacore chips, according to the final part of the protocol and using the following times of reaction:

- Activation step with 50 mM NHS, 200 mM EDAC in water: 7 min.
- Covalent immobilisation of 200 ppm streptavidin in 10 mM acetate buffer, pH 5.0: 7 min.
- Saturation of free carboxylic groups with 1M ethanolamine hydrochloride, pH 8.6: 7 min.
- Aptamer immobilisation after a thermal treatment (95 °C 1 min, 0 °C 10 min) [138,139]: 20 min. The thermal treatment can unfold the aptamer strand making the biotin label at 5' end available for the interaction with streptavidin on the chip surface. Therefore, before the immobilisation, the biotinylated aptamer was heated at 90 °C for 1 min to unfold the DNA strand and then cooled in ice for 10 min in order to block the DNA in its unfolded structure.

After the aptamer immobilisation, the surface was blocked with 500 ppm biotin (Sigma; Milan, Italy) solution in immobilisation buffer (20 min), to saturate the free streptavidin sites. The immobilisation procedure was performed at a constant flow rate of 5 µl/min at 25 °C, using as running buffer the same solution as binding buffer, degassed daily prior to use.

## 2.2.2. Immobilisation of thiolated aptamer

The gold sensor surface was modified with a thiolated aptamer and a blocking thiol by chemisorption via SH-Au interaction [140, 141]. The use of a blocking thiol such as 6-mercapto-1-hexanol (MCH; Sigma, Milan, Italy) improved the immobilisation efficiency; the thiolated probe alone could lie flat onto the surface because of non-

specific interactions between the oligonucleotide bases and the gold surface, while MCH attached to the unoccupied gold regions replacing non-specifically adsorbed probes. In this way, a better orientation of the probe could be achieved. The immobilisation methodology based on thiolated probes is illustrated in Figure 17.

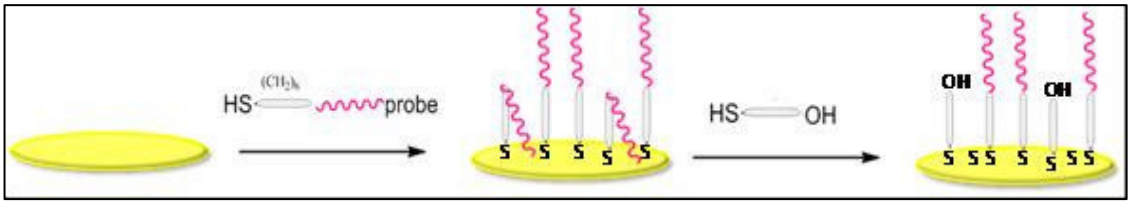


**Figure 17. Immobilisation of thiolated probes.**

For thiolated aptamer immobilisation on QCM device, the resonator was washed with a boiling solution of $H_2O_2$, $NH_3$ (30%) and MilliQ water in a ratio 1:1:5. The crystal was dipped in this solution for 10 minutes, then washed with MilliQ water and air dried. Then the crystal was housed in the cell and treated with a 1 µM solution of thiolated probe in immobilisation solution (1 M $KH_2PO_4$, pH 3.8) for two hours, then washed with immobilisation solution and MilliQ water. Afterwards, 200 µl of blocking thiol solution (MCH) was injected into the cell and the reaction was allowed to proceed for 1 h, before the final washing with MilliQ water. As a final step, MilliQ water was replaced by 100 µl of binding buffer and the frequency was allowed to stabilise.

## 2.3 Binding measurement procedures

After the aptamer immobilisation on the piezoelectric crystal or on the Biacore chip, the binding between the immobilised receptor and the target protein was monitored. The measurement cycle consisted of recording the baseline, followed by target injection, washing with buffer and surface regeneration. The regeneration step consisted of an

acid, basic or highly saline treatment, which released the sensor-bound analyte from the aptamer without affecting its capacity to further bind the protein and allowing a multiple use of the sensor.

### 2.3.1. Binding protocol for Thrombin detection with piezoelectric device

During the piezoelectric aptasensor development for thrombin detection, 50 mM Tris-HCl, pH 7.4, 140 mM NaCl, 1 mM $MgCl_2$ was used as binding buffer. Human α-Thrombin was purchased by Sigma (Milan, Italy). Thrombin is shipped as lyophilised powder containing 417 NIH Units of protein (3093 NIH Units/mg). Thrombin stock solution (3.6 μM in 20 μl binding buffer) was stored at -20 °C and further dilutions in binding buffer were stored in ice during measurements. Human serum albumin (HSA; Sigma, Milan, Italy; Product Number A9511) was used as negative control. Albumin was shipped lyophilised and stored at 4 °C. Further dilutions were prepared in the same binding buffer and used after preparation.

A generic example of an interaction between the immobilised thrombin aptamer and its protein target in solution is reported in Figure 17. A stable baseline was initially recorded when the crystal together with the immobilised probe was in contact with 100 μl of binding buffer. The aptamer-protein interaction was performed by replacing the binding buffer with an equal volume (100 μl) of a solution containing the target molecule (in the concentration range 50 - 200 nM), prepared using the same buffer. At the end of the time necessary for the interaction to occur, the surface was washed with binding buffer to remove the unbounded molecules or the molecules that could non-specifically absorb on the crystal surface. When the frequency had reached a stable value, the frequency value was recorded. The frequency shifts reported in this work are always the difference between two stable frequency values (± 1 Hz) recorded in binding buffer: in particular, the frequency shift is reported as the difference between the final

value (D) and the value displayed before the binding reaction (A). Since both frequency values are taken when the crystal is in contact with the same buffer solution (binding buffer), the shift is only due to compounds fixed on the gold surface during the reaction [18]. A signal generated by the aptamer-protein interaction is considered significant when the difference between the frequency values corresponding to the buffers is higher than 3 Hz. Different concentrations of the protein were used to build a calibration plot.

After each cycle of binding, the aptamer-thrombin interaction was regenerated (E) by 1 min treatment with 2M NaCl. With this treatment the sensor-bound analyte was released from the surface, and the baseline was reached again, allowing multiuse of the sensor (F). All the experiments were performed at room temperature.

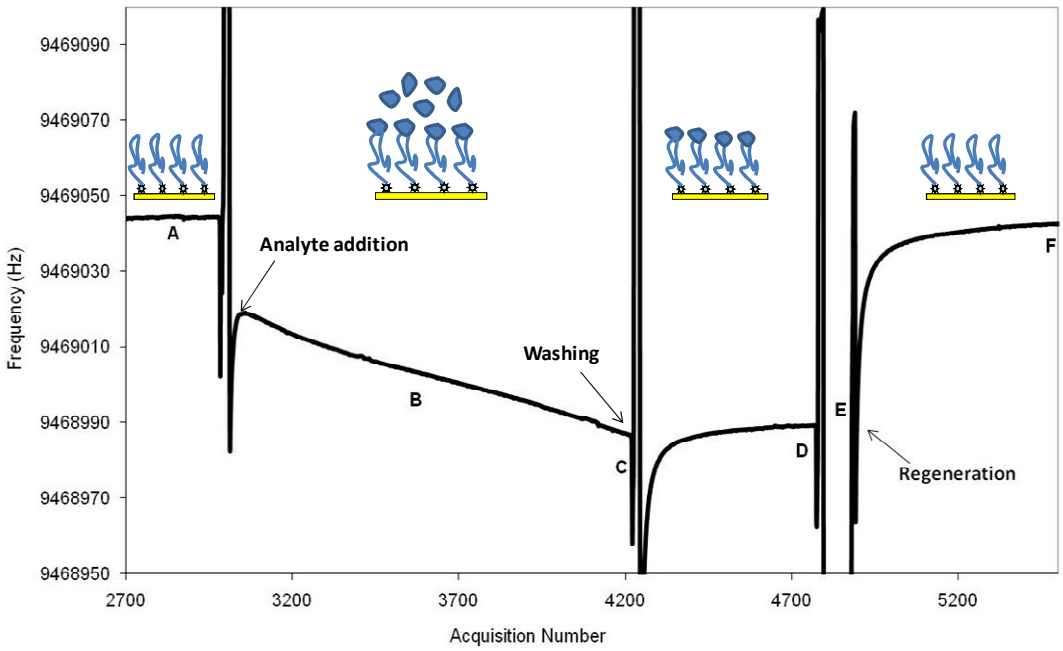


**Figure 18. Schematic diagram of a piezoelectric measurement. Typical sensorgram recorded during a binding reaction. A) The probe is immobilised on the sensor surface. Recording of the baseline in binding buffer. B) Injection of the protein solution. The aptamer-protein interaction was monitored in real time. C) Removing the DNA solution and washing with binding buffer. D) Baseline in binding buffer. The analytical signal due to the complex formation is given by $\Delta F(Hz)=F(D)-F(A)$. E) Regeneration and washing with binding buffer. F) Baseline in binding buffer after regeneration.**

With the same procedure, HSA was used as negative control, to test the specificity of the interaction and the presence of non-specific adsorption on the surface.

## 2.3.2. Binding protocol with optical device

For SPR measurements, after aptamer immobilisation the binding between the immobilised receptor and proteins was monitored with an interaction time of 15 minutes, followed by washing with running buffer and surface regeneration. Binding interactions were monitored at a constant flow rate of 2 µl/min at 25°C. A schematic representation of a sensorgram is reported in Figure 19, where the SPR signal is expressed in Resonant Units (RU).

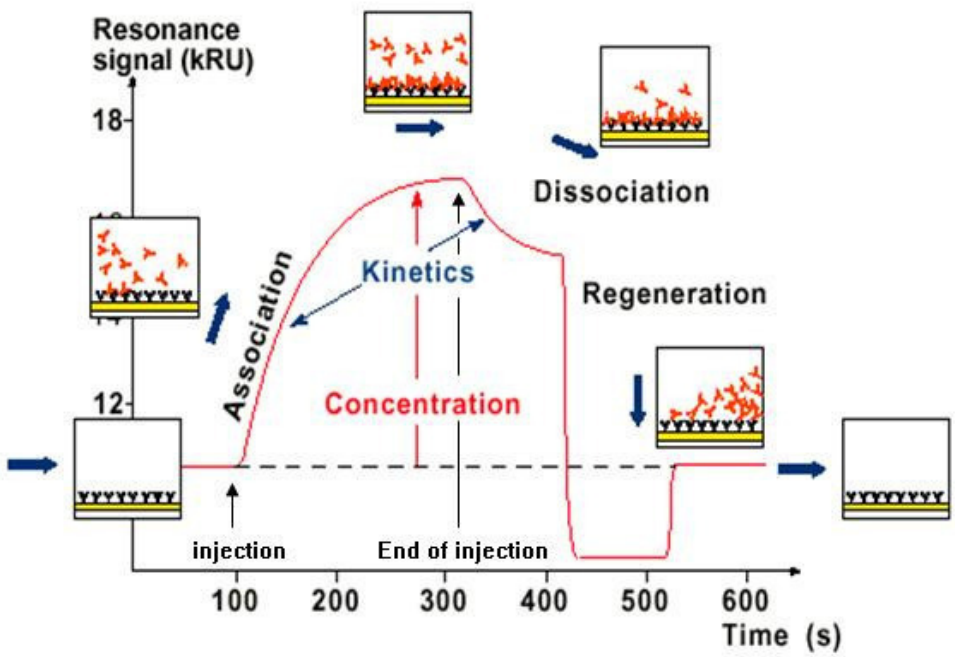


**Figure 19. Schematic representation of a SPR sensorgram (from http://www.biacore.com).**

*a) Thrombin*

For the optimisation of the binding procedure between the immobilised aptamer and thrombin by SPR experiments, different binding buffers and regeneration solutions were tested. 4-(2-hydroxyethyl)piperazine-1-ethanesulonic acid (HEPES), tris-(hydroxymethyl)aminomethane (Tris-HCl), polyoxyethylene-sorbitan monolaurate (Tween 20) and all the other reagents for the buffers and the regenerating solutions were purchased from Sigma (Milan, Itlay). The following buffers were tested both as running solutions and protein dilution to 20 nM: 10 mM HEPES pH 7.4, 150 mM NaCl, 0.005% Tween 20; 50 mM Tris-HCl pH 7.4, 140 mM NaCl, 5 mM KCl, 1 mM $MgCl_2$; 50 mM Tris-HCl pH 7.4, 140 mM NaCl, 1 mM $MgCl_2$; 10 mM HEPES pH 8. The following solutions were tested to release the protein from the surface: SDS (0.025%); 12 mM NaOH with 1.2% EtOH; 50 mM HCl; 2 M NaCl.

*b) C-Reactive Protein*

For the optical aptasensor development for CRP detection, purified human C-Reactive Protein was purchased by Biodesign (Milan, Italy) in concentration 2000 ppm in buffer 0.1 M Tris, 0.2 M NaCl, 2 mM $CaCl_2$, pH 7.5 containing 0.1 % $NaN_3$ as preservative. The protein solution was stored at 4°C. Further dilutions were performed and kept in ice during the experiments to prevent denaturation.

Concentration of CRP solutions was expressed as mg/l (ppm), in order to allow a direct comparison of the results obtained in this work with other results reported in literature, where clinically-relevant proteins are usually measured as mg/l. In contrast, thrombin solutions were reported as molarities, according to other papers cited in this work.

2-(N-morpholino)ethanesulfonic acid (MES) and all the other reagents for the buffers were purchased from Sigma (Milan, Itlay). The following binding buffers were tested both as running buffer and for protein dilutions, in order to find the one granting the highest sensitivity for CRP: 10 mM MES pH 6.0; 10 mM HEPES pH 6.0; 10 mM Tris-HCl pH 6.0; 10 mM MES pH 6.5; 10 mM HEPES pH 6.5; 10 mM Tris-HCl pH 6.5; 10 mM HEPES pH 7.0; 10 mM Tris-HCl pH 7.0; 10 mM HEPES pH 7.5; 10 mM Tris-HCl

pH 7.5. The selected binding buffer was further added with 0.005% (v/v) of Tween 20 and 2 mM $CaCl_2$.

HSA and human immunoglobulin G (IgG; Sigma, Milan, Italy) were used as negative controls. The aptamer-CRP binding was dissociated with 1 min injection of HCl at different concentrations (1, 10 or 25 mM), depending upon the entity of the binding shift to be regenerated. With this treatment the sensor-bound analyte was released from the immobilised aptamer.

## 2.4. Experiments in complex matrices

### 2.4.1. Treatment of human serum and plasma for Thrombin detection

Human serum from clotted male whole blood (Product Number H1388) and Human citrated plasma (Product Number P9523), provided by Sigma (Milan, Italy), were divided into aliquots and stored at -20 °C. Standard solutions of thrombin were added to serum or plasma to test the performance of the piezoelectric aptasensor in complex matrices. Since serum does not contain coagulation factors, the addition of thrombin did not affect the samples. On the contrary, the addition of thrombin to plasma, which contains all the proteins involved in the coagulation cascade including fibrinogen, leads to the formation of fibrin and to rapid sample clotting. To avoid this phenomenon, fibrinogen was precipitated from plasma before the addition of thrombin in the preparation of spiked samples. Such selective precipitation is based on the use of ammonium sulfate as precipitant: 250 µL of plasma was treated with 1250 µL of 2 M ammonium sulfate and 1000 µL of 0.1 M sodium chloride. The solution was mixed for 3-4 min, then centrifuged for 2 min at 15000 rounds per minutes (RPM), and the supernatant was collected and eluted with binding buffer using NAP™ 10 columns for

rapid desalting and buffer exchange (Amersham Biosciences; Milan, Italy). The amount of protein in the raw plasma and the eluted solution was evaluated by spectrophotometric measurements at λ = 280 nm, and a loss of protein content (~40%) was detected after precipitation of fibrinogen.

### 2.4.2. Treatment of human serum for C-Reactive Protein detection

For the complex matrix treatment, different approaches were tested:

- Magnetic beads coupled with protein G with diameter 2.8 ± 0.2 μm were purchased from Dynal Biotech (Milan, Italy). Standard solutions of CRP (0.01 ppm), HSA (500 ppm), hIgG (240 ppm) or a mixture of them with and without addition of CRP were incubated with 200 μL of magnetic beads suspension for 20 minutes; then the magnetic separation between the beads and the solution was performed by the use of a magnetic bar. The solutions were further diluted (1:2) in order to reach the relative concentrations corresponding to a 1:100 serum dilution. The quantity of protein recovered after the treatment was roughly estimated by spectrophotometric measurements at λ = 280 nm. The treated solutions were then tested using the optical aptasensor.

- Affinity columns removing both hIgG and HSA (IgG Removal Kit) were purchased by GE Healthcare and used for the treatment of undiluted human serum. The serum eluted from the column resulted diluted 30 times and was further diluted 3 times to reach a final dilution 1:90. This solution was then added with a commercial product able to further reduce the matrix effect: in particular, a non specific binding reducer (NSB-Reducer™; Biacore, Sweden) containing carboxymethyl dextran sodium salt (10 mg/ml) in 0.15 M NaCl, 0.02% $NaN_3$ was employed. Standard solutions of CRP in the concentration range 0.1– 0.4 ppm were spiked in the treated matrix.

## 2.5. Computational approach to the study of aptamer-thrombin interaction using Openeye Scientific Software

With the aim of calculating through simulations the interaction energy between thrombin and DNA sequences, a library of oligonucleotides was created and screened by computational methods in order to identify potentially binding sequences.

For this purpose, 15-mer DNA sequences were virtually created using the software package Hyperchem 7.5, which performs molecular modeling and simulations. All the other modeling steps were then performed using Openeye Scientific Software Inc. This free software resource offers large-scale modeling applications and toolkits. All the experiments were performed on a Acer Veriton T661, RAM 3 GBytes, supported by platform Microsoft Windows XP.

The Openeye application VIDA was used to visualise images of the molecule structures and to handle very large data sets. The other Openeye applications (with the exception of Fred-Receptor) are command line driven programs. Once the library of 15-mer mutated sequences was generated starting from the TBA sequence, the proposed general procedure consisted of several steps:

a. Creation of the binding box where each sequence will be docked, using the Openeye application Fred-Receptor
b. Energy minimisation of each sequence structure in the library, using the Openeye application Szybki-1.2.2
c. Generation of conformers for each minimised sequence, using the Openeye application Omega2-2.2.1
d. Docking of each sequence in the receptor site and scoring, using FRED2.2.3 (Fast Rigid Exhaustive Scoring), which is the Openeye protein-ligand docking program.

### 2.5.1. Creation of the library

The 15-mer TBA aptamer (5'-GGTTGGTGTGGTTGG-3') was drawn as a single strand in helix conformation by means of HyperChem 7.5 and used as a reference structure where mutations have to be introduced. HyperChem allows the substitution of nucleotide residues with others present in the database.

The automatic creation of mutated sequences as single strands in helix conformation in HyperChem 7.5 was realised by using a special script equipped with a modifiable input file. The program had been written and kindly provided by Mr. Leonid Sislo, a student in Computer Science at Kanaus University of Technology (Lithuania) during his visit to our laboratory. This special script performed the generation of combinations with the aid of AutoIt v3 framework, which is a freeware BASIC-like automation language used to script simple Windows-based tasks. The special script was equipped with an input file which stored modifiable rules for limiting the number of sequences to be generated, in order to complete the library generation in a working day. In particular, the number of mutations to be performed, i.e. the number of mutated nucleotides with respect to the TBA sequence, can be varied at will, with the aim of reducing the search space with respect to the number of possible mutated DNA sequences. In this way the generation of a library of 990 different sequences each containing a maximum of two mutations with respect to the TBA sequence was performed. The script output file consisted of a set of oligonucleotide structures saved in format .pdb, which is compatible with both the HyperChem 7.5 and Openeye software packages. In order to briefly indicate the mutations performed, the following procedure was adopted: the central number indicating the position in the sequence was squeezed between the symbol indicating the nucleotide in the TBA sequence for that position (on the left) and the symbol indicating the mutated nucleotide (on the right).

The library was added with three virtually generated sequences, which in literature have been experimentally tested for weakly binding to thrombin:

- 5'-GGT GGT GGT TGT GGT-3', having 6 mutations (Mutations T4G, G6T, T7G, G10T, T13G, G15T) with respect to the TBA sequence and referred to as sequence "a" [54]
- 5'-GGT AGG GTC GGA TGG-3' (Mutations T4A, T7G, G8T, T9C, T12A) referred to as sequence "b" [55]
- 5'-GGT AGG GCA GGT TGG-3' (Mutations T4A, T7G, G8C, T9A), referred to as sequence "c" [55]

As a consequence, the library contained 994 different sequences as single strands in helix conformation.

### 2.5.2. Creation of the binding box

The binding box is defined as the area comprising the ligand and the site of the protein interacting with the ligand. For binding box design, the ligand-protein complex structure was downloaded from the Protein Data Bank and the Openeye Scientific Software toolkit Fred-Receptor was used. Fred-Receptor is a wizard like graphics utility that designs the box for subsequent docking with FRED, the Openeye docking program. To design the box, the ligand structure was selected as reference (reference ligand) and a 3D rectangular box was automatically generated. The binding box describes the general area of the protein where ligands are expected to bind. Any molecule that FRED will dock, must fit within the binding box, although this is only one of several criterion required for docking. Since box size indirectly influences docking speed, the receptor site contours can be varied. Typical box sizes range from 1000 to 8000 cubic Ångstroms.

Thrombin shows two different binding sites for aptamers, but only the aptamer-thrombin complex, where the 15-mer TBA interacts with the fibrinogen-binding exosite, has been solved by NMR [67] and it is present in Protein Data Bank (code

1HAO). Therefore, the TBA aptamer-thrombin complex structure 1HAO was downloaded from Protein Data Bank in order to define by using Fred-Receptor the binding box, around the aptamer, in the Fibrinogen-binding exosite. With the aim of studying the aptamer-thrombin interaction also in the heparin-binding exosite, the heparin-thrombin complex (code 1TB6) was downloaded from Protein Data Bank and a box was automatically created around heparin by Fred-Receptor. The binding box contours were then modified, in order to define a binding box of dimensions similar to that in the fibrinogen-binding exosite, so that the aptamer should fit in.

Fred-Receptor docks the reference ligand (in this case the 15-mer TBA) to the protein and scores the resulting interaction on the basis of a scoring function. The scoring function used in this work was ShapeGauss [45], that is a shape-based fitting scoring function proprietary of Openeye. This attempts to quantitate how well a pair of atoms interact using a Gaussian representation of atomic volumes. The score is best (more negative) when atomic surfaces touch, but do not interpenetrate. The two receptor site boxes and the Shapegauss scoring function were also employed by FRED to dock each sequence in the library, after the minimisation step and the generation of conformers.

### 2.5.3. Energy minimisation and conformational search

The library of nucleotide sequences (in format .pdb) was visualized in VIDA and saved as a multi-file of structures in format .oeb, which is the molecular file format that Openeye toolkits Szybki-1.2.2. and Omega2-1.2.2 support. The energy of the molecules contained in this multi-file was then minimized by Szybki-1.2.2, which uses the Merck Molecular Force Field (MMFF) [142] for energy optimisation. The MMFF potential expression is given by the sum of seven terms: bond stretching, angle bending, stretch-bending, out-of-plane bending, torsion, Van der Waals and electrostatic interactions.

For Szybki-1.2.2 running, default settings were kept with the exception of max_iter = 4000.

Once each structure was minimised, conformers of each molecule were discovered using Omega2-2.2.1. Omega is designed to be used with the large libraries of compounds required by computer-aided drug design, and it is able to rapidly generate multi-conformer structure databases. This toolkit splits a molecule into parts and then adopts the use of advanced algorithms to link the structures together in order to produce a stable conformer. Molecular modeling results generally depend on the quality of the conformers generated, upon which results are rationalised and predictions are made. For running Omega2-2.2.1, default settings were retained.

### 2.5.4. Docking and Scoring

Using the multi-conformer library and the binding box file as input, the docking program FRED-2.2.3 outputs the molecules of the database most likely to bind to the receptor. Typical docking time for FRED is a few seconds per ligand. For each multi-conformer ligand, FRED generates candidate poses and exhaustively examines all possible poses within the binding box, translating and rotating each molecule of the multi-conformer library within the box by specified angular and translational step (by default, 1.5 Å and 1 Å respectively). Poses that do not fit within the active box or do not match the defined constraints are rejected. All remaining poses are ranked on the basis of a scoring function. As explained above, in this work ShapeGauss was used as scoring function. A systematic solid body optimisation of the top-ranked poses is then performed against ShapeGauss, by rigidly rotating and translating the molecule at half the step-size used in the exhaustive docking. As an output file, FRED returns a hit-list of scored docked structures.

# RESULTS

## 3.1. Development of a piezoelectric aptasensor to detect Thrombin

A piezoelectric aptamer-based affinity biosensor to detect label-free Thrombin was developed. The best conditions for the assay had to be found, in order to critically evaluate the aptasensor's analytical performance, in terms of selectivity, linearity ($R^2$), reproducibility (coefficient of variation CV%) and stability (number of cycles).

### 3.1.1. Optimisation of experimental conditions with Biacore

As a first optimisation step, SPR measurements were performed in order to determine the optimal aptamer-analyte binding protocol. For this purpose, the 5' biotinylated 15-mer thrombin aptamer with polyT tail was immobilised onto the SPR chip at a concentration of 1μM. Different binding buffers (in terms of ionic strength, pH, $Mg^{2+}$ content) were tested for the dilution of thrombin to 20 nM and the binding with the immobilised aptamer was then monitored, in order to valuate which buffer promoted the binding step. The best performance in terms of sensitivity and reproducibility were observed with Tris-HCl pH 7.4, independently by the presence of KCl (Figure 20).

However Tris-HCl pH 7.4 not containing KCl was chosen as the binding buffer to be used for further experiments.

Different regeneration solutions were also tested, such as 0.025 % SDS, 0.1 M NaOH, 2 M NaCl, 50 mM HCl, with the aim of releasing the bound analyte from the sensor without affecting the aptamer's capacity to bind thrombin. A complete surface regeneration was achieved by a treatment with NaCl 2M (1 min). These optimised binding conditions (binding buffer and regeneration solution) were then transferred to the piezoelectric system.

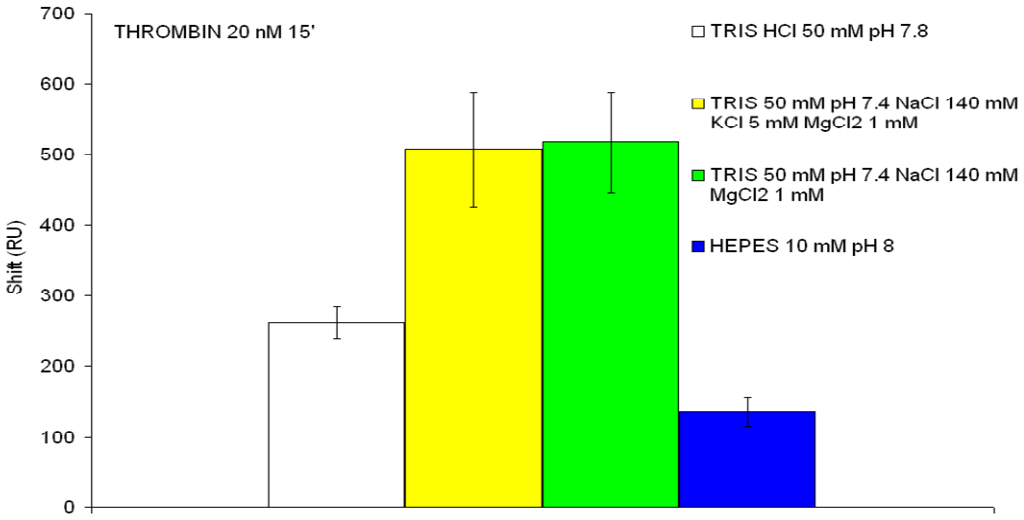


**Figure 20. Comparison between different binding buffers (Biacore CM5 chip with biotinylated 15-mer aptamer with PolyT tail). Each error bar represents standard deviation of three replicates (n=3).**

## 3.1.2. Analytical performance of Thrombin detection with the piezoelectric device

For the development of the piezoelectric aptasensor, the 15-mer TBA was immobilised on the gold surface of 9.5 MHz piezoelectric crystals and the analyte (Thrombin) in

solution was added. The analytical signal (Frequency vs. Time) was recorded in real-time without the use of any label.

In the development of aptasensors, it is important to select a proper immobilisation protocol to ensure good analytical performances. For this reason, two immobilisation protocols were compared, in order to choose which aptamer design assured higher sensitivity and reproducibility: 1µM aptamer modified at its 5' with a biotin group and a polyT (20-mer) tail was immobilised onto the gold surface of a quartz crystal previously modified with streptavidin amino-coupled to a carboxylated dextran layer, according to the procedure described in paragraph 2.2.1. (Figure 21); 1 µM aptamer modified at its 5' end with a thiol group was directly attached to bare gold crystal surface, according to the procedure described in paragraph 2.2.2 (Figure 22).

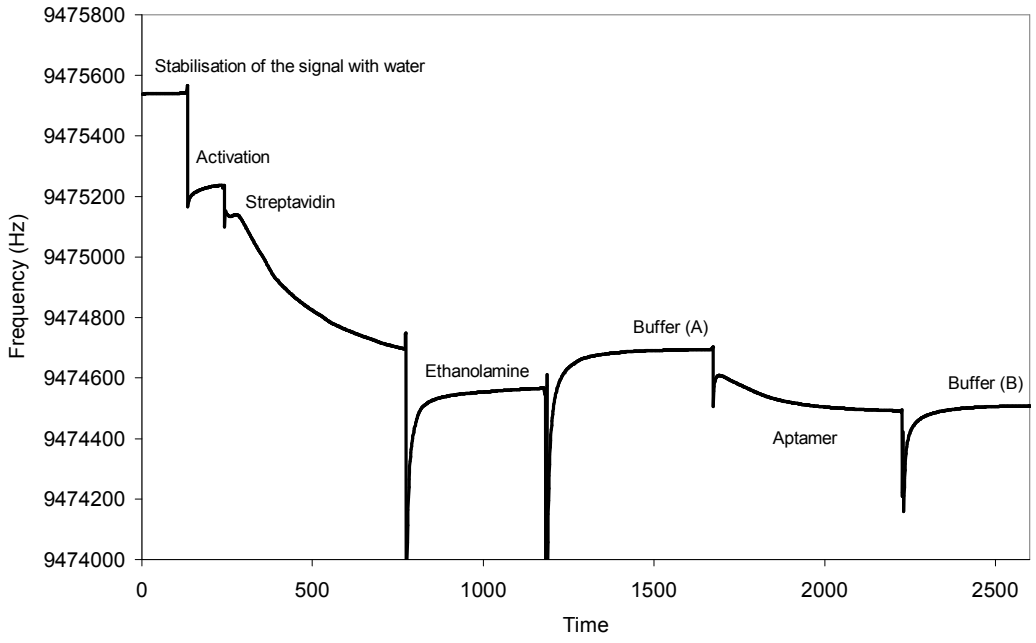


**Figure 21. Typical frequency variation (*vs.* Time) recorded during the functionalisation of the crystal and the biotinylated aptamer immobilisation. The entity of the immobilisation can be evaluated by the difference between the frequency shift of the two steps Buffer (B) – Buffer (A).**

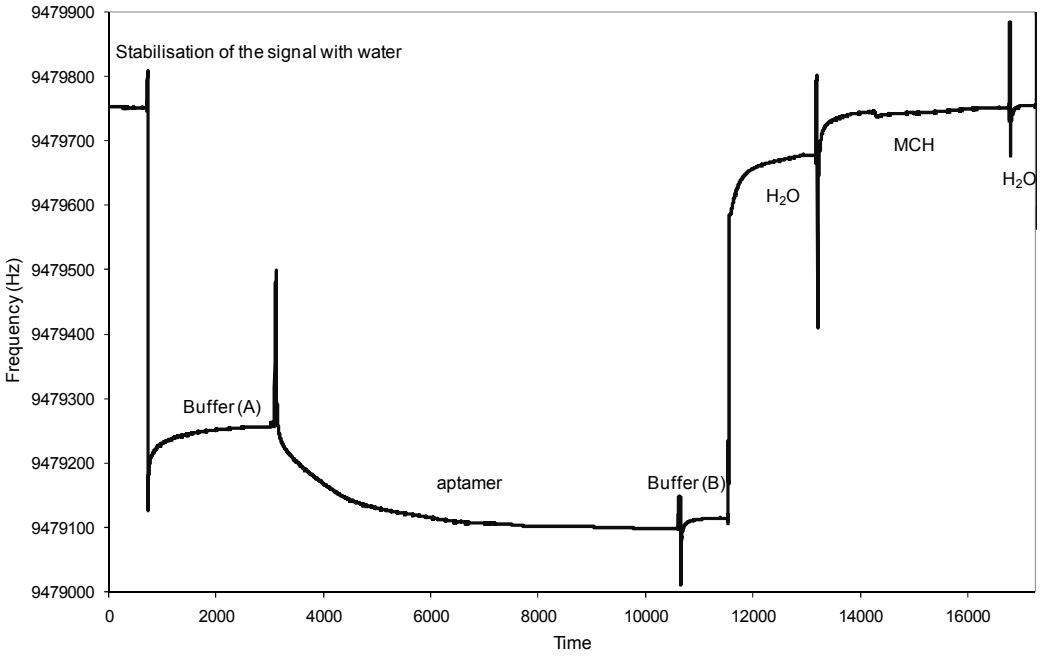


**Figure 22. Typical frequency variation (vs. Time) recorded during the immobilisation of the thiolated aptamer on the crystal surface. The entity of the immobilisation can be evaluated by the difference between the frequency shift of the two steps Buffer (B) – Buffer (A).**

From the shifts resulting from the immobilisation of the two different aptamers, a similar density of immobilised molecules was estimated considering 1 Hz = 2 ng/cm$^2$, according to the Sauerbrey equation (Equation 1.1). This density similarity allowed a correct comparison between the different aptamers when evaluating their sensitivity for the detection of thrombin. For this purpose, the binding between the immobilised aptamer and 100 and 200 nM thrombin was studied with an interaction time of 20 min and the sensor surface was then regenerated with 1 minute treatment with NaCl 2M (Figure 23). The regeneration was considered successful if the frequency value registered with buffer returned to the frequency value corresponding to the same buffer before the analyte binding.

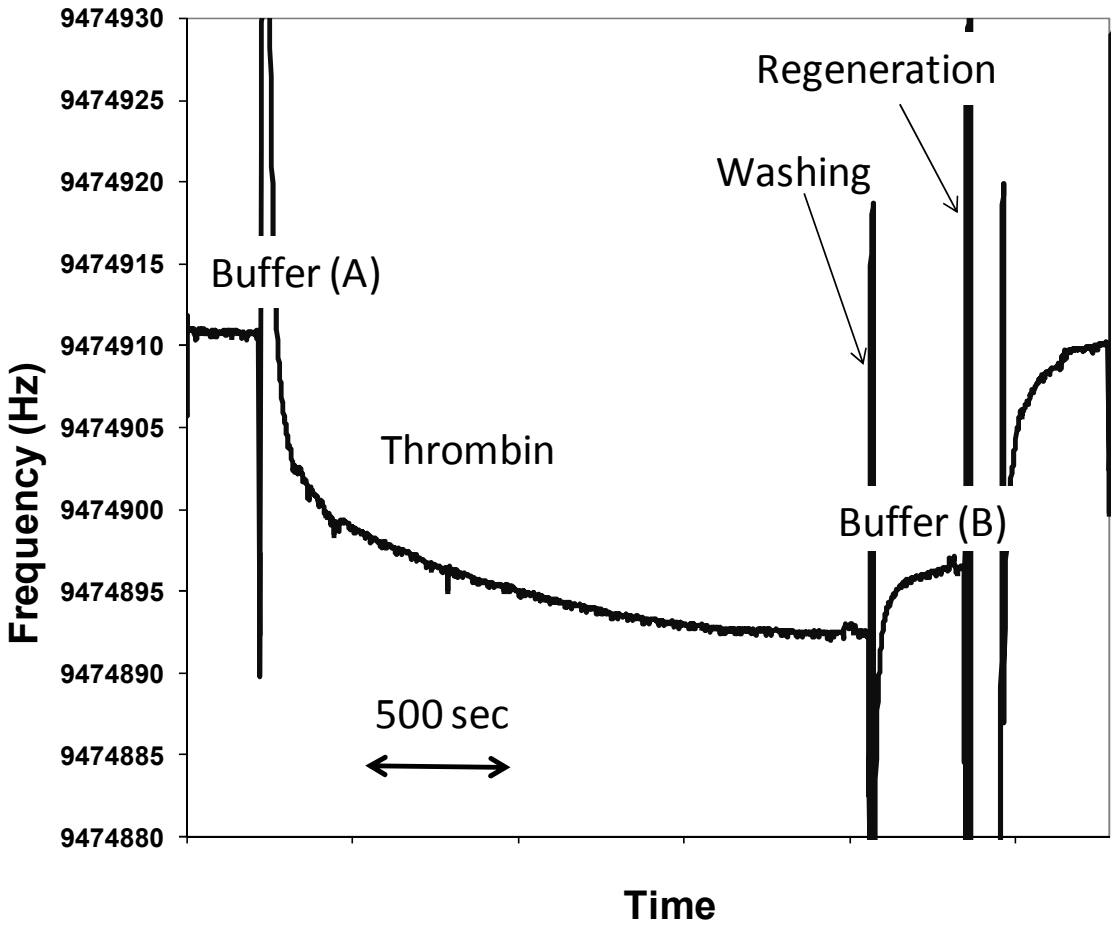


**Figure 23. Typical frequency variations (vs. time) recorded during the binding of thrombin (100 nM) to the immobilised aptamer. The reported analytical datum is the difference in frequency between Buffer (B) and Buffer (A) which represent the baseline.**

The immobilisation results for the biotinylated and the thiolated aptamer are reported in Table 3. The aptamers tested were compared in terms of signal amplitude and reproducibility: the results indicated that the best performances were obtained when immobilising the biotinylated aptamer rather than the thiolated one.

| Immobilised aptamer | Immobilisation shift (Hz) | Density (molecules/cm$^2$) | Thrombin 100 nM (Hz) | Thrombin 200 nM (Hz) |
|---|---|---|---|---|
| Biotinylated aptamer (with tail) | -225 ± 36 | 2.4 x $10^{13}$ | -16 ± 9 | -48 ± 10 |
| Thiolated aptamer | -138 ± 30 | 3.4 x $10^{13}$ | -12 ± 13 | -23 ± 13 |

**Table 3. Comparison between the results obtained with the aptasensor when immobilizing the Biotinylated or the Thiolated Aptamer (aptamer concentration: 1 µM; interaction time with thrombin: 20 min). Sample size of n = 3. Density was calculated from the immobilisation shift by applying Sauerbrey equation [equation 1.1] and it was reported as molecules/cm$^2$ considering the molecular weight of each sequence and the Avogadro number.**

As a second optimisation step, the influence of a spacer in the aptamer-binding behaviour was studied. In a heterogeneous-phase assay, the probe has to be fixed on the sensor surface in order to obtain an ordered and oriented layer, so that the flexibility of the bioreceptor is assured without altering the affinity for the target molecule [25]. For this reason, the influence of a spacer was investigated, by testing the 5' biotinylated 15-mer aptamer in presence or absence of a tail of 20 thymins. Since the 15-mer aptamer sequence contained only thymine and guanine bases, the presence of a spacer consisting only of thymine avoids A:T base pairing, therefore the aptamer secondary structure was probably not affected. The best analytical performances were observed with the aptamer carrying the polyT tail (Figure 24), which showed a good sensitivity and reproducibility (CV for the two concentrations, 13%). The higher sensitivity obtained with this aptamer was probably due to the presence of the spacer, which maintains the aptamer far from the sensor surface, avoiding steric hindrance and allowing the proper conformation for molecular recognition. On the contrary, when the biotinylated aptamer without polyT tail was immobilised, very low sensitivity was found ($\Delta F$ for 200 nM Thrombin < 20 Hz), even if comparable surface density occurred (2.1 x $10^{13}$ molecules/cm$^2$).

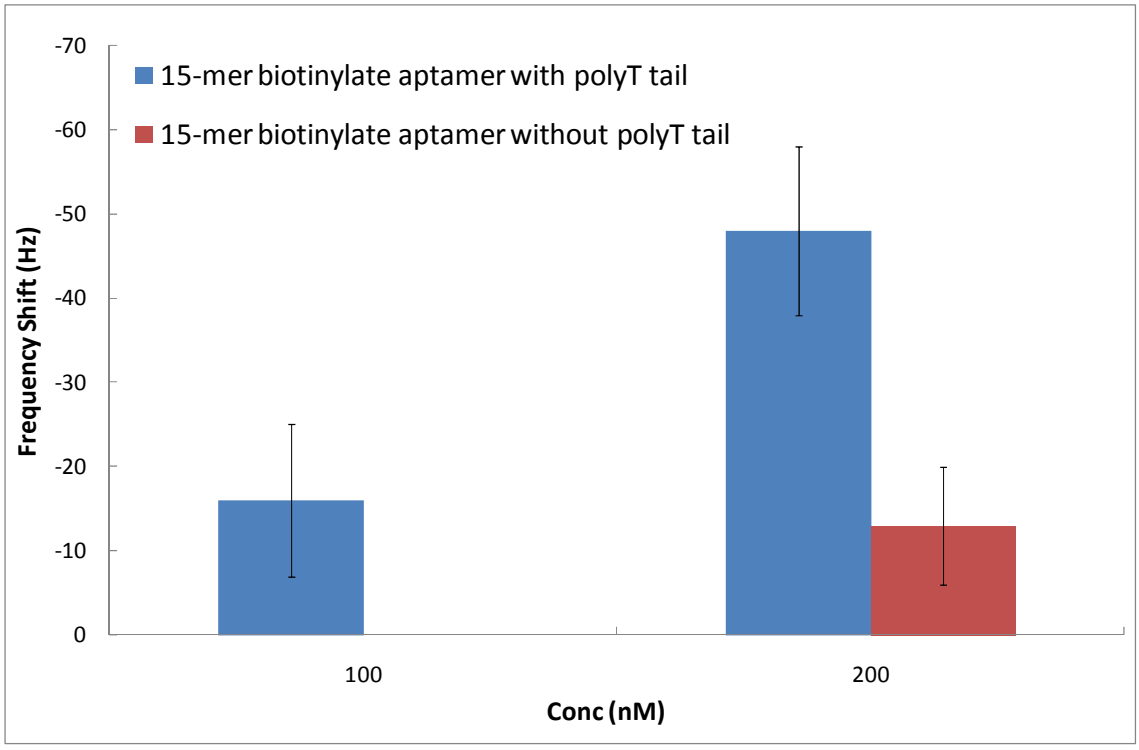


**Figure 24. Comparison between the results obtained with the aptasensor when 100 and 200 nM Thrombin was bound to the immobilised Biotinylated Aptamer with polyT tail or without the polyT tail. Each error bar represents standard deviation of three replicates (n=3). (aptamer concentration: 1 µM; interaction time with thrombin: 20 min).**

Further investigation were then conducted with the biotinylated aptamer carrying the polyT tail, in order to study the different parameters influencing the aptamer immobilisation and consequently its binding to the protein. In particular, the influences of a thermal treatment of the aptamer (heating at 95 °C for 1 min and then cooling in ice for 10 min) and its concentration (varied from 0.1 to 1 µM) were investigated. Moreover, during the optimisation of the binding conditions, the interaction time was increased from 20 to 30 min. The results are reported in Table 4, which shows the improvements in terms of sensitivity, linearity, reproducibility and reusability, by varying these parameters. Three repetitions were carried out for each standard solution in order to evaluate the reproducibility. Thrombin calibration curves obtained in the different experimental conditions are reported in Appendix. Despite the importance of these simple key steps for aptasensor analytical performance, the minimum detectable

amount using the assay, defined as the lowest concentration of analyte giving a measurable signal, remained 50 nM in all cases.

| Immobilised aptamer concentration | Density (molecules/cm$^2$) | Binding Time | Linear Regression | $R^2$ | Cycles |
|---|---|---|---|---|---|
| 1 µM | 2.4 x $10^{13}$ | 20 min | $y$ = -0.22$x$ + 1.94 | 0.933 | 14 |
| 1 µM thermal treatment | 2.5 x $10^{13}$ | 20 min | $y$ = -0.23$x$ + 0.42 | 0.977 | 18 |
| 0.5 µM thermal treatment | 2.0 x $10^{13}$ | 20 min | $y$ = -0.23$x$ + 0.68 | 0.988 | 18 |
| 0.5 µM thermal treatment | | 30 min | $y$ = -0.22$x$ | 0.998 | 22 |

**Table 4. Comparison between the analytical characteristics of the sensor obtained when immobilising the biotinylated aptamer with a polyT tail. Density was calculated from immobilisation shift by applying Sauerbrey equation [equation 1.1] and it was reported as molecules/cm$^2$ considering the molecular weight of the immobilised sequence and the Avogadro number.**

The thermal treatment unfolds the aptamer DNA strand making the 5'-end of the biotin label available for interaction with streptavidin on the crystal surface. Even if the thermal treatment has no effect on the aptamer surface density (2.5 x $10^{13}$ molecules/cm$^2$), the linearity in the thrombin range 0-200 nM ($R^2$ = 0.977) significantly improved, probably because the thermal treatment ensures correct intramolecular folding.

The aptamer concentration was reduced in order to decrease the steric hindrance on the sensor surface and to allow the correct aptamer folding upon thrombin binding. The results indicated that the surface capacity was not affected by the dilution from 1 to 0.5 $\mu$M of the aptamer (2.0 x $10^{13}$ molecules/cm$^2$), but the sensor analytical performances further improved in terms of linearity ($R^2$ = 0.988). On the contrary, a further dilution to 0.1 $\mu$M dramatically reduced the sensor sensitivity (Table 5).

| Immobilised aptamer concentration | Density (molecules/cm$^2$) | 100 nM Thrombin Binding (Hz) |
|---|---|---|
| 0.5 μM thermal treatment | 2.0 x $10^{13}$ | -20 ± 2 |
| 0.1 μM thermal treatment | 6.0 x $10^{12}$ | -13 ± 6 |

**Table 5. Comparison between the analytical characteristics of the sensor obtained when immobilising the biotinylated aptamer with a polyT tail in concentration 0.5 or 0.1 μM after thermal treatment (binding time 20 min, sample size of n = 3). Density was calculated from immobilisation shift by applying Sauerbrey equation [equation 1.1] and it was reported as molecules/cm$^2$ considering the molecular weight of the immobilised sequence and the Avogadro number.**

Finally, the increase in the interaction time from 20 to 30 min, which allowed the binding curve to reach a plateau, resulted in further improved linearity ($R^2$ = 0.998). Using the crystal modified with 0.5 μM aptamer with polyT tail after thermal treatment, a calibration curve for thrombin was constructed in the concentration range 0-200 nM, allowing the binding reaction to proceed for 30 minutes (Figure 25).

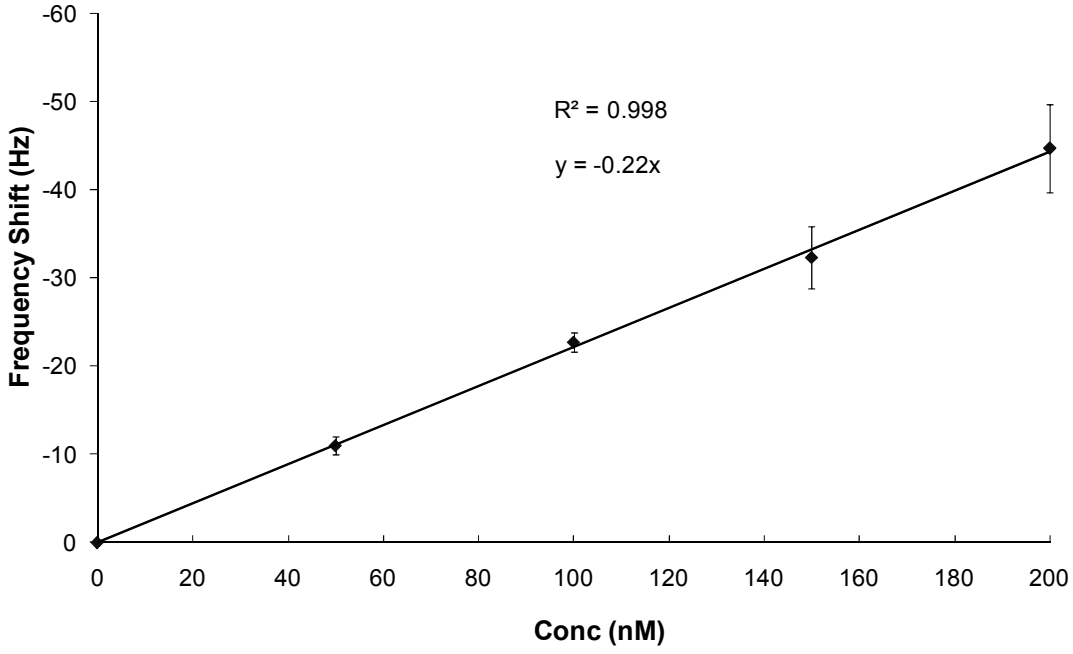


**Figure 25. Calibration curve for thrombin in the range 0 – 200 nM in binding buffer. Each error bar represents standard deviation of three replicates (n=3). (Binding time 30 min; concentration of 15-mer biotinylated aptamer with polyT tail 0.5 μM).**

Negative controls were tested to demonstrate the specificity of the interaction. Human serum albumin is present in plasma and serum at high concentration (~ 50000 mg/l, i.e. 770 μM). The absence of non-specific adsorption was tested using HSA as negative control, at a concentration of 77 $\mu$M in binding buffer, in a 1400-fold excess with respect to thrombin. The interaction did not result in a measurable frequency decrease ($\Delta F < 3$ Hz), demonstrating the high specificity of the sensor (Figure 26).

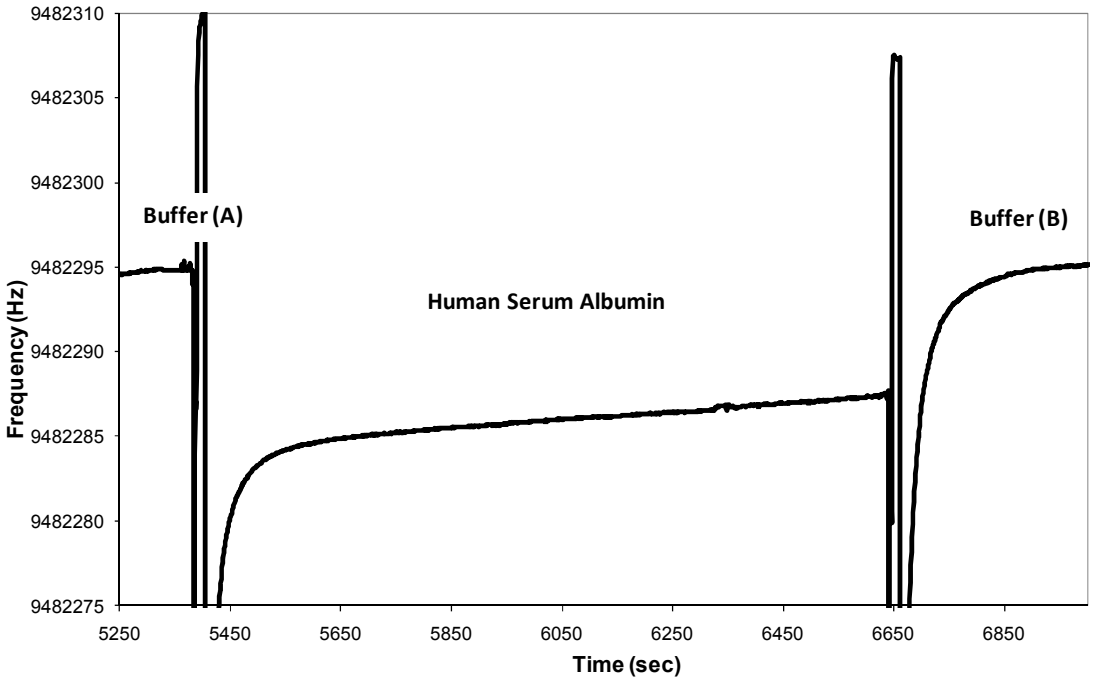


**Figure 26. Typical curve obtained with 77 μM Human Serum Albumin interacting with the immobilised aptamer (Interaction time 30 min). The reported analytical datum will be the difference in frequency between Buffer (B) and Buffer (A) which represents the baseline.**

### 3.1.3. Detection of Thrombin in complex matrix

The ability of the aptasensor to detect the analyte in complex matrices was tested. Thrombin is the last enzyme protease involved in the coagulation cascade and it converts fibrinogen to insoluble fibrin that forms the fibrin gel [57]. Since the detection of thrombin in plasma or blood is clinically relevant, an aptamer-based sensor as an alternative diagnostic tool for thrombin analysis or blood coagulation investigation could be of considerable interest in the clinical diagnostics. Standard solutions of thrombin were added to serum and plasma to test the performance of the aptasensor in these complex matrices.

Since serum does not contain coagulation factors, the addition of thrombin does not affect the samples. Thrombin was detected in serum diluted 1:100 spiked with thrombin in a concentration range 0-200 nM, with a blank value of -32 ± 8 Hz. The recorded signals increased with the concentration of added thrombin, demonstrating that the aptasensor was able to operate in this complex matrix (Figure 27).

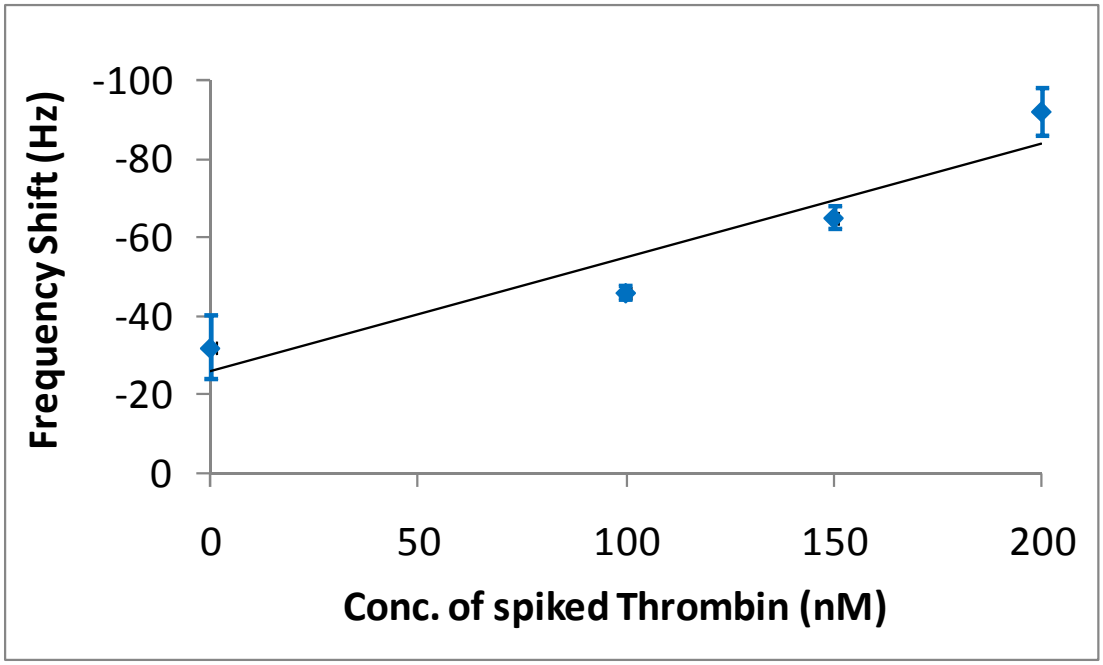


**Figure 27. Frequency shifts obtained with different concentrations of thrombin (0-200 nM) interacting with the immobilised aptamer. Thrombin was added to serum (1:100 in binding buffer). Each error bar represents standard deviation of three replicates (n=3). Interaction time 30 min.**

Since serum does not contain the proteins involved in coagulation, further experiments were carried out with plasma, which is the matrix where normally thrombin is detected. The addition of thrombin to plasma, which contains all the proteins involved in the coagulation cascade including fibrinogen, leads to the formation of fibrin and to rapid sample clotting. To avoid this phenomenon, fibrinogen was selectively precipitated from plasma before the addition of thrombin in the preparation of spiked samples, using ammonium sulphate as precipitant. A loss of protein content (~ 40%) was detected after precipitation of fibrinogen by spectrophotometric measurements at 280 nm. Figure 28 shows the signals obtained in spiked plasma without fibrinogen (final dilution 1:100). Reproducibility was good (CV% = 13%), and the response was linear in the tested concentration range, 0-200 nM ($R^2$ = 0.990). In this range, no saturation of the surface was observed. The matrix effect with a blank signal of -21 Hz is present, but despite the high complexity of the matrix, the increase in thrombin concentration could be detected.

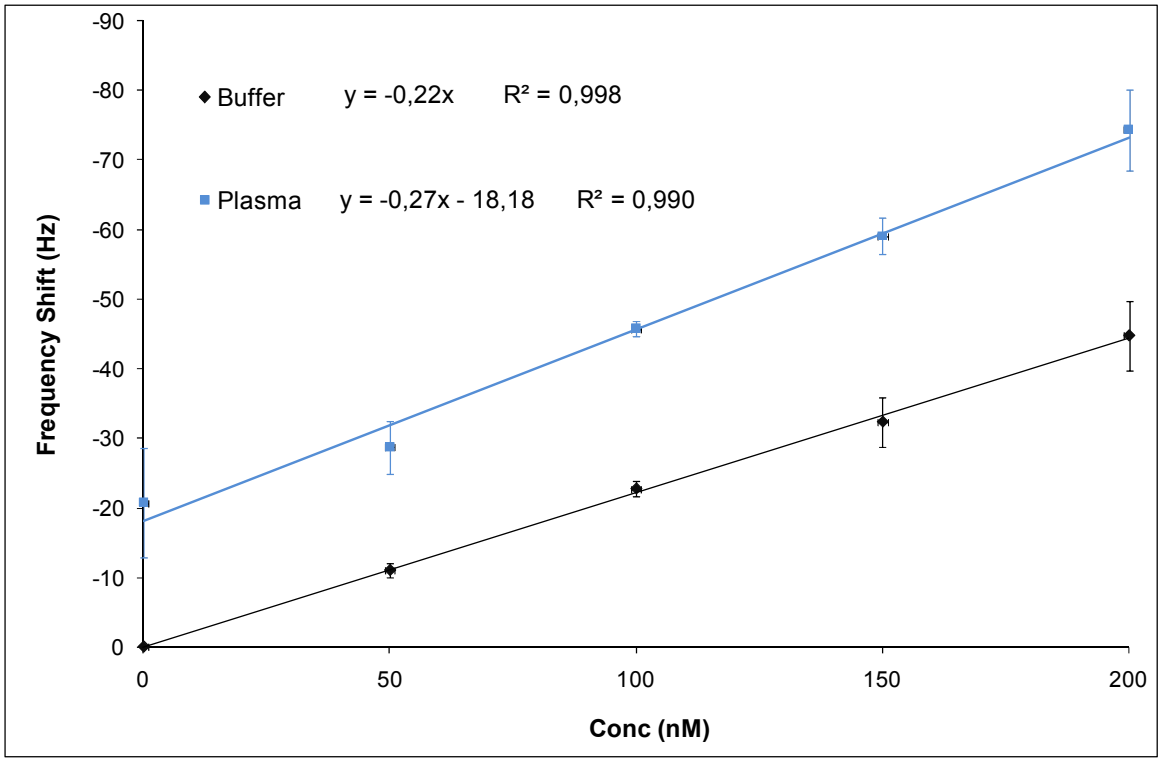


**Figure 28. Calibration plot obtained with different concentrations of thrombin in buffer and plasma. Each error bar represents standard deviation of three replicates (n=3).**

## 3.2. Development of an optical aptasensor to detect C-Reactive Protein

The development of an RNA aptamer-based optical biosensor was realized by immobilising the 44-mer aptamer specific for CRP on the gold surface of Biacore CM5 chips and monitoring the interaction with the label-free target analyte. Also in this case study, the optimal conditions for the binding in the heterogeneous phase were to be found by optimisation of some simple but critical parameters, in order to reach acceptable analytical performances of the aptasensor.

### 3.2.1. Analytical performance of C-Reactive Protein detection with the optical device

In aptasensor development, good analytical performance can be ensured by selecting a proper immobilisation protocol. Studies with thrombin reported above had shown that improved sensor performance could be obtained by the addition of a spacer to the aptamer sequence, in order to facilitate a correct aptamer-protein binding. For this reason, also in the case of CRP a polyT tail consisting of 20 thymins was linked to the 5' end of the aptamer, together with a biotin group to ensure that it was anchored correctly to the streptavidin-modified surface. Because of the presence of the four kinds of nucleotides in the CRP aptamer sequence, an oligonucleotides tail could cause the formation of intra-molecular folding in the aptamer structure. To avoid this problem, a non-oligonucleotide tail could be necessary. For this reason a TEG tail at the 5' end of the aptamer was also considered, consisting of a 16-atom mixed polarity spacer arm, which gives flexibility and optimal capture by streptavidin. In both cases, before immobilization, the aptamer solution was subjected to a thermal treatment (95 °C for 1 min, 0 °C for 10 min), which unfolded the aptamer, making the biotin label at the 5′ end available for interaction with streptavidin on the surface. Finally, the surface was

saturated with biotin. In Figure 29, the immobilisation of the aptamer with the BioTEG tail on the dextran-streptavidin-modified chip is reported versus the SPR signal.

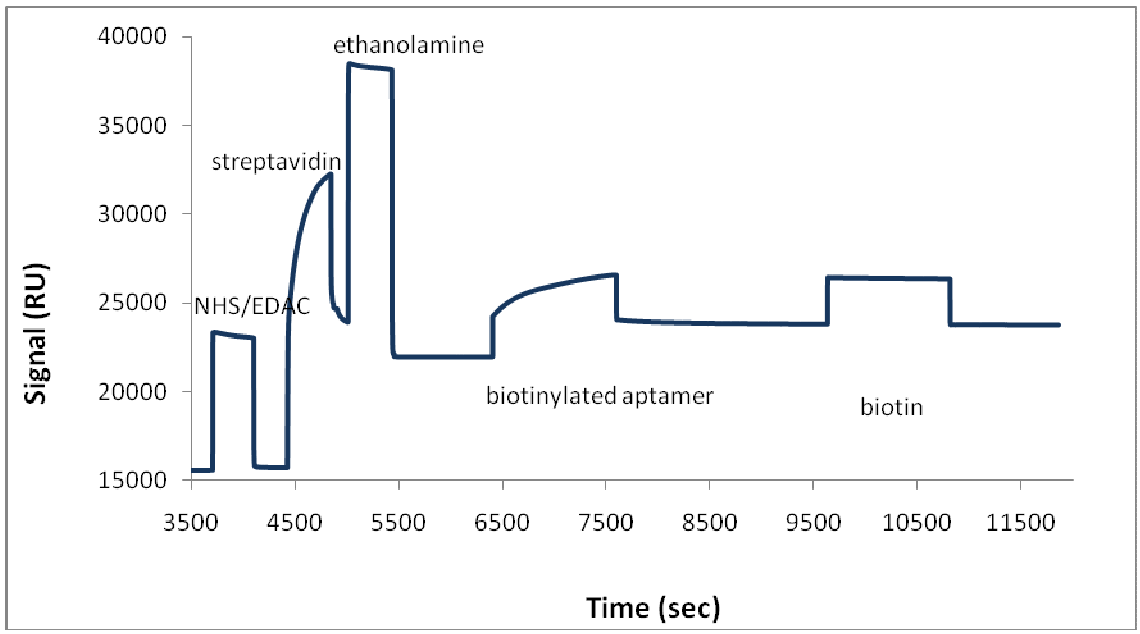


**Figure 29. Immobilisation of the CRP aptamer with the BioTEG tail on CM5 chip modified with streptavidin. After the activation with NHS/EDAC, streptavidin (200 ppm) was covalently bound to the carboxylic groups present on the dextran and finally saturated with ethanolamine. The RNA aptamer (1 µM in immobilisation buffer), thermally treated, was anchored to the surface via biotin-streptavidin binding, with a resulting shift in the resonance signal of 1988 RU. Finally biotin (500 ppm) was added to saturate the free sites of streptavidin.**

### 3.2.1.1. Optimisation of the binding conditions

When developing an aptasensor, the first step is to optimise the buffer to be employed in the assay. After the immobilisation of the aptamer with the polyT tail, the interaction between the immobilised receptor and 1 ppm CRP was monitored with an association time of 15 min followed by washing with running buffer. The experiments were conducted at 25 °C. The analyte CRP was dissolved in several buffers differing in salts

composition and pH. The effect of the pH in the range 6-7.5 was studied. During the experiments the same buffer was used as a solvent to dissolve the analyte (binding buffer) and as running buffer, flowing on the chip surface before and after CRP injection. The following buffers were tested: MES 10 mM pH 6.0, HEPES 10 mM pH 6.0, Tris/HCl 10 mM pH 6.0, MES 10 mM pH 6.5, HEPES 10 mM pH 6.5, Tris/HCl 10 mM pH 6.5, HEPES 10 mM pH 7.0, Tris/HCl 10 mM pH 7.0, HEPES 10 mM pH 7.5, Tris/HCl 10 mM pH 7.5. Tris/HCl buffer was tested since a similar buffer was used for the aptamer selection in the SELEX process [88]. The results are shown in Figure 30, where the frequency shifts recorded for the interaction of the immobilized aptamer with 1 ppm CRP as well as with 100 ppm HSA are reported.

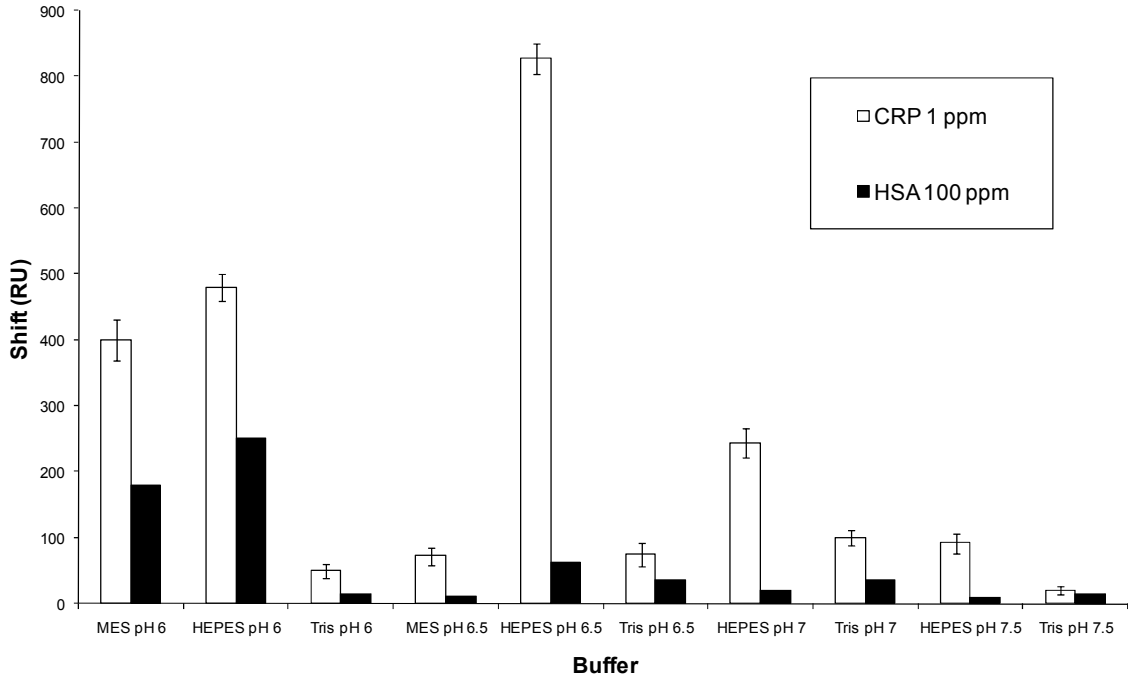


**Figure 30. Binding buffer optimisation using 1 ppm CRP and 100 fold-excess concentration of human serum albumin (100 ppm HSA) as negative control. The same buffer used in the binding assay was also employed as running buffer. Each error bar represents standard deviation of three replicates (n=3).**

HSA was chosen as negative control since it is the most abundant protein in serum. HEPES 10 mM at pH 6.5 was chosen as binding and running buffer, since in this buffer

the best ratio between the specific signal (in presence of CRP) and the unspecific signal (in presence of HSA) was found. For the following experiments, the optimised buffer (Hepes 10 mM pH 6.5) was added with 0.005% Tween 20 in order to remove the slight baseline drift, as suggested in Biacore X™ manual.

After each binding cycle, the surface was regenerated by 1 min treatment with HCl (1, 10 or 25 mM depending upon the entity of the binding shift to be regenerated) or with 1 mM NaOH.

### 3.2.1.2. Effect of calcium ions

It is reported that in the absence of calcium ions CRP in neutral or mildly acid environment self-dissociates, slowly but persistently [95]. Therefore the pentameric CRP (pCRP) is stored in buffer containing $CaCl_2$ to prevent spontaneous formation of monomeric CRP (mCRP) [94]. In fact, the purified CRP purchased for this study was stored in buffer containing 2 mM $CaCl_2$. Despite the important role that calcium ions play in the CRP pentameric structure maintenance, it should be considered that the selection process for generating the CRP aptamer was conducted in absence of calcium ions [88]. For this reason the influence of calcium ions on the binding was also investigated, in the case of both polyT and TEG modified aptamers.

The binding curve for 0.05 ppm CRP prepared in the optimised buffer (Hepes 10 mM pH 6.5, 0.005% Tween 20), i.e. in the absence of calcium ions, is reported in Figure 31. The aptamer-CRP interaction time was set to 15 minutes, but it was observed that as soon as the injection ended, CRP slowly dissociated. For this reason the binding shift was recorded 15 min from the end of the injection.

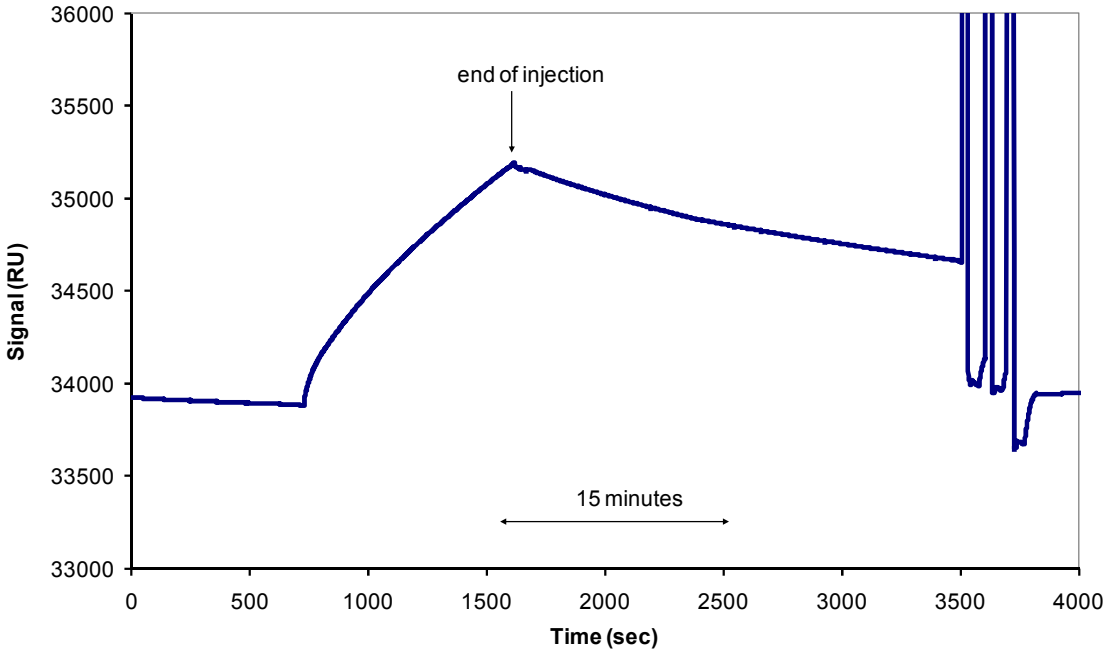


**Figure 31. CRP binding curve in the absence of calcium ions in the binding buffer. Immobilised aptamer: CRP aptamer with polyT tail. CRP concentration: 0.5 ppm. Binding time: 15 min. Binding and running buffer: Hepes 10 mM, pH 6.5, 0.005% Tween 20. Flowrate 2 µl/min, T 25 °C. Binding shift recorded 15 min after the end of injection: 784 RU. Regeneration: HCl 1 mM (3 injections).**

*a) Optimisation of the aptamer concentration*

The aptamer concentration is one of the critical parameters that influence the analytical performances of the assay; for this reason it was decreased from 1 µM to 0.1 µM in order to reduce the steric hindrance on the surface.

The analytical performance of the CRP aptamer with the TEG tail were studied in the absence of calcium ions using as running and binding buffer the one resulted from the optimisation step (Hepes 10 mM pH 6.5) and added with 0.005% Tween 20 for the baseline stabilisation. Calibration curves were obtained using the CRP aptamer with the TEG tail immobilised at two different concentrations (1 and 0.1 µM) and they are compared in Figure 32. The reported measurements (in RU) were referred to three repetitions (n=3) of each protein concentration and were registered 15 min after the end

of injection because of the dissociation. A sensitivity increase (10 times) was found when 0.1 μM aptamer was used for immobilisation, probably as a consequence of the decreased steric hindrance on the surface. The analytical characteristics of the assay for the two different concentrations of the aptamer with the TEG tail are compared in Table 6.

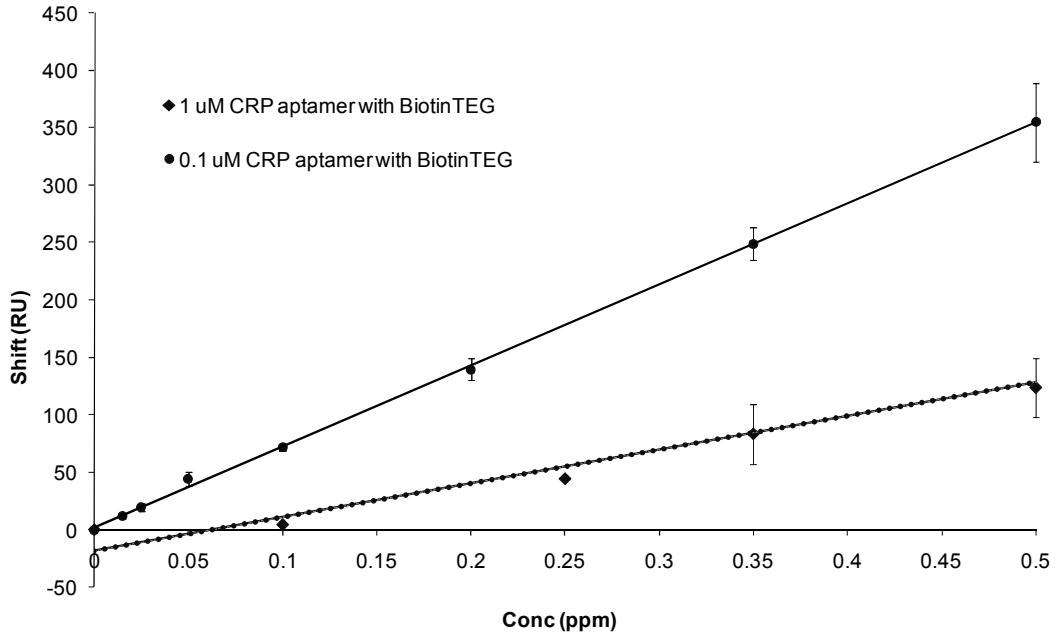


**Figure 32. Calibration curves obtained by immobilising CRP aptamer with the TEG tail at two different concentrations (1 μM and 0.1 μM) in Hepes 10 mM, pH 6.5, 0.005% Tween 20 on CM5 Biacore chip. Each error bar represents standard deviation of three replicates (n=3). Flowrate 2 μl/min, 25 °C. Binding shifts were recorded 15 min after the end of injection.**

| Aptamer concentration (μM) | 1 | 0.1 |
|---|---|---|
| Linear range (ppm) | 0 – 1 | 0 – 0.5 |
| Experimental DL (ppm) | 0.1 | 0.015 |
| $R^2$ | 0.990 | 0.999 |
| Linear Regression | $y = 293.0x - 17.9$ | $y = 703.8x + 2.3$ |

**Table 6. Analytical characteristics of the assay using the aptamer with the TEG tail immobilised on the chip at two different concentrations (1 and 0.1 μM). Binding Buffer Hepes 10 mM, pH 6.5, 0.005% Tween 20. Interaction time 15 min.**

*b) Comparison between the two different tails*

The surfaces carrying the aptamers modified with the two different tails were tested for their ability to bind the target analyte in the absence of calcium ions. The most suitable tail was identified by investigating the effect of the two different spacers on the aptasensor performance, following the same identical procedure for the immobilisation of the two aptamers and using the optimised running and binding buffer (Hepes 10 mM pH 6.5, 0.005% Tween 20). Since the best analytical results in the case of the CRP aptamer with the TEG tail were obtained by using a concentration of 0.1 μM for the immobilisation, the same concentration was used also for the immobilisation of the CRP aptamer with the polyT tail. A comparison of the analytical characteristics of the assays is reported in Table 7. From the comparison, a slightly superior analytical behaviour for the TEG tail aptamer was found in terms of linearity ($R^2$) and the minimum detectable amount of the analyte, defined as the lowest concentration giving a measurable signal.

| Aptamer modification | TEG | PolyT |
|---|---|---|
| Aptamer concentration (μM) | 0.1 | 0.1 |
| Linear Range (ppm) | 0 – 0.5 | 0 – 0.5 |
| Experimental DL (ppm) | 0.015 | 0.05 |
| $R^2$ | 0.999 | 0.997 |
| Binding Buffer | Hepes 10 mM pH 6.5, 0.005% Tween 20 | |

**Table 7. Analytical characteristics of the assay using the 0.1 μM aptamer with TEG tail or with polyT tail immobilised on the chip. Data recorded in the absence of calcium ions.**

*c) Calibration in presence of calcium ions*

The influence of the calcium ions on the analytical performances of the assay was studied. Physiological calcium concentration is 2 mM as total calcium and 1.3 mM as $Ca^{2+}$ free ion. To mimic the physiological conditions, 2 mM $Ca^{2+}$ was added to the

binding and running buffer. As can be observed from the sensorgram recorded during the binding of 0.025 ppm CRP to the immobilised TEG aptamer (Figure 33), the complex aptamer–CRP curve did not dissociate at the end of the injection, indicating a higher stability of the complex in the presence of $Ca^{2+}$.

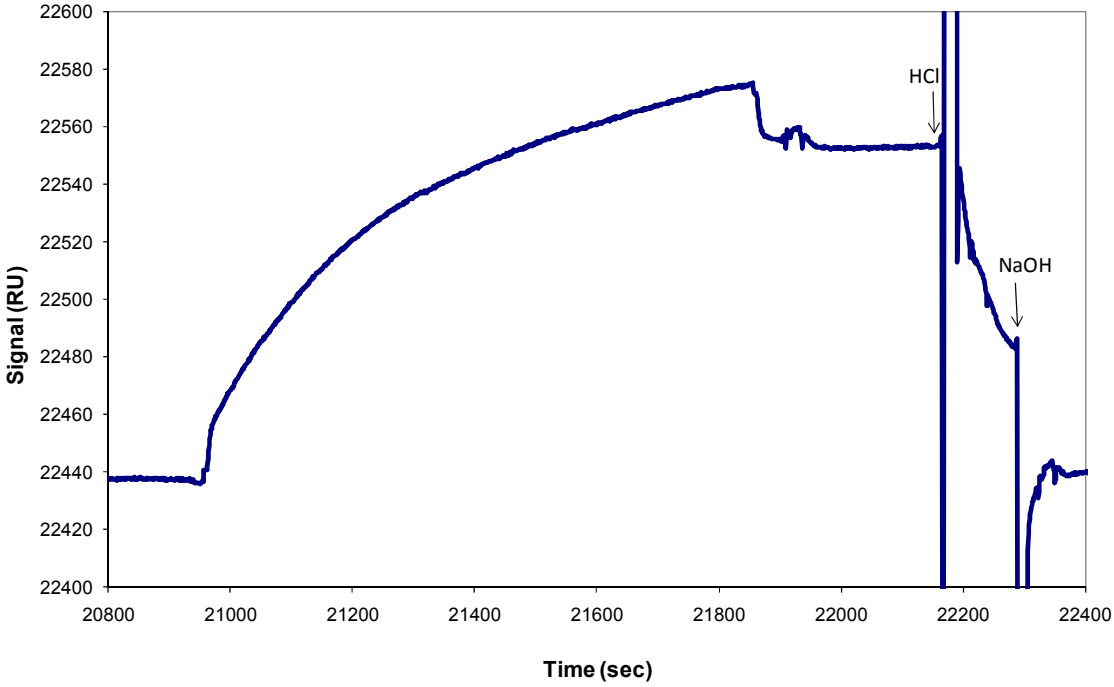


**Figure 33. CRP binding curve in the presence of calcium ions. CRP aptamer with the TEG tail, CRP concentration 0.025 ppm, binding and running buffer: Hepes 10 mM, pH 6.5, 0.005 %, Tween 20, $CaCl_2$ 2 mM. Binding shift at the end of injection: 115 RU. Regeneration injections in order to return to the baseline: 1 mM HCl, 1 mM NaOH.**

As a consequence of the CRP-aptamer complex stability, higher RU signals were recorded after 15 min of interaction. As can be observed from the calibration curves reported in Figure 34, an increase of sensitivity was registered using chips modified with either the TEG aptamer or the polyT aptamer: in both cases, the minimum detectable amount of the analyte was reduced to 0.005 ppm. Nevertheless, the sensor carrying the aptamer with the TEG tail showed a higher sensitivity, expressed as the slope of the regression line, while the reproducibility obtained using the aptamer modified by both tails was similar (Table 8). The binding constant, using the

BIAevaluation 3.1 program, was estimated to be 0.5 nM (expressed as $K_D$). This value, calculated with the TEG modified aptamer, was lower than the one reported in literature (125 nM), calculated in solution, but in absence of calcium [88].

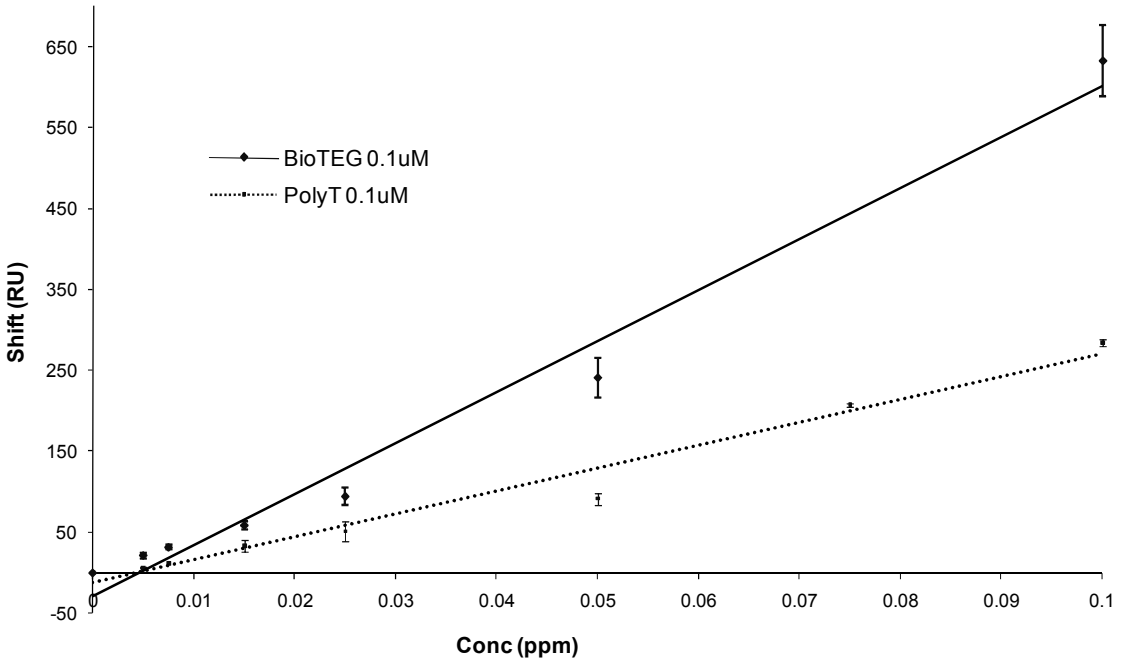


**Figure 34. Calibration curves obtained by immobilizing CRP aptamer 0.1 µM with the polyT tail or the TEG tail . Each error bar represents standard deviation of three replicates (n=3). Flowrate 2 µl/min, 25°C. Binding shifts were recorded at the end of injection.**

| Aptamer modification | PolyT | TEG |
|---|---|---|
| Binding Buffer | Hepes 10 mM, pH 6.5, 0.005% Tween 20, $CaCl_2$ 2mM | |
| Linear Range (ppm) | 0 – 0.1 | 0 – 0.1 |
| Experimental DL (ppm) | 0.005 | 0.005 |
| $R^2$ | 0.975 | 0.982 |
| Linear Regression | y = 2827.3x -12.3 | y = 6297.9 x -27.7 |
| Cycles | 50 | 50 |

**Table 8. Analytical characteristics of the assay using chips modified with the polyT-tail or the TEG-tail aptamer (concentration 0.1 µM), in presence of calcium ions in the binding buffer.**

Using the TEG aptamer, the sensor was also tested by decreasing the calcium concentration down to 1 mM. Similar results as to those obtained for 2 mM $Ca^{2+}$ were found. In particular, when a low (0.025 ppm) CRP concentration was tested, 358 RU and 327 RU were recorded, respectively in presence of 1 mM and 2 mM $Ca^{2+}$. Similar findings were obtained with 0.1 ppm CRP: 78 RU and 95 RU were found, respectively for 1 mM and 2mM $Ca^{2+}$.

*d) Specificity*

The specificity of the aptasensor was tested using 500 ppm HSA under the optimised binding conditions (binding buffer Hepes 10 mM, pH 6.5, 2 mM $CaCl_2$, 0.005% Tween 20). When the aptamer with TEG tail was used as immobilised probe, the recorded response was 10% of the CRP signal at the same dilution factor (10 ± 4 RU vs 58 ± 5 RU). Furthermore, the TEG tail assured a better specificity towards HSA than the PolyT tail (Figure 35).

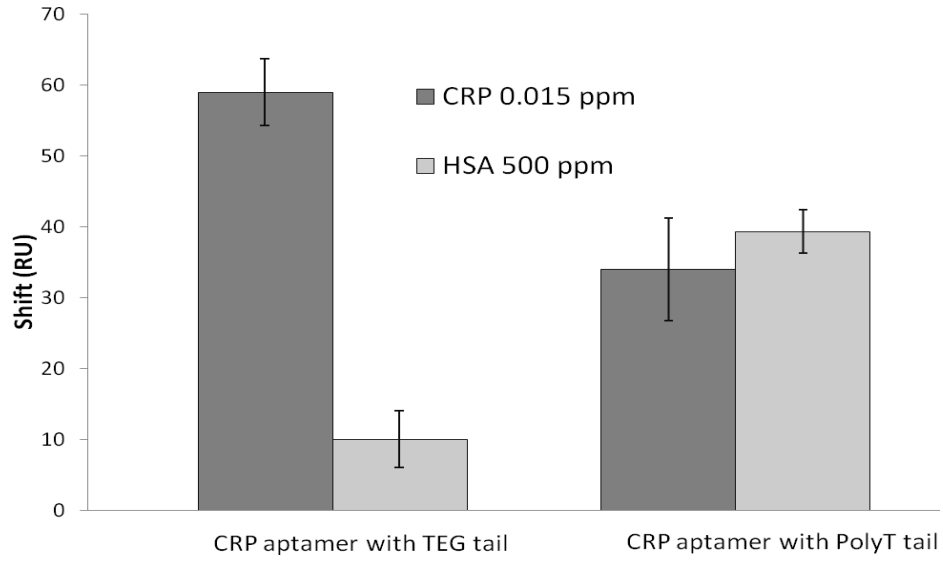


**Figure 35. Specificity test with negative control: comparison between the two spacers. HSA and CRP diluted 1:100 respect to the physiological conditions. Each error bar represents standard deviation of three replicates (n=3). Binding and running buffer: Hepes 10 mM, pH 6.5, 0.005 %, Tween 20, $CaCl_2$ 2 mM. Binding shifts recorded at the end of injection.**

### 3.2.2. Detection of C-Reactive Protein in complex matrix

The possibility to detect C-Reactive Protein directly in a complex matrix such as serum samples was evaluated. For this purpose, serum samples were diluted 1:100 and filtered (0.2 μm filter) in order to remove the particulate matter and avoid clogging of the Biacore microfluidic system. The SPR sensor, modified by immobilisation of the CRP aptamer with the TEG tail, was directly exposed to the serum solutions and the response recorded. Unfortunately, a very high RU signal (>17000 RU) was measured. Furthermore, after the exposure to diluted serum the sensor surface could not be completely regenerated and following further injection of CRP standard solution, the aptamer was unable to bind the analyte anymore.

Simulated serum solutions were produced in RNase-free environment in order to estimate the matrix effect. Since one important protein class in serum is represented by immunoglobulins (IgG), the aptasensor was exposed to an IgG solution, prepared in RNase-free binding buffer. The concentration of IgG injected into the chip was 120 ppm, because it is the concentration present in a 1:100 diluted serum. The relative results indicated a very important RU shift (>17000 RU) induced by IgG, demonstrating a clear interfering effect in the assay. However, the surface was completely regenerated and the ability of the aptamer to bind its target was preserved. From this preliminary study, it was evident that a sample clean up had to be conducted to minimise such matrix effects.

#### 3.2.2.1. Pre-treatment of simulated serum samples with magnetic beads

An additional sample pre-treatment was applied, in order to remove IgG from simulated serum solutions by using magnetic beads coupled with protein G, able to bind the Fc portion of IgG. Different standard solutions containing CRP or HSA or IgG or a mixture of them with and without addition of CRP, were tested at a concentration corresponding

to a 1:100 serum dilution. The recovery of the proteins after such sample pre-treatment was evaluated by spectrophotometric measurements at λ=280 nm. The results are shown in Table 9. The recovery data and the RU signals indicated that CRP and HSA were not retained by the beads; whereas IgG was partially removed from the sample and a recovery of 16% was observed, resulting in a significant RU shift. In the case of the mixtures containing HSA and IgG or HSA, IgG and CRP, the recorded RU signals were always lower than those related to each single component. This could be due to an interaction effect between IgG and the other proteins.

| Solution | Recovery of proteins after treatment | Shift (RU) |
|---|---|---|
| CRP 0.01 ppm | 99 % | 38 |
| IgG 120 ppm | 16 % | 158 |
| HSA 500 ppm | 100 % | 22 |
| HSA 500 ppm + IgG 120 ppm | 58 % | 70 |
| HSA 500 ppm + IgG 120 ppm + CRP 0.01 ppm | 51 % | 83 |

**Table 9. Summary of the standard solutions that were pre-treated by magnetic beads coupled to protein G and then tested with the aptasensor. The proteins recovery after this pre-treatment were estimated by spectrophotometric measurements.**

### 3.2.2.2. Pretreatment of human serum with purification columns

An affinity column was used to treat human serum in order to remove IgG and HSA from the matrix and consequently minimise the non-specific signal. The treated serum eluted from the column resulted diluted 1:27 and it was further diluted 1:3 with binding buffer. The resulting solution was then added with a commercial non-specific binding reducer (NSB Reducer), to further reduce the matrix effect. As a first step, the concentration of NSB reducer to be added and the incubation time was optimised. For

this purpose, serum treated using an affinity column and further diluted 1:3 was added with different concentrations of NSB reducer (1000, 2000 and 4000 ppm), using various incubation times prior of the injection (0, 5, 10, 20 min). As it can be observed in Figure 36, the addition of 1000 ppm NSB reducer to pre-treated serum, with 5 min incubation time, caused a significant decrease in the non-specific signal, from thousands of RU to 513 RU.

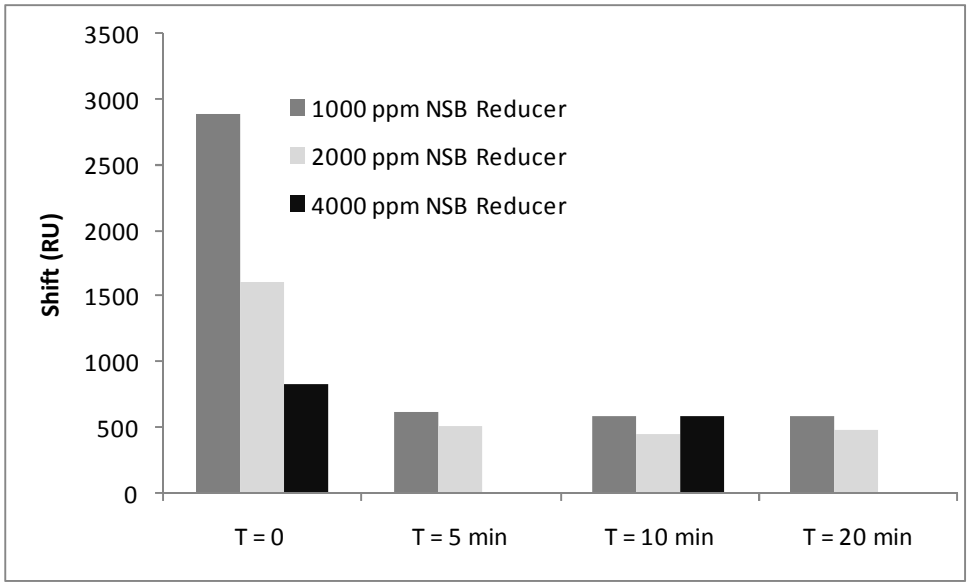


**Figure 36. Decrease of the non-specific signal of pre-treated serum by incubation with NSB Reducer. Sample size of n = 1.**

However, when a standard solution of CRP was spiked to the treated solution (serum eluted from the affinity column, further diluted 1:3 and added with 1000 ppm NSB Reducer, incubation time 5 min), a significant signal variation was not observed, even at high CRP concentrations. In fact, after the addition of 0.2 or 0.3 ppm of CRP signals corresponding to 531 and 549 RU, respectively, were recorded, in comparison with 513 RU caused by non-specific signal.

### 3.2.2.3. Comparison between modified and non-modified aptamer for C-Reactive Protein

The RNA aptamer is sensitive to degradation by RNase, which are present in any biological sample. Consequently the possibility that the CRP aptamer was destroyed when dealing with serum solutions exists. For this reason the CRP aptamer was purchased modified with 2' F-pyrimidines to increase its stability, with the aim of directly detecting CRP in serum samples.

In order to understand if the modification altered the affinity of the aptamer towards CRP, the analytical characteristics of the modified aptamer were compared with those obtained with the non-modified aptamer under the same experimental conditions. For this purpose, 0.1 μM of modified CRP aptamer with the BioTEG tail was immobilised on a SPR chip and standard solutions of the analyte at different concentrations were made up in binding buffer containing calcium ions (Hepes 10 mM, pH 6.5, 2 mM $CaCl_2$, 0.005% Tween 20) prepared in MilliQ water not treated with DEPC. Surface regeneration after CRP binding was realised with 1 minute treatment of 1 mM NaOH. The CRP calibration plot obtained with the modified aptamer is reported in Figure 37. The aptasensor realised with the modified aptamer showed a good linearity in the range 0 – 0.2 ppm ($R^2$ = 0.997) and good reproducibility (CV av % = 16 %). The aptasensor specificity was also tested using 5000 ppm HSA as negative control (1:10 dilution with respect to physiological concentration) and a shift of 557 ± 29 RU was recorded.

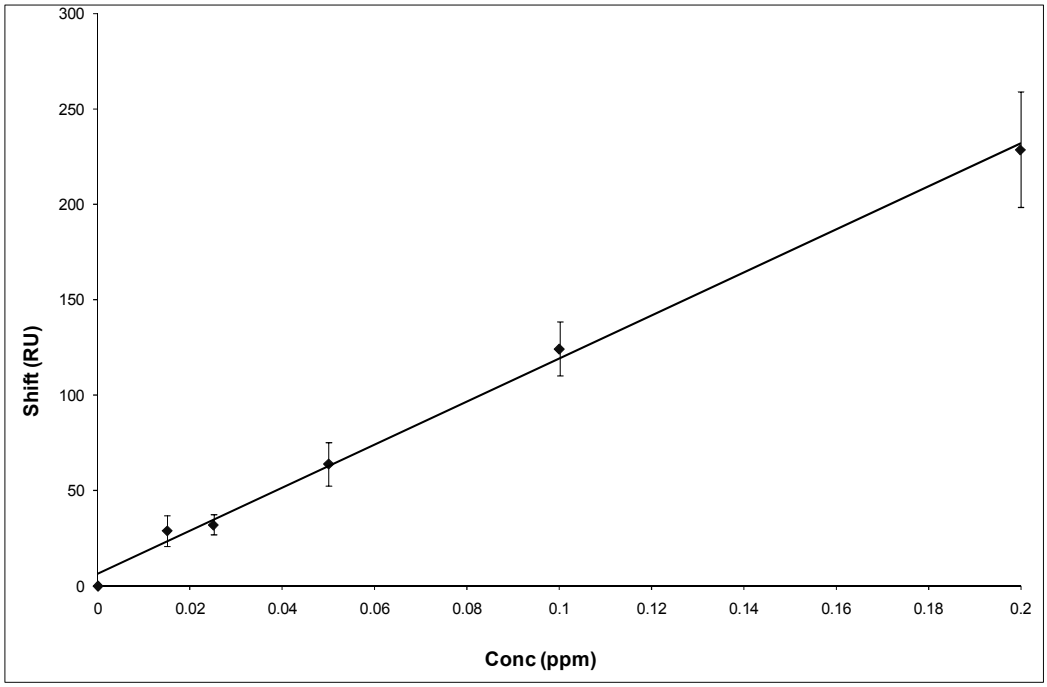


**Figure 37. Calibration plot for the CRP aptamer modified with 2'-F-pyrimidines. Each error bar represents standard deviation of three replicates (n=3). Interaction time 15 min. Flowrate 2 µl/min, 25 °C. Binding shifts recorded at the end of injection.**

The difference between the modified and non-modified RNA aptamer is compared in Table 10. The sensitivity (expressed by the slope of the curve) and the minimum detectable amount of the analyte for the modified aptamer were worse than for the un-modified one, but sufficient to detect normal levels of CRP in diluted serum.

| | Biotin-TEG CRP aptamer | |
|---|---|---|
| | modified | Non-modified |
| Binding Buffer | Hepes 10 mM, pH 6.5, 0.005% Tween 20, $CaCl_2$ 2mM | |
| Linear Range (ppm) | 0 – 0.2 | 0 – 0.1 |
| Experimental DL (ppm) | 0.015 | 0.005 |
| $R^2$ | 0.997 | 0.982 |
| Linear Regression | $y = 1126.0\,x + 6.5$ | $y = 6297.9\,x - 27.7$ |

**Table 10. Comparison of analytical parameters of the aptasensor realised by immobilising RNA aptamer non-modified and modified with 2'-F-pyrimidines.**

The immobilised aptamer modified with 2'-F-pyrimidines was exposed to human serum diluted 1:100 and again a very high non-specific signal corresponding to thousands of RU was recorded. However, the surface was completely regenerated and the capacity of the aptamer to bind CRP was not affected.

### 3.2.2.4. Sandwich assay

The possibility to realise a sandwich assay using the CRP aptamer as secondary ligand was evaluated. For this purpose, 2'-F-pyrimidine modified CRP aptamer immobilised onto CM5 Biacore chip was exposed to a standard solution of 0.2 ppm CRP and then to a standard solution of 0.1 μM CRP aptamer, prepared in binding buffer (interaction time 15 minutes). As a result, a shift of 284 ± 5 RU was recorded for 0.2 ppm CRP and the SPR signal was further enhanced by 48 ± 2 RU by the secondary aptamer (Figure 38). This result suggests that CRP aptamer was able to bind the aptamer-protein complex formed at the chip surface. Since the shift of 1000 RU corresponds to 0.8 ng/mm$^2$ (Biacore User Manual), the density of bound molecules was calculated from the binding shifts relative to CRP and to the secondary aptamer, taking into account the molecular weight of each molecule and the Avogadro number. As a result, 1.2 x $10^{11}$ molecules/cm$^2$ of CRP were bound to the primary aptamer and 1.7 x $10^{11}$ molecules/cm$^2$ of secondary aptamer were bound to CRP, suggesting a 1:1 stechiometry.

This result could be exploited to develop an indirect sandwich assay for CRP detection in real samples, in order to reduce the matrix effect observed in the direct assay.

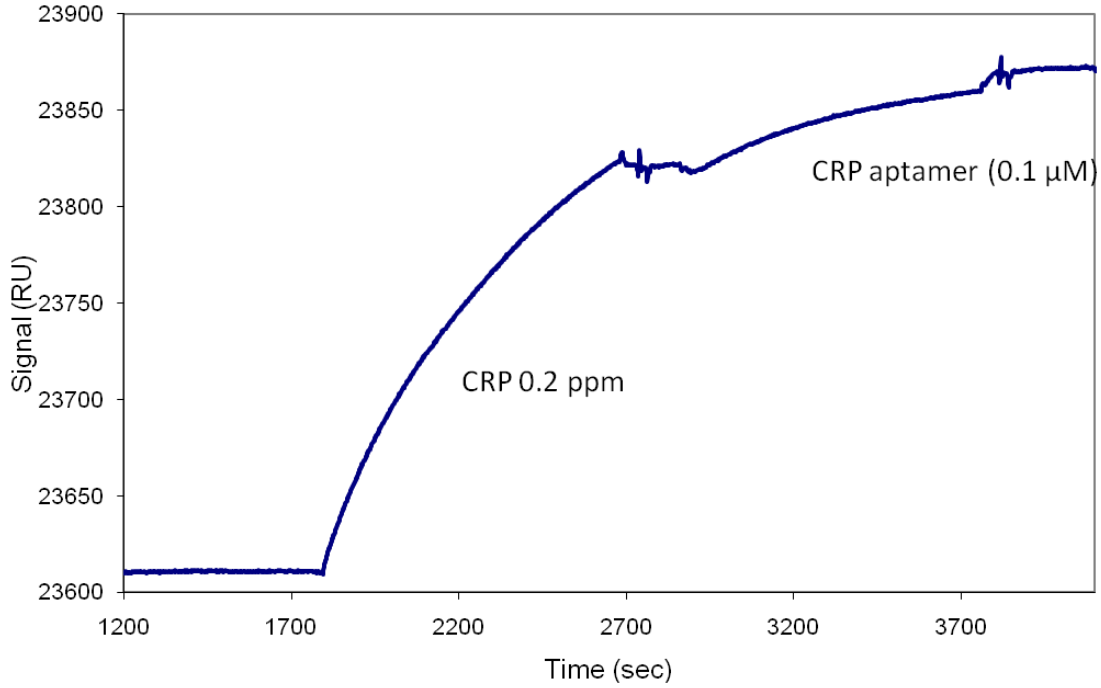


**Figure 38. Sandwich assay: 0.2 ppm CRP was bound to the immobilised CRP aptamer (Interaction time 15 min, binding shift 221 RU), then the secondary aptamer at a concentration of 0.1 µM was added (Interaction time 15 min, binding shift 50 RU). Immobilised aptamer: 0.1 µM CRP aptamer modified with 2'-F-pyrimidines. Flowrate 2 µl/min, 25 °C.**

## 3.3. Selection of Thrombin-binding aptamers by a computational approach

The aptamer-thrombin complex NMR structure (1HAO), in which the 15-mer TBA in its typical chair-conformation interacts with the fibrinogen-binding exosite, was downloaded from Protein Data Bank. By means of Fred-Receptor, a 25803 $Å^3$ binding box was defined (Figure 39a) and the 15-mer TBA in the chair-shaped conformation was docked to the protein as a reference ligand. Using Shapegauss as scoring function, 100 possible binding poses were ranked for the chair-shaped aptamer, with binding scores comprised in the range -1762 ÷ -1549 (Figure 39b). Binding scores were expressed as arbitrary units describing the affinity between aptamer and protein.

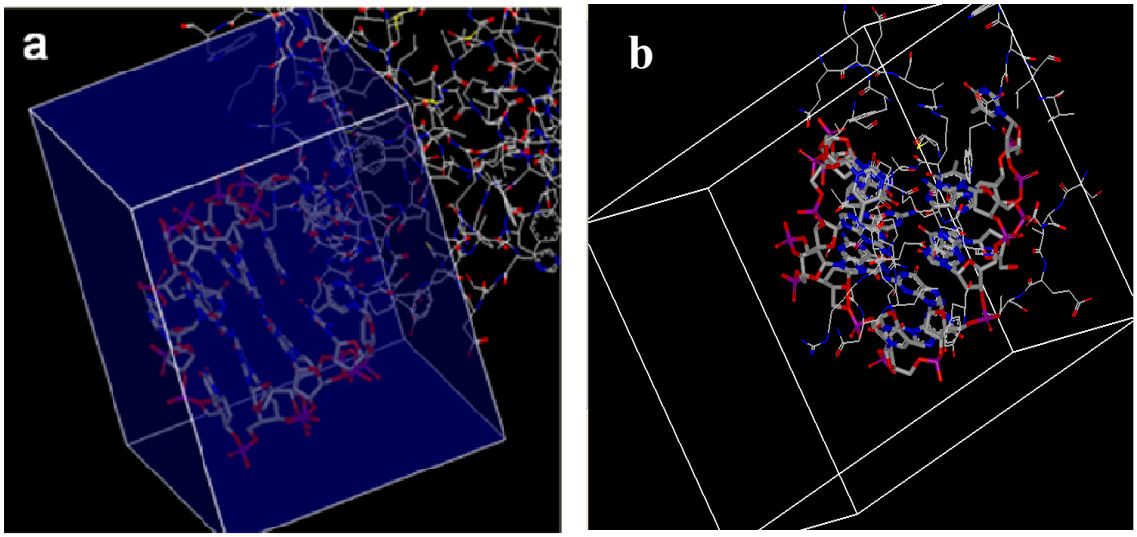


**Figure 39. Creation of the binding box. a) A 25803 $Å^3$ rectangular box was created for the 15-mer TBA aptamer, in the aptamer-thrombin complex (1HAO) downloaded from Protein Data Bank. b) The 15-mer TBA in the chair-shaped conformation was docked to the protein and the relative poses were scored; the top-ranked pose received a binding score of -1762.**

With the aim of studying the aptamer-thrombin interaction also in the heparin-binding exosite, the heparin-thrombin complex (code 1TB6) was downloaded from Protein Data Bank and a binding box was automatically created for heparin. The binding box

contours were then modified, in order to define a 28427 $Å^3$ protein receptor site, in which the aptamer should fit (Figure 40a). Using Shapegauss as scoring function, 100 possible binding poses were ranked for the chair-shaped aptamer, with binding scores comprise in the range -1373 ÷ -1141 (Figure 40b).

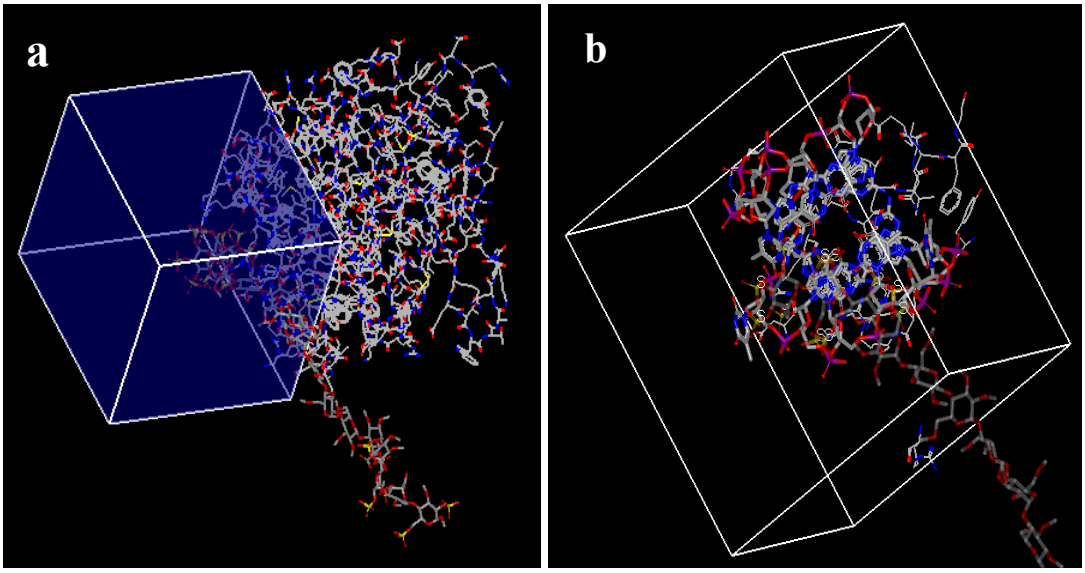


**Figure 40. a) A 28427 $Å^3$ rectangular box was created in the heparin-binding exosite using the heparin-thrombin complex (1TB6) downloaded from Protein Data Bank. b) The 15-mer TBA in the chair-shaped conformation was docked to the protein receptor site and the relative poses were scored; the top-ranked pose received a binding score of -1373.**

The library of sequences created in Hyperchem by the use of the special algorithm contained the TBA sequence, 990 different sequences having one or two mutations respect to the TBA and the three low-binding sequences reported in literature (named sequences “a”, “b” and “c”). As a result, the library contained 994 sequences, which were minimised (computing time 1 day, 2 h, 29 min). To take into account the flexibility of the oligonucleotides, overcoming the serious limitation of considering nucleotides as rigid, conformers were generated for each sequence: the Openeye software OMEGA generated an average of 53 conformers for each sequence, in 5 days, 5 h, 1 min. Consequently, the database was represented by the conformers of the 994 oligonucleotide, around 53000 units. In order to give an idea of the minimisation energy

and number of conformers obtained, the results for the sequences selected for the following experimental part and for the three low binding sequences were quantitatively reported in Table 11.

| Code | Sequence | Mutations | Minimisation Energy (Kcal/mol) | Conformers |
|---|---|---|---|---|
| TBA | 5'-GGT TGG TGT GGT TGG-3' | - | -1030 | 44 |
| Best | 5'-GGT TTG TGT GGT TAG-3' | G5T, G14A | -993 | 91 |
| Medium | 5'-GGC TGG TGT GAT TGG-3' | T3C, G11A | -959 | 112 |
| Worst | 5'-GGT AGG TGT GGT TGC-3' | T4A, G15C | -996 | 61 |
| "a" | 5'-GGT GGT GGT TGT GGT-3' | T4G, G6T, T7G, G10T, T13G, G15T | -1050 | 45 |
| "b" | 5'-GGT AGG GTC GGA TGG | T4A, T7G, G8T, T9C, T12A | -833 | 39 |
| "c" | 5'-GGT AGG GCA GGT TGG-3' | T4A, T7G, G8C, T9A | -834 | 80 |

**Table 11. Computational summary results for the oligonucleotide sequences selected for experimental screening. The oligonucleotide sequences, the mutations with respect to the TBA sequence, the minimisation energy and the number of conformers generated are reported.**

After these preliminary steps for the binding box and preparing conformers, FRED (the protein-ligand docking program by Openeye) was run with Shapegauss as scoring function. The run completed in 1 day, 12 hours, 33 minutes when docking was performed in the Fibrinogen-binding exosite and in 1 day, 10 hours, 31 minutes when

docking was performed in the Heparin-binding exosite. Therefore, the binding score together with a molecule file containing the docked structures of the top scored conformer for each sequence was generated. The binding score obtained was given only by one component, i.e. the shape score, while the hydrogen atoms were ignored.

### 3.3.1. Analysis of the binding scores

From the docking simulation in the Fibrinogen binding exosite, 174 sequences were not scored since no valid pose was found. The best conformer in terms of binding score was that coming from the mutated sequence G5T,G14A, with a total score of −1748. Considering the full ligand library, the total score ranged from −1748 to −667, but only 98 elements reached a score between −1748 and −1500, while the majority of oligonucleotides ( 657 elements) had total score between −1500 and −1000 and 65 sequences had a total score higher than -1000 (Figure 41).

The docking step in the Heparin binding exosite failed for 194 sequences, which was not scored since no valid pose was found. The best conformer in term of binding score was that coming from the mutated sequence G6T, with a total score of -1486. Considering the full ligand library, the total score was comprised between -1486 and -404, therefore lower binding scores were in general found in the heparin binding exosite with respect to the fibrinogen binding exosite (Figure 42). Only 90 elements reached a score between −1486 and −1200, while the majority of oligonucleotides (672 elements) had total score between −1200 and −700 and 38 sequences had a total score higher than -700.

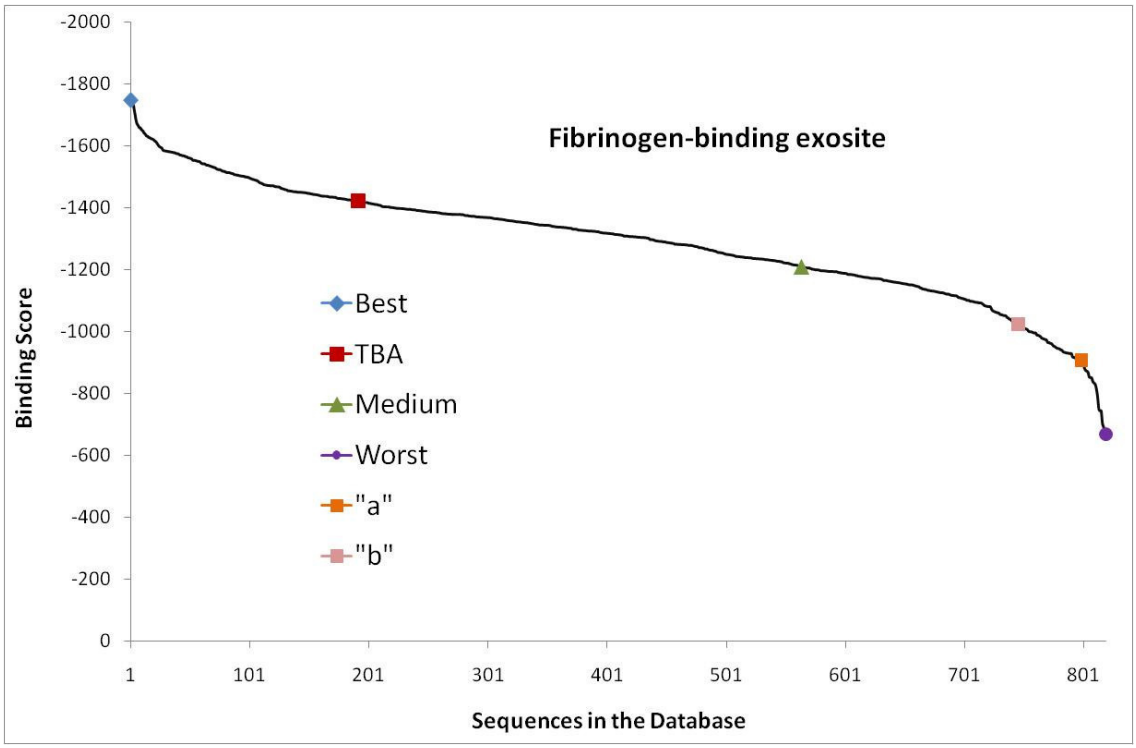


**Figure 41. Binding score for each sequence in the database docked to the Fibrinogen-binding exosite.**

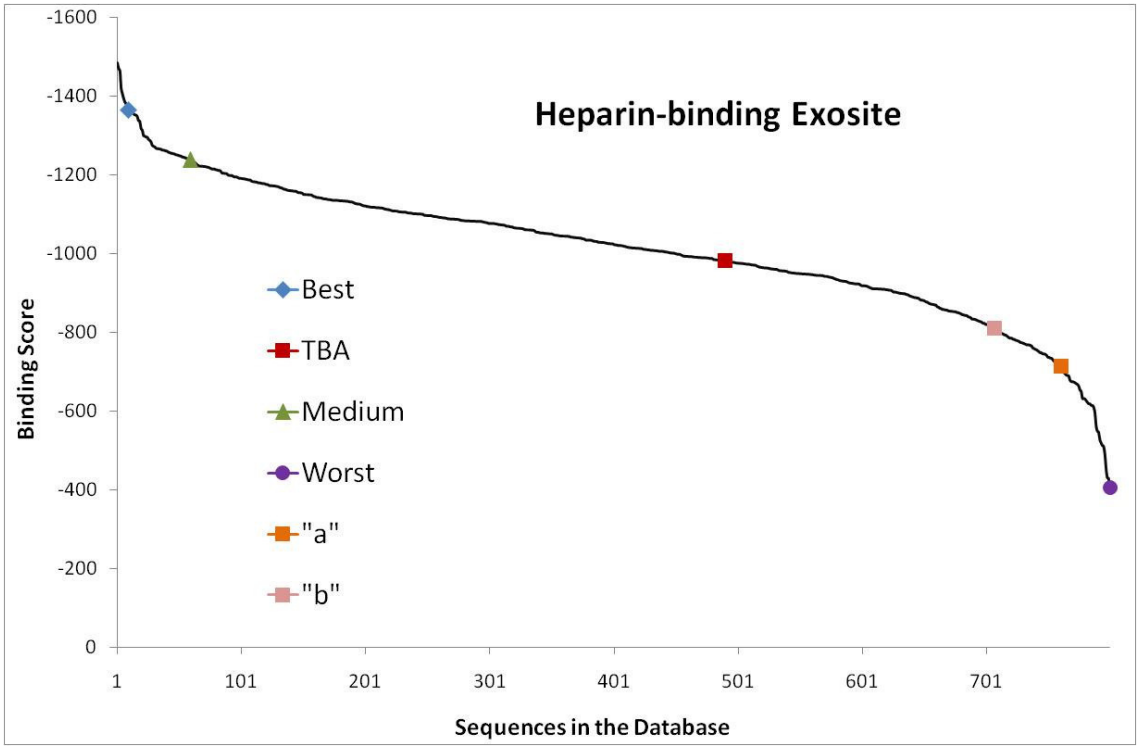


**Figure 42. Binding score for each sequence in the database docked to the Heparin-binding exosite.**

The binding scores obtained for library docking in each exosite were divided in three parts, in order to classify high-binding sequences from low-binding sequences. Calculations were carried out in order to quantitate how many times a mutation appeared in each position and results are reported in Table 12. Among the 98 sequences having the most favourable binding score in the fibrinogen binding site (Binding score < -1500), positions G1, G2 and G6 were the most mutated, while positions T9, G10, T12 and G15 were the less mutated. Up to 12 mutated sequences among 19 showed mutation G1T, but in general a trend towards a particular mutation was not observed. Among 93 sequences having the most favourable binding score in the heparin binding site (Binding score < -1200), positions most mutated were G1, T7, T13 and G14, while G10 was the less mutated position. Also in this case, a bias was observed for mutation G1T (10 sequences among 16), but in general there was not a clear prevalence of a mutation with respect to the others. However, for both the binding sites mutations in cytosine were unfavoured in comparison to mutations in adenine, in all the positions. In contrast with results reported by Tasset *et al*. [55], mutation of position 4 with an adenine (T4A) did not seem to promote the oligonucleotide binding to the heparin-binding site. In fact, only one sequence having mutation T4A achieved a highly favourable binding score.

| Binding Score | TBA | G | G | T | T | G | G | T | G | T | G | G | T | T | G | G |
|---|---|---|---|---|---|---|---|---|---|---|---|---|---|---|---|---|
| | Mutation | **Fibrinogen-Binding Site** | | | | | | | | | | | | | | |
| **< -1500** | | **4** | **9** | **6** | **4** | **4** | **6** | **6** | **6** | **3** | **3** | **3** | **1** | **7** | **7** | **2** |
| -1500 <BS< -1000 | **A** | 26 | 26 | 29 | 28 | 30 | 29 | 28 | 33 | 32 | 34 | 33 | 25 | 23 | 26 | 30 |
| > -1000 | | 4 | 5 | 3 | 3 | 2 | 3 | 1 | 2 | 0 | 2 | 2 | 11 | 3 | 4 | 4 |
| **< -1500** | | **3** | **6** | **6** | **0** | **3** | **6** | **3** | **5** | **2** | **2** | **4** | **2** | **4** | **2** | **2** |
| -1500 <BS< -1000 | **C** | 34 | 31 | 29 | 23 | 24 | 30 | 33 | 24 | 29 | 25 | 35 | 34 | 28 | 29 | 35 |
| > -1000 | | 0 | 1 | 5 | 6 | 2 | 1 | 2 | 5 | 1 | 3 | 2 | 2 | 2 | 4 | 3 |
| < -1500 | | **-** | **-** | **1** | **8** | **-** | **-** | **5** | **-** | **3** | **-** | **-** | **3** | **3** | **-** | **-** |
| -1500 <BS< -1000 | **G** | - | - | 34 | 23 | - | - | 31 | - | 32 | - | - | 25 | 30 | - | - |
| < -1000 | | - | - | 0 | 2 | - | - | 1 | - | 4 | - | - | 8 | 3 | - | - |
| **< -1500** | | **12** | **6** | **-** | **-** | **3** | **10** | **-** | **3** | **-** | **1** | **5** | **-** | **-** | **7** | **4** |
| -1500 <BS< -1000 | **T** | 27 | 23 | - | - | 28 | 23 | - | 22 | - | 17 | 26 | - | - | 27 | 32 |
| > -1000 | | 1 | 0 | - | - | 2 | 1 | - | 6 | - | 5 | 2 | - | - | 1 | 2 |
| Binding Score | Mutation | **Heparin-Binding Site** | | | | | | | | | | | | | | |
| **< -1200** | | **4** | **5** | **5** | **1** | **4** | **3** | **6** | **6** | **4** | **4** | **5** | **0** | **6** | **5** | **4** |
| -1200 <BS< -700 | **A** | 26 | 33 | 32 | 32 | 31 | 33 | 28 | 33 | 31 | 31 | 30 | 25 | 26 | 30 | 29 |
| > -700 | | 2 | 0 | 1 | 2 | 0 | 1 | 1 | 2 | 0 | 4 | 2 | 1 | 2 | 3 | 2 |
| < -1200 | | **2** | **2** | **3** | **0** | **1** | **3** | **5** | **2** | **1** | **0** | **4** | **4** | **2** | **6** | **5** |
| -1200 <BS< -700 | **C** | 36 | 36 | 34 | 23 | 26 | 34 | 32 | 29 | 26 | 32 | 31 | 27 | 28 | 23 | 32 |
| > -700 | | 1 | 1 | 2 | 7 | 2 | 2 | 0 | 3 | 4 | 0 | 1 | 3 | 1 | 3 | 1 |
| **< -1200** | | **-** | **-** | **2** | **8** | **-** | **-** | **6** | **-** | **5** | **-** | **-** | **7** | **7** | **-** | **-** |
| -1200 <BS< -700 | **G** | - | - | 34 | 22 | - | - | 31 | - | 33 | - | - | 21 | 27 | - | - |
| > -700 | | - | - | 1 | 2 | - | - | 0 | - | 1 | - | - | 0 | 1 | - | - |
| **< -1200** | | **10** | **3** | **-** | **-** | **4** | **7** | **-** | **2** | **-** | **2** | **2** | **-** | **-** | **5** | **4** |
| -1200 <BS< -700 | **T** | 29 | 25 | - | - | 26 | 28 | - | 22 | - | 18 | 30 | - | - | 30 | 32 |
| > -700 | | 1 | 1 | - | - | 6 | 0 | - | 3 | - | 2 | 1 | - | - | 1 | 1 |

**Table 12. Tabulation of the data resulting from the analysis of binding scores for docking the oligonucleotides library in both the thrombin binding sites. Binding scores were divided in three classes for each exosite in order to distinguish sequences having the highest affinity from those having the lowest affinity. Quantification of how many times a mutation appeared in each position was reported.**

Taking into consideration the two binding exosites, the mutated sequence G5T,G14A (named "Best") was the top scored in the Fibrinogen-binding exosite and the tenth scored in the Heparin-binding exosite; the TBA sequence was ranked 192$^{th}$ and 490$^{th}$ in the two exosites respectively, the mutated sequence T3C,G11A (named "Medium") was ranked 564$^{th}$ and 60$^{th}$ respectively and the mutated sequence T4A,G15C (named "Worst") was bottom ranked in both the binding sites. These binding scores were taken into consideration in the choice of the ligands for the experimental test, in order to have a variety of candidates: the best and worst ranked, for which a huge difference in term of binding scores was highlighted, plus a sequence for which an intermediate behavior had to be expected. A binding score % was calculated by assigning value 100 to the mutated sequence G5T,G14 ("Best") for the Fibrinogen-binding site and to the mutated sequence G6T for the Heparin-binding site.

Regarding the three sequences experimentally tested in literature for low-binding, docking of sequence "c" failed in both the exosites, while sequences "a" and "b" were ranked bottom in both the exosites (Binding Score sequence "a": -907 and -713 respectively; Binding Score sequence "b": -1023 and -811 respectively).
The simulation results for the most interesting sequences are summarized in Table 13.

| Code | Fibrinogen Binding Exosite 820 docked sequences | | | Heparin Binding Exosite 800 docked sequences | | |
|---|---|---|---|---|---|---|
| | Binding Score | Hit-list position | Binding Score % | Binding Score | Hit-list position | Binding Score % |
| Best | -1748 | 1 | 100 | -1364 | 10 | 91.8 |
| TBA | -1422 | 192 | 81.3 | -982 | 490 | 66.1 |
| Medium | -1209 | 564 | 69.2 | -1256 | 60 | 83.3 |
| Worst | -667 | 820 | 38.2 | -404 | 800 | 27.2 |
| "a" | -907 | 799 | 51.9 | -713 | 761 | 48.0 |
| "b" | -1023 | 746 | 58.5 | -811 | 707 | 54.6 |

**Table 13. Binding Scores and relative hit list position for the oligonucleotide sequences chosen for the experimental test and for the docked sequences reported in literature for low-binding to Thrombin.**

Binding scores obtained by docking the database in the fibrinogen-binding exosite were graphically correlated with the binding scores obtained by docking the library in the heparin-binding exosite (Figure 43). This aimed to immediately represent the behaviour of each docked sequence in both the binding sites. As can be observed, most of the sequences tended to bind the fibrinogen binding site rather than the heparin site, and the mutated sequence named "Medium" obtained the same binding scores for both the exosites.

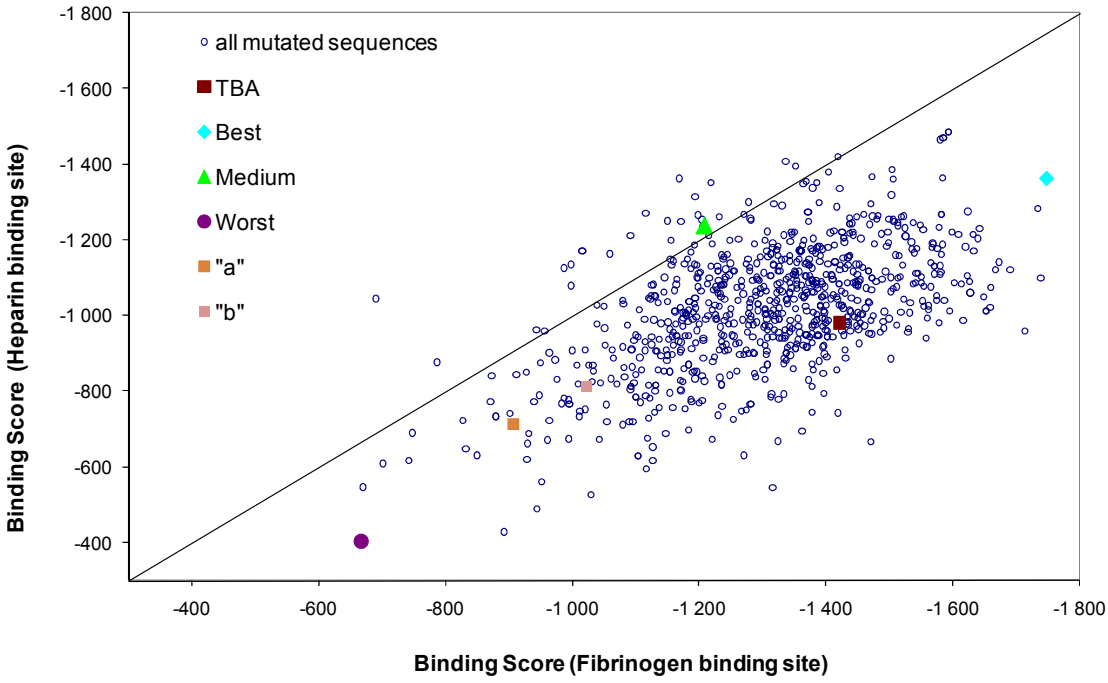


**Figure 43. Scatter plot of the binding scores obtained by docking the database in the Fibrinogen-binding site versus the binding scores obtained by docking the database in the Heparin-binding site. The line represents the graph diagonal.**

### 3.3.2. Experimental tests

Experimental tests were conducted in order to verify if the binding scores agreed with the analytical behaviour of the sequences. For this purpose, the 15-mer Thrombin-binding aptamer as well as the best sequence, the worst sequence and the sequence with intermediate behaviour resulting from the simulation experiments were immobilised on CM5 Biacore chips, in concentration 0.5 μM, following the procedure described in paragraph 2.2.1. To assure each immobilised sequence a certain flexibility, a no oligonucleotide spacer (BioTEG tail) was chosen in order to avoid base-pairing, which affects the aptamer's secondary structure. Two chips were employed for each sequence and, from the resulting immobilisation shifts, a similar density of immobilised molecules was estimated considering 1000 RU = 0.8 ng/mm$^2$ (Biacore User Manual). This density similarity allowed a direct comparison among the different sequences when testing their sensitivity for the detection of thrombin. The results for the immobilisation step are reported in Table 14.

| Sequence Code | Chip 1 | | Chip 2 | |
|---|---|---|---|---|
| | Immobilisation Shift (RU) | Density (molecules/cm$^2$) | Immobilisation Shift (RU) | Density (molecules/cm$^2$) |
| TBA | 1116 | 1.0 x $10^{13}$ | 1194 | 1.1 x $10^{13}$ |
| Best | 931 | 8.5 x $10^{12}$ | 918 | 8.4 x $10^{12}$ |
| Medium | 1126 | 1.0 x $10^{13}$ | 1080 | 9.9 x $10^{12}$ |
| Worst | 957 | 8.8 x $10^{12}$ | 911 | 8.3 x $10^{12}$ |

**Table 14. Comparison between different immobilised BiotinTEG sequences onto Biacore CM5 Chips. Concentration of each sequence: 0.5 μM. Density was calculated from immobilisation shifts (1000 RU = 0.8 ng/mm2, according to the Biacore User Manual) and it was reported as molecules/cm$^2$ considering the molecular weight of each immobilised sequence and the Avogadro number.**

### 3.3.2.1. Binding Buffer optimisation

Binding experiments were performed with the target thrombin solution prepared in the previously optimised buffer (50 mM Tris-HCl pH 7.4, 140 mM NaCl, 1 mM $MgCl_2$, 0.005% Tween 20), as reported in paragraph 3.1.1. The same buffer was used also as running solution. The thrombin-aptamer interaction time was 15 minutes and the surface was regenerated after each binding cycle by a treatment with 1 mM or 5 mM NaOH.

When testing the TBA sequence, a binding shift was recorded in the thrombin concentration range 0-10 nM, with a minimum detectable amount of the analyte of 0.5 nM (Figure 44). On the contrary, when testing the mutated sequences, a change in refractive index was observed during the protein injection, but no binding shift was recorded, even at very high thrombin concentration (Figure 45)

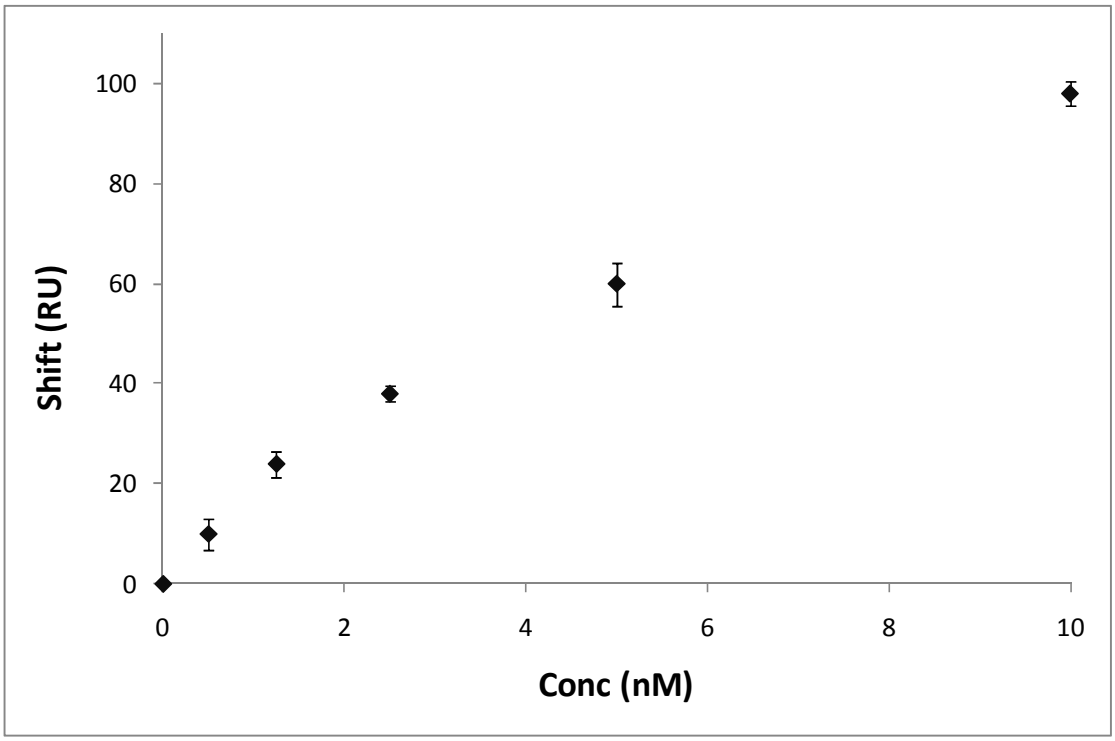


**Figure 44. Binding shifts recorded for different concentrations of thrombin when the TBA sequence was immobilised on a CM5 chip. Each error bar represents standard deviation of three replicates (n=3). The thrombin solution was prepared in buffer 50 mM Tris-HCl pH 7.4, 140 mM NaCl, 1 mM $MgCl_2$, 0.005% Tween 20.**

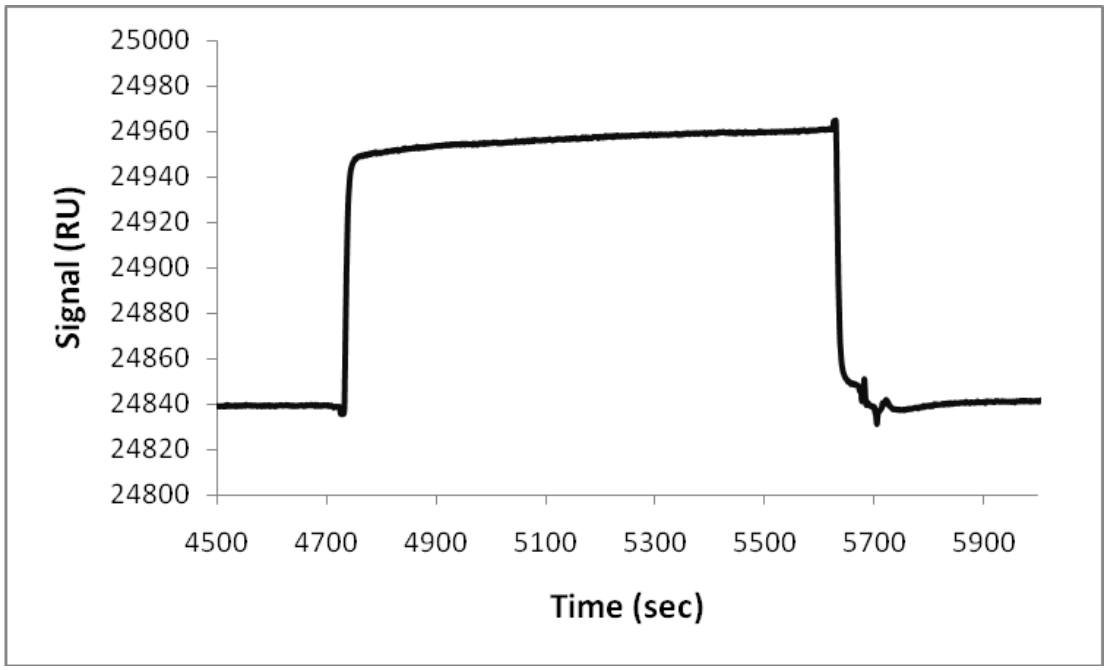


**Figure 45. Interaction between 400 nM Thrombin and the immobilised mutated sequence G5T,G14A (named "Best"). No binding shift was recorded after 15 min interaction. Running and Binding buffer: 50 mM Tris-HCl, pH 7.4, 140 mM NaCl, 1 mM $MgCl_2$, 0.005% Tween 20.**

It should be noticed that in the computational experiments, phenomena occurring in solution such as ionic strength, pH and in trace compounds interferences could not be taken into account. In fact, Openeye Scientific Software performs modelling experiments in vacuum or in solution, by introducing an implicit solvation model that simulate an aqueous solution. For this reason, in the experimental test the ionic strength of the binding buffer was drastically reduced, in order to reproduce the binding conditions of the simulation: for this purpose, a 400 nM thrombin solution was prepared by diluting the 4000 nM stock solution (in 50 mM Tris-HCl, pH 7.4, 140 mM NaCl, 1 mM $MgCl_2$) in MilliQ water and the binding curve was registered, using the binding buffer as running solution. Under these conditions, a binding curve was registered, but a complete dissociation was observed at the end of injection (Figure 46).

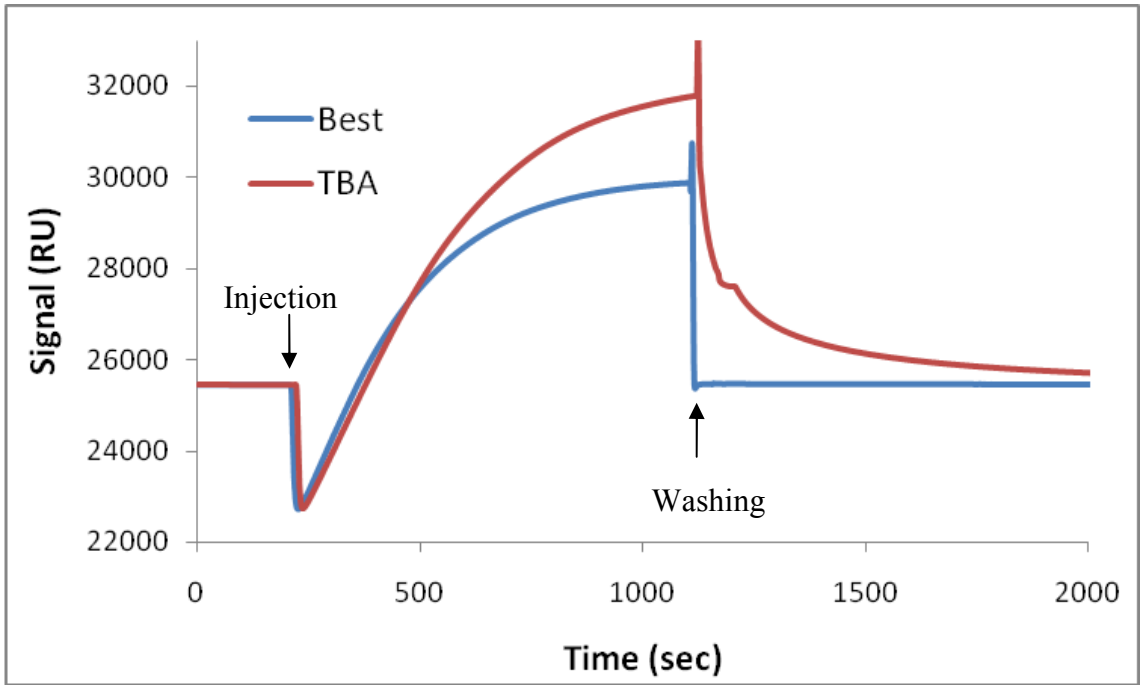


**Figure 46. Binding curves for 400 nM thrombin interacting with the immobilised mutated sequence G5T,G14A ("Best") and the TBA sequence. The thrombin solution was prepared by diluting 1:10 the thrombin stock solution with MilliQ water. The previously optimised binding buffer was used as running solution (50 mM Tris-HCl, pH 7.4, 140 mM NaCl, 1 mM $MgCl_2$, 0.005% Tween 20). A dissociation curve was observed as soon as the injection ended.**

On the contrary, when MilliQ water was used as running buffer as well as for the preparation of 400 nM thrombin, the binding curve did not dissociate at the end of the injection and the measurement of a binding shift was possible (Figure 47).

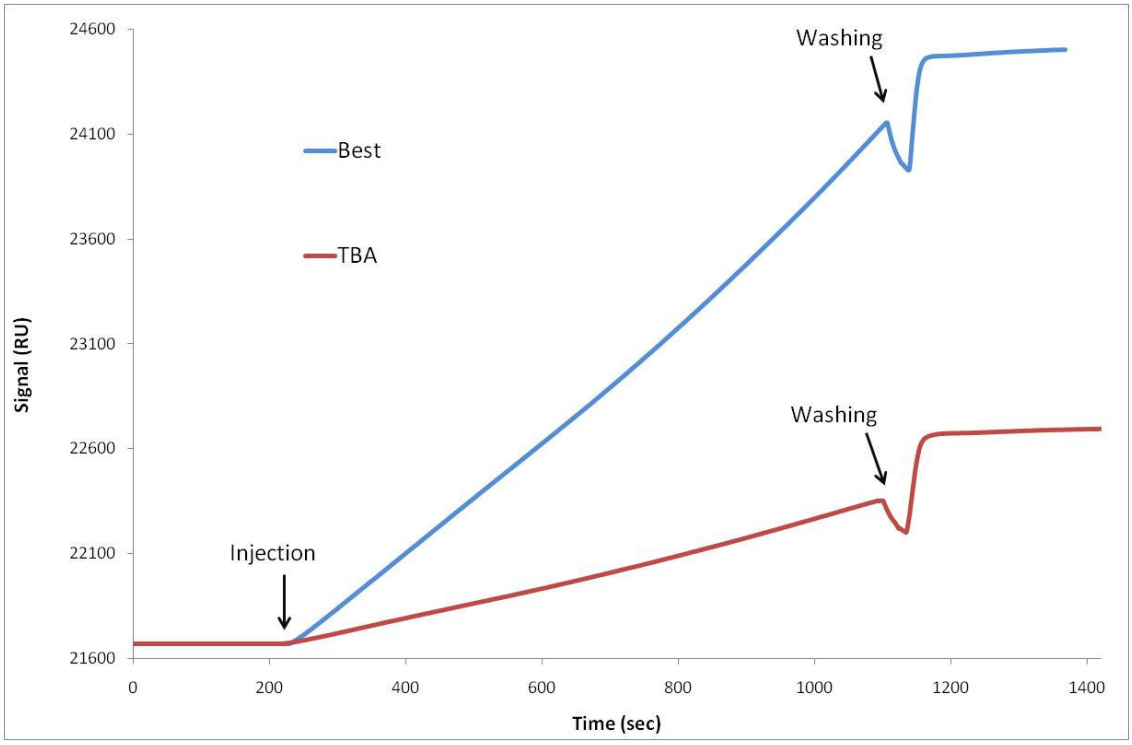


**Figure 47. Binding curve for 100 nM thrombin interacting with the immobilised mutated sequence G5T,G14A ("Best") and the TBA sequence. MilliQ water was used as running buffer. The thrombin solution was prepared by diluting 1:10 the thrombin stock solution with MilliQ water. Binding shifts of 2455 RU and 1013 RU were registered when the immobilised sequence was G5T,G14A or TBA, respectively.**

It seemed that the binding curve shape as well as the binding shift depended upon the ionic strength of the binding and running buffer, which had to be minimised to reproduce the conditions used in the computational experiments. Curve shape suggested that a successful rapid binding to a stable plateau was not achieved when experiments were performed in water; on the contrary, a slow binding was observed, without reaching a plateau during the ligand pulse. This could cause a irreproducible binding, probably due to the binding buffer conditions (Biacore User Manual). In addition, several problems were encountered when using MilliQ water as running and binding buffer: since the 4 μM thrombin stock solution was prepared in 50 mM Tris-HCl, pH 7.4, 140 mM NaCl, 1 mM $MgCl_2$, different dilutions of this buffer were made up when preparing different concentrations of thrombin; secondly, the protein structure could be affected in a highly diluted environment; finally, a baseline drift was observed when

working in MilliQ water. To overcome these problems, further experiments were performed in order to find the lowest ionic strength which supported a binding curve without departing from the computational conditions. For this purpose, the optimised binding buffer was diluted 1:10 or 1:50 with MilliQ water and the resulting solutions were used as running and binding buffer. Using the buffer diluted 1:10, a slight dissociation was observed when 100 nM thrombin was bound to the mutated sequence G5T,G14A ("Best") (Figure 48). On the contrary, using the buffer diluted 1:50 the binding curve did not dissociate at the end of the injection. Therefore, this solution (1 mM Tris-HCl, pH 7.4, 2.8 mM NaCl, 0.02 mM $MgCl_2$) was chosen for the following experiments, aimed to verify if the experimental and computational analysis agreed.

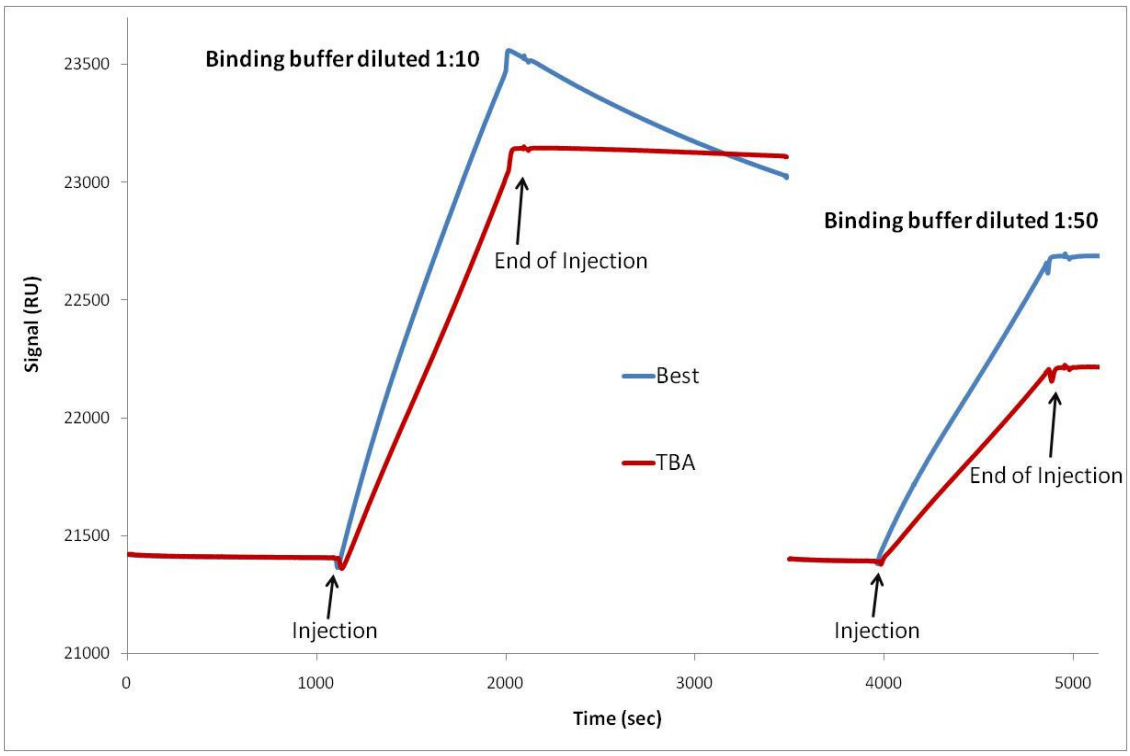


**Figure 48. Binding curves for 100 nM thrombin interacting with the immobilised mutated sequence G5T,G14A ("Best") and the TBA sequence, when binding buffer diluted 1:10 or 1:50 was used as running solution as well as for the dilution of the stock thrombin solution. In the case of binding buffer diluted 1:50, binding shifts of 1296 RU and 824 RU were recorded when the immobilised sequence was G5T,G14A or TBA, respectively.**

### 3.3.2.2. Comparison between the experimentally tested sequences

Using the binding buffer diluted 1:50, the analytical performances of the four oligonucleotide sequences were compared in terms of signal amplitude, sensitivity (slope), linearity ($R^2$) and reproducibility. The results indicated that a slightly better performance was obtained with the mutated sequence G5T,G14A ("Best"), while a slightly worse performance was obtained with the mutated sequence T4A,G15C ("Worst"), in agreement with the simulation findings (Table 15). The behaviours of the TBA and the mutated sequence T3C,G11A ("Medium") were very similar and intermediate between the other two sequences (Figure 49).

| Sequence Code | Linear Regression | $R^2$ |
|---|---|---|
| TBA | y = 5.35x – 10.7 | $R^2 = 0.992$ |
| Best | y = 7.86x - 18.8 | $R^2 = 0.994$ |
| Medium | y = 5.05x – 8.2 | $R^2 = 0.997$ |
| Worst | y = 3.33x – 7.5 | $R^2 = 0.985$ |

**Table 15. Analytical behaviour of the four experimentally tested immobilised sequences in the optimised binding conditions (Binding buffer diluted 1:50)**

As a consequence of the reduction in ionic strength, thrombin was detected in the concentration range 0-50 nM with a minimum detectable amount of the analyte of 5 nM, with all the four sequences tested. In contrast, a thrombin concentration range of 0-10 nM was achieved with the immobilised TBA sequence, using the optimised buffer as binding and running buffer, with a minimum detectable amount of analyte of 0.5 nM.

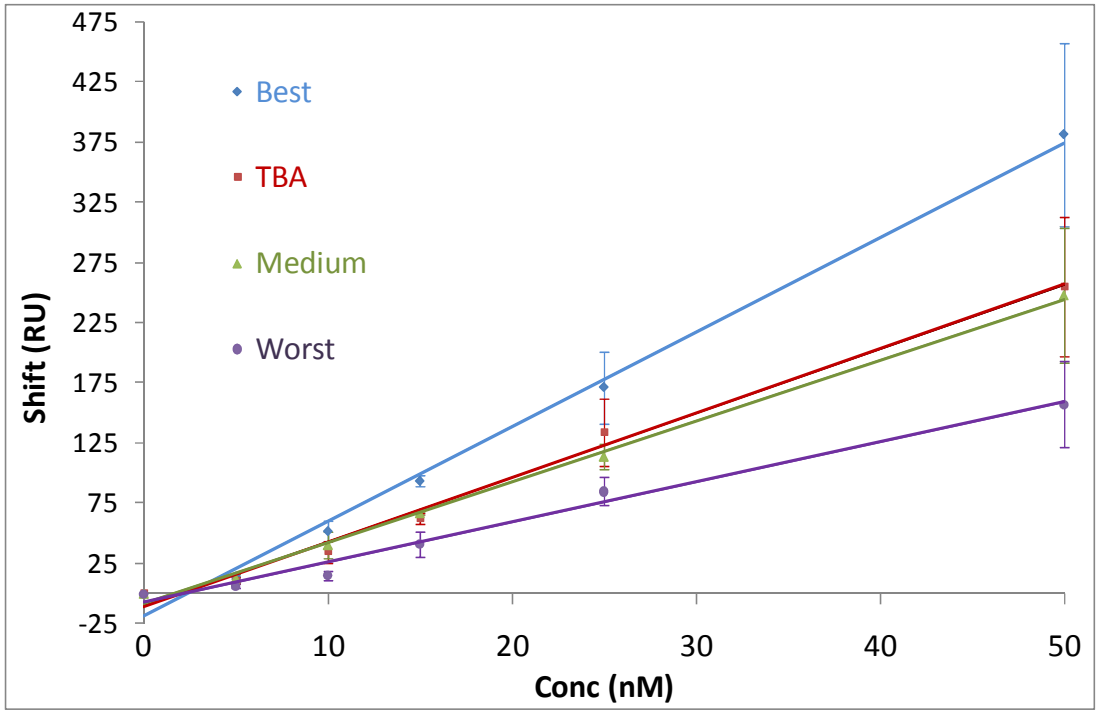


**Figure 49. Thrombin calibration plots obtained with the four experimentally tested immobilised sequences in the optimised binding conditions (Binding buffer diluted 1:50). Each error bar represents standard deviation of three replicates (n=3).**

The specificity of each sequence was tested in the optimised binding conditions using human serum albumin as negative control. Using binding buffer diluted 1:50, HSA solutions were prepared in concentration 77 µM, corresponding to a dilution 1:100 with respect to physiological concentrations. Very similar results were recorded when HSA was exposed to each of the immobilised sequence, with a slightly higher unspecific signal observed in the case of sequence "Medium" (Figure 50). However it is worthy to note that *in silico* experiments only evaluated the affinity of each ligand to thrombin, independently by their specificity towards other proteins.

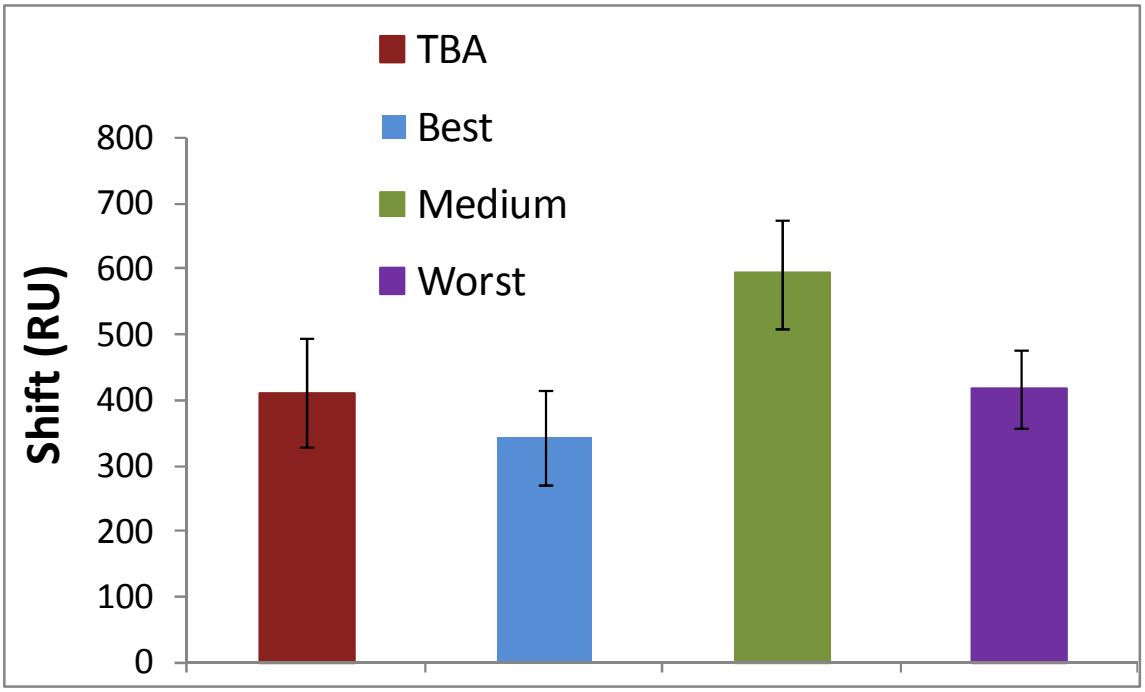


**Figure 50. Specificity test with HSA 77 µM for the four experimentally tested immobilised sequence in the optimised binding conditions (Binding buffer diluted 1:50). Each error bar represents standard deviation of three replicates (n = 3).**

# DISCUSSION

## 4.1. Optimisation of critical parameters influencing the aptamer-protein affinity reaction

Aptamers represent a very interesting affinity reagent with potential application in diagnostics, rivalling antibodies due to several advantages, mainly deriving from their chemical synthesis. In this thesis the suitability of aptamers as receptor molecules on solid surfaces for protein detection was investigated. For this purpose a well described and studied DNA aptamer specific for thrombin was chosen as a model system for biosensor development and coupled to label-free piezoelectric transduction. Furthermore, optical transduction was also used for another case study, where an RNA aptamer specific for C-Reactive Protein was employed. This latter aptamer was coupled to an optical chip and the principle of Surface Plasmon Resonance was used to study the interaction. So far, no application of CRP aptamer nor any studies on its employment have been described. Only its selection using the SELEX process has been reported in the literature [88].

Both QCM and SPR techniques have their own strengths and weaknesses for the development of aptamer-based biosensors. QCM is rather more likely to be used for the development of a new commercial aptasensor than SPR with the Biacore device, due to its simple and cheap costruction. However, because of RNA sensitivity to nucleases, SPR was used for the optimisation process of the CRP-binding aptamer, since the Biacore facilitated a relatively controlled environment. In addition, since both transduction methods involve direct affinity sensing on a gold surface, many parallels

exist between the two approaches. The advantage of QCM and SPR-based biosensing over other technologies is their fast and reliable analysis in real-time, without the use of labels, together with the possibility of repeated use of the sensor surface. Thus, direct aptamer-based assays were developed for thrombin and CRP detection without the use of any label and the experimental conditions for binding in heterogeneous phase were found. The optimisation step was of paramount importance since the behaviour of aptamers fixed onto solid supports (i.e. in heterogeneous phase) can vary considerably with respect to their performances in solution. It has been demonstrated [143] that some of the conditions optimised for an aptamer (such as kind of binding buffer, pH, ionic strength, regeneration solution) are not universal for all aptamers; on the contrary, these assay conditions have to be optimised on an individual aptamer basis since each aptamer possess a unique structure for target binding that must be considered. For this reason, the working conditions from one optimised system cannot be directly transferred to another one. However, despite the individual characteristics of each aptamer, other critical parameters for optimal aptamer performance are of general applicability in aptasensing development (for example, the presence of a spacer in the aptamer sequence), when other transduction principles are employed.

Therefore a critical evaluation of important simple key steps in development of both aptasensors studied was conducted, because of their significant implications for analytical performance in terms of selectivity, linearity ($R^2$), reproducibility and stability (cycles). In particular, the influence of the aptamer immobilisation procedure (chemistry, length, concentration and pre-treatment of the aptamer) as well as the binding conditions employed in the assays was studied.

### 4.1.1. Optimisation of the immobilisation step

To date, a rational evaluation of different important key steps in aptasensor development has been reported only for an enzyme linked oligonucleotide assay

(ELONA) assay [143]. In this thesis work the TBA and CRP aptamers were immobilised onto the gold surfaces of a quartz crystal or of a SPR chip through the biotin- or thiol- derived 5' end. For this purpose, two standardized procedures for coupling of oligonucleotide sequences onto gold surfaces were applied [144]. In particular, immobilisation of biotinylated probe was realised on a layer of streptavidin linked to carboxylated dextran, fixed onto the gold surface on a self-assembled monolayer of 11-mercaptoundecanol; self assembly of the thiol-labelled probe was achieved on the gold surface via direct chemisorption. The two immobilisation methods were used for the modification of the piezoelectric crystal with the TBA probe and compared in terms of sensitivity and reproducibility: despite the long-time required for crystal preparation, the best procedure turned out to be the one based on dextran and streptavidin, in accordance with other reports [145]. For this reason this procedure was also used in the case of CRP detection, by immobilising the biotinylated CRP aptamer onto CM5 Biacore chips, already modified with a dextran layer.

As reported in paragraph 1.4.2.3. of this thesis, the TBA aptamer immobilisation through the 5' [79; 68; 78; 80; 75] or 3' [72; 73] modified end has been successfully demonstrated in numerous works. Studies of TBA aptamer showed that chemical modification of the 5' or 3' termini minimally perturbed thrombin-binding [71], since the interaction with thrombin is thought to occur adjacent to the T3T4 and T12T13 loops. However, other authors reported that an increased binding efficiency was observed when TBA was immobilised through its 3'-termini instead of 5' [143].

Since aptamers require the adoption of a particular structure to facilitate protein binding, the presence of a spacer arm in the aptamer sequence was studied in the case of both thrombin and CRP, in order to evaluate whether this spacer allowed increased flexibility of the aptamers to form the binding conformation. The results with TBA aptamer showed that coupling the receptors to the gold surface via a linker molecule (a polyT or a TEG tail) was advantageous to sterically assist the analyte binding. Improved target binding was observed in presence of a spacer, presumably due to the decreased steric hindrance, with consequent improved folding and analyte recognition. These findings correlated well with others previously reported. In particular, when developing an

aptamer-based quartz crystal biosensor to detect IgE, Liss *et al*. [146] demonstrated that the folded aptamer structure was stabilised by extending the sequence with the addition of other bases, in order to allow the formation of a longer stem and consequently a more stable tertiary structure. Other authors showed that the addition of a linker consisting of six carbon atoms correlated with improved thrombin binding [143].

In the case of CRP, the analytical characteristics of the assay using the aptamer modified with a polyT or a TEG tail were compared and an improved performance was observed in the case of TEG, probably because this non-oligonucleotide spacer avoids intra-molecular folding in the aptamer structure. Intra-molecular folding in presence of the polyT tail was not observed in the case of the TBA, since this aptamer was formed only by guanines and thymines and consequently A·T base pairing was avoided. This problem was, however, taken into account in the choice of the spacer for the mutated TBA sequences, which contained all of the four nucleotides. Thereby, it has been shown the necessity to identify the most suitable tail to be used as a spacer when immobilising the aptamer of interest on a solid surface.

From the immobilisation shifts, the density of immobilised aptamer on the solid surface was evaluated in terms of molecules/cm$^2$. In the case of the SPR device, a density of about $10^{13}$ molecules/cm$^2$ was calculated for different 15-mer oligonucleotide sequences, assuming that a shift of 1000 RU corresponds to 0.8 ng/mm$^2$, as reported in the Biacore User Manual. In the case of the QCM device, a density of about $10^{13}$ molecules/cm$^2$ was also calculated assuming 1 Hz = 2 ng/cm$^2$, according to the Sauerbrey equation (Equation 1.1). However, it should be noted that the Sauerbrey equation is valid only for a dry crystal operating in air. When working in solution, additional viscoelastic contributions to frequency changes should be taken into account at the level of the layer absorbed at the crystal and the surrounding electrolyte. Furthermore, water molecules entrapped into the layer could also give a contribution to the mass increase at the sensor surface. In order to correct changes of frequency connected with viscoelesticity, some authors have suggested the introduction of a correction factor of approximately 2 to the calculated number of molecules/cm$^2$ [73;

147; 148]. However, even if this correction had been taken into account, similar surface densities would have been calculated for all the analysed oligonucleotide sequences.

Both in the cases of thrombin and CRP, improved analytical performances of the assays were observed on decreasing the aptamer concentration from 1 μM to 0.5 or 0.1 μM, respectively, even if the dilution did not affect the surface capacity. In addition, the influence of a thermal treatment on the aptamer was studied. Prior to the immobilisation step, the aptamers were denatured by incubation for 10 minutes at 95 °C, followed by rapid cooling on ice. This methodology is routinely executed with DNA or RNA probes with the aim of unfolding any pre-existing 3-D structures that may interfere with target binding [147; 146; 139]. Results for thrombin detection showed that aptamer denaturation improved the efficiency of the assay in terms of linearity and reproducibility and for this reason the thermal treatment was adopted also for C-Reactive Protein detection. However, Baldrich *et al.* [143] reported that TBA denaturation was not needed for the assay's optimal performance, but this result might be due to the presence of KCl, which promoted the folding of the quadruplex structure.

### 4.1.2. Optimisation of the binding conditions

The first critical parameter to be taken into account in the optimisation of the binding event was the binding buffer. The buffer system applied during the SELEX process is of critical importance for subsequent aptamer-ligand binding experiments [149]. Even though the binding buffer used in the SELEX process for the aptamer identification should ensure the optimum protein-aptamer interaction in solution, the effect of factors such as pH, ionic strength and presence of particular ions could affect or promote the binding in the heterogeneous phase. For this reason, the binding buffer to be used in the assay had to be optimised both in the case of thrombin and CRP detection.

In the case of thrombin, 20 mM Tris-acetate, pH 7.4, 140 mM NaCl, 5 mM KCl, 1 mM $CaCl_2$, 1 mM $MgCl_2$ was employed by Bock *et al.* [54] for the selection of the 15-mer thrombin aptamer, while the use of 50 mM Tris HCl, pH 7.5, 100 mM NaCl, 1 mM $MgCl_2$ resulted in the selection of the 29-mer aptamer [55]. In this work, different binding buffers were tested in order to find the best interaction conditions with thrombin and improved performances in terms of sensitivity and reproducibility were obtained with a buffer very similar to that employed by Tasset *et al.* (50 mM Tris-HCl, pH 7.4, 140 mM NaCl, 1 mM $MgCl_2$), not containing potassium ions. Several authors demonstrated that $K^+$ had a stabilising effect on the thrombin-aptamer interaction in aqueous solution, because $K^+$ is believed to shift the equilibrium toward the TBA quadruplex conformation [54; 56; 64; 150; 151]. The various aptasensors for thrombin detection reported in literature were employed with binding buffers at neutral pH, but a slightly different ionic strengths and in the presence of $K^+$ compared to the ones used in the SELEX processes. Nevertheless, it has been reported that the quadruplex structure of the TBA is thermodynamically stable even in the absence of KCl, at temperature lower than the TBA melting temperature, which depends upon the ionic strength [143]. The aptamer-thrombin interaction upon DNA folding has been observed even in pure water [152]. However, the quadruplex structure that was formed in the absence of $K^+$ or other small ions had an intramolecular configuration different from that existing in the presence of cations [153], while the formation of a bimolecular, and not monomolecular, guanine quadruplex was observed at very low ionic strength [154].

In the case of CRP detection, the best analytical performances were found when employing 10 mM HEPES pH 6.5, a buffer slightly different in ionic strength, pH and salt content compared to the one used in the SELEX process for the aptamer selection (50 mM Tris-HCl, pH 7.4, 100 mM NaCl, 5 mM KCl, 1 mM $MgCl_2$, 0.1 % $NaN_3$) [88]. Furthermore, it was observed that the addition of calcium ions to the binding buffer promoted the binding event with CRP, resulting in an increase in the aptamer-protein complex stability, with consequent increase in aptasensor sensitivity. In fact, it has been reported that in the absence of calcium, the pentameric CRP structure dissociated to monomers [94]. Under the optimised working conditions, the minimum detectable amount of analyte was 0.005 ppm CRP using the SPR device, in the CRP concentration

range 0 - 0.1 ppm, with good linearity ($R^2$ = 0.982). As a comparison, a minimum detectable amount of analyte of 1 ppm was found with another label-free biosensor based on surface plasmon resonance for CRP detection in standard solution, using antibodies as recognition elements [108].

In the case of thrombin detection with the QCM device, a minimum detectable amount of analyte of 50 nM thrombin was recorded employing the optimised working conditions, in the thrombin concentration range 0 - 200 nM. An increase in the aptamer-protein interaction time (from 20 min to 30 min) resulted in an improved binding efficiency in terms of linearity ($R^2$ = 0.998), in accordance with other reports [143], where up to 90 minutes of incubation had been employed. Other label-free aptasensors for thrombin detection have been reported, based on the quartz crystal microbalance [73] and surface acoustic wave (SAW) devices [69; 155]. In the case of QCM [73], a detection limit for thrombin of 1 nM in buffer was reported, even if this datum was not supported by the study of other important analytical parameters such as specificity, reproducibility or matrix effect. For SAW devices [69; 155], the reported sensitivity was in the same order of magnitude (submicromolar) as the proposed approach, but the analysis was limited to standard solutions.

Unlike proteins, which are irreversibly denatured in unfavourable conditions, oligonucleotides are capable of reversible denaturation. Consequently, aptamers can be subjected to repeated use, thereby realising a device where the analyte binding with the immobilised receptor is an almost completely reversible process. Target dissociation is generally realised by rinsing the surfaces with acid or basic solutions, as was observed in the case of CRP, where solutions of HCl or NaOH were employed for surface regeneration. In other cases, solutions having a high ionic strength were used to remove the target analyte from the surface, while the receptor layer was completely reconstituted simply by returning to the original buffer conditions. In fact, high concentrations of salt cause disruption of hydrogen bonds and electrostatic interactions responsible for most of the aptamer-target association. In agreement with the result reported by Baldrich *et al.* [143], the best regenerating solution for the TBA-thrombin complex was 2 M NaCl, probably because this solution induced a change in TBA or

thrombin folding, thus affecting their binding without damaging the oligomer structure. As a consequence, recovery of the quadruplex was facilitated as soon as the regeneration solution was replaced by the binding solution. Under the specific optimised working conditions, up to 22 cycles were realised on the same piezoelectric crystal for thrombin detection and up to 50 cycles were performed on the same SPR chip for CRP detection without decrease in sensitivity.

The specificity of the biosensor was tested for TBA aptamer as well as for CRP aptamer by the use of high concentrations of HSA, under the same experimental conditions as the target proteins. Since HSA is the most abundant protein in serum and plasma, where it is present at high concentration (~ 50000 ppm, i.e. 770 μM), human serum albumin was chosen as negative control. In the case of the TBA aptamer, the specificity of the piezoelectric aptasensor was demonstrated by employing a concentration of HSA corresponding to a 1400-fold excess with respect to thrombin, i.e. a 1:10 dilution of HSA with respect to the physiological concentration. In the case of the aptamer for CRP, the negative control test with the SPR device was conducted employing HSA diluted 1:100 with respect to the physiological concentration and a non-specific response was observed, corresponding to the 10% of the specific signal given by CRP at the same dilution factor. This poorer specificity of CRP aptamer with respect to TBA reflected its lower affinity constant ($K_D$ = 125 nM for CRP aptamer [88] *vs.* $K_D$ = 26 nM for TBA [54]), even if it compares favourably with the affinity of anti-CRP antibodies, with reported values for different clones of 440 and 550 nM, respectively [111; 113].

## 4.2. Aptamers as receptors for detection of proteins in complex matrices

One of the greatest challenges of protein assays is the development of fast, easy-to-use devices for detection of protein in complex matrices, with potentially wide applicability in diagnostics. Biosensors represent an interesting approach for protein detection because of their intrinsic characteristics such as real-time detection, fast analysis time, low cost and label-free analysis. The major problem currently encountered in biosensor development, when working with complex matrices such as serum and plasma, is the non-specific binding of protein, which results in high signal backgrounds and consequent decrease of assay sensitivity. In this work, the capability of aptamers to specifically detect their targets in complex matrix samples was investigated, using the different biosensor formats.

A few aptamer-based biosensors have been developed for detection of proteins of clinical interest (such as thrombin, platelet-derived growth factor (PDGF) and vascular endothelial growth factor (VEGF)) in real matrices by making use of labels to enhance the signal. In particular, Lai *et al.* [156] reported the fabrication and characterisation of an electrochemical aptamer-beacon sensor (E-AB) directed against the blood protein PDGF, using Methylene Blue (MB)-modified PDGF-binding aptamer attached to a gold electrode. The E-AB sensor was employed directly in complex, contaminant-ridden samples, such as serum diluted 1:1 and undiluted blood serum and yielded a detection limit of 50 pM and rapid sensor response (10 min – 1 h). After a regeneration step, the sensor was reusable up to 5 times before unacceptable degradation was observed. On the basis of the same principle, a MB-modified thrombin-binding aptamer was employed for electronic detection of the analyte in 50 % diluted human serum spiked with thrombin [75].

Drolet *et al.* [157] used the anti-VEGF aptamer to quantify the analyte in serum via a sandwich type microtitre plate assay. An enzyme-linked oligonucleotide assay (ELONA) was realised using a monoclonal antibody directed against hVEGF as capture

reagent and a fluorescein-tagged version of the hVEGF-binding oligonucleotide as detection reagent. After a final incubation with alkaline phosphatase conjugated with antifluorescein Fab fragments, signal was generated using a chemiluminescent alkaline phosphatase detection system. The theoretical DL in rat serum was 25 ppt, with no significant cross-reactivity for other serum proteins, such as Placental growth factor (PlGF), PDGF, fibroblast growth factor (bFGF), thrombin and cytokines.

A recent electrochemical sandwich approach based on the use of an enzyme as traditional amplifying label and aptamer-functionalised magnetic beads was developed and applied to the detection of spiked thrombin directly in human plasma [84].

### 4.2.1. Detection of Thrombin in a complex matrix

In this work, a direct approach to detection of human proteins in complex matrix was attempted using label-free aptamer-based biosensor formats. In the case of the TBA aptamer immobilised on the gold surface of a quartz crystal microbalance, the detection of thrombin spiked in complex media was successfully demonstrated. In particular, human serum diluted 1:100 and human plasma diluted 1:100, after the selective precipitation of fibrinogen to avoid sample clotting, were employed. The selective semi-quantitative precipitation of fibrinogen by addition of a high ionic strength solution is a standardised procedure in clinical analysis [158; 159]. Different thrombin concentrations in the analytical range 0 - 200 nM could be detected in treated human plasma with good linearity ($R^2 = 0.990$) despite a high background signal (-21 Hz) due to the complexity of the solution. Thus, the ability of the TBA to detect the analyte in complex matrices demonstrated the potential of aptamer-based sensing for medical investigations. However, due to the high dilution factor, the sensitivity achieved was not sufficient for a direct application of the aptasensor to the detection of thrombin in real samples. Compared to other reported aptamer-based protein detection biosensing methods which have been applied to complex matrices analysis [75; 84], the proposed

approach was able to directly detect the analyte in human biological fluids with negligible matrix effect. Conventional assays for the detection of thrombosis markers in blood include immunochemical assays for active pro-coagulants or activation peptides. The conventional assays of blood coagulation are usually indirect because the end point is represented by the clotting fibrinogen, which is dependant not only on thrombin levels but also on many other factors [59]. In addition, by using the available technologies for evaluating clinical hemorrhagic risk or thrombosis, i.e. the addiction of tissue factor, most of the generated thrombin is ignored since the formation of the fibrin clot occurs at 10-30 nM thrombin, which is the 3% of the total amount of thrombin produced during the reaction [160]. For these reasons, a direct label-free assay for the detection of the presence of thrombin in blood could have an important diagnostic value for the study of diseases associated with coagulation abnormalities [59].

### 4.2.2. Detection of C- Reactive Protein in a complex matrix

In this work a direct detection of CRP in diluted human serum was also attempted, by the use of CRP aptamer immobilised on a SPR chip. Unfortunately, despite filtration, dilution and introduction of a sample pre-treatment, the measurement of spiked CRP in human serum was not achieved because of a large matrix effect.

It has been generally recognised that matrix interference limited the success of SPR biosensor system in the study of binding events in complex biological samples, because of the inability to control non-specific adsorption [161]. Actually, SPR measures any change of refractive index at the probe surface, thus non-specific binding will produce a signal indistinguishable from specific binding, despite the use of carboxylated-dextran derived chips. In fact, dextran flexible chains which extend approximately 100 nm in aqueous solution, form a highly hydrophilic surface with little tendency for non-specific adsorption of proteins and other biomolecules, providing a barrier between biomolecules and the gold substrate [136]. Various strategies have been employed to

resolve the problem of non-specific binding in real-time biospecific interaction analysis, such as a method for measuring anti-myoglobin in bovine serum by SPR using chips where CM-dextran was replaced by other biocompatible polymers [162]. Recently, a method for minimising non-specific binding of bovine serum components to the surface of CM-dextran coated chips has been proposed [163]. Bovine leptine protein (in concentration > 10 ppm) was measured in bovine serum diluted 1:10 in an optimised buffer having high ionic strength and containing carboxymethylated dextran to reduce the non-specific adsorption on the surface. However, direct detection of proteins in a complex matrix by SPR measurements using Biacore CM5 chips has been successfully demonstrated [164], by immobilising an antibody specific for vitellogenin and adding a solution of target protein spiked in fish plasma diluted 1:500. Furthermore, SPR-based immunosensing was very recently applied to CRP detection in human serum [109], but the main limitation of this approach was the single use of a valuable chip, the functionalisation of which via amide-linked NHS-dextran was time-consuming. In fact the CRP, spiked in serum diluted 1:10, was directly immobilised on the chip and probed with anti-CRP antibody, the signal was further enhanced by using anti-IgG as a secondary antibody. Protein immobilisation on the sensor chip prevented any reuse of the surface, thus each measurement was conducted on a different chip. In contrast, the approach proposed in this work is based on the reuse of the sensing surface, facilitated by dissociation of the affinity complex.

In the proposed approach, filtration and dilution 1:100 of human serum with binding buffer did not appear to have an effect on reducing unspecific adsorption on the surface modified with the CRP aptamer, since a clear matrix effect was observed, mostly caused by immunoglobulins, which represent the main class of proteins in serum. As with other proteins of interest as potential biomarkers for diseases, CRP is present in serum at ppm levels, making it difficult to detect among abundant proteins such as IgG and HSA, which constitute more than 85% of the bulk mass of the total proteins in plasma [165]. Further dilution of serum was avoided, since the minimum detectable amount of analyte of CRP in standard solution corresponded to a dilution of 1:200 with respect to its physiological concentration (1 ppm).

Since high abundance proteins tend to mask lower abundance ones in serum analysis, different commercial methods for specific depletion of IgG and HSA have been proposed at high removal rates (> 95%) [166]. Among these, magnetic beads and purification columns are used coupled to Protein G, which specifically binds the Fc region of IgG, realising a biological affinity separation. In another approach [167], a column packed with Immunoglobulins Y immobilised on microbeads was used to remove serum abundant proteins, but successful detection of CRP was realised only at very high concentrations (370 ppm), which was completely out of the significant range as a clinical biomarker (1-10 ppm). In fact, the major problem with separation methods is the potential loss of non-abundant proteins by inadvertent capture, which causes depletion of important biomarker candidates during the protein depletion process. A comparison among different commercial kits for removing high abundant proteins from serum samples has been recently reported, showing the importance of this up-to-date issue and confirming the lost of several clinically interested proteins upon elution, due to interaction with HSA or binding to column [168]. As a consequence, some proteins might be completely withdrawn from the analysis.

In this work, different sample pre-treatments, such as magnetic beads, affinity columns and a commercial reducer of non-specific binding (NSB-Reducer) were introduced, with the aim of removing IgG or both IgG and HSA from the matrix, and reducing the non-specific adsorption on the surface. In particular, the contribution of HSA and IgG to the matrix effect was studied by using magnetic beads for the treatment of simulated serum solutions containing hIgG and HSA or hIgG, HSA and CRP corresponding to a dilution 1:100 with respect to physiological concentration. Since the recorded SPR signals were lower than those recorded for each single component, an interaction effect between the proteins occurred. In fact, albumin is a well known carrier and transport protein in serum [166].

Based on the same principle, disposable affinity columns for depletion of both IgG and HSA were used to treat human serum and the treated solution was supplemented with a commercial non-specific binding reducer. Since NSB-Reducer contained carboxymethyl dextran, its structure was similar to the dextran matrix on the sensor

surface. Consequently, by adding NSB-Reducer to the complex matrix prior of injection, the non-specific binding of complex sample components to the surface was reduced via a competition effect. It has been reported that non-specific binding levels should be reduced in the range 69-98 % without affecting the measurements of specific binding interactions (www.biacore.com). In this work, a drastic reduction of interfering signal was achieved by combining purification columns with the commercial non-specific binding reducer, but it was not possible to measure significant concentrations (0.2 – 0.3 ppm) of CRP spiked in these treated matrices. Probably, spiked CRP was captured by NSB-Reducer in solution and as a consequence only a weak interaction with the immobilised aptamer was observed upon injection.

The low ability of the CRP immobilised aptamer to recognize its target in complex matrix could be also due to a lack of specificity and stability, since this is an RNA aptamer, which is subject to RNase degradation. For this reason the pyrimidine nucleotides of the CRP aptamer sequence were chemically modified with 2' fluorine functional groups, with the aim of increasing the aptamer stability in biological fluids [169]. A lower sensitivity and reproducibility for the modified aptamer was found together with a higher minimum detectable amount of analyte compared to the unmodified aptamer (0.015 ppm vs 0.005 ppm). Probably the 2'-F modification affected the folding of the oligonucleotide sequence upon binding to the target protein. The main advantage that 2'-F modification offered was the possibility to facilitate the working conditions, operating in buffers prepared in MilliQ water and avoiding those special precautions necessary for working with RNA sequences, in the attempt to realise a "RNase free" environment. As a consequence, experimental time was reduced and ease of analysis was achieved. Despite the increase in aptamer stability, direct detection of spiked CRP in diluted serum was not yet achieved due to the matrix effect. For this reason the possibility to realise a sandwich assay with CRP aptamer as immobilised receptor as well as secondary affinity ligand was evaluated, with the aim of amplifying the specific signal or realising an indirect assay for CRP detection in complex matrices.

## 4.3. Selection of Thrombin-binding aptamers by a computational approach

Combinatorial techniques are used to generate libraries of millions of oligonucleotides [170]. Huge libraries have been employed in selection techniques to discover new sequences capable of binding with high affinity and selectivity to a target molecule. The introduction of a computationally-assisted prediction could reduce the experimental work currently employed in SELEX or non-SELEX methods for aptamer selection. It might also avoid experimental issues currently encountered, such as reagent instability and inaccuracy as well as lack of sensitivity and selectivity of each of the employed techniques in a multi-step selection processes.

Computational approaches are routinely applied to identify candidate compounds for new drugs using information obtained from the target structure, because of the necessity to use cost- and time- effective ways to find lead compounds [171]. Docking methods are used to identify the pose of a ligand in the protein binding site and to predict the affinity between a protein and a ligand, by screening a library of potential candidates as ligands. Information required for the docking approach are the three-dimensional structures of protein and ligand at atomic resolution. A huge number of protein and ligands complexes have been resolved by X-Ray crystallography, NMR, mass spectrometry and other spectroscopic techniques and their structures have been deposited into public repositories such as Protein Data Bank.

In this work, a computational method developed to screen databases of drug-like molecules was adapted to screen a database of oligonucleotides, with the aim of introducing a novel technique able to find new aptamers. The DNA aptamer that binds to thrombin (TBA) was chosen as a model, because it is one of the most well characterised. Its structure has been determined [56], as well as its binding site [66; 67] and its stability *in vivo* and *in vitro* [172]. The 15-mer TBA sequence was identified by SELEX as the minimal consensus sequence (5'-GGTTGGTGTGGTTGG-3') from a pool of ~$10^{13}$ 96-mer oligonucleotides containing a randomised 60-mer sequence [54].

Actually, the TBA sequence was one of a family of DNA oligonucleotides containing the consensus sequence d(GGNTGG$N_{2\text{-}5}$GGNTGG), where G and T were invariant nucleotides and N was variable, but with a bias for a particular nucleotide. Starting from the TBA sequence, an *in silico* post-SELEX procedure was introduced by performing mutations in one or two positions of the 15-mer and calculating the affinity of each ligand for thrombin on the basis of a binding score. For this purpose, the three-dimensional NMR structure of the thrombin-aptamer complex was used to study the interaction between thrombin and different nucleotide sequences, in order to investigate the influence of different mutations in different positions of the sequence on the binding affinity towards thrombin.

The three-dimensional structures of TBA and 990 mutated sequences were virtually created in Hyperchem 7.5 in helix conformation. Using the open-source Openeye Scientific Software Inc., this library of oligonucleotides was screened for the ability of each compound to bind thrombin, after energy minimisation and conformational search steps. The theoretical number of mutated sequence to be created was astronomical, but had to be reduced to 990 by restricting to 2 the maximum number of mutations performed in each sequence, in order to reduce the calculation time. Since the TBA sequence was formed only by guanines and thymines, and a maximum of two mutations were introduced, a library of G-rich oligonucleotides was generated.

The ability of G-rich oligonucleotides to bind a specific protein is not related to the nucleic acid primary sequence, but rather binding specificity depends upon the three-dimensional structure [173]. A typical characteristic of G-rich nucleic acids sequences is the formation of G-quartets. Many kinds of guanine quadruplexes have been observed, depending upon the number of molecules in the quadruplex (intramolecular, bimolecular, tetramolecular and octamolecular), mutual orientations of strands (parallel, antiparallel), position of the loops in the quadruplex, and syn-anti glycosidic orientations of guanine residues [154]. Therefore, G-rich nucleic acids can form a variety of possible quadruplex structures depending on both thermodynamic and kinetic considerations [174]. In the case of TBA, the aptamer folded structure, referred to as the "chair conformation", presents four guanines forming two G-quartets through base-

pairing, aligning in a planar arrangement [64] and connected by two TT loops and a TGT loop [56]. However, the aptamer binding conformation depends upon the binding conditions. NMR studies have shown that the quadruplex structure formed in the absence of $K^+$ or other small ions had an intramolecular configuration different from that existing in the presence of cations [153]. In addition, circular dichroism studies showed that TBA generated a bimolecular, and not monomolecular, guanine quadruplex at very low ionic strength, i.e. in 1 mM sodium phosphate, at pH 7 [154].

In this work a database of G-rich oligonucleotides was screened for their binding affinity towards thrombin by means of *in silico* docking experiments. Current research is focused on solving several issues of computational docking, such as ligand flexibility, molecular size, tautomeric equilibrium, protonation state of ligands and aminoacids in the binding pocket [175]. Because of the high computational cost that flexibility implicates, most docking programs assume the protein to be rigid and the ligand to be flexible. In the case of Openeye Scientific Software, the docking program FRED applied a Gaussian shape fitting function to optimise the contact surface between the ligand and the protein, thereby allowing an extremely fast rigid-docking procedure. The flexibility of the ligand was represented by a set of conformers for each ligand, generated by the tool Omega, thus improving the rigid-body docking accuracy. In this work, an average of 53 conformers was generated for each sequence and this average number was consistent with other work making use of Omega [176; 177].

Docking of a virtual database of ligands against a specific target aims to distinguish binders from non binders and even high affinity binders from low affinity binders on the basis of a binding score. Each docked pose is scored and ranked according to the protein-ligand binding affinity, represented by the binding score, which allows a direct comparison between different ligands. Different scoring functions have been developed [178], but the choice of the proper scoring function for a particular protein-ligand system still remains a challenge in molecular modelling. In fact none of the scoring functions can be generally applied to different targets and databases, since systematic docking errors occur in all programs [175]. In particular, in this work FRED was applied to dock ligands having a 3-fold higher molecular weight than the maximum one

(1500 g/mol) for which FRED was designed to work. When ligands having high molecular weight are docked, the binding scores are overestimated because of the large molecular surface area, resulting in a larger number of unspecific interactions with the protein [46; 175]. Among the scoring functions that FRED supports, Shapegauss was the only one that could be fit to work with large ligands, because it only finds shape complementarity instead of chemical complementarity and uses less computational memory (Warren, G., Openeye Scientific Sofware, Inc., personal communication). Together with physical-chemical features, shape complementarity is essential in determining protein-ligand binding affinities. As an example, Shapegauss and other open-source methods have been developed for performing shape-complementarity search as a first step to rapidly reduce the size of a large compound database, prior to use more accurate but slow docking/scoring computations [177].

The FRED strategy is to exhaustively dock and score all possible positions of each ligand by performing rigid rotations and translations of each conformer within a binding box created by the user. Poses that clashes with the protein or that do not have enough contacts with the receptor are rejected. In this work the aptamer-thrombin docking area was defined as a box of 25803 $Å^3$ for the fibrinogen binding site and of 28427 $Å^3$ for the heparin binding site, in order to contain the whole aptamer structure. The chair-shaped aptamer was docked as a reference and the top-ranked pose received a binding score of –1762 and -1373, in the fibrinogen and heparin exosite respectively. These reference binding scores were significant lower than the ones obtained from docking of TBA structure drawn in helix conformation and minimised (binding score -1422 and -982, respectively in the fibrinogen and heparin binding site). However, these reference binding scores were very similar to those obtained from docking of the candidate mutated sequence subjected to the same procedure of TBA (drawing in Hyperchem, energy minimisation and conformer search) and named “Best” because of the top-ranked hit-list positions (binding score -1748 and -1364, respectively).

Thrombin displays two positively charged exosites where DNA sequences are expected to bind and both these binding sites were taken into account for the simulations. In fact, the two basic sites which are able to interact with acidic regions of thrombin-binding

molecules (fibrinogen, heparin, hirudin, thrombomodulin), are likely targets for oligonucleotides, because of the polyanionic nature of the nucleic acid phosphodiester backbone [64; 179]. X-Ray and NMR studies showed that TBA interacted in the fibrinogen binding site of thrombin as well as in the heparin binding site of a symmetry-related molecule [66; 67]. From the analysis of the binding scores it appeared that TBA and the most of the mutated sequences preferably bound to the fibrinogen than to the heparin binding site. However, in this study only 15-mer nucleotides were considered starting from the TBA sequence isolated by Bock *et al.* [54]. The 29-mer thrombin aptamer isolated by Tasset *et al.* [55] and reported to interact in the heparin binding site, forming a more stable complex with thrombin than TBA, was not taken into account because of the dimensions and the molecular weight of this structure, with consequent problems in docking accuracy and computational time and memory.

Results extrapolated from computational procedure were verified by correlating the binding scores with the analytical performance of biosensors developed by immobilising TBA and other mutated oligonucleotides, selected on the basis of their binding score, onto optical chips. Other comparative studies between binding scores obtained from a database of candidates and experimental results obtained by testing the ability of ligands to bind a target were reported, but only oligopeptides [180; 7; 181; 176] or small organic compounds [182; 183; 184; 185] were employed as potential ligands. Few of these reports [176; 184; 185] used Openeye Scientific Software to perform docking simulations. In particular, a computational study making use of Hyperchem for library creation and of the Openeye algorithm FRED for database screening was applied to select oligopeptides binding to protein internalin, and an experimental verification was carried out by colorimetric competition assays [176]. Other studies employed different docking programs such as Leapfrog® [180] or Gold [7] to select rational designed oligopeptides to be experimentally tested using a QCM in a biosensor format.

For the aim of this work, three mutated sequences were experimentally tested by SPR measurements. In particular, a sequence mutated in position 5 with a thymine and in

position 14 with an adenine was selected because of strong binding to thrombin, both in the fibrinogen and heparin binding site. A sequence mutated in position 4 with an adenine and in position 15 with a cytosine was selected by virtue of being the worst candidate for binding thrombin in both the exosites. Finally, a sequence mutated in position 3 with a cytosine and in position 11 with an adenine was selected because it was docked with similar binding scores in the two exosites. Despite successful immobilisation of all the tested sequences, preliminary results showed that, in contrast to the TBA, the immobilised mutated sequences were not able to recognise the target under the previously optimised binding conditions. On the contrary, a binding interaction for all the probed sequences was observed upon a harsh reduction in ionic strength of the binding buffer. Therefore, it appeared that the mutated sequences identified by computational approach were able to recognise the target only when the experimental conditions were close to the conditions employed in the simulations. In fact, affects associated with solvent such as ionic strength and presence of particular ions were not taken into account in the computations. For this reason, in the SPR measurements the binding buffer routinely employed in thrombin-aptamer recognition assays was diluted, in order to find the minimum ionic strength able to assure the formation of a stable complex between thrombin and the mutated sequence. Even at extremely low ionic strength an interaction between aptamer and thrombin was observed. In fact it has been shown that the TBA-thrombin recognition event upon aptamer folding in the quadruplex structure, occurred at very low ionic strength [154] and also in pure water solution [152]. Only the binding buffer ionic strength was changed, while its pH was maintained at 7.4, which was the optimum pH found in this study and in reports by other workers [147], because it avoided the protein becoming charged during the binding event. In fact, thrombin is known to have a pI of 7.0-7.3-7.6 in three isoionic forms [186] and thus is expected to remain almost neutral when the binding buffer pH is equal to its pI, and to readily adhere to both apolar and negatively charged surfaces [187; 188].

Experimental results obtained using binding buffer diluted 1:50 confirmed the computational results, since slightly improved analytical performances in terms of sensitivity and reproducibility were obtained for the sequence named “Best” compared

to TBA or "Medium", while significantly poorer results were obtained for the sequence named "Worst". These results appeared to prove the ability of FRED to discriminate between high binding and low binding sequences through the *in silico* procedure adopted in this work. This finding was surprising given the numerous limitations of computational experiments mentioned above, but also because top-ranked docked molecules are often unable to bind the target at reasonable concentrations [44]. Indeed, in this work four calibration curves were obtained in the same thrombin concentration range (0-50 nM), with the same experimental detection limit (5 nM), but differing in sensitivity and reproducibility of measurements. High error bars observed were probably due to the sub-optimal working conditions, but also to thrombin degradation once the stock solution was unfrozen and diluted.

The findings of other workers [54; 55; 189; 190] were consistent with these computational results. In fact, several mutated sequences are reported in literature for their lower ability to inhibit thrombin in comparison with TBA. The capability of these sequences to inhibit thrombin-catalysed conversion of fibrinogen to fibrin was determined by measuring the clotting time. Unfortunately, clotting times determined for the same sequence by different groups were not directly comparable because they were calculated for different experimental conditions, in terms of dilution buffer, thrombin concentration, oligonucleotide concentration and matrix (purified fibrinogen or human plasma).

Three 15-mer sequences (named "a" [54], "b" and "c" [55]) known for their low capability to inhibit thrombin were drawn in Hyperchem and added to the library of mutated oligonucleotides to perform docking experiments. Two of these sequences were bottom-ranked in the binding score lists referred to both the thrombin exosites, while the docking of sequence "c" failed in both the binding sites. Bock *et al.* [54] carried out inhibition tests by incubating TBA or "a" sequence (in concentration 100 nM) in a solution of 2 mg/ml of purified fibrinogen (in selection buffer) for 1 min at 37 °C and measuring the clotting time after the addition of thrombin (13 nM). Fibrin formation was observed after 169 seconds in presence of TBA, compared with 26 seconds in presence of the scrambled sequence "a" and with 25 seconds in the absence of DNA.

The inhibition test was carried out also in human plasma, where the TBA aptamer showed a less potent anti-clotting activity (43 sec) compared to the solution of purified fibrinogen.

Tasset *et al.* [55] identified the low-binding mutated sequences "b" and "c" by measuring dissociation constants for the thrombin-aptamer complexes: $K_D$ > 1000 nM were determined for both "b" and "c" sequences, in comparison with $K_D$ = 26 nM for TBA [54] and $K_D$ = 0.5 nM for the 29-mer thrombin aptamer interacting with the heparin-binding exosite [55]. Furthermore, inhibition tests were carried out in 2 mg/ml of purified fibrinogen, after the addition of 200 nM DNA sequence and thrombin. The clotting time was 156 sec for TBA, compared with 17 sec for sequence "b" and 34 sec for the 29-mer aptamer.
Making use of the SELEX process Macaya *et al.* [189] identified a group of DNA structures able to bind thrombin more strongly than TBA. These sequences contained a quadruplex/duplex motif consisting of a central 15-mer that could be mutated in the TGT or TT loops with respect to the 15-mer TBA, flanked by additional 4-7 complementary base pairs. Since these selected oligonucleotides were longer (24 - 48 mer) than the 15-mer, a direct comparison with the computational results could not be performed. However, a 15-mer sequence mutated in position 9 with an adenine (Code T9A) was identified for binding to thrombin and its inhibition activity was evaluated by measuring the clotting time following the procedure described by Bock *et al.* [54]. Computational result was consistent with that reported by Macaya *et al.* [189], since a decrease in binding score % corresponded to a worse inhibition activity.

A correlation between binding scores and inhibition ability of sequences identified by Bock *et al.* [54], Tasset *et al.* [55], and Macaya *et al.* [189] is reported in Table 16, with regards to the binding scores obtained for the Fibrinogen-binding site, where the 15-mer sequences are expected to bind, inhibiting the fibrinogen conversion to fibrin.

| Code | Binding score % (Fibrinogen binding site) | DNA concentration for inhibition test (nM) | Clotting Time (sec) | Ref |
|---|---|---|---|---|
| TBA | 81.3 | 100<br>200<br>100 | 169<br>156<br>172 | [54]<br>[55]<br>[189] |
| a | 51.9 | 100 | 26 | [54] |
| b | 58.5 | 200 | 17 | [55] |
| T9A | 77.5 | 100 | 123 | [189] |

**Table 16. Correlation between binding score and clotting time for different 15-mer DNA sequences having a lower capability to inhibit thrombin compared to TBA. Mutated sequences "a", "b" and T9A were identified and tested by Bock *et al.* [54], Tasset *et al.* [55] and Macaya *et al.* [189], respectively.**

In addition, the findings reported by Ikebukuro *et al.* [190] were correlated with the computational results. Ikebukuro *et al.* described an evolution-mimicking algorithm (i.e. a genetic algorithm which mimics Darwinian evolution) for searching aptamers showing an inhibitory activity towards thrombin, in order to restrict the number of aptamers to be assayed. In fact, since binding sequences identified by SELEX might bind to the target protein without affecting its activity, inhibition assays of different nucleotide sequences are usually carried out one by one. Making use of the described evolution-mimicking algorithm, 16384 sequences were virtually generated by introducing mutations. Ten of these sequences were synthesized and clot-inhibition assays were carried out by measuring the clotting time. A decrease in the inhibitory effect was observed if the TGT loop or the T12T13 loop was mutated, because of the alteration of the binding structure. Five of the analyzed sequences presented only one or two mutations with respect to the TBA, therefore the results for these oligonucleotides were correlated with the results achieved in this study, taking into account the binding scores obtained for the Fibrinogen-binding site (Table 17), where the 15-mer sequences are expected to bind inhibiting the fibrinogen conversion to fibrin. This comparison study showed a good correlation between the inhibition activity reported by Ikebukuro *et al.* [190] and the evaluation of the thrombin-aptamer interaction resulting from the

computational method. In fact, a decrease in inhibition activity corresponded to a lower binding score compared to TBA.

| Code | Binding Score %<br>(Fibrinogen binding site) | Clotting time (sec)<br>Ref. [190] |
|---|---|---|
| TBA | 81.3 | 63 |
| G8T,T9G | 73.4 | 30 |
| T7G,G8C | 71.1 | 19 |
| T7A | 69.8 | 20 |
| T7G | 66.6 | 31 |
| G8C | 63.0 | 18 |

**Table 17. Correlation between binding score and clotting time for different 15-mer DNA sequences having a lower capability to inhibit thrombin compared to TBA. Mutated sequences were identified and tested by Ikebukuro *et al* [190].**

To sum up, a good correlation was found between binding score and preliminary SPR experimental results conducted with TBA and the three mutated sequences "Best", "Medium" and "Worst". In addition, computational results corroborated with experimental results carried out by other groups, which performed inhibition tests in order to verify the lower potential inhibiting activity of mutated sequences compared to TBA. Sequences mutated in the 15-mer motif and binding to thrombin with higher affinity than TBA were identified [189], but unfortunately it was not possible to correlate their clotting times with the binding score because these oligonucleotides were longer than 15-mer, having additional motifs attached to the 15-mer.

# CONCLUSIONS AND FUTURE WORK

Artificial receptors such as aptamers represent an attractive alternative to antibodies for analytical assays and devices. Aptamers are generated through selection methods carried out *in vitro*, which allow chemical production of DNA or RNA affinity molecules showing high specificity and selectivity comparable to antibodies. So far, aptamers have found different applications in analytical chemistry, ranging from separation techniques to biosensors.

In this work, aptamers have been employed as new receptors for the development of biosensors. The DNA aptamer specific for thrombin (TBA) was chosen as a model for biosensor development, being one of the most well known and characterised. In fact, TBA was the first aptamer to be selected by the SELEX procedure [54] for a protein with no known physiological binding to nucleic acids. This highly specific aptamer was coupled with a piezoelectric transducer with the aim of realising detection of a protein target in heterogeneous assays. Different parameters influencing the analytical performance (linearity, reproducibility, stability, selectivity) of this label-free and reusable sensor were considered, such as immobilisation procedure, presence of a spacer in the nucleotide sequence, thermal treatment of the aptamer, concentration of the aptamer, type of binding buffer, interaction time with thrombin and specificity against HSA. This work demonstrated how small variations in simple steps in the assay development could lead to much improved analytical performance. Therefore, the proposed study can be considered as a reference approach in aptasensor development.

In this work, the ability of label-free aptasensing to operate in complex matrixes was also studied. Even though the TBA aptamer has been used in several studies already, in only few cases has the possibility of detecting this protein in biological fluids been investigated, mainly making use of methods for signal enhancement. Indeed, in this work the direct detection of spiked thrombin in diluted serum and plasma was demonstrated, yielding the same minimum detectable amount as recorded in standard solution (50 nM), despite a relatively high background signal due to matrix effects. This result is of paramount importance for practical application of aptasensors as new, interesting and attractive devices for clinical diagnostics, and also for environmental and food analysis. In addition, in future, efforts could include the development of microarrays, which represent an interesting tool in aptamer-based methods, since a current challenge in diagnostics is the simultaneous detection of different proteins, with consequent reduction of analysis costs.

Because of the successful application of TBA as a receptor molecule for thrombin detection, another aptamer, i.e. the recently selected RNA aptamer targeted towards C-Reactive Protein [88], was used as recognition element in the development of an optical biosensor based on a Surface Plasmon Resonance transducer. So far, no application of this aptamer, studies on its employment, its structure nor the location of its binding on CRP have been described. Therefore, this work represents the first study of the interaction between the immobilised RNA aptamer and its target analyte, starting from the basic information available, i.e. the aptamer sequence.

Since each aptamer is unique in the three-dimensional binding configuration adopted upon binding to its specific target, extensive studies of assay parameters were necessary to obtain the optimal analytical system. For this reason, also in the case of CRP, different critical parameters potentially affecting the analytical performances of the aptasensor were evaluated. In particular the importance of a non-nucleotide spacer for an aptamer containing all the four nucleotides and the influence of calcium ions on aptamer-CRP complex stability was clearly demonstrated, together with studies on aptamer concentration, type of binding buffer and specificity towards HSA. Under the optimised working conditions a minimum detectable amount of 0.005 ppm CRP in

standard solution was achieved, which was a significant improvement on a previously described SPR antibody-based biosensor [108].

Since the experimental detection limit and the linear range were such as to allow quantification of CRP in physiological concentration, the detection of CRP spiked in real matrix was attempted. Experiments performed in 1:100 diluted serum suggested the need for a sample pretreatment to apply this aptasensor in complex solutions. Studies to reduce the interfering effect, mainly caused by IgG, were conducted by sample treatment with magnetic beads or affinity columns coupled with protein G, together with the introduction of a commercial non-specific binding reducer. Unfortunately, the low concentration of CRP in serum as well as its interaction with other proteins, or with the different methods employed to reduce the matrix effect, prevented the detection of spiked CRP in real samples. Also the use of the CRP aptamer modified with 2'-fluoropyrimidines, in order to increase its stability, did not result in a successful detection of physiological concentrations of CRP in serum. However, the possibility to realise a sandwich assay by interaction of the CRP aptamer with the CRP-aptamer complex can open a new route for detection of CRP in real matrix by signal enhancing or competitive assay. In addition, further efforts to minimise the matrix effect could be performed by diluting serum 1:500, thanks to the high sensitivity of the assay in standard solution. Finally, this study represents the starting point for future applications of the CRP aptamer with different transducers.

In the third part of this work, the possibility of introducing a computational method for aptamer selection was evaluated. Docking methods are routinely applied for drug discovery, but have also been successfully employed for selection of bio-mimetic peptides as well as for MIP design. The introduction of an *in silico* approach to aptamer selection could reduce the drawbacks and limitations currently faced by SELEX and other experimental procedures. For this reason, a computational method formerly developed for docking of small molecules to a protein active site has been adapted to docking of nucleotide sequences to the thrombin-binding exosites, with the aim of studying the interaction between protein and mutated oligonucleotides with respect to the thrombin-binding aptamer. The affinity of each mutated sequence towards thrombin

was described by a binding score, compared with the one obtained with the TBA. Therefore, a retrospective docking study was developed, also making use in this case of TBA as a model, since it is the most studied aptamer.

On the basis of their binding scores, three mutated sequences were chosen to be further employed in experimental tests performed with the SPR device, in order to test the reliability of computational results. In particular, the sequences showing the best, medium and worst binding score among the docked oligonucleotides were employed for the development of optical biosensors, the analytical characteristics of which were compared with those obtained for TBA. A good correlation between *in silico* selection and experimental results was found, although different working conditions (in terms of ionic strength) with respect to those previously optimised in this work were employed, in order to reproduce an experimental environment close to that computationally simulated. In addition, *in silico* results corroborated other experimental results reported in literature [54; 55; 189; 190]. In fact, eight mutated sequences tested for their lower capability of inhibit thrombin with respect to TBA received a worse binding score than TBA. Despite TBA the binding score corresponding to only 81.3% of the best candidate, the computational approach partially confirmed results observed in SELEX, identifying high affinity binding sequences (TBA) from low affinity binding sequences reported in literature. Further studies should be carried out in order to validate the proposed computational approach to aptamer selection. In particular, inhibition tests of the three experimentally probed mutated sequences should be performed and other mutated aptamers should be experimentally tested. In addition, consideration should be given to the mutated aptamers' binding mode to thrombin. This work could have a significant impact on future aptamer selection for sensors and diagnostics. In addition, this new research approach may encourage significant collaborative research in this field, with the objective of facilitating the development of new and improved algorithms.

# Appendix

For piezoelectric aptamer-based biosensor development for thrombin detection, the biotinylated 15-mer aptamer with polyT tail was immobilised on piezoelectric crystals and different parameters influencing the aptasensor analytical performance were evaluated. In particular, the influence of simple key steps (such as aptamer thermal treatment, aptamer concentration and binding time with the analyte) on aptasensor linearity, sensitivity and reproducibility was studied. Thrombin calibration curves obtained by varying these parameters are reported in Figure A1, A2, A3 and A4.

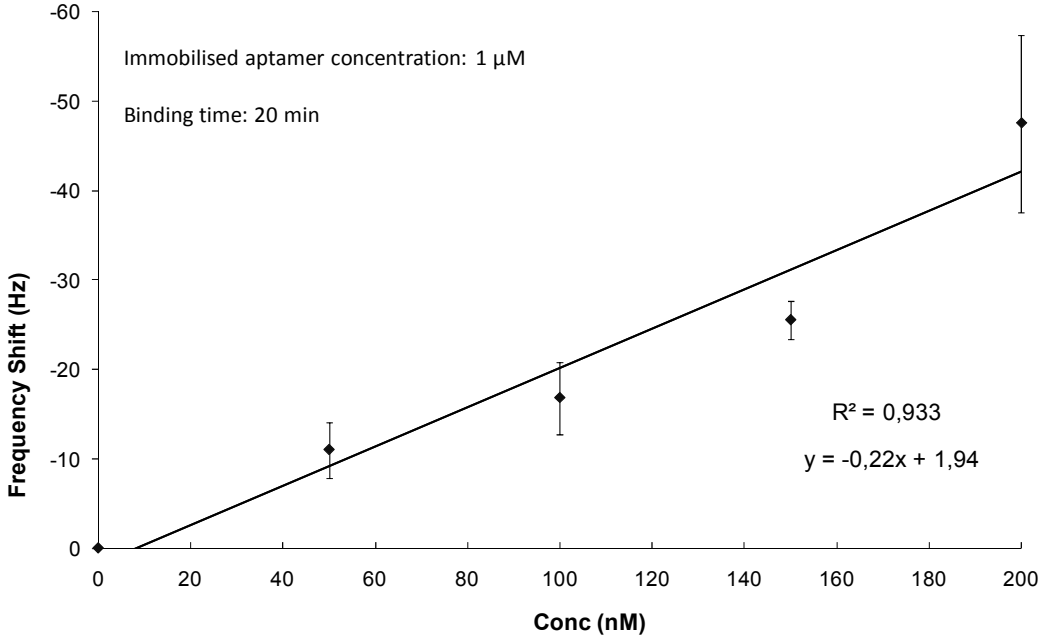


**Figure A1. Calibration curve for thrombin in the range 0-200 nM in binding buffer. Experimental parameters: concentration of 15-mer biotinylated aptamer with PolyT tail 1 µM; no aptamer thermal treatment; binding time 20 min. Each error bar represents standard deviation of three replicates (n = 3).**

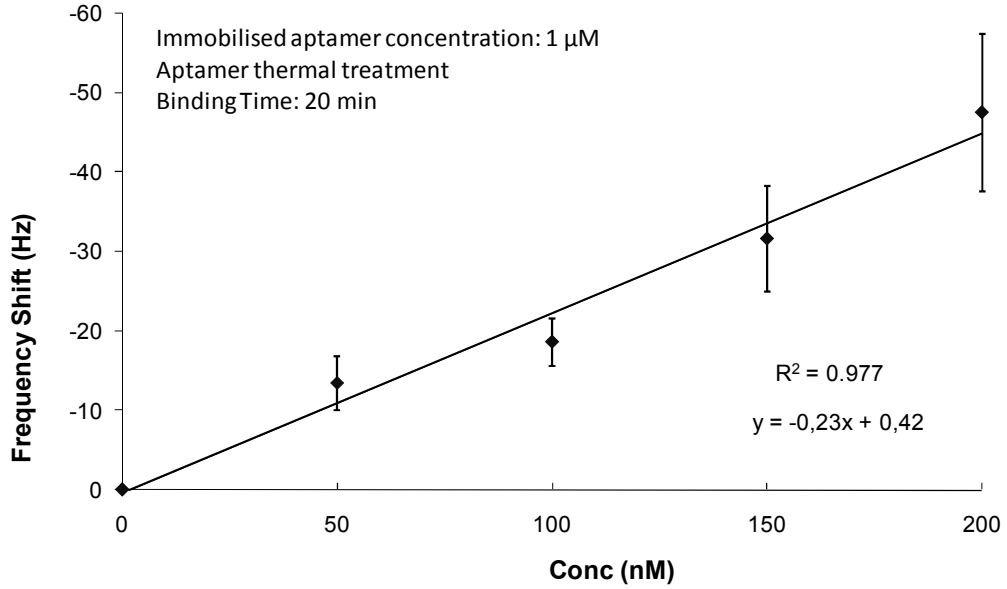


**Figure A2. Calibration curve for thrombin in the range 0-200 nM in binding buffer. Experimental parameters: concentration of 15-mer biotinylated aptamer with PolyT tail 1 µM; aptamer thermal treatment 95 °C 1 min, 0 °C 10 min; binding time 20 min. Each error bar represents standard deviation of three replicates (n = 3).**

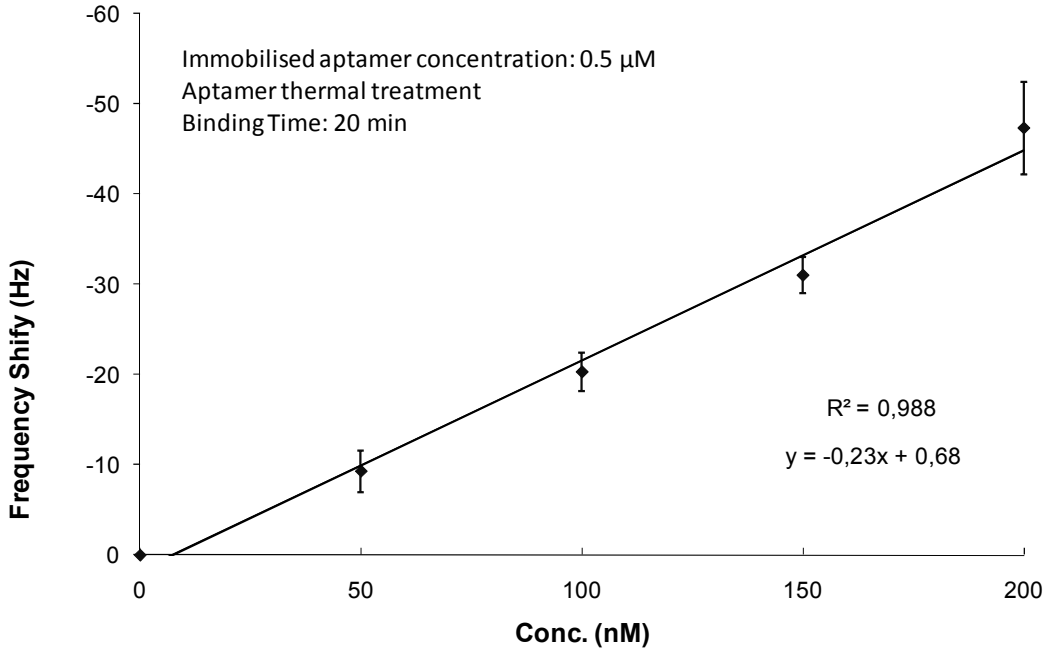


**Figure A3. Calibration curve for thrombin in the range 0-200 nM in binding buffer. Experimental parameters: concentration of 15-mer biotinylated aptamer with PolyT tail 0.5 µM; aptamer thermal treatment 95 °C 1 min, 0 °C 10 min; binding time 20 min. Each error bar represents standard deviation of three replicates (n = 3).**

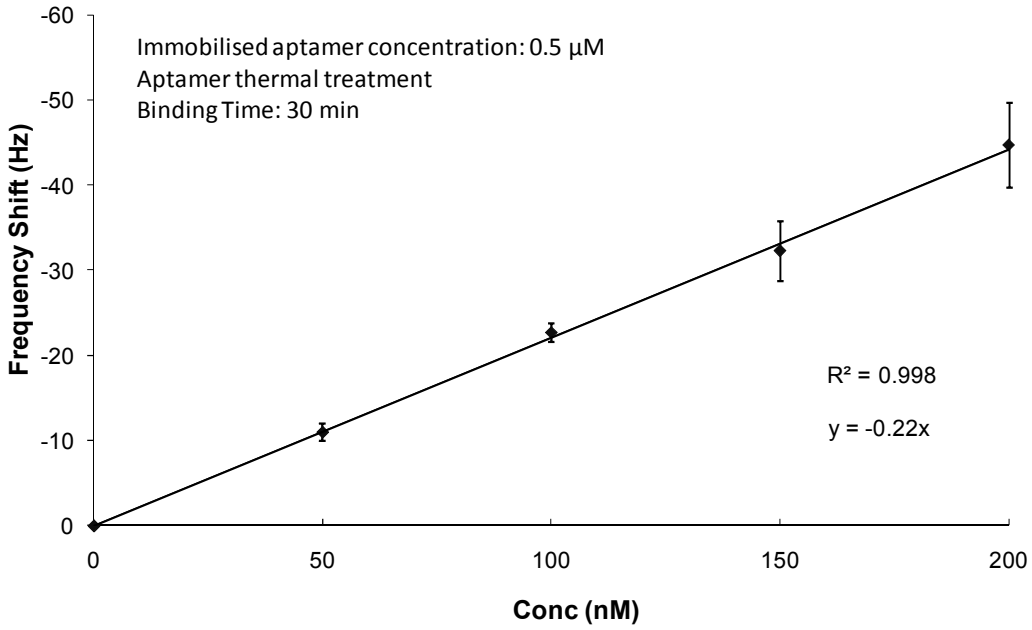


**Figure A4. Calibration curve for thrombin in the range 0-200 nM in binding buffer. Experimental parameters: concentration of 15-mer biotinylated aptamer with PolyT tail 0.5 µM; aptamer thermal treatment 95 °C 1 min, 0 °C 10 min; binding time 30 min. Each error bar represents standard deviation of three replicates (n = 3).**

[1] Ellington, A. D.; Szostak, J. W. (1990) In vitro selection of RNA molecules that bind specific ligands. *Nature* **346**, 818-822.

[2] Tuerk, C.; Gold, L. (1990). Systematic evolution of ligands by exponential enrichment. *Science* **249**, 505-510.

[3] Turner, A.P.F. (2000) Biosensors - sense and sensitivity. *Science* **290**, 1315-1317.

[4] Saerens, D.; Huang, L.; Bonroy, K.; Muyldermans, S. (2008) Antibody fragments as probe in biosensor development. *Sensors* **8**, 4669-4686.

[5] Mathonet, P.; Fastrez, J. (2004) Engineering of non-natural receptors. *Current opinion in structural biology* **14**, 505-511.

[6] Clark, S. L.; Remcho, V. T. (2002) Aptamers as analytical reagents. *Electrophoresis* **23**, 1335-1340.

[7] Mascini, M.; Del Carlo, M.; Compagnone, D.; Cozzani, I.; Tiscar, P. G.; Mpmhanga, C. P.; Chen, B. (2006) Piezoelectric sensors based on biomimetic peptides for the detection of heat shock proteins (HSPs) in mussels. *Analytical Letters* **39**, 1627-1642.

[8] Piletsky, S. A.; Piletska, E. V.; Bossi, A.; Karim, K.; Lowe, P.; Turner, A. P. F. (2001) Substitution of antibodies and receptors with molecularly imprinted polymers in enzyme-linked and fluorescent assays. *Biosensors and Bioelectronics* **16**, 701-707.

[9] Cummings M. D.; DesJarlais R. L.; Gibbs A. C.; Mohan V.; Jaeger E. P. (2005) Comparison of Automated Docking Programs as Virtual Screening Tools. *Journal of Medicinal Chemistry* **48**, 962-976

[10] Griffiths, D.; Hall, G. (1993) Biosensor – what real progress in being made? *Trends in Biotechnology* **11**, 122-130.

[11] Scheller, G.; Schubert, F.; Pfeiffer, D.; Wollenberg, U.; Riedel, K. (1989) Research and development of biosensors – a review. *Analyst* **114**, 653-662.

[12] Tothill, I.E..; Turner, A.P.F. (2003). Biosensors. In: Encyclopaedia of Food Sciences and Nutrition, edited by B. Caballero, L. Trugo and P. Finglas. Academic Press, New York.

[13] Turner, A. P. F.; Karube, I.; Wilson, G. S. (1987) Biosensors: Fundamentals and applications. Oxford University Press, Oxford, U. K.

[14] Scott, A.O. (1998) Introduction. In: Biosensors for Food Analysis, edited by A.O. Scott. The Royal Society of Chemistry, Cambridge.

[15] D'Orazio, P. (2003) Biosensors in clinical chemistry. *Clinica Chimica Acta* **334**, 41-69.

[16] Chaplin, M.F.; Bucke. C. (1990) Enzyme technology. Cambridge University Press, Cambridge, U.K.

[17] Leech, D. (1994) Affinity biosensors. *Chemical society reviews* **23**, 205-213.

[18] Skladal, P. (2003) Piezoelectric quartz crystal sensor applied for bioanalytical assays and characterization of affinity biosensors. *Journal of the Brazilian Chemical Society* **14**, 491-502.

[19] Jayasena, S. D. (1999) Aptamers: an emerging class of molecules that rival antibodies in diagnostics. *Clinical Chemistry* **45**, 1628-1650

[20] Proske, D.; Blank, M.; Buhmann, R.; Resch, A. (2005) Aptamers-basic research, drug development and clinical application. *Applied Microbiology and Biotechnology* **69**, 367-374.

[21] Hermann, T.; Patel, D. J. (2000) Adaptive recognition by nucleic acid aptamers. *Science* **287**, 820-825.

[22] You, K. M.; Lee, S. H.; Im, A.; Lee, S. B. (2003) Aptamers as functional nucleic acids: *in vitro* selection and biotechnological applications. *Biotechnology and Bioprocess Engineering* **8**, 64-75.

[23] Jenison, R.D; Gill, S.C.; Pardi, A.; Polisky, B. (1994) High-resolution molecular discrimination by RNA. *Science* **263**, 1425-1429.

[24] Tombelli, S.; Minunni, M.; Mascini, M. (2007) Aptamer-based assays for diagnostics, environmental and food analysis. *Biomolecular Engineering* **24**, 191-200.

[25] Tombelli, S.; Minunni, M.; Mascini, M. (2005) Analytical applications of aptamers. *Biosensors and Bioelectronics* **20**, 2424-2434.

[26] Osborne, SE; Ellington, A. (1997) Nucleic acids selection and the challenge of combinatorial chemistry. *Chemical Reviews* **97**, 349-370.

[27] Luzi, E.; Minunni, M.; Tombelli, S.; Mascini, M. (2003) New trends in affinity sensing: aptamers for ligand binding. *Trends in Analytical Chemistry*, **22**, 810-818.

[28] Cox, J. C.; Ellington, A. D. (2001) Automated selection of anti-protein aptamers. *Bioorganic and Medicinal Chemistry* **9**, 2525-2531.

[29] Golden, M. C.; Collins, B. D; Willis, M. C.; Koch, T. H. (2000) Diagnostic potential of PhotoSELEX-evolved ssDNA aptamers. *Journal of Biotechnology* **81**, 167-178.

[30] O'Sullivan, C. K. (2002) Aptasensors – the future of biosensing? *Analytical and Bioanalytical Chemistry* **372**, 44-48.

[31] Geiger, A.; Burgstaller, P.; von der Eltz, H.; Roeder, A.; Famulok, M. (1996) RNA aptamers that bind L-arginine with sub-micromolar dissociation constants and high enantioselectivity. *Nucleic Acids Research* **24**, 1029-1036.

[32] Liao, W; Cui, XT. (2007) Reagentless aptamer-based impedance biosensor for monitoring a neuro-inflammatory citokine PDGF. *Biosensors and Bioelectronics* **23**, 218-224.

[33] Kim, N; Gan, H. H.; Schlick, T. (2007) A computational proposal for designing structured RNA pools for in vitro selection of RNAs. *Bioinformatics* **13**, 478-492.

[34] Hamula, C. L. A.; Guthrie, J. W.; Zhang, H; Li, X; Le, X. C. (2006) Selection and analytical applications of aptamers. *Trends in Analytical Chemistry* **25**, 681-691.

[35] Gold, L. (2006) Epilogue. A personal perspective: aptamers after 15 years. In: The Aptamer Handbook, edited by S. Klussmann, Wiley-VCH Verlag GmbH & Co. KGaA, Weinheim.

[36] Cox, J. C.; Rudolph, P.; Ellington, A. D. (1998) Automated RNA selection. *Biotechnology Progress* **14**, 845 – 850.

[37] Eulberg, D.; Buchner, K.; Maasch, C.; Klussmann, S. (2005) Development of an automated in vitro selection protocol to obtain RNA-based aptamers: identification of a biostable substance P antagonist. *Nucleic Acids Research* **33**, 45-55.

[38] Berezovski, M.; Musheev, M.; Drabovich, A.; Krylov, S. N. (2006) Non-SELEX selection of aptamers. *Journal of American Chemical Society* **128**, 1410-1411.

[39] Famulok, M.; Mayer, G.; Blind, M. (2000) Nucleic acid aptamers – from selection in vitro to applications in vivo. *Accounts of Chemical Research* **33**, 591-599.

[40] Kusser, W. (2000) Chemically modified nucleic acid aptamers for in vitro selections: evolving evolution. *Reviews in Molecular Biotechnology* **74**, 27-38.

[41] Burmeister, P. E.; Lewis, S. D.; Silva, R. F.; Preiss, J. R.; Horwitz, L. R.; Pendergrast, P. S.; McCauley, T. G.; Kurz, J. C.; Epstein, D. M.; Wilson, C.; Keefe A. D. (2005) Direct in vitro selection of 2'-O-methyl aptamer to VEGF. *Chemistry and Biology* **12**, 25-33.

[42] Klussmann, S.; Nolte, A.; Bald, R.; Erdmann, V. A.; Furst, J. P. (1996) Mirror-image RNA that binds D-adenosine. *Nature Biotechnology* **14**, 1112-1115.

[43] Jhaveri, S.; Rajendran, M.; Ellington, A. D. (2000) In vitro selection of signaling aptamers. *Nature Biotechnology* **18**, 1293-1297.

[44] Leach, A. R.; Shoichet, B. K.; Peishoff, C. E. (2006) Prediction of protein-ligand interactions. Docking and Scoring: successes and gaps. *Journal of Medicinal Chemistry* **49**, 5851-5855.

[45] McGann, M. R.; Almond, H. R.; Nicholls, A.; Grant, J. A.; Brown, F. K. (2003) Gaussian Docking Functions. *Biopolymers* **68**, 76-90.

[46] Carta, G.; Knox, A. J. S.; Lloyd, D. G. (2007) Unbiasing scoring functions: a new normalization and rescoring strategy. *Journal of Chemical Information and Modeling* **47**, 1564-1571.

[47] Schulz-Gasch, T.; Stahl, M. (2003) Binding site characteristics in structure-based virtual screening: evaluation of current docking tools. *Journal of Molecular Modeling* **9**, 47-57.

[48] Ferrara, P.; Gohlke, H.; Price, D. J.; Klebe, G.; Brooks, C. L. III (2004) Assessing Scoring Functions for Protein-Ligand Interactions. J*ournal of Medicinal Chemistry* **47**, 3032-3047.

[49] Rajamani, R.; Good, A. C. (2007) Ranking poses in structure-based lead discovery and optimisation: current trends in scoring function development. *Current Opinion in Drug Discovery & Development* **10**, 308-315.

[50] Woodbury, N; Greving, M. (2006) WO 2007109067 20070927, patent application serial no. 60/784,496.

[51] Hall, B; Hesselberth, J. R.; Ellington, A. D. (2007) Computational selection of nucleic acid biosensors via a slip structure model. *Biosensors and Bioelectronics* **22**, 1939-1947.

[52] Fang, X.; Cao, Z.; Beck, T.; Tan, W. (2001) Molecular aptamer for real-time oncoprotein platelet-derived growth factor monitoring by fluorescence anisotropy. *Analytical Chemistry*. **73**, 5752-5757.

[53] Brody, E. N.; Gold L. (2000). Aptamers as therapeutic and diagnostic agents. *Molecular Biotechnology* **74**, 5-13.

[54] Bock, L. C.; Griffin, L. C.; Latham, J. A.; Vermaas, E. H; Toole, J. J. (1992) Selection of single-stranded DNA molecules that bind and inhibit human thrombin. *Nature* **355**, 564-566.

[55] Tasset, D; Kubik, M. F.; Steiner, W. (1997) Oligonucleotide inhibitors of human thrombin that bind distinct epitopes. *Journal of Molecular Biology* **272**, 688-698.

[56] Macaya, R. F; Schultze, P; Smith, F. W.; Roe, J. A.; Feigon, J. (1993) Thrombin-binding DNA aptamer forms an unimolecular quadruplex structure in solution. *Proceedings of the National Academy of Sciences* **90**, 3745-3749.

[57] Holland, C.A.; Henry, A. T.; Whinna, H. C.; Church, F. C. (2000) Effect of oligodeoxynucleotide thrombin aptamer on thrombin inhibition by heparin cofactor II and antithrombin. *FEBS Lett*ers **484**, 87-91.

[58] Stubbs, M.T.; Bode, W. (1993). A player of many parts: the spot light falls on thrombins structure. *Thrombosis Research* **69**, 1-58.

[59] Shuman, M.A.; Majerus, P. W. (1976) The measurement of thrombin in clotting blood by radioimmunoassay. *Journal of Clinical Investigation* **58**, 1249-1258.

[60] Bichler, J; Heit, J. A. ; Owen, W. G. Detection of thrombin in human blood by ex-vivo hirudin. (1996) *Thrombosis Research* **84**, 289-294.

[61] Carville, D. G. M.; Guyer, K. E. (2000) Hemostasis testing: Past, present and future. *IVD Technology Magazine* **Sep**, 49-56.

[62] Hemker, H. C.; Giesen, P.; AlDieri, R.; de Smed, E.; Wagenvoord, R. et al. (2002) The calibrated automated Thrombogram (CAT): a universal routine test for hyper and hypocoagulability. *Pathophysiology of Haemostasis and Thrombosis* **32**, 249-253.

[63] Brummel, E. K.; Paradis, S. G.; Butenas, S.; Mann, K.G. (2002) Thrombin functions during tissue factor-induced blood coagulation. *Blood* **100**, 148-152.

[64] Padmanhabhan, K; Tulinsky, A. (1993) The structure of α-Thrombin inhibited by a 15-mer single stranded DNA aptamer. *The Journal of Biological Chemistry* **268**, 17651-17654.

[65] Wu, Q.; Tsiang, M.; Sadler, J. E. (1992) Localization of the single stranded DNA binding site in the thrombin anion binding exosite. *The Journal of Biological Chemistry* **267**, 24408-24412.

[66] Kelly, J. A.; Feigon, J.; Yeates, T. O. (1996) Reconciliation of the X-ray and NMR structures of the thrombin-binding aptamer d(GGTTGGTGTGGTTGG). *Journal of Molecular Biology* **256**, 417-422.

[67] Padmanhabhan, K.; Tulinsky, A. (1996) An ambiguous structure of a DNA 15-mer thrombin complex. *Acta Crystallographica* D**52**, 272-282.

[68] Lee, M; Walt, D. R. (2000) A fiber-optic microarray biosensor using aptamers as receptors. *Analytical Biochemistry* **282**, 142-146.

[69] Schlensog, M. D.; Gronewold, T. M. A.; Tewes, M; Famulok, M.; Quandt, E. (2004) A Love-wave biosensor using nucleic acids as ligands. *Sensors and Actuators B* **101**, 308-315.

[70] Cao, Z.; Tan, W. (2005) Molecular aptamers for real-time protein-protein interactions study. *Chemistry - A European Journal* **11**, 4502-4508.

[71] Potyrailo, R. A.; Conrad, R. C.; Ellington, A. D.; Hieftje, G. M. (1998) Adapting selected nucleic acid ligands (aptamers) to biosensors. *Analytical Chemistry* **70**, 3419-3425.

[72] So, H. M.; Won, K.; Kim, Y. H.; Kim, B. K.; Ryu, B. H. et al. (2005) Single-walled carbon nanotube biosensors using aptamers as molecular recognition elements. *Journal of American Chemical Society* **127**, 11906-11907.

[73] Hianik, T.; Ostatna, V.; Zajacova, Z.; Stoikova, E.; Evtugyn, G. (2005) Detection of aptamer-protein interactions using QCM and electrochemical indicator methods. *Bioorganic and Medicinal Chemistry Letters* **15**, 291-295.

[74] Lin, C.; Katilius, E.; Liu, Y.; Zhang, J.; Yan, H. (2006) Self-assembled signaling aptamer DNA arrays for protein detection. *Angewandte Chemie International Edition* **45**, 5296-5301.

[75] Xiao, Y., Lubin, A.A., Heeger, A.J., Plaxco, K.W. (2005). Label-Free Electronic Detection of Thrombin in Blood Serum by Using an Aptamer-Based Sensor. *Angewandte Chemie International Edition* **44**, 5456-5459.

[76] Xiao, Y.; Piorek, B. D.; Plaxco, K. W.; Heeger, A. J. (2005) A reagentless signal-on architecture for electronic, aptamer-based sensors via target-induce strand displacement. *Journal of American Chemical Society* **127**, 17990-17991.

[77] Radi, A. E.; Sanchez, J. L. A.; Baldrich, E.; O'Sullivan, C. K. (2005) Reagentless, reusable, ultrasensitive electrochemical molecular beacon aptasensor. *Journal of American Chemical Society* **128**, 117-124.

[78] Ikebukuro, K.; Kiyohara, C.; Sode, K. (2005) Novel electrochemical sensor system for protein using the aptamers in sandwich manner. *Biosensors and Bioelectronics* **20**, 2168-2172.

[79] Mir, M.; Vreeke, M.; Katakis, I. (2006) Different strategies to develop an electrochemical thrombin aptasensor. *Electrochemistry Communications* **8**, 505-511.

[80] Pavlov, V.; Xiao, Y.; Shlyahovsky, B; Willner, I. (2004) Aptamer-functionalized Au nanoparticles for the amplified optical detection of Thrombin. *Journal of American Chemical Society* **126**, 11768-11769.

[81] Polsky, R; Gill, R; Kaganovsky, L; Willner, I. (2006) Nucleic acid-functionalised Pt nanoparticles: catalytic labels for the amplified electrochemical detection of biomolecules. *Analytical Chemistry* **78**, 2268-2271.

[82] Li, B; Wang, Y; Wei, H; Dong, S. Amplified electrochemical aptasensor taking AuNPs based sandwich sensing platform as a model. (2008) *Biosensors and Bioelectronics* **23**, 965-970.

[83] He, P; Shen, L; Cao, Y; Li, D. (2007) Ultrasensitive electrochemical detection of proteins by amplification of aptamer-nanoparticle bio bar codes. *Analytical Chemistry* **79**, 8024-8029.

[84] Centi, S., Tombelli, S., Minunni, M., Mascini, M. (2007) Aptamer-based detection of plasma proteins by an electrochemical assay coupled to magnetic beads. *Analytical Chemistry* **79**, 1466-1473.

[85] Zheng, J; Feng, W; Lin, L; Zhang, F; Cheng, G; He, P; Fang, Y. (2007) A new amplification strategy for ultrasensitive electrochemical aptasensor with network-like thiocyanuric acid/gold nanoparticles. *Biosensors and Bioelectronics* **23**, 341-347.

[86] McCauley, TG; Nobuko, H; Stanto, M. (2003) Aptamer-based biosensor arrays for detection and quantification of biological macromolecules. *Analytical Biochem*istry **319**, 244-250.

[87] Li, Y; Lee, HJ; Corn, RM. (2007) Detection of protein biomarkers using RNA aptamer microarrays and enzimatically amplified Surface Plasmon Resonance Imaging. *Analytical Chemistry* **79**, 1082-1088.

[88] Kim, S. D.; Ryu, J. S.; Yi, H. K.; Kim, S. C.; Zhang, B. T. (2004) Construction of C-Reactive Protein-binding aptamer as a module of the DNA computing system for diagnosing cardiovascular diseases. *Proceedings of the 10th international meeting on DNA computing* 334-343

[89] Pepys, M. B.; Hirschfield, G. M. (2003) C-Reactive Protein: a critical update. *The Journal of Clinical Investigation* **111**, 1805-1812.

[90] Ledue, T. B.; Rifai, N. (2001) High sensitivity immunoassay for C-Reactive Protein: promises and pitfalls. *Clinical Chemistry and Laboratory Medicine* **39**, 1171-1176.

[91] Yeh E.T.H.(2005) A new perspective on the biology of C-Reactive Protein *Circulation Research* **97** 609-611.

[92] Black, S.; Kushner, I.; Samols, D. (2004) Minireview. C-Reactive Protein. *The Journal of Biological Chemistry* **279**, 48487-48490.

[93] Potempa, L. A.; Siegel, K.; Fiefel, B. A.; Potempa, R. T.; Gewurz, H. (1987) Expression, detection and assay of neoantigen (Neo-CRP) associated with free, human C-Reactive Protein subunit. *Molecular Immunology* **24**, 531-541.

[94] Khreiss, T.; Jòzsef, L.; Potempa, A.; Filep, J. G. (2004) Conformational rearrangement in C-Reactive Protein is required for proinflammatory actions on human endothelial cells. *Circulation* **109**, 2016-2022.

[95] Wang, H-W.; Wu, Y.; Chen, Y.; Sui, S-F. (2002) Polymorphism of structural forms of C-Reactive Protein. *International Journal of Molecular Medicine* **9**, 665-671.

[96] Lee, R. T.; Lee, Y. C. (2003) Carbohydrate-binding properties of human neo-CRP and its relationship to phosphorylcholine-binding site. *Glycobiology* **13**, 11-21.

[97] Ridker, P. M. (2003) C-Reactive Protein. A simple test to help predict risk of heart attack and stroke. *Circulation* **108**, 81-85.

[98] Willerson, J. T.; Ridker, P. M. (2004) Inflammation as a cardiovascular risk factor. *Circulation* **109**, suppl. II, 2-10.

[99] Lagrand, W. K.; Visser, C. A.; Hermens, W. T.; Niessen, H. W. M.; Verheugt, W. A.; Wolbink, G-J.; Hack, C. E. (1999) C-Reactive Protein as a cardiovascular risk factor. More than an epiphenomenon? *Circulation* **100**, 96-102.

[100] Malik, S.; Wong, N. D.; Franklin, S.; Pio, J.; Fairchild, C.; Chen, R. (2005) Cardiovascular disease in U.S. patients with metabolic syndrome, diabetes and elevated C-Reactive Protein. *Diabetes Care* **28**, 690-693.

[101] Verma, S.; Szmitko, P. E.; Yeh, E. T. H. (2004) C-Reactive Protein: structure affects function. *Circulation* **109**, 1914-1917.

[102] Guidance for Industry and FDA Staff (2005) Review criteria for assessment of C-Reactive Protein (CRP), high sensitivity C-Reactive Protein (hsCRP) and cardiac C-Reactive Protein (cCRP) assay. U.S. Food and Drug Administration, Department of Health and Human Services http://www.fda.gov/cdrh/oivd/guidance/1246.html

[103] Aziz, N.; Fahey, J. L.; Detels, R.; Butch, A. W. (2003) Analytical performances of a highly sensitive C-Reactive protein-based immunoassay and the effects of laboratory variables on levels of protein in blood. *Clinical and Diagnostic Laboratory* **10**, 652-657.

[104] Clearfield, M. B. (2005) C-Reactive Protein: a new risk assessment tool for cardiovascular disease. *Journal of the American Osteopathic Association* **105**, 409-416.

[105] Zhan, W.; Bard, A. (2007) Electrogenerated chemiluminescence immunoassay of human C-Reactive Protein by using $Ru(bpy)_3^{2+}$-encapsulated liposomes as labels. *Analytical Chemistry* **79**, 459-463.

[106] Kriz, K.; Ibraimi, F.; Lu, M.; Hansson, L-O.; Kriz, D. (2005) Detection of C-Reactive Protein utilizing magnetic permeability detection based immunoassay. *Analytical Chemistry* **77**, 5920-5924.

[107] Kartalov, E. P.; Zhong, J. F.; Scherer, A.; Quake, S. R. Taylor, C. R.; Anderson, W. F. (2006) High-throughput multi-antigen microfluidic fluorescence immunoassay. *BioTechniques* **40**, 85-90.

[108] Hu, W. P.; Hsu, H-Y.; Chiou, A.; Tseng, K. Y.; Lin, H-Y.; Chang, G. L.; Chen, S-J. (2006) Immunodetection of pentamer and modified C-Reactive Protein using surface plasmon resonance biosensing. *Biosensors and Bioelectronics* **21**, 1631-1637.

[109] Jung, S-H.; Jung, J-W.; Suh, I-B.; Yuk, J. S.; Kim, W-J.; Choi, E. Y.; Kim, Y-M.; Ha, K-S. (2007) Analysis of C-Reactive Protein on amide-linked N-hydrosxysuccinimide-dextran arrays with a spectral surface plasmon resonance biosensor for serodiagnosis. *Analytical Chemistry* **79**, 5703-5710.

[110] Kim, H-C.; Lee, S-K.; Jeon, W. B.; Lyu, H-K-; Lee, S. W.; Jeong, S. W. (2008) Detection of C-Reactive Protein on a functional poly(thiophene) self-assembled monolayer using surface plasmon resonance. *Ultramicroscopy*, in press

[111] Lin, S.; Lee, C-K.; Lin, Y-H.; Lee, S-Y.; Sheu, B-C.; Tsai, J-C.; Hsu, S-M. (2006) Homopolyvalent antibody-antigen interaction kinetic studies with use of a dual-polarization interferometric biosensor. *Biosensors and Bioelectronics* **22**, 715-721.

[112] Chen, X.; Wang, Y.; Zhou, J.; Yan, W.; Li, X.; Zhu, J-J. (2008) Electrochemical impedance immunosensor based on three-dimensional ordered macropouros gold film. *Analytical Chemistry* **80**, 2133-2140.

[113] Meyer, M. H. F.; Hartmann, M.; Krause, H-J.; Blankenstein, G.; Mueller-Chorus, B.; Oster, J.; Miethe, P.; Keusgen, M. (2007) CRP determination based on a novel magnetic biosensor. *Biosensors and Bioelectronics* **22**, 973-979.

[114] McBride, J.; Cooper, M. A. (2008) A high sensitivity assay for the inflammatory marker C-Reactive Protein employing acoustic biosensing. *Journal of Nanotechnology* **6**, 1-8.

[115] Albrecht, C.; Kaeppel, N.; Gauglitz, G. (2008) Two immunoassay formats for fully automated CRP detection in human serum. *Analytical and Bioanalytical Chemistry* **391**, 1845-1852.

[116] Curie, J.; Curie, P. (1880) An oscillating quartz crystal mass detector. *Rendu* **91**, 294-297.

[117] Drafts, B. (2001) Acoustic wave technology sensors. *IEEE Transactions on microwave theory and techniques* **49**, 795-802.

[118] Janshoff, A.; Steinem, C. (2001) Quartz crystal microbalance for bioanalytical applications. *Sensor Update* **9**, 313-354.

[119] Bruckenstein, S.; Shay, M. (1985) Experimental aspects of the use of quartz crystal microbalance solution. *Electrochimica Acta* **30**, 1295-1300.

[120] O'Sullivan, C. K.; Guilbault, G. G. (1999) Commercial quartz crystal microbalances – theory and applications. *Biosensors and Bioelectronics* **14**, 663-670.

[121] Sauerbrey, G. (1959) The use of quartz oscillators for weighing thin layers and for microweighing. *Zeitschrift für Physik* **155**, 206-222.

[122] Hiller, A. C.; Ward, M. D. (1992) Scanning electrochemical mass sensitivity mapping of the quartz crystal. *Analytical Chemistry* **64**, 2539-2554.

[123] Kanazawa, K.K.; Gordon, J.G. (1985). Frequency of a Quartz Microbalance in contact with liquid. *Analytical Chemistry* **57**, 1770-1771.

[124] Chang, S; Muramatsu H.; Nakamura, C.; Miyake, J. (2000) The principle and applications of piezoelectric crystal sensors. *Material science and Engineering C* **12**, 111-123.

[125] Minunni, M.; Mascini, M.; Guilbault, G. G. (1995) The quartz crystal microbalance as biosensor. A status report on its future. *Analytical Letters* **28**, 749-764.

[126] Kim, N.; Park, I-S.; Kim, D-K. (2004) Characteristics of a label-free piezoelectric immunosensor detecting *Pseudomonas aeruginosa*. *Sensors and Actuators B: Chemical* **100**, 432-438.

[127] Mannelli, I.; Minunni, M.; Tombelli, S.; Mascini, M. (2003) Bulk acoustic wave (BAW) affinity biosensor for genetically modified organisms (GMOs) detection. *IEEE Sensor Journal* **3**, 369-375.

[128] Sklàdal, P.; dos Santos Riccardi, C.; Yamanaka, H.; Inàcio da Costa, P. (2004) Piezoelectric biosensor for real time monitoring of hybridization and detection of hepatitis C virus. *Journal of Virological Methods* **117**, 145-151.

[129] Dell'Atti, D.; Tombelli, S.; Minunni, M.; Mascini, M. (2006) Detection of clinically relevant point mutations by a novel piezoelectric biosensor. *Biosensors and Bioelectronics* **21**, 1876-1879.

[130] Earp, R. L.; Dessy, R. E. (1998) Surface Plasmon Resonance. In: Commercial biosensors: applications to clinical, bioprocess and environmental samples. Edited by Graham Ramsey. John Wiley & Sons, Inc., New York.

[131] Fan, X.; White, I. M.; Shopova, S. I.; Zhu, H.; Suter, J. D.; Sun, Y. (2008) Sensitive optical biosensors for unlabeled targets: a review. *Analytica Chimica Acta* **620**, 8-26.

[132] Homola, J. (2003) Present and future of surface plasmon resonance biosensors. *Analytical and Bioanalytical Chemistry* **377**, 528-539.

[133] Campbell, C. T.; Kim, G. (2007) SPR microscopy and its applications to high-throughput analyses of biomolecular binding events and their kinetics. *Biomaterials* **28**, 2380-2392.

[134] Green, R. J.; Frazier, R. A.; Shakesheff, K. M.; Davies, M. C.; Roberts, C. J.; Tendler, S.J.B. (2000) Surface plasmon resonance analysis of dynamic biological interactions with biomaterials. *Biomaterials* **21**, 1823-1835.

[135] Homola, J. (2008) Surface Plasmon Resonance sensors for detection of chemical and biological species. *Chemical Reviews* **108**, 462-493.

[136] Löfås, S.; Jöhnsson, B. (1990) A novel hydrogel matrix on gold surfaces in surface plasmon resonance sensors for fast and efficient covalent immobilisation of ligands. *Journal of Chemical Society and Chemical Communications* **21**, 1526-1528.

[137] Storri, S.; Santoni, T.; Minunni, M.; Mascini, M. (1998) Surface modifications for the development of piezoimmunosensors. *Biosensors and Bioelectronics* **13**, 347-357.

[138] Ducongè, F.; Di Primo, C.; Toulmè, J.J. (2000) Is a closing "GA pair" a rule for stable loop-loop RNA complexes? *Journal of Biological Chemistry* **275**, 21287-21294.

[139] Minunni, M.; Tombelli, S.; Gullotto, A.; Luzi, E.; Mascini, M. (2004) Development of biosensors with aptamers as bio-recognition element: the case of HIV-1 Tat protein. *Biosensors and Bioelectronics* **20**, 1149-1156.

[140] Herne, T. M.; Tarlov, M. J. (1997) Characterization of DNA probes immobilized on gold surfaces. *Journal of American Chemical Society* **119**, 8916-8920.

[141] Chaky, N. K.; Vijayamohanan, K. (2002) Review. Self-assembled monolayers as tunable platform for biosensor applications. *Biosensors and Bioelectronics* **17**, 1-12.

[142] Halgren T. A. (1996) Merck Molecular Force Field I. Basis, form, scope, parameterization and performances of MMFF94. *Journal of Computational Chemistry* **17**, 490-519.

[143] Baldrich, E.; Restrepo, A.; O'Sullivan, K. (2004) Aptasensor development: elucidation of critical parameters for optimal aptamer performance. *Analytical Chemistry* **76**, 7053-7063.

[144] Wang, R.; Tombelli, S.; Minunni, M. Spiriti, M.; Mascini, M. (2004) Immobilisation of DNA probes for the development of SPR-based sensing. *Biosensors and Bioelectronics* **20**, 967-974.

[145] Tombelli, S.; Mascini, M.; Turner, A. P. F. (2002) Improved procedures for immobilisation of oligonucleotides on gold-coated piezoelectric quartz crystals. *Biosensors and Bioelectronics* **17**, 929-936.

[146] Liss, M.; Peterson, B.; Prohaska, E. (2002) An aptamer-based quartz crystal protein biosensor. *Analytical Chemistry* **74**, 4488-4495.

[147] Hianik, T.; Ostatnà, V.; Sonlajtnerova, M.; Grman, I. (2007) Influence of ionic strenght, pH and aptamer configuration for binding affinity to thrombin. *Bioelectrochemistry* **70**, 127-133.

[148] Zhou, X. C.; Huang, L. Q.; Li, S. F. Y. (2001) Microgavimetric DNA sensor based on quartz crystal microbalance: comparison of oligonucleotide immobilisation methods and the application in genetic diagnosis. *Biosensors and Bioelectronics* **16**, 85-95.

[149] Stadtherr, K.; Wolf, H.; Lindner, P. (2005) An aptamer-based protein biochip. *Analytical Chemistry* **77**, 3437-3443.

[150] Li, J. J.; Fang, X.; Tan, W. (2002) Molecular aptamer beacons for real-time protein recognition. *Biochemical and Biophysical Research Communications* **292**, 31-40.

[151] Keniry, M. A. (2001) Quadruplex structures in nucleic acids. *Biopolymers* **56**, 123-146.

[152] Ho, H-A.; Leclerc, M. (2004) Optical sensor based on hybrid aptamer/conjugated polymer complexes. *Journal of American Chemical Society* **126**, 1384-1387.

[153] Baldrich, E.; O'Sullivan, C. K. (2005) Ability of thrombin to act as molecular chaperone, inducing formation of quadruplex structure of thrombin-binding aptamer. *Analytical Biochemistry* **341**, 194-197.

[154] Fialovà, M.; Kypr, J.; Vorlìčkovà, M. (2006) The thrombin binding aptamer GGTTGGTGTGGTTGG forms a bimolecular guanine tetraplex. *Biochemical and Biophysical Research Communications* **344**, 50-54.

[155] Gronewold, T. M. A.; Glass, S.; Quandt, E.; Famulok, M. (2005) Monitoring complex formation in the blood-coagulation cascade using aptamer-coated SAW sensors. *Biosensors and Bioelectronics* **20**, 2044-2052.

[156] Lai, RY; Plaxco, KW; Heeger, AJ. (2007) Aptamer-based electrochemical detection of picomolar Platelet-Derived Growth Factor directly in blood serum. *Analytical Chemistry* **79**, 229-233.

[157] Drolet, DW; Moon-McDermott, L; Romig, TS. (1996) An enzyme-linked oligonucleotide assay. *Nature Biotechnology* **14**, 1021-1025.

[158] Silver, F. H.; Wang, M-C.; Pins, G. D. (1995) Preparation and use of fibrin glue in surgery. *Biomaterials* **16**, 891-903.

[159] Loewy, A. G.; Dunathan, K.; Kriel, R.; Wolfinger, H. L. Jr. (1960) Fibrinase. *The Journal of Biological Chemistry* **236**, 2625-2633.

[160] Mann, K. G.; Butenas, S.; Brummel, K. (2003) The dynamics of thrombin formation. *Arteriosclerosis Thrombosis and Vascular Biol*ogy **23**, 17-25.

[161] Masson, J-F.; Hamersky, K.; Beadouin, S.; Booksh, K. S. (2003) *In vitro* biochemical monitoring with fiber optic based Surface Plasmon Resonance sensors. *SPIE Proceedings* **5261**, 123-134.

[162] Masson, J-F.; Battaglia, T. M.; Kim, Y-C; Prakash, A.; Beaudoin, S.; Booksh, K. S. (2004) Preparation of analyte-sensitive polymeric supports for biochemical sensors. *Talanta* **64**, 716-725.

[163] Situ, C.; Wylie, A. R. G.; Douglas, A.; Elliott, C. T. (2008) Reduction of severe bovine serum associated matrix effects on carboxymethylated dextran coated biosensors surfaces. *Talanta* **76**, 832-836.

[164] Bulukin, E.; Meucci, V.; Minunni, M.; Pretti, C.; Intorre, L.; Soldani, G.; Mascini, M. (2007) An optical immunosensor for rapid vitellogenin detection in plasma from carp *(Cyprinus carpio)*. *Talanta* **72**, 785-790.

[165] Anderson, N. L.; Anderson, N. G. (2002) The human plasma proteome: history, character, and diagnostic prospects. *Molecular and Cellular Proteomics* **1**, 845-867.

[166] Altintaş E. B.; Denizli, A. (2006) Efficient removal of albumin from human serum by monosize dye-affinity beads. *Journal of Chromatography B* **832**, 216-223.

[167] Huang, L.; Harvie, G.; Feitelson, J. S.; Gramatikoff, K.; Herold, D. A.; Allen, D. L.; Amunngama, R.; Hagler, R. A.; Pisano, M. R.; Zhang, W-W.; Fang, X. (2005) Immunoaffinity separation of plasma proteins by IgY microbeads: meeting the needs of proteomic sample preparation and analysis. *Proteomics* **5**, 3314-3328.

[168] Stempfer, R.; Kubicek, M.; Lang, I. M.; Christa, N.; Gerner, C. (2008) Quantitative assessment of human serum high-abundance protein depletion. *Electrophoresis* **29**, 1-8.

[169] Heidenreich, O.; Eckstein, F. (1992) Hammerhead ribozyme-mediated cleavage of the long terminal repeat RNA of human immunodeficiency virus Type 1. *Journal of Biological Chemistry* **267**, 1904-1909.

[170] Silverman, S. K.; Hergenrother, P. J. (2006) Combinatorial chemistry and molecular diversity. Tools for molecular diversification and their applications in chemical biology. *Current Opinion in Chemical Biology* **10**, 185-187.

[171] Goldenhuys, W. J.; Gaasch, K. E.; Watson, M.; Allen, D. D.; Van der Schyf, C. J. (2006) Optimizing the use of open-source software applications in drug discovery. *Drug Discovery Today* **11**, 127-132.

[172] Keefe, A. D.; Schaub, R. G. (2008) Aptamers as candidate therapeutics for cardiovascular interactions. *Current Opinion in Pharmacology* **8**, 147-152.

[173] Bates, P. J.; Kahlon, J. B.; Thomas, S. D.; Trent, J. O.; Miller, D. M. (1999) Antiproliferative activity of G-rich oligonucleotides correlates with protein binding. *The Journal of Biological Chemistry* **274**, 26369-26377.

[174] Dapić, V.; Abdomerović, V.; Marrington, R.; Pederby, J.; Rodger, A.; Trent, J. O.; Bates, P. J. (2003) Biophysical and biological properties of quadruplex oligodeoxyribonucleotides. *Nucleic Acids Research* **31**, 2097-2107.

[175] Krovat, E. M.; Steindl, T.; Langer, T. (2005) Recent advances in docking and scoring. *Current Computer-Aided Drug Design* **I**, 93-102.

[176] Mascini, M.; Guilbault, G. G.; Monk, I. R.; Hill, C.; Del Carlo, M.; Compagnone, D. (2008) Screening of rationally designed oligopeptides for *Listeria monocytogenes* detection by means of a high density colorimetric microarray. *Microchimica Acta* DOI 10.1007/s00604-008-0035-0.

[177] Sauton, N.; Lagorce, D.; O Villoutreix, B.; Miteva, M. A. (2008) MS-DOCK: Accurate multiple conformation generator and rigid docking protocol for multi-step virtual ligand screening. *BMC Bioinformatics* **9**, 184-195.

[178] Stahl, M.; Rarey, M. (2001) Detailed analysis of scoring functions for virtual screening. *Journal of Medicinal Chemistry* **44**, 1035-1042.

[179] Paborsky. L. R.; McCurdy S. N.; Griffin, L. C.; Toole, J. J.; Leung, L. L. K. (1993) The single-stranded DNA aptamer-binding site of human thrombin. *The Journal of Biological Chemistry* **268**, 20808-20811.

[180] Mascini, M.; Macagnano, A.; Monti, D.; Del Carlo, M.; Paolesse, R.; Chen, B.; Warner, P.; D'Amico, A.; Di Natale, C.; Compagnone, D. (2004) Piezoelectric sensors for dioxins: a biomimetic approach. *Biosensors and Bioelectronics* **20**, 1203-1210.

[181] Mascini, M.; Sergi, M.; Monti, D.; Del Carlo, M.; Compagnone, D. (2008) Oligopeptides as mimic of acethylcholinesterase: from the rational design to the application in solid-phase exctraction for pesticedes. *Analytical Chemistry*, in press.

[182] Chianella, I.; Lotierzo, M.; Piletsky, S. A.; Tothill, I. E.; Chen, B.; Karim, K.; Turner, A. P. F. (2002) Rational design of a polymer specific for microcystin-LR using a computational approach. *Analytical Chemistry* **74**, 1288-1293.

[183] Piletska, E.V.; Tuner, N.W.; Turner, A. P. F.; Piletsky, S. A. (2005) Controlled release of the herbicide simazine from computationally designed molecular imprinted polymers. *Journal of controlled release* **108**, 132-139.

[184] Yakaiah, T., Lingaiah, B. P. V.; Narsaiah, B.; Shireesha, B.; Ashok Kumar, B.; Gururaj, S.; Parthasarathy, T.; Sridhar, B. (2007) Synthesis and structure activity relationship of novel pyrimido[1,2-b]indazoles as potential anticancer agents against A-549 cell lines. *Bioorganic & Medicinal Chemistry Letters* **17**, 3445-3453.

[185] Li, M.; Huang, Y-J.; Tai, P. C.; Wang. B. (2008) Discovery of the first SecA inhibitors using structure-based virtual screening. *Biochemical and Biophysical Research Communications* **368**, 839-845.

[186] Fenton, J. W. II; Fasco, M. J.; Stackrow, A. B.; Aronson, D. L.; Young, A. M.; Finlayson, J. S. (1977) Human Thrombins. Production, evaluation and properties of α-Thrombin. *The Journal of Biological Chemistry* **252**, 3587-3598.

[187] Sonder, S. A.; Fenton, J. W. II (1984) Proflavin binding within the fibropeptide groove adjacent to the catalytic site of human α-Thrombin. *Biochemistry* **23**, 1818-1823.

[188] Berliner, L. J.; Sugawara, Y.; Fenton, J. W. II (1985) Human α-Thrombin binding to nonpolymerized fibrin-sepharose: evidence for an anionic binding region. *Biochemistry* **24**, 7005-7009.

[189] Macaya, R. F.; Waldron, J. A.; Beutel, B. A.; Gao, H.; Joesten, M. E.; Yang, M.; Patel, R.; Bertelsen, A, H., Cook, A. F. (1995) Structural and functional characterization of potent antithrombotic oligonucleotides possessing both quadruplex and duplex motifs. *Biochemistry* **34**, 4478-4492.

[190] Ikebukuro K.; Okumara, Y.; Sumikura, K.; Karube, I. (2005) A novel method of screening thrombin-inhibiting DNA aptamers using an evolution-mimicking algorithm. *Nucleic Acids Research* **33**, 108-113.

## Publications

Development of an optical RNA-based aptasensor for C-Reactive Protein.
A. Bini; S. Centi; S. Tombelli; M. Minunni; M. Mascini. (2008) *Analytical and Bioanalytical Chemistry* **390**, 1077-1086

Piezoelectric biosensors for aptamer-protein interaction.
S. Tombelli; A. Bini; M. Minunni; M. Mascini. (2008) *Methods in Molecular Biology: Biosensors and Biodetection* **54**, 23-36. Humana Press, Ed. A. Rasooly and K. E. Herold, Totowa NJ (USA).

Analytical performances of aptamer-based sensing for Thrombin detection.
A. Bini; M. Minunni; S. Tombelli; S. Centi; M. Mascini. (2007) *Analytical Chemistry* **79**, 3016-19.

Anal Bioanal Chem (2008) 390:1077–1086
DOI 10.1007/s00216-007-1736-7

ORIGINAL PAPER

# Development of an optical RNA-based aptasensor for C-reactive protein

**A. Bini · S. Centi · S. Tombelli · M. Minunni · M. Mascini**

Received: 4 July 2007 / Revised: 4 October 2007 / Accepted: 5 November 2007 / Published online: 9 December 2007


**Abstract** The development of a RNA-aptamer-based optical biosensor (aptasensor) for C-reactive protein (CRP) is reported. CRP is an important clinical biomarker; it was the first acute-phase protein to be discovered (1930) and is a sensitive systemic marker of inflammation and tissue damage. It has also a prognostic value for patients with acute coronary syndrome. The average concentration of CRP in serum is 0.8 ppm and it increases in response to a variety of inflammatory stimuli, such as trauma, tissue necrosis, infection and myocardial infarction. The interaction between the 44-base RNA aptamer and the target analyte CRP is studied. In particular, the influence of the aptamer immobilization procedure (chemistry, length, concentration), as well as the binding conditions, i.e., the influence on the binding of different buffers, the presence of $Ca^{2+}$ ion and the specificity (against human serum albumin) have been evaluated. Using the best working conditions, we achieved a detection limit of 0.005 ppm, with good selectivity towards human serum albumin. Some preliminary experiments in serum are reported.

**Keywords** Aptamer · C-reactive protein · Surface plasmon resonance

## Introduction

The detection and quantification of proteins play an essential role in fundamental research as well as in clinical practice. To date, the antibody-based assays are the most commonly used diagnostic methods; however, a new class of receptors called aptamers has appeared in the literature [1]. Aptamers are DNA or RNA molecules isolated from a library of random sequences by an "in vitro" selection and amplification process, called Systematic Evolution of Ligands by EXponential enrichment (SELEX) [2, 3]. They have been shown to be useful for the detection of proteins and can rival antibodies in diagnostic applications. In this regard, numerous aptamers have been selected for a broad range of proteins. Aptamers bind the relative target with affinity and specificity comparable to those of monoclonal antibodies. They offer several advantages over antibodies, making them very promising in analytical and diagnostic applications. Avoiding the use of animals, the in vitro selection and chemical synthesis of aptamers allow reduction of the batch-to-batch variation encountered with antibody production. Moreover, they can be easily chemically modified and are more resistant to degradation and denaturation if working in harsh conditions [4, 5].

Different aptamer-based bioanalytical assays have been developed and reviewed [6–12]. Among these, biosensors represent an interesting approach because of their intrinsic characteristics such as real-time detection, fast analysis time, low cost and label-free analysis. Many aptamer-based biosensors (aptasensors) have been developed for protein detection using different assay formats. Very recently, aptasensors for proteins with innovative approaches, i.e., immunoglobulin E using carbon nanotube field-effect transistors [13] and vascular endothelial growth factor using new surface plasmon resonance (SPR) imaging instrumentation [14], have been reported.

Few papers concern the detection of proteins of clinical interest (for example, thrombin and platelet-derived growth factor) in real matrices such as plasma and serum [15–19].

A. Bini · S. Centi · S. Tombelli · M. Minunni · M. Mascini (✉)
Dipartimento di Chimica, Università degli Studi di Firenze,
Polo Scientifico,
Via della Lastruccia 3, 50019 Sesto Fiorentino,
Florence, Italy
e-mail: marco.mascini@unifi.it

C-reactive protein (CRP) represents an important analyte in clinical analysis. This protein has been selected as a relevant analyte in the Integrated Project founded by the European Community, entitled "Healthcare by biosensor measurements and networking (Care-Man)," for developing innovative analytical devices for fast molecular diagnostic. CRP is one of the cytokine-induced "acute-phase" proteins whose blood levels rise during a general, unspecific response to infections and noninfectious inflammatory processes. Moreover, CRP is an acute-phase reactant and a factor in the development of atherosclerosis plaques. Although CRP was initially believed to be only a marker of vascular inflammation, a recent research indicates that it also plays an active role in atherogenesis [20]. CRP is normally present in serum at concentrations below 10 ppm; in adults the average concentration is 0.8 ppm. CRP serum levels increase in response to a variety of inflammatory stimuli, such as trauma, tissue necrosis, infection and myocardial infarction. Following an acute-phase stimulus, the levels may increase to more than 500 ppm, resulting in the release of elevated quantities into the circulation.

Commercially available immunochemical methods for CRP detection include qualitative, semiquantitative and quantitative assays. Enzyme-linked immunosorbent assay (ELISA) is applied in highly sensitive detection of CRP with a detection limit of 100 ppb [21].

Other immunochemical approaches for CRP detection have been reported. Among these, a competitive liposome-based immunosorbent assay to detect human CRP in standard solutions (detection limit 0.1 ppm) by an electrogenerated chemiluminescence technique has been described [22]. More recently alternative new approaches for CRP detection in complex matrices such as whole blood, serum and plasma have also been studied. In particular, Kartalov et al. [23] developed a multianalyte ELISA test for simultaneous CRP, prostate-specific antigen, ferritin and vascular endothelial growth factor detection in blood by fluorescence. A magnetic permeability detection in whole blood [24] and a magnetic assay in serum, saliva and urine [25], both using magnetic beads, have been also reported.

Finally, immunosensors for CRP analysis have been described. Some optical biosensors, with the antibody immobilized on the sensing surface and the sample analyte added directly, have been reported only for CRP detection in buffer solutions [26–28]. CRP detection in human serum has been achieved by SPR-based immunosensing [29], in which the analyte, instead of being added in solution for receptor binding, was directly immobilized on dextran-modified chips by adding serum drops (diluted 1:10).

Although immunosensors showed very interesting performances, the availability of a CRP RNA-aptamer [30] encouraged the development of the relative RNA-based aptasensor. The affinity constant of the aptamer for CRP, expressed as $K_D$, is 125 nM. This affinity competes with antibody affinities, whose reported values for different clones are, respectively, 440 and 550 nM [28] and 720 nM [27].

In this work the RNA aptamer specific for CRP was immobilized on the chip surface and the interaction was monitored by SPR.

To our knowledge, this is the first paper regarding the interaction between the RNA aptamer and its target analyte. On the basis of this, the main goal of this work was to find the conditions for the binding in the heterogeneous phase and then to improve the analytical performances of the aptasensor by optimization of some simple but critical parameters. Such parameters that could affect the analytical performance of the aptasensor [16] in terms of selectivity, linearity ($R^2$), reproducibility (coefficient of variation) and stability (cycles) have been studied. In particular, the influence of the aptamer immobilization procedure (chemistry, length, concentration), as well as the binding conditions, i.e., the influence of different buffers on the binding, the presence of $Ca^{2+}$ ion and the specificity (against human serum albumin, HSA) were evaluated. Preliminary assays in human serum were performed.

## Materials

### Reagents

1-Ethyl-3-(dimethylaminopropyl) carbodiimide (EDAC), diethyl pyrocarbonate (DEPC), RnaseZAP™, polyoxyethylene-sorbitan monolaurate (Tween 20), 4-(2-hydroxyethyl) piperazine-1-ethanesulfonic acid (HEPES), 2-(*N*-morpholino) ethanesulfonic acid (MES), tris(hydroxymethyl)aminomethane (Tris) and all the other reagents for the buffers were purchased from Sigma (Milan, Italy). EDTA and calcium chloride were purchased from Merck (Milan, Italy).

All the solutions used in the experiments were prepared in DEPC-treated water, filtered with 0.22-μm-pore size filters (Nalgene, Milan, Italy) and degassed daily prior to use. DEPC-treated water was prepared adding 1 ml DEPC to 1 l Milli-Q water and the mixture was stirred overnight. The solution was then autoclaved at 1 atm for 20 min.

The sequence of the CRP 44-mer RNA aptamer is as follows: 5′-GCCUGUAAGGUGGUCGGUGUGGCGAGUGUGUUAGGAGAGAUUGC-3′.

This aptamer was selected through ten SELEX rounds [30]. Two of the possible secondary structures that the CRP aptamer can adopt were calculated using freely available software (RNA mfold version 2.3 server, available from http://www.bioinfo.rpi.edu/applications/mfold/, by M. Zuker and D.H. Turner) and are reported in Fig. 1.

The RNA aptamer biotinylated at the 5′ end was purchased by IBA (Germany) with two different spacers, a

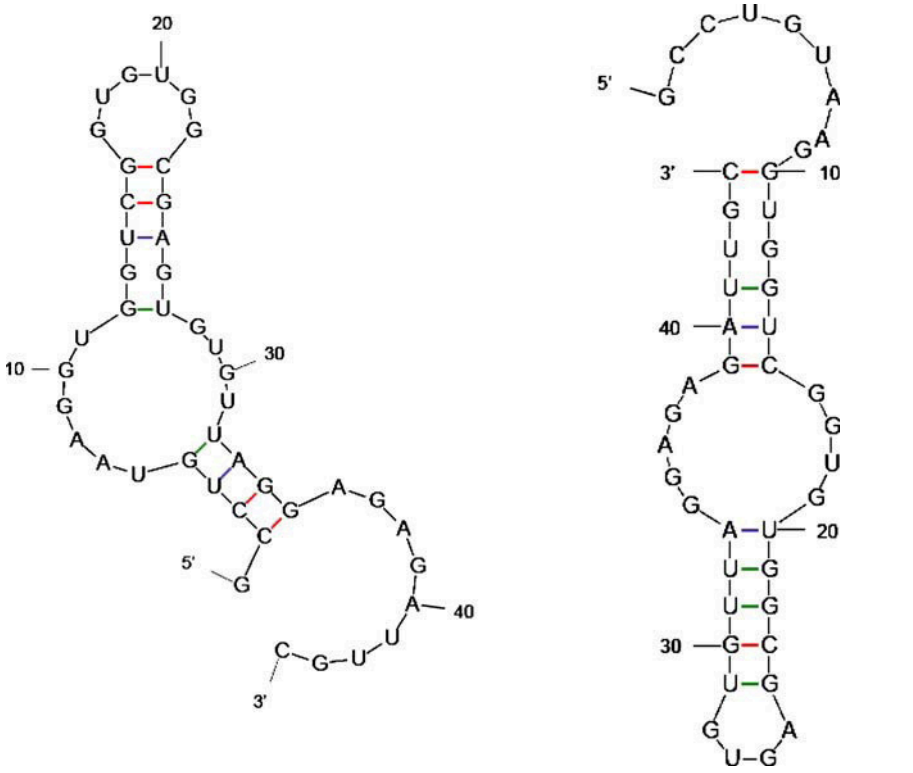


**Fig. 1** Two of the possible secondary structures of the C-reactive protein (CRP) RNA aptamer, calculated using RNA mfold version 2.3 server. These structures have a comparable energy ($\Delta G$)

polyT and a triethylene glycol (TEG) tail. The polyT tail is formed by 20 thymines, while the TEG tail ($C_6H_{14}O_4$) is a spacer arm based on a triethylene glycol, containing four oxygen atoms. The functionalization of the aptamer with a spacer confers a certain flexibility to the molecule without interfering with the binding to streptavidin. The sequence of the aptamer with the two modifications is reported below:

- 5′-biotin-TT TTT TTT TTT TTT TTT TTT-GCCUGU AAGGUGGUCGGUGUGGCGAGUGUGUUAGGAG AGAUUGC-3′,
- 5′-biotin-TEG-GCCUGUAAGGUGGUCGGUGUGG CGAGUGUGUUAGGAGAGAUUGC-3′.

Purified human CRP (molecular mass 115.135 g/mol) was purchased from Biodesign (Milan, Italy) with a concentration of 2,000 ppm in 0.1 M Tris, 0.2 M NaCl, 2 mM $CaCl_2$, pH 7.5 buffer containing 0.1% $NaN_3$ as a preservative and it was stored at 4 °C. Further dilutions were performed and the solutions were kept in ice during the experiments to prevent denaturation.

Biotin, HSA, human immuoglobulin G (IgG) and human serum were obtained from Sigma (Milan, Italy). HSA and human IgG were used as negative controls.

Magnetic beads coupled with protein G with a diameter of 2.8±0.2 μm were obtained from Dynal Biotech (Milan, Italy).

The buffers tested in this study were as follows: 10 mM MES pH 6.0, 10 mM HEPES pH 6.0, 10 mM Tris/HCl pH 6.0, 10 mM MES pH 6.5, 10 mM HEPES pH 6.5, 10 mM Tris/HCl pH 6.5, 10 mM HEPES pH 7.0, 10 mM Tris/HCl pH 7.0, 10 mM HEPES pH 7.5, and 10 mM Tris/HCl pH 7.5. The immobilization buffer was 300 mM NaCl, 20 mM $Na_2HPO_4$, 0.1 mM EDTA pH 7.4.

### Instrumentation

SPR measurements were performed using the BIACORE X™ instrument (Biacore, Uppsala, Sweden) and carboxylated dextran-coated chips (CM5 chip, Biacore, Uppsala, Sweden). The SPR signal is expressed in resonance units (RU).

## Methods

### Aptamer immobilization

To prevent the RNA sequence from undergoing RNase degradation, a “nuclease-free” environment was necessary. For this reason careful cleaning of the glassware, vials and instrumentation was necessary. Before use, the instrumentation (the fluid cartridge and the tubing) was treated with cleaning solutions by running specific Biacore cleaning procedures (BIAcore Desorb and Sanitaze methods). Moreover, all the external instrumental components (the needle and the tubing) were treated with specific RNase inhibitors. Finally, before chip docking, an RNase-inhibiting solution (20 μl RNaseZap™ solution at 20 μl/min) was injected

followed by ten subsequent injections of DEPC-treated water [31].

The immobilization procedure was performed at a constant flow rate of 5 μl/min at 25.0 °C. For the immobilization of the CRP aptamer, the dextran surface of the chip was further modified with streptavidin (35 μl, 200 μg/ml in 10 mM acetate buffer, pH 5.0) after an activation step (35 μl) with 50 mM *N*-hydroxysuccinimide and 200 mM EDAC [32]. The remaining carboxylated sites on dextran were blocked with ethanolamine (1 M pH 8.6, 35 μl), then the biotinylated aptamer in immobilization buffer was injected (100 μl) after the thermal treatment (95 °C for 1 min, 0 °C for 10 min) [33, 34]. Finally, the surface was blocked with biotin (500 ppm in immobilization buffer, 100 μl) to saturate the remaining free streptavidin sites.

### Binding measurement procedure

After the immobilization of the CRP aptamer on the chip, the binding between the immobilized receptor and CRP, in different concentrations, was monitored with an interaction time of 15 min followed by washing with running buffer. Binding interactions were monitored at a constant flow rate of 2 μl/min at 25 °C.

The measurement cycle consisted of recording the baseline, followed by sample injection, washing with buffer, signal recording and surface regeneration.

A schematic representation of the assay is reported in Fig. 2.

### Surface regeneration

The aptamer-CRP binding was dissociated with 1-min injection of HCl at different concentrations (1, 10 or 25 mM), depending upon the entity of the binding shift to be regenerated. With this treatment the sensor-bound analyte is released from the aptamer.

### Sample pretreatment with magnetic beads

Standard solutions of CRP (0.01 ppm), HSA (500 ppm), IgG (240 ppm) or a mixture of them with and without addition of CRP were incubated with 200 μl of magnetic beads coupled with a protein G suspension for 20 min; then the magnetic separation between the beads and the solution was performed with the use of a magnetic bar. The solutions were further diluted (1:2) in order to reach the relative concentrations corresponding to a 1:100 serum dilution, then these were tested with the aptasensor.

## Results and discussion

In aptasensor development it is important to select a proper immobilization protocol to ensure good analytical performances. Improved sensor performances can be obtained by the addition of tails to the aptamer sequence [16]. Thus, it is necessary to identify the most suitable tail to be used as a spacer when immobilizing the aptamer of interest on a solid surface.

First we investigated the effect of two different tails consisting of a 20-mer polyT and a TEG tail. In both cases the aptamer carried a biotin at the 5′ end to ensure its anchoring to streptavidin-modified surfaces.

In Fig. 3 the immobilization of the aptamer with the TEG tail on the dextran-streptavidin-modified chip is reported versus the SPR signal. Before immobilization, 1 μM aptamer solution was subjected to a thermal treatment (95 °C for 1 min, 0 °C for 10 min), which unfolded the aptamer, making the biotin label at the 5′ end available for interaction with streptavidin on the surface [35]. Finally, the surface was saturated with biotin. The signal recorded for the aptamer binding was 1,988 RU.

When developing an aptasensor, the first step is to optimize the buffer to be employed in the assay. In fact it has been

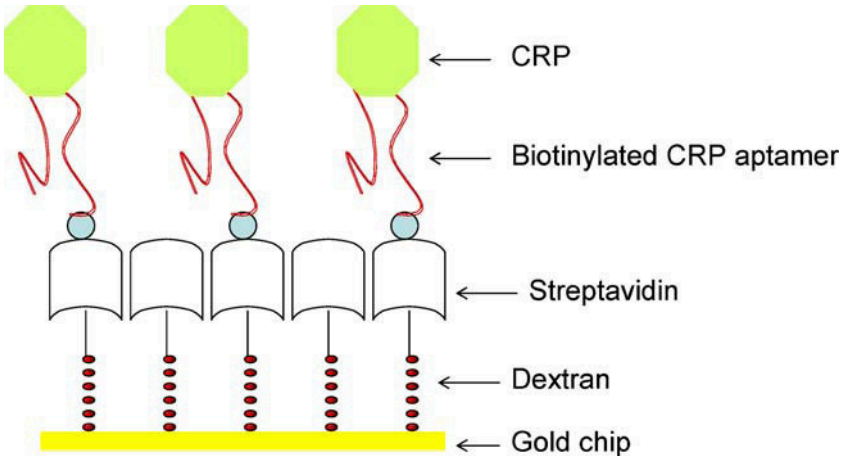


**Fig. 2** A schematic representation of the assay on the CM5 chip

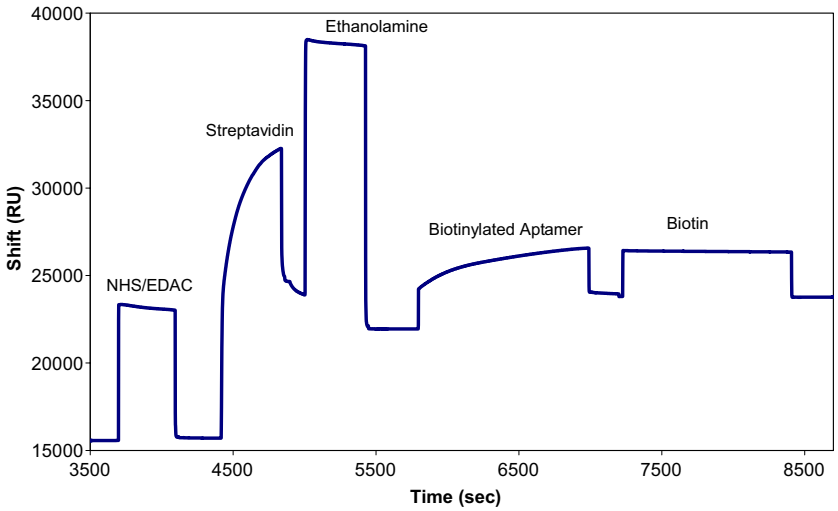


**Fig. 3** Immobilization of the CRP aptamer with the polyT tail on the CM5 chip modified with streptavidin. After the activation with *N*-hydroxysuccinimide (*NHS*)/1-ethyl-3-(dimethylaminopropyl)carbodiimide (*EDAC*), streptavidin (200 ppm) was covalently bound to the carboxylic groups present on the dextran, finally saturated with ethanolamine. The RNA aptamer (1 μM in immobilization buffer), thermally treated, was anchored to the surface via biotin-streptavidin binding, with a resulting shift in the resonance signal of 1,988 RU. Finally biotin (500 ppm) was added to saturate the free sites of streptavidin. *RU* resonance units

reported [16] that this parameter differs from one interaction to another, thus it is difficult to directly transfer the working conditions from an optimized system to a new one.

## Binding buffer optimization

After the immobilization of the aptamer with the polyT tail, the interaction between the immobilized receptor and 1 ppm CRP was monitored with an association time of 15 min followed by washing with running buffer. The experiments were conducted at 25.0 °C. The analyte CRP was dissolved in several buffers differing in salt composition and pH. The effect of the pH in the range 6–7.5 was studied. During the experiments the same buffer was used as a solvent to dissolve the analyte (binding buffer) and as a running buffer, flowing on the chip surface before and after CRP injection.

The following buffers were tested: 10 mM MES pH 6.0, 10 mM HEPES pH 6.0, 10 mM Tris/HCl pH 6.0, 10 mM

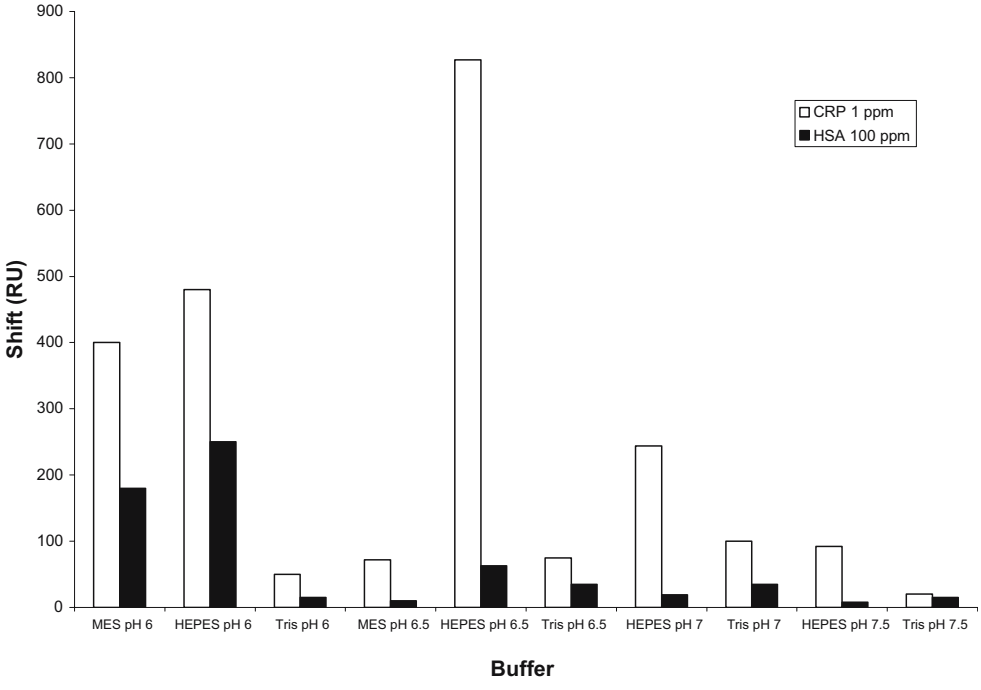


**Fig. 4** Binding buffer optimization using 1 ppm CRP and 100-fold excess concentration of human serum albumin (*HSA*; 100 ppm), as a negative control. The same buffer used in the binding assay was also employed as the running buffer. *MES* 2-(*N*-morpholino)ethanesulfonic acid, *HEPES* 4-(2-hydroxyethyl)piperazine-1-ethanesulfonic acid, *Tris* tris (hydroxymethyl)aminomethane

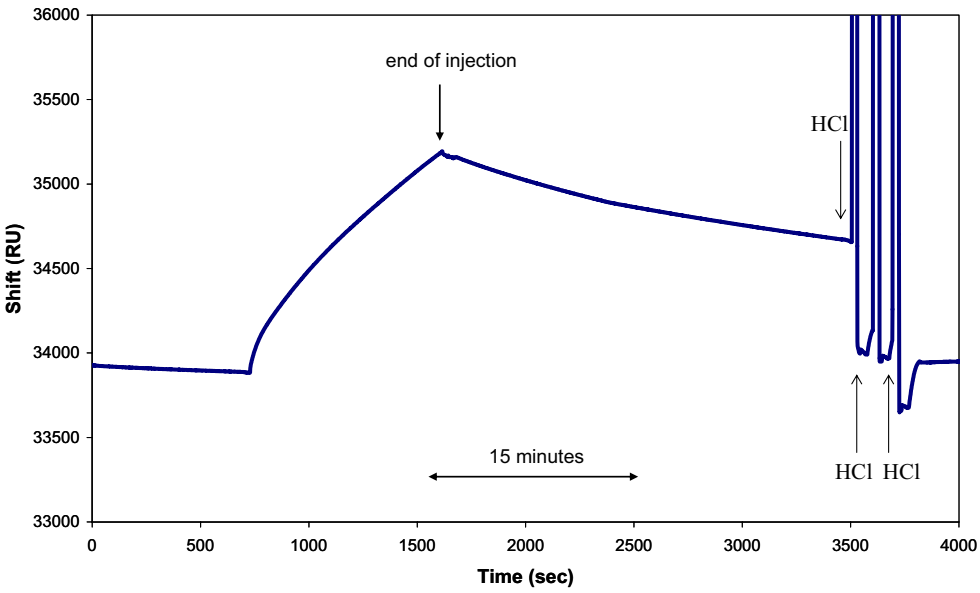


**Fig. 5** CRP binding curve in the absence of calcium ions. CRP aptamer with the polyT tail, CRP concentration 0.5 ppm, binding time 15 min. Binding and running buffer 10 mM HEPES pH 6.5, flow rate 2 μl/min, 25 °C. Binding shift recorded 15 min after the end of the injection 784 RU. Regeneration with 1 mM HCl (three injections)

MES pH 6.5, 10 mM HEPES pH 6.5, 10 mM Tris/HCl pH 6.5, 10 mM HEPES pH 7.0, 10 mM Tris/HCl pH 7.0, 10 mM HEPES pH 7.5, and 10 mM Tris/HCl pH 7.5.

Tris/HCl buffer was tested since a similar buffer was used for the aptamer selection in the SELEX process. The results are shown in Fig. 4, where the frequency shifts recorded for the interaction of the immobilized aptamer with 1 ppm CRP as well as with 100 ppm HSA are reported. HSA was chosen as a negative control since it is the most abundant protein in serum.

HEPES (10 mM at pH 6.5) was chosen as the binding and running buffer, since in this buffer the best ratio between the specific signal (in the presence of CRP) and the unspecific signal (in the presence of HSA) was found.

The surfaces carrying the aptamers modified with the two different tails were tested for their ability to bind the target analyte, in the presence and absence of calcium ion. It should also be noted that the selection process for generating the CRP aptamer was performed in the absence of calcium ions, but on the other hand, calcium ions play an important role in the maintenance of the CRP pentameric structure.

CRP is a soluble $Ca^{2+}$-dependent ligand-binding serum protein (115 kDa) and it has been reported that $Ca^{2+}$ influences the stability of the protein in its pentameric form. In particular, CRP is composed of five identical non-glycosylated polypeptide subunits (206 amino acids, molecular mass 23 kDa), held together by noncovalent interactions to form a circular structure (pentraxin). The ligand-binding site of each protomer is composed of loops with two calcium ions [36]. Human CRP circulates in blood as a stable pentamer (pCRP) in soluble form, but another structural form of CRP exists, known as monomeric CRP (mCRP) [37]. In serum as well as in the purified state CRP has a variable molecular

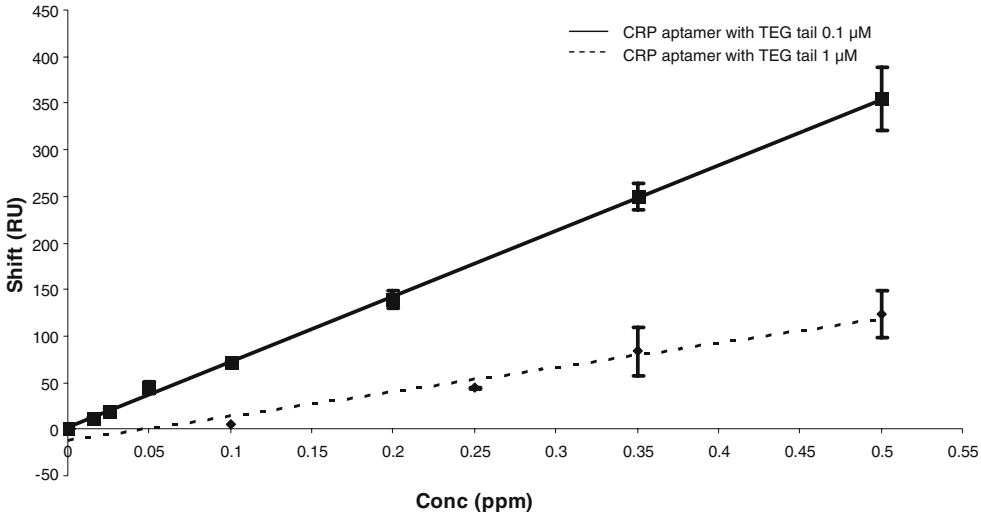


**Fig. 6** Calibration curves obtained by immobilizing CRP aptamer with the triethylene glycol (*TEG*) tail at two different concentrations (1 and 0.1 μM) in 10 mM HEPES pH 6.5, 0.005% Tween 20 on the CM5 Biacore chip. Flow rate 2 μl/min, 25 °C. Binding shifts were recorded 15 min after the end of injection

**Table 1** Analytical characteristics of the assay using the aptamer with the triethylene glycol (*TEG*) and the polyT tails immobilized on the chip (solution used for the immobilization 0.1 μM)

| Aptamer modification | TEG | PolyT |
|---|---|---|
| Aptamer concentration (μM) | 0.1 | 0.1 |
| Linear range (ppm) | 0–0.5 | 0–0.5 |
| Experimental DL (ppm) | 0.015 | 0.05 |
| $R^2$ | 0.999 | 0.977 |
| Average CV (%) | 8 | 8 |
| Binding buffer | 10 mM HEPES pH 6.5, 0.005% Tween 20 | |

*DL* detection limit, *CV* coefficient of variation, *HEPES* 4-(2-hydroxyethyl)piperazine-1-ethanesulfonic acid
Data recorded in the absence of calcium ions

mass ranging from 110 to 144 kDa [38]. It is reported that in the absence of calcium, CRP in a neutral and mildly acid environment self-dissociates, slowly but persistently [39]. Therefore, pCRP is stored in buffer containing $CaCl_2$ to prevent spontaneous formation of mCRP [40]. The purified CRP used in this study was stored in a buffer containing 2 mM $CaCl_2$.

For this reason, the influence of the calcium ions on the binding was first investigated in the case of both polyT- and TEG-modified aptamers immobilized on the chip.

In Fig. 5 a CRP (0.5 ppm) binding curve for binding on the polyT tail aptamer, in the absence of calcium ions, is shown. The aptamer-CRP interaction time was set at 15 min. It was observed that as soon as the injection ended, CRP slowly dissociated. For this reason the binding shift was recorded every time 15 min after the end of the injection. The aptamer-CRP binding was dissociated by using HCl solutions. Up to 45 cycles of binding/regeneration cycles were performed on the same chip without losing sensitivity (data not shown). The slight baseline drift was removed by adding 0.005% Tween 20 both to the running buffer and to the binding buffer, as reported in the BiacoreX™ manual. So the final solution used as the running and binding buffer was 10 mM HEPES pH 6.5, 0.005% Tween 20 with or without the addition of calcium ions.

## Influence of calcium ions on the aptasensor

### *Calibration of CRP in the absence of calcium ions using the CRP aptamer modified with the TEG tail*

The aptamer concentration is one of the critical parameters that influence the analytical performances of the assay; for this reason it was decreased from 1 to 0.1 μM in order to reduce the steric hindrance on the surface.

The analytical performances of the CRP aptamer with the TEG tail was studied in the absence of calcium ions. Calibration curves obtained using the CRP aptamer with the TEG tail immobilized at two different concentrations (1 and 0.1 μM) are compared in Fig. 6. The reported measurements are referred to three repetitions ($n$=3) of each protein concentration. A sensitivity increase (10 times) was found when 0.1 μM aptamer was used for the immobilization. This could be due to the decreased steric hindrance on the surface, in agreement with what was previously reported [16].

### *Calibration without calcium ions: CRP aptamer modified with a 20-mer polyT tail*

Since the best analytical results were obtained using a 0.1 μM solution of the TEG aptamer, the same concentration was also tested for the immobilization of the CRP aptamer by the polyT tail.

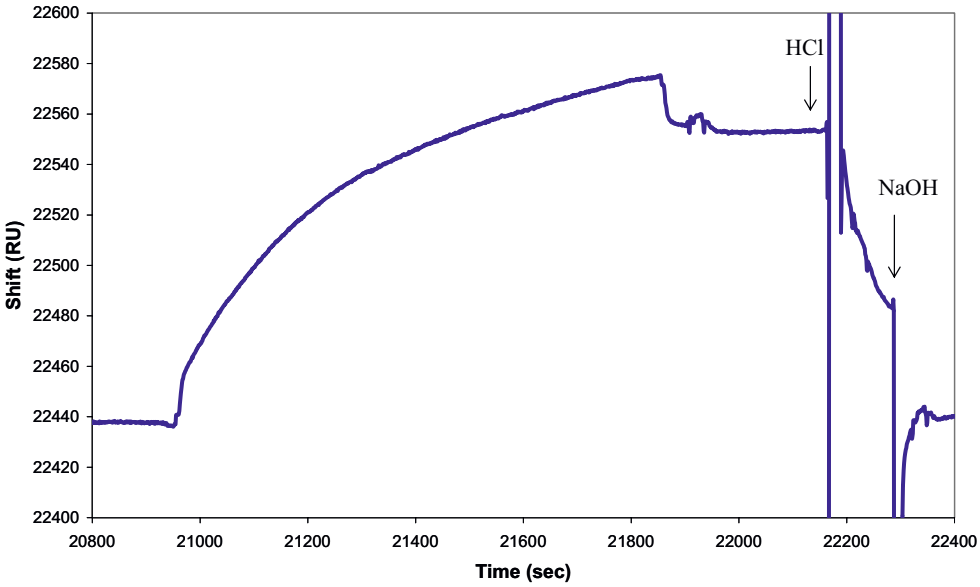


**Fig. 7** CRP binding curve in the presence of calcium ions. CRP aptamer with the TEG tail, CRP concentration 0.025 ppm, binding and running buffer 10 mM HEPES pH 6.5, 0.005%, Tween 20, $CaCl_2$ 2 mM. Binding shift at the end of the injection 115 RU. Regeneration injections in order to return to the baseline 1 mM HCl, 1 mM NaOH

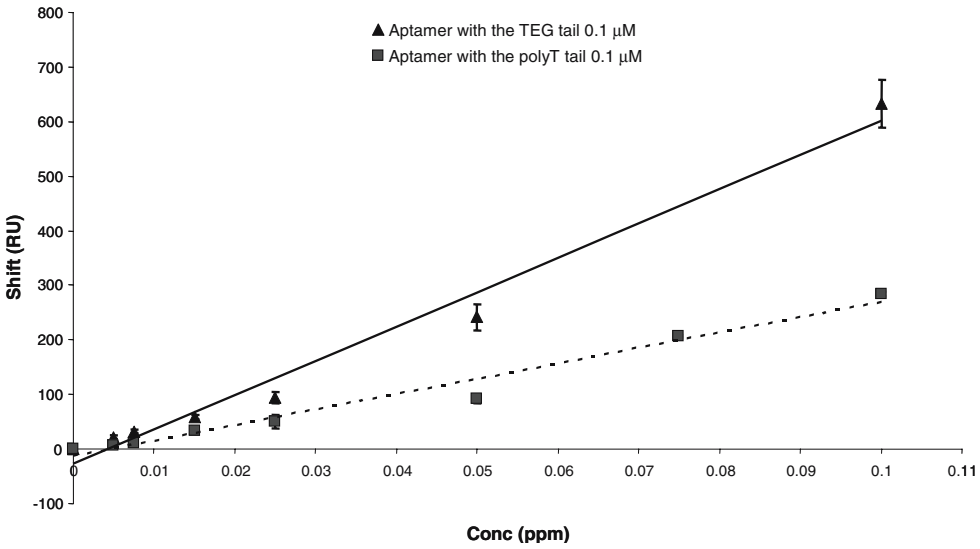


**Fig. 8** Calibration curves obtained by immobilizing 0.1 μM CRP aptamer with the polyT tail or the TEG tail. Flow rate 2 μl/min, 25 °C. Binding shifts were recorded at the end of the injection

Also in this case the CRP-aptamer binding was monitored using 10 mM HEPES pH 6.5 with 0.005% Tween 20 as the running and binding buffer and HCl as the regeneration solution. The analytical characteristics of the assay using the aptamer modified with the polyT and TEG tails, respectively, are reported in Table 1. From the comparison, a slightly superior analytical behavior for the TEG tail aptamer was found.

*Calibration in the presence of calcium ions*

The influence of calcium ions on the analytical performances of the assay was studied. The physiological concentration of calcium is 2 mM as total calcium and 1.3 mM as $Ca^{2+}$ free ion. To mimic the physiological conditions, 2 mM $Ca^{2+}$ was added to the binding and running buffer. The sensorgram recorded during the binding of CRP to the immobilized TEG aptamer is shown in Fig. 7.

The aptamer-CRP complex did not dissociate at the end of the injection, indicating a higher stability of the complex in the presence of $Ca^{2+}$. Consequently, higher RU signals were recorded after 15 min of interaction, with an increase of sensitivity (the experimental detection limit was reduced to 0.005 ppm), using chips modified with either the TEG aptamer or the polyT aptamer. The binding constant, using the BIAevaluation 3.1 program, was estimated to be 0.5 nM (expressed as $K_D$). This value, calculated with the TEG-modified aptamer, is lower than the one reported in the literature (125 nM) [30], calculated in solution but in the absence of calcium.

In Fig. 8 the relative calibration curves are reported. The sensor carrying the aptamer with the TEG tail shows a higher sensitivity, expressed as the slope of the regression line, and the reproducibilities obtained using the aptamer modified by both tails were similar (Table 2). Using the TEG aptamer, we also tested the sensor by decreasing the calcium concentration to 1 mM. Similar results to those

**Table 2** Analytical characteristics of the assay using chips modified with the polyT-tail or the TEG-tail aptamer (concentration 0.1 μM), in presence of calcium ions in the binding buffer

| Aptamer modification | PolyT | TEG |
|---|---|---|
| Binding buffer | 10 mM HEPES pH 6.5, 0.005% Tween 20, 2 mM $CaCl_2$ | |
| Linear range (ppm) | 0–0.1 | 0 – 0.1 |
| Experimental DL (ppm) | 0.005 | 0.005 |
| $R^2$ | 0.975 | 0.982 |
| Linear regression | $y$=2827.3$x$−12.3 | $y$=6297.9$x$−27.7 |
| Average CV (%) | 9 | 11 |
| Cycles | 50 | 50 |

**Table 3** Summary of the standard solutions, that were pretreated by magnetic beads coupled to protein G and then tested with the aptasensor

| Solution | Recovery of proteins after treatment (%) | Shift (RU) |
|---|---|---|
| 0.01 ppm CRP | 99 | 38 |
| 120 ppm IgG | 16 | 158 |
| 500 ppm HSA | 100 | 22 |
| 500 ppm HSA + 120 ppm IgG | 58 | 70 |
| 500 ppm HSA + 120 ppm IgG + 0.01 ppm CRP | 51 | 83 |

*CRP* C–reactive protein, *IgG* immunoglobulin G, *HSA* human serum albumin, *RU* resonance units
The recovery of the proteins after this pretreatment was estimated by spectrophotometric measurements

obtained for 2 mM $Ca^{2+}$ were obtained. In particular, when a low (0.025 ppm) CRP concentration was tested, 358 and 327 RU were recorded, respectively, in the presence of 1 and 2 mM $Ca^{2+}$. Similar findings were obtained at 0.1 ppm CRP. In particular 78 and 95 RU were found, respectively, for 1 and 2 mM $Ca^{2+}$.

To test the specificity of the aptasensor, 500 ppm HSA was used and the recorded response was 10% of the CRP signal at the same dilution factor (10±4 compared with 58± 5 RU).

### Matrix effect evaluation and sample pretreatment

The final goal of this new aptasensor would be the detection of CRP directly in complex matrices like serum samples. SPR-based immunosensing has very recently been applied to CRP detection in human serum [30], but the main limitation of this approach is the single use of a valuable chip, whose functionalization is time-consuming. In fact the CRP, present in serum diluted 1:10, was immobilized directly on the chip, preventing any reuse of the surface. In contrast, our approach is based on the reuse of the sensing surface, allowed by affinity complex dissociation.

For this reason the aptamer was immobilized on the SPR chip and directly exposed to the analyte in solution. Thus, some preliminary experiments in a diluted serum sample were performed to estimate the applicability of the CRP aptasensor to complex matrices.

The sensor, modified by immobilization of the aptamer with the TEG tail, was exposed to serum solutions, diluted 1:100 and filtered (0.2-μm filter) and the response was recorded. Unfortunately, a clear matrix effect was found since a very high RU signal was measured. Since one important protein class in serum is represented by immunoglobulins (IgG), the aptasensor was exposed to an IgG solution. The concentration of IgG injected on the chip was 120 ppm because this is the concentration present in a 1:100 diluted serum. The relative results indicated a very important RU shift induced by IgG, demonstrating a clear interfering effect in the assay.

From this preliminary study, it is evident that a sample clean-up should be conducted to minimize such a matrix effect. For this reason an additional sample pretreatment was applied, in order to remove IgG from serum by using magnetic beads coupled with protein G, able to bind the Fc portion of IgG. Different standard solutions containing CRP or HSA or IgG or a mixture of them, with and without addition of CRP, were tested at a concentration corresponding to a 1:100 serum dilution. The recovery of the proteins after such sample pretreatment was evaluated by spectrophotometric measurements at 280 nm. The results are shown in Table 3. The recovery data and the RU signals indicated that CRP and HSA were not retained by the beads, whereas IgG was partially removed from the sample and a recovery of 16% was observed, resulting in a significant RU shift. In the case of the mixtures containing HSA and IgG or HSA, IgG and CRP, the recorded RU signals are always lower than those related to each single component. This could be due to an interaction effect between IgG and the other proteins. In conclusion, the interesting analytical performances obtained with the aptasensor represent the prerequisite for the possible application of the device to real matrices. However, further work is required on sample pretreatment in order to reduce the interferences that have not yet been completely identified.

## Conclusions

Different parameters potentially affecting the analytical performances [selectivity, linearity ($R^2$), reproducibility and stability] of the aptasensor were evaluated. In particular, the influence of the aptamer immobilization procedure (chemistry, length, concentration), as well as the binding conditions, i.e., the influence of different buffers on the binding, the presence of $Ca^{2+}$ ions and the specificity (against HSA), were evaluated. Regarding the immobilization step, it has been demonstrated that the TEG tail was more suitable for aptamer immobilization than the polyT tail. Then it was found that HEPES at pH 6.5 with 0.005% Tween 20 was the best buffer to use in the binding step, giving the highest specific CRP response. The influence of calcium ions on the sensor performances was clearly demonstrated. In the presence of 2 mM $Ca^{2+}$, the aptamer-CRP complex was stabilized and higher signals were recorded. The reproducibility of the system, expressed as the coefficient of variation was estimated to be 11% and the experimental detection limit (0.005 ppm) was very good and compatible with clinical applications. Experiments performed in serum suggest the need for a sample pretreatment to apply this aptasensor in complex solutions. Preliminary studies to reduce the interfering effect caused by IgG were conducted by a sample treatment with magnetic beads coupled with protein G. Further efforts will be made to minimize the matrix effect by diluting serum 1:500, thanks to the high sensitivity of the assay.

This study is important for future analytical applications of the sensor, eventually using different transduction principles. To our knowledge, the interaction between the RNA aptamer, immobilized on the sensing surface, and its target analyte had not been studied before. On the basis of this, the main goal of this work was to find the conditions for the binding in the heterogeneous phase and then to improve the analytical performances of the aptasensor by optimization of some simple but critical parameters.

**Acknowledgements** We thank the European Community for partially funding this work with the Integrated Project CARE-MAN, Healthcare by Biosensor Measurements and Networking (NMP4-CT-2006-017333).

## References

1. Jayasena SD (1999) Clin Chem 45:1628–1650
2. Tuerk C, Gold L (1990) Science 249:505–510
3. Ellington AD, Szostak JW (1990) Nature 346:818–822
4. Luzi E, Minunni M, Tombelli S, Mascini M (2003) Trends Anal Chem 22:810–818
5. Tombelli, S, Minunni M, Mascini M (2005) Biosens Bioelectron 20:2424–2434
6. Yang L, Fung CW, Cho EJ, Ellington AD (2007) Anal Chem 79:3320–3329
7. Tombelli S, Minunni M, Mascini M (2007) Biomed Eng 24:191–200
8. Li YY, Zhang C, Li BS, Zhao LF, Li XB, Yang WJ, Xu SQ (2007) Clin Chem 56:1061–1066
9. Tombelli S, Minunni M, Mascini M (2007) In: Van Emon JM (Ed) Immunoassays and other bioanalytical techniques. CRC, New York
10. Wang J (2007) Electroanalysis 19:769–776
11. Hamula CLA, Guthrie JW, Zhang H, Li XF, Le XC (2006) Trends Anal Chem 25:681–691
12. Lin C, Katilius E, Liu Y, Zhang J, Yan H (2006) Angew Chem Int Ed 45:5296–5301
13. Maehashi K, Katsura T, Kerman K, Takamura Y, Matsumoto K, Tamiya E (2007) Anal Chem 79:782–787
14. Li Y, Hye Jin Lee HJ, Corn RM (2007) Anal Chem 79:1082–1088
15. Centi S, Tombelli S, Minunni M, Mascini M (2007) Anal Chem 79:1466–1473
16. Bini A, Minunni M, Tombelli S, Centi S, Mascini M (2007) Anal Chem 79:3016–3019
17. Xiao Y, Lubin AA, Heeger AJ, Plaxco KW (2005) Angew Chem Int Ed 44:5456–5459
18. Heyduk E, Heyduk T (2005) Anal Chem 77:1147–1156
19. Lai RY, Plaxco KW, Heeger AJ (2007) Anal Chem 79:229–233
20. Clearfield MB (2005) J Am Osteopath Assoc 105:409–416
21. Ledue TB, Rifai N (2001) Clin Chem Lab Med 39:1171–1176
22. Zhan W, Bar AJ (2007) Anal Chem 79:459–463
23. Kartalov EP, Zhong JF, Scherer A, Quake SR, Taylor CR, Anderson WF (2006) BioTechniques 40:85–90
24. Kriz K, Ibraimi F, Lu M, Hansson LO, Kriz D (2005) Anal Chem 77:5920–5924
25. Meyer MHF, Hartmann M, Krause HJ, Blankenstein G, Mueller-Chorus B, Oster J, Miethe P, Keusgen M (2007) Biosens Bioelectron 22:973–979
26. Hu WP, Hsu HY, Chiou A, Tseng KY, Lin HY, Chang GL, Chen SJ (2006) Biosens Bioelectron 21:1631–1637
27. Meyer MHF, Hartmann M, Keusgen M (2006) Biosens Bioelectron 21:1987–1990
28. Lin S, Lee C-K, Lin Y-H, Lee S-Y, Sheu B-C, Tsai J-C, Hsu S-M, (2006) Biosens Bioelectron 22:715–721
29. Jung S-H, Jung J-W, Suh I-B, Yuk JS, Kim W-J, Choi EY, Kim Y-M, Ha K-S (2007) Anal Chem 79:5703–5710
30. Kim SD, Ryu JS, Yi HK, Kim SC, Zhang BT (2004) In: Proceedings of the 10th international meeting on DNA computing, pp 334–343
31. Davis TM, Wilson WD (2001) Methods Enzymol 340:22–50
32. Lofas S, Johnsson B (1990) J Chem Soc Chem Commun 21: 1526–1528
33. Ducongè F, Di Primo C, Toulmè JJ (2000) J Biol Chem 275: 21287–21294
34. Minunni M, Tombelli S, Gullotto A, Luzi E, Mascini M (2004) Biosens Bioelectron 20:1149–1156
35. Tombelli S, Minunni M, Luzi E, Mascini M (2005) Bioelectrochemistry 67:135–141
36. Shrive AK, Gheetham GMT, Holden D, Myles DAA, Turnell WG, Volanakis JE, Pepys MB, Bloomer AC, Greenhough, TJ (1996) Nat Struct Mol Biol 3:346–354
37. Potempa LA, Siegel JN, Fedel BA, Potempa RT, Gewurz H (1987) Mol Immunol 24:531–541
38. Oliveira EB, Gotschlich EC, Liu TY (1977) Proc Natl Acad Sci USA 74:3148–3151
39. Wang HW, Wu Y, Chen Y, Sui SF (2002) Int J Mol Med 9:665–671
40. Khreiss T, Jozsef L, Potempa A, Filep JG (2004) Circulation 109:2016–2022

# Chapter 2

# Piezoelectric Biosensors for Aptamer–Protein Interaction

**Sara Tombelli, Alessandra Bini, Maria Minunni, and Marco Mascini**

## Summary

Aptamers can be considered as a valid alternative to antibodies or other biomimetic receptors for the development of biosensors and other analytical methods. The production of aptamers is commonly performed by the SELEX (Systematic Evolution of Ligands by Exponential Enrichment) process, which, starting from large libraries of oligonucleotides, allows the isolation of large amounts of functional nucleic acids by an iterative process of in vitro selection and subsequent amplification through polymerase chain reaction. Aptamers are suitable for applications based on molecular recognition as analytical, diagnostic, and therapeutic tools.

The use of aptamers as biorecognition element in piezoelectric biosensors will be here reported with particular application to the detection of thrombin.

**Key words:** Biosensor, DNA, Aptamers, Thrombin, Quartz crystal microbalance.

## 2.1. Introduction

Aptamers are single-stranded DNA or RNA ligands, which can be selected for different targets starting from a large library of molecules containing randomly created sequences *(1)*. The selection process is called SELEX (Systematic Evolution of Ligands by Exponential enrichment), first reported in 1990 *(2, 3)*. The SELEX process involves iterative cycles of selection and amplification starting from a large library of oligonucleotides with different sequences (generally $10^{15}$ different structures). After the incubation with the specific target and the partitioning of the binding from the nonbinding molecules, the oligonucleotides that are selected are amplified to create a new mixture enriched in those nucleic acid molecules having a higher affinity for the target. After several cycles

Avraham Rasooly and Keith E. Herold (eds.), *Methods in Molecular Biology: Biosensors and Biodetection, Vol. 504*

Book doi: 10.1007/978-1-60327-569-9_2

of the selection process, the pool is enriched in the high affinity sequences at the expense of the low affinity binders.

Aptamers can offer advantages over antibodies that make them very promising for analytical applications *(4, 5)*. The main advantage is the overcoming of the use of animals or cell lines for the production of the molecules. Antibodies against molecules that are not immunogenic are difficult to generate. On the contrary, aptamers are isolated by in vitro methods that are independent on animals, since an in vitro combinatorial library can be generated against any target. Moreover, the aptamer selection process can be manipulated to obtain aptamers that bind a specific region of the target and with specific binding properties in different binding conditions. After selection, aptamers are produced by chemical synthesis and purified to a very high degree by eliminating the batch-to-batch variation found when using antibodies. Another advantage over antibodies can be seen in the higher temperature stability of aptamers; in fact antibodies are large proteins sensitive to the temperature and they can undergo irreversible denaturation. On the contrary, aptamers are very stable and they can recover their native active conformation after denaturation.

Besides antibodies, the selections process itself, with the amplification step, gives some advantages to aptamer with respect to other "nonnatural" receptors, such as oligopeptides, which cannot be amplified during their selection procedure.

The additional attractive aspect of aptamers for researchers in the analytical field is the wide range of molecules for which they can be selected, including organic dyes *(6)*, amino acids *(7)*, antibiotics *(8)*, peptides *(9)*, proteins ***(10)***, vitamins *(11)*, and also whole cells *(12)* or micro-organisms such as bacteria *(13)*.

With respect to their application, aptamers were selected in the past mainly for their use as therapeutic agents. In addition to the therapeutic field, aptamers have been then used in several analytical methodologies, such as affinity chromatography (Michaud et al. 2004), capillary electrophoresis *(14)*, mass spectrometry *(15)*, or biosensors *(1)*. These aptamers-based methods have been mainly employed in the clinical area for the development of diagnostic assays.

A very attracting application is the exploitation of aptamers as biorecognition elements in biosensors and the majority of the reported aptamer-based biosensors make use of the thrombin-binding aptamer (15-mer, 5′-GGTTGGTGTGGTTGG-3′). This DNA aptamer was the first one selected in vitro, specific for a protein without nucleic acids-binding properties[5], and it has been studied as anticlotting therapeutic tool *(16, 17)*. The thrombin-binding aptamer has been extensively investigated: its G-quartet structure has been established *(18, 19)* and the binding site has been identified *(20)*. This aptamer has been coupled to different transduction principles to demonstrate the wide

applicability of aptamers as bioreceptors in biosensors *(21–27)*. These studies clearly indicate the suitability of aptamer-based systems for analytical applications.

Thrombin (factor IIa) is the last enzyme protease involved in the coagulation cascade, and it converts fibrinogen to insoluble fibrin that forms the fibrin gel either in physiological conditions or in a pathological thrombus *(28)*. Thrombin has also hormone-like properties, and it is involved in thrombosis and platelet activation. Therefore, thrombin plays a central role in a number of cardiovascular diseases *(29)*, and it is thought to regulate many processes in inflammation and tissue repair at the vessel wall.

The concentration of thrombin in blood can vary considerably: thrombin, not present in blood under normal conditions, can reach low micromolar concentrations during the coagulation process but low levels (low nM) of thrombin generated early in haemostasis are also important to the overall process *(30)*. Out of the haemostatic process, circulating thrombin has been detected at high pM range in blood of patients suffering from diseases known to be associated with coagulation abnormalities.

This chapter deals with the coupling of the thrombin aptamer with quartz crystal microbalance devices for the development of aptamer-based piezoelectric biosensors.

The term "piezoelectric" derived from the Greek word *piezen* meaning "to press." The first investigation on the piezoelectricity was performed in 1880 by Jacques and Pierre Curie *(31)*, who observed that a mechanical stress applied to the surfaces of various crystals caused a corresponding electrical potential across the crystal, whose magnitude was proportional to the applied stress. The Curies also verified the converse piezoelectric effect in which application of a voltage across these crystals caused a corresponding mechanical strain. Application of an alternating electric field across the crystal substrate results in an alternating strain field. This causes a vibrational, or oscillatory, motion in the crystal, resulting in the generation of acoustic standing waves. Depending on various criteria, the oscillator vibrates at a characteristic resonant frequency.

The most used devices in biosensors are generally bulk acoustic wave (BAW)-based employing AT-cut quartz crystals.

An AT-cut crystal is typically cut at an angle of + 35°15′ and has a zero frequency temperature coefficient at or near room temperature that results in minimal frequency changes due to temperature *(32)*. AT-cut crystals oscillate in the thickness shear mode *(33)*.

The first quantitative investigation of the piezoelectric effect was performed by Sauerbrey, who derived the relationship for the change in frequency $\Delta F$ (in Hz) caused by the added mass $\Delta m$ (in g):

$$\Delta F = -\frac{2F_0^2}{A\sqrt{\mu_Q \rho_Q}} \cdot \Delta m$$

where $F_0$ is the fundamental resonant frequency of unloaded quartz, $\mu_Q$ is the shear modulus of AT-cut quartz ($2.947 \times 10^{11}$ g cm$^{-1}$s$^{-2}$), $\rho_Q$ is the density of the quartz (2.648 g cm$^{-3}$) and $A$ is the surface area in cm$^2$ *(34)*. The Sauerbrey equation assumes a uniform distribution of mass on the entire electrode portion of an AT-cut quartz crystal. Mass sensitivity decreases monotonically with the radius, in a Gaussian manner becoming negligible at and beyond the electrode boundary *(35)*. Another assumption of this equation is that the mass added or lost at the crystal surface does not experience any deformation during the oscillation: this is true for thin, rigid layers. For thicker, less rigid layers, a more complex theory is necessary.

Piezoelectric crystals have been used as microbalances and as a microviscometer owing to their small size, high sensitivity, simplicity of construction and operation, light weight and the low power required *(36)*. The quartz–crystal microbalance (QCM) has traditionally been used in many applications such as thin film deposition control, etching studies, aerosol mass measurements, and space system contamination studies *(37)*. Recently, however, the interest in the application of piezoelectric devices in the field of analysis has increased, since it was realized that many opportunities for molecular sensing can be opened up once a suitable recognition layer or molecule is coated on the crystal. In particular, piezoelectric biosensors have found a wide range of applications in food *(38, 39)*, environmental, and clinical *(40, 41)* analysis.

## 2.2. Materials

### 2.2.1. Aptamer and Target Protein

1. α-Thro mbin from human plasma, MW 37 kDa (Sigma, Milan, Italy) (Product number: T6884). Thrombin is shipped as lyophilized powder containing 417 NIH Units of protein (3,093 MIH Units/mg). Thrombin stock solution (aliquots: 20 µL, 3.6 µM in binding buffer) was stored at −20°C and for the experiments further dilutions in binding buffer were stored in ice during measurements.
2. 15-mer DNA aptamer for thrombin (MWG Biotech, Milan, Italy) with the following sequence: 5′ biotin TTTTTTTTTTTTTTTTTTTT GGT TGG TGT GGT TGG 3′ *(42)*. The aptamer (MW 5053 g/mol) is received lyophilized and then diluted in MilliQ water. The diluted aptamer can be stored at −20°C. The aptamer is biotinylated a the 5′ end to allow its immobilization onto streptavidin-modified surfaces. The insertion of the polyT (20-mer) tail at the 5′ end

of the aptamer sequence is necessary for the optimal immobilization of the aptamer onto a solid support (*see* **Note 1**).

3. *Immobilization buffer*: 300 mM NaCl, 20 mM $Na_2HPO_4$, 0.1 mM EDTA, pH 7.4.
4. *Binding buffer*: 50 mM Tris–HCl, 140 mM NaCl, 1 mM $MgCl_2$, pH 7.4.
5. Human serum albumin (Sigma, Milan, Italy) (Product number: A9511) was used as negative control. Albumin was shipped lyophilized and stored at 4°C. Further dilutions were prepared in binding buffer and used after preparation.
6. Human serum from clotted male whole blood (Sigma, Milan, Italy) (Product number: H1388) was used to study the effect of a complex matrix. Serum can be divided into aliquots and stored at –20°C. Human citrated plasma (Sigma, Milan, Italy) (Product number: P9523) was used as naturally containing complex matrix.

### 2.2.2. Other Reagents

1. Streptavidin, bis-2-methoxyethyl ether (diglyme), bromoacetic acid, bovine serum albumin, ethanolamine hydrochloride, Tween 20, mercaptoundecanol, *N*-(3-Dimethylaminopropyl)-*N'*-ethylcarbodiimide hydrochloride (EDAC) (Sigma, Milan, Italy).
2. Ammonium sulphate, $NH_3$, $H_2O_2$, ethanol, NaOH, EDTA (Merck, Milan, Italy).
3. Epichlorohydrin, *N*-hydroxysuccinimide (NHS) (Fluka, Milan, Italy).
4. Dextran T500 (Amersham Biosciences Europe, Milan, Italy).
5. NAP™ 10 Columns (17–0854–01, GE Healthcare, Uppsala, Sweden) as exchanging buffer system for plasma purification.

### 2.2.3. Instrumentation

1. The complete measuring system is illustrated in **Fig. 2.1**. 9.5 MHz AT cut quartz crystals (14 mm, 165 µm) with gold evaporated on both sides (42.6 $mm^2$ area, Ø 7.4 mm) (International Crystal Manufacturing (USA)). The quartz crystal (**Fig. 2.1A**) is housed inside the measurement cell such that only one side of the resonator is in contact with the solution in the cell well; in this way two measurement series can be performed on the same resonator, one for each side. The cell is made of methacrylate, which is resistant and inert toward the chemicals used in the experiment, rigid, allowing to fix it to a support with a pincer and transparent, so that it is possible to observe any anomalies (air bubbles) that could be present into the well. The cell consists in two blocks of methacrylate, which are hold together by two screws (**Fig. 2.1B**). The crystal is housed between these two blocks, and it is sandwiched between two *o*-rings. This kind of cell is used for batch measurements, and the solution of the reagents is inserted into the

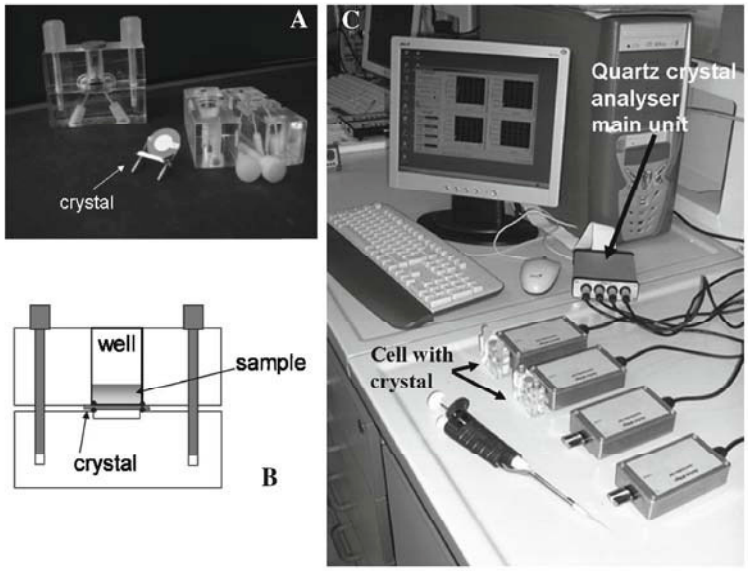


Fig. 2.1. (A) Quartz crystal and working cell; (B) Schematic view of the working cell. The crystal is hold between two -rings, and the sample is injected into the cell well. Only one side of the crystal is in contact with the solution; (C) Photograph of the whole measuring system with the cells and the quartz crystal analyser.

cell by pipetting it directly in the upper cell well. The volume of the well is around 1 mL but for the typical volumes used the measurements are between 100 and 200 µL.

2. The frequency variations are continuously recorded using a quartz crystal analyser, QCMagic from Elbatech (Marciana, LI, Italy) (**Fig. 2.1C**). A detailed diagram with all the measurements components is illustrated in **Fig. 2.2**. QCMagic is a measuring instrument for the recovery of the oscillation frequency of a working quartz crystal. The system is interfaced to the driving personal computer (PC) by means of a digital counter PCI board. One single PCI board can drive up to four oscillator units, thus allowing operating with up to four independent quartz crystal. QCMagic makes use of an internal reference crystal, used as a timebase comparator. Depending on the frequency of this internal timebase, each unit can be tuned to work with a specific working crystal, chosen between 1 and 10 MHz. When more units are used, they are cross-connected by means of one single cable carrying both power supply and signals. QCMagic is interfaced with a PC for data acquisition and storage. The system is driven by a software running under MS-Windows™. Oscillating frequency vs. time measurements can be performed following the data acquisition in real time on the computer screen, by means of strip chart plotting. Examples are given in **Figs. 2.3** and **2.4**. The analytical data are the differences between two stable frequency values (±0.5 Hz).

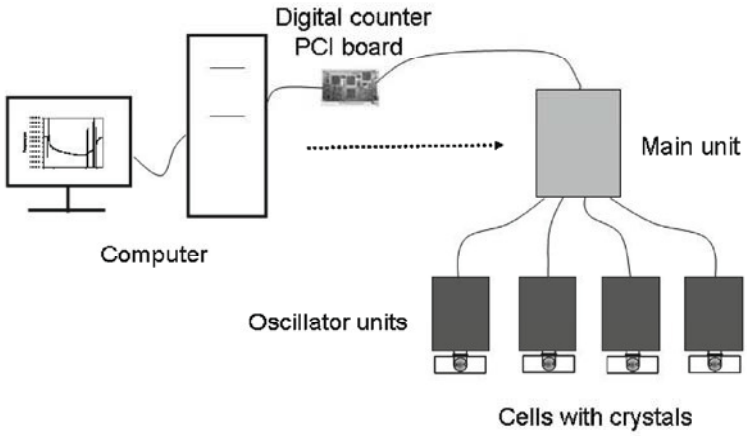


Fig. 2.2. The components of the measuring system.

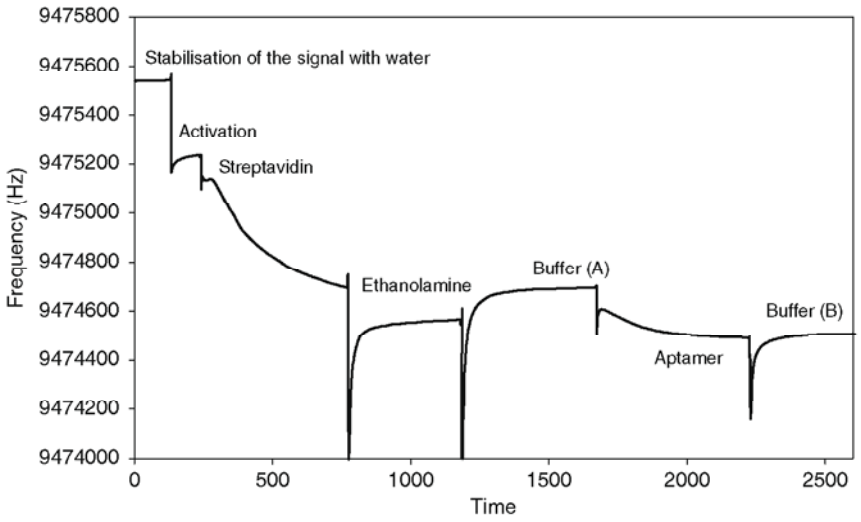


Fig. 2.3. Typical frequency variations (vs. time) recorded during the functionalization of the crystal and the immobilization of the aptamer. The entity of the immobilization can be evaluated by the difference between the frequency shift of the two steps Buffer (B) – Buffer (A).

## 2.3. Methods

### *2.3.1. Immobilization of the Aptamer onto Piezoelectric Crystals*

1. The immobilization chemistry adopted follows the approach described in Tombelli et al. *(43)*. In particular, before the immobilization of the aptamer, the electrode surface of the quartz crystal needs to be cleaned with a boiling solution consisting of $H_2O_2$ (33%), $NH_3$ (33%), and milliQ water in a 1:1:5 ratio. The crystals are immersed in the solution for 10 min. They are then thoroughly washed with distilled water and used immediately afterwards.

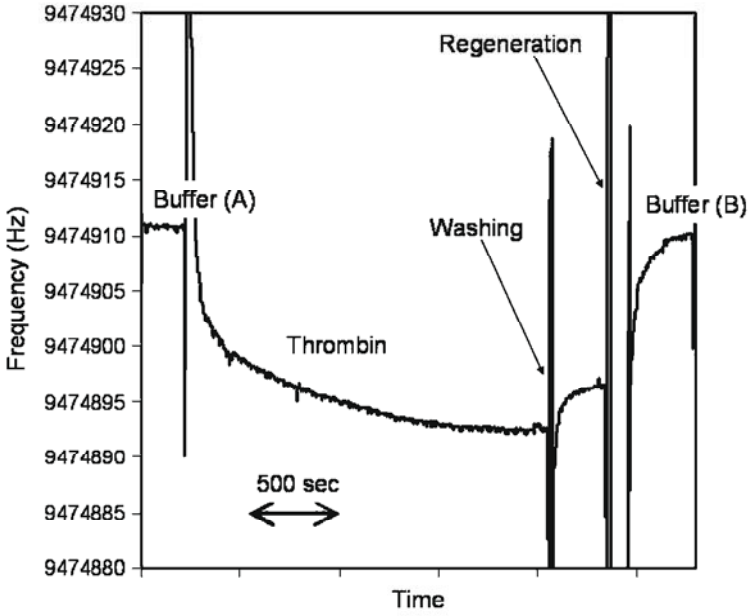


Fig. 2.4. Typical frequency variations (vs. time) recorded during the binding of thrombin (50 nM) to the immobilized aptamer. The reported analytical datum will be the difference in frequency between Buffer (B) and Buffer (A), which represents the baseline.

2. The freshly cleaned crystal is immersed in an unstirred 1 mM ethanolic solution of 11-mercaptoundecanol at room temperature, in the dark, for 48 h. The solution of 11-mercaptoundecanol is freshly prepared before use (2 mg of the thiol in 10 mL of ethanol). The crystal is then washed with ethanol and milliQ water and sonicated for 10 min in ethanol to remove the excess of thiol. The hydroxylic surface is treated with a 600 mM solution of epichlorohydrin in a 1:1 mixture of 400 mM NaOH and bis-2-methoxyethyl ether (diglyme) for 4 h. After washing with water and ethanol, the crystal is immersed for 20 h in a basic dextran solution (3 g of dextran in 10 mL of NaOH 100 mM). The surface is further functionalized with a carboxymethyl group using bromoacetic acid (1 M solution in 2 M NaOH for 16 h). All the reactions are performed at room temperature. The coated crystals can be stored at 4°C immersed in milliQ water for 15 days. For their use, the crystals are washed with water and placed in the cell.
3. For further functionalization, the surface of the crystal is activated prior to covalent coupling with 200 µL of a solution of NHS 50 mM and EDAC 200 mM in water (*see* **Note 2**). After 5 min, the activating solution is replaced by streptavidin 200 µg/mL in acetate buffer 10 mM, pH 5 for 20 min. The residual reacting sites are blocked with 200 µL of a solution

of ethanolamine hydrochloride (pH 8.6, 1 M water solution). After washing with the immobilization buffer, the biotinylated aptamer is added (200 µL of a solution 1.0 µM of the probe in immobilization buffer). The immobilization is allowed to proceed for 20 min (**Fig. 2.3**).

4. The biotinylated aptamer (0.5 µM, (*see* **Note 3**)) is thermally treated before its immobilization. The thermal treatment can unfold the aptamer strand making the biotin label at the 5′ end available for the interaction with streptavidin on the chip surface. Before the immobilization, the biotinylated aptamer is heated at 90°C for 1 min to unfold the DNA strand and then cooled in ice for 10 min to block the DNA in its unfolded structure *(44)* (*see* **Note 4**).
5. The cell with the immobilized aptamer is stored at 4°C with 200 µL of binding buffer.

### 2.3.2. Binding Measurements

1. After the immobilization of the aptamer, the frequency is stabilized by keeping the crystal in contact with 100 µL of binding buffer. Thrombin (100 µL) is then added to the cell and left in contact with the immobilized aptamer for 30 min. The surface is then washed with buffer to remove the unbound protein (**Fig. 2.4**).
2. The analytical data, expressed as frequency shift, are the differences in the frequency of the crystal before the addition of thrombin and after the washing with buffer subsequent to the affinity interaction. A signal generated by the aptamer–protein interaction is considered significative when the difference between the frequency values corresponding to the two buffers is higher than 3 Hz. Different concentrations of the protein can be used to build a calibration plot. An example of calibration plot is shown in **Fig. 2.5**.
3. After each cycle of binding, the crystal surface can be regenerated by 1 min treatment with 2 M NaCl. With this treatment, the sensor-bound analyte is released at increased ionic strength that unfolds the three-dimensional structure of the aptamer without damaging the oligomer structure, and the baseline is reached again, allowing the multiuse of the sensor. The regeneration is considered successful when the frequency value of buffer (B) (**Fig. 2.4**) has reached again the frequency value corresponding to buffer (A) (**Fig. 2.4**). Generally, on the same crystal surface, 20 measurements can be performed without loss in sensitivity.
4. Negative controls can be tested to prove the specificity of the interaction. Human serum albumin is present in plasma and serum at high concentration (~50,000 mg/L), and it must be tested to prove the absence of nonspecific adsorption due to this high concentration in real matrices (*see* **Note 5**).

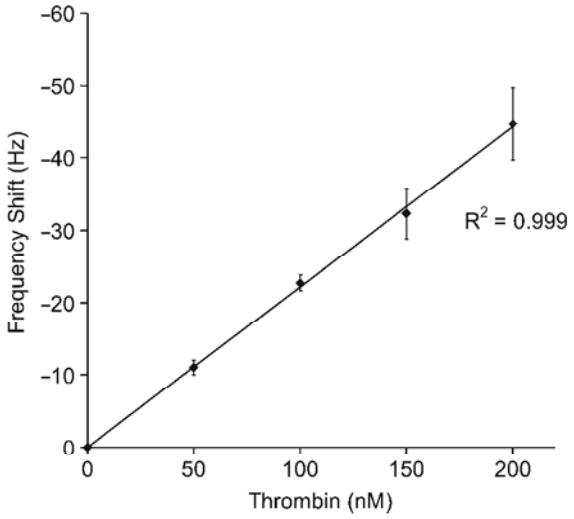


Fig. 2.5. Typical calibration plot obtained with different concentrations of thrombin (0–200 nM) interacting with the immobilized aptamer. Thrombin is diluted in binding buffer; interaction time 30 min.

5. Standard solutions of thrombin can be added to serum or plasma to test the performance of the biosensor in complex matrices. Since serum is not containing coagulation factors, the addition of thrombin is not affecting the samples (*see* **Note 6**). On the contrary, the addition of thrombin to plasma, which contains all the proteins involved in the coagulation cascade including fibrinogen, leads to the formation of fibrin and to the rapid sample clotting. To avoid this phenomenon, fibrinogen has to be precipitated from plasma before the addition of thrombin in the preparation of spiked samples (*see* **Note 7**). After precipitation of fibrinogen thrombin can be added to plasma (*see* **Note 8**).

## 2.4. Notes

1. The procedure to fix the aptamer to a solid surface is of paramount importance to obtain an ordered and oriented layer able to assure, as much as possible, the flexibility of the bioreceptor without altering the affinity for the target molecule (Tombelli 2005). For this reason, both the influence of a spacer in the aptamer binding behavior and of the immobilization protocol have to be studied. The spacer can consist in a polyT(20) added to the binding sequence of the aptamer. When examining the performances obtained with this aptamer on the

piezoelectric biosensor for thrombin, it showed a good reproducibility (average CV% for the concentrations of thrombin, 100 and 200 nM: 13%) and a very good selectivity as demonstrated by the low signal ($\Delta F < 3$ Hz) obtained with a high concentration of human serum albumin (77 μM HSA), used as negative control. The higher sensitivity obtained with this aptamer is probably due to the presence of the spacer that maintains the aptamer far from the sensor surface allowing the proper conformation for molecular recognition. When the biotinylated aptamer without the polyT tail was immobilized, very low sensitivity ($\Delta F$ for thrombin 200 nM < 20 Hz) was found, even if comparable surface density occurred.

2. The NHS and EDAC solution must be prepared immediately before use to avoid loss of activity.
3. By changing the concentration of aptamer for its immobilization, the surface capacity is not affected by the dilution from 1 to 0.5 μM of the aptamer. On the contrary, a further dilution to 0.1 μM dramatically reduced the biosensor sensitivity.
4. Even if the thermal treatment has no effect on the aptamer surface density ($2.5 \times 10^{13}$ molecules/cm$^2$ with or without the treatment), the linearity in the thrombin range 0–200 nM ($R^2 = 0.977$) and the reproducibility of the binding step (CV% = 21%) significantly improved. This result confirms that the thermal treatment ensures correct intramolecular folding.
5. To check the specificity of the sensor HSA at high concentration (77 μM), in a 1,400-fold excess respect to thrombin, is used. The interaction did not result in a measurable frequency decrease ($\Delta F < 3$ Hz), demonstrating the high specificity of the sensor.
6. Thrombin was detected in serum diluted 1:100 spiked with thrombin in a concentration range 0–200 nM, with a blank value of −32 Hz. The recorded signals increased with the concentration of added thrombin demonstrating that the aptasensor was able to operate in this complex matrix. However, since serum is not containing the proteins involved in coagulation, further experiments have to be carried out with plasma, which is the matrix where normally thrombin is detected.
7. The selective precipitation of fibrinogen is based on the use of ammonium sulphate as precipitant: 250 μL of plasma are treated with 1,250 μL of 2 M ammonium sulphate and 1,000 μL of 0.1 M sodium chloride. The solution is mixed for 3–4 min, then centrifuged, and the supernatant is eluted in a NAP column for a rapid desalting and buffer exchange. The protein amount of the raw plasma and of the eluted solution was evaluated by spectrophotometric measurements at $\lambda = 280$ nm to estimate the loss of protein content after precipitation of fibrinogen.

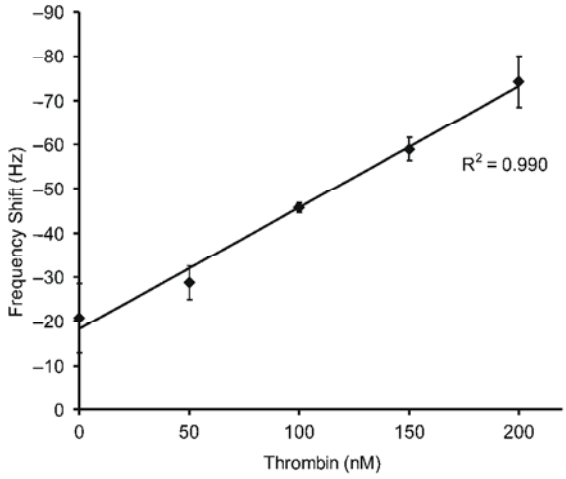


Fig. 2.6. Typical calibration plot obtained with different concentrations of thrombin (0–200 nM) interacting with the immobilized aptamer. Thrombin is added to plasma (1:10 in binding buffer); interaction time 30 min.

8. Thrombin is added to plasma diluted 1:100 in a concentration range 0–200 nM. The response is linear in the tested concentration range ($R^2$ = 0.990) and reproducibility was good (CV% = 13%). The matrix effect with a blank signal of –21 Hz is present but, despite the high complexity of the matrix, the increase in thrombin concentration could be detected (**Fig. 2.6**).

## References


1. Tombelli, S., Minunni, M., Mascini, M. (2005). Analytical applications of aptamers. Biosens. Bioelectron. 20, 2424–2434
2. Tuerk, C., Gold, L. (1990). Systematic evolution of ligands by exponential enrichment. Science 249, 505–510
3. Ellington, A.D., Szostak, J.W. (1990). In vitro selection of RNA molecules that bind specific ligands. Nature 346, 818–822
4. Luzi, E., Minunni, M., Tombelli, S., Mascini, M. (2003). New trends in affinity sensing: aptamers for ligand binding. TrAC. Trends Analyt. Chem. 22, 810–818
5. O'Sullivan, C.K. (2002). Aptasensors-the future of biosensing? Anal. Bioanal. Chem. 372, 44–48
6. Ellington, A.D., Szostak, J.W. (1992). Selection in vitro of single-stranded DNA molecules that fold into specific ligand-binding structures. Nature 355, 850–852
7. Geiger, A., Burgstaller, P., Von der Eltz, H., Roeder, A., Famulok, M. (1996). RNA aptamers that bind L-arginine with sub-micromolar dissociation constants and high enantioselectivity. Nucleic Acids Res. 24, 1029–1036
8. Tereshko, V., Skripkin, E., Patel, D.J. (2003). Encapsulating streptomycin within a small 40-mer RNA. Chem. Biol. 10, 175–187
9. Baskerville, S., Zapp, M., Ellington, A.D. (1999). Anti-Rex aptamers as mimics of the Rex-binding element. J. Virol. 73, 4962–4971
10. Wen, J.D., Gray, C.W., Gray, D.M. (2001). SELEX selection of high-affinity oligonucleotides for bacteriophage Ff gene 5 protein. Biochemistry 40, 9300–9310
11. Wilson, C., Nix, J., Szostak, J.W. (1998). Functional requirements for specific ligand recognition by a biotin-binding RNA pseudoknot. Biochemistry 37, 14410–14419
12. Herr, J.K., Smith, J.E., Medley, C.D., Shangguan, D., Tan, W. (2006). Aptamer-conjugated nanoparticles for selective collection and detection of cancer cells. Anal. Chem. 78, 2918–2924
13. Homann, M., Göringer, H.U. (1999). Combinatorial selection of high affinity RNA ligands

to live African trypanosomes. Nucleic Acids Res. **27**, 2006–2014

14. Kotia, R.B., Li, L., McGown, L.B. (2000). Separation of nontarget compounds by DNA aptamers. Anal. Chem. **72**, 827–831
15. Cole, J.R., Dick, L.W., Jr., Morgan, E.J., McGown, L.B. (2007). Affinity capture and detection of immunoglobulin E in human serum using an aptamer-modified surface in matrix-assisted laser desorption/ionization mass spectrometry. Anal. Chem. **79**, 273–279
16. Hamaguchi, N., Ellington, A., Stanton, M. (2001). Aptamer beacons for the direct detection of proteins. Anal. Biochem. **294**, 126–131
17. Li, J.J., Fang, X., Tan, W. (2002). Molecular aptamer beacons for real-time protein recognition. Biochem. Biophys. Res. Commun. **292**, 31–40
18. Macaya, P., Schultze, F.W., Smith, J.A., Roe, F.J. (1993). Thrombin-binding DNA aptamer forms a unimolecular quadruplex structure in solution. Proc. Natl. Acad. Sci. U.S.A **90**, 3745–3749
19. Smirnov, I., Shafer, R.H. (2000). Effect of loop sequence and size on DNA aptamer stability. Biochemistry **39**, 1462–1468
20. Paborsky, L.R., McCurdy, S.N., Griffin, L.C., Toole, J.J., Leung, L.L. (1993). The single-stranded DNA aptamer-binding site of human thrombin. J. Biol. Chem. **268**, 20808–20811
21. Baldrich, E., Restrepo, A., O'Sullivan, C.K. (2004). Aptasensor development: elucidation of critical parameters for optimal aptamer performance. Anal. Chem. **76**, 7053–7063
22. Radi, A.E., Acero Sanchez, J.L., Baldrich, E., O'Sullivan, C.K. (2006). Reagentless, reusable, ultrasensitive electrochemical molecular beacon aptasensor. J. Am. Chem. Soc. **128**, 117–124
23. Gronewold, T.M.A., Glass, S., Quandt, E., Famulok, M. (2005). Monitoring complex formation in the blood coagulation cascade using aptamer-coated SAW sensors. Biosens. Bioelectron. **20**, 2044–2052
24. Mir, M., Vreeke, M., Katakis, I. (2006). Different strategies to develop an electrochemical thrombin aptasensor. Electrochem. Commun. **8**, 505–511
25. Zhang, H., Wang, Z., Li, X.F., Le, X.C. (2006). Ultrasensitive detection of proteins by amplification of affinity aptamers. Angew. Chem. Int. Ed. **45**, 1576 –1580
26. Centi, S., Tombelli, S., Minunni, M., Mascini, M. (2007). Aptamer-based detection of plasma proteins by an electrochemical assay coupled to magnetic beads. Anal. Chem. **79**, 1466–1473
27. Bini, A., Minunni, M., Tombelli, S., Centi, S., Mascini, M. (2007). Analytical performances of aptamer-based sensing for thrombin detection. Anal. Chem. **79**, 3016–3019
28. Holland, C.A., Henry, A.T., Whinna, H.C., Church, F.C. (2000). Effect of oligodeoxynucleotide thrombin aptamer on thrombin inhibition by heparin cofactor II and antithrombin. FEBS Lett. **484**, 87–91
29. Stubbs, M.T., Bode, W. (1993). A player of many parts: the spotlight falls on thrombin's structure. Thrombosis Res. **69**, 1–58
30. Shuman, M.A., Majerus, P.W. (1976). The measurement of thrombin in clotting blood by radioimmunoassay. J. Clin. Invest. **58**, 1249–1258
31. Curie, J., Curie, P. (1880). An oscillating quartz crystal mass detector. Rendu **91**, 294–297
32. Janshoff, A., Steinem, C. (2001). Quartz crystal microbalance for bioanalytical applications. Sensor Update **9**, 313–354
33. Bruckenstein, S., Shay, M. (1985). Experimental aspects of the use of quartz crystal microbalance solution. Electrochim. Acta **30**, 1295–1300
34. Sauerbrey, G. (1959). The use of quartz oscillators for weighing thin layers and for microweighing. Z. Physik. **155**, 206–222
35. Hillier, A.C., Ward, M.D. (1992). Scanning electrochemical mass sensitivity mapping of the quartz crystal. Anal. Chem. **64**, 2539–2554
36. Chang, S., Muramatsu, H., Nakamura, C., Miyake, J. (2000). The principle and application of piezoelectric crystal sensors. Mater. Sci. Eng. C **12**, 111–123
37. O'Sullivan, C.K., Guilbault, G.G. (1999). Commercial quartz crystal. Microbalances. Biosens. Bioelectron. **14**, 663–670
38. Kim, N., Park, I.S., Kim, D.K. (2004). Characteristics of a label-free piezoelectric immunosensor detecting *Pseudomonas aeruginosa*. Sens. Actuators B Chem. **100**, 432–438
39. Mannelli, I., Minunni, M., Tombelli, S., Mascini, M. (2003). Bulk acoustic wave (BAW) affinity biosensor for genetically modified organisms (GMOs) detection. IEEE Sens. J. **3**, 369–375
40. Skládal, P., dos Santos Riccardi, C., Yamanaka, H., Inácio da Costa, P. (2004). Piezoelectric biosensors for real-time monitoring of hybridization and detection of hepatitis C virus. J. Virol. Methods **117**, 145–151
41. Dell'Atti, D., Tombelli, S., Minunni, M., Mascini, M. (2006). Detection of clinically relevant point mutations by a novel piezoelectric

biosensor. Biosens. Bioelectron. 21, 1876–1879

42. Bock, L.C., Griffin, L.C., Latham, J.A., Vermaas, E.H., Toole, J.J. (1992). Selection of single-stranded DNA molecules that bind and inhibit human thrombin. Nature 355, 564–566
43. Tombelli, S., Mascini, M., Braccini, L., Anichini, M., Turner, A.P.F. (2000). Coupling of a DNA piezoelectric biosensor and polymerase chain reaction to detect apolipoprotein E polymorphisms. Biosens. Bioelectron. 15, 363–370
44. Ducongè, F., Di Primo, C., Toulmè, J.J. (2000). Is a closing GA pair a rule for stable loop-loop DNA complexes? J. Biol. Chem. 275, 21287–21294

*Anal. Chem.* **2007,** *79,* 3016−3019

# Analytical Performances of Aptamer-Based Sensing for Thrombin Detection

**Alessandra Bini, Maria Minunni, Sara Tombelli, Sonia Centi, and Marco Mascini***

*Università degli Studi di Firenze, Via della Lastruccia 3, 50019 Sesto Fiorentino, Italy*

**Aptamer-based assays represent a modern and attractive approach in bioanalytical chemistry. The DNA thrombin aptamer has been extensively investigated, and the coupling of this aptamer to different transduction principles has demonstrated the wide applicability of aptamers as bioreceptors in bioanalytical assays. The goal of this work was to critically evaluate all the parameters that can influence the sensor performances by using the thrombin aptamer immobilized onto piezoelectric quartz crystals. The optimization of the immobilization and the binding protocol was of paramount importance, and improvements in analytical performances could be obtained by optimizing simple steps in immobilization and assay conditions. Moreover, the work demonstrated the possibility of using aptamer-based sensors in complex matrixes, opening the possibility of a real application to diagnostics or medical investigation.**

Bioanalytical approaches based on aptamers as affinity ligands represent an interesting tool for protein detection,[1,2] and homogeneous or heterogeneous assays have been proposed for the analysis of the relative target.[3,4] A very interesting application is the exploitation of aptamers as biorecognition elements in biosensors,[5−7] where most of the work refers to the thrombin-binding aptamer, with or without labels.[8−18] However, even if aptamer-based sensing represents a modern and attractive approach, a critical evaluation of the key steps (immobilization, binding assay format, and conditions) in developing such devices is still needed.[19] Moreover, most of the reported work deals with standard solutions of the analyte, but very important applications of aptasensing would interest real matrixes, which have been considered only in very few cases.[6,20,21]

In this paper, a study conducted with the aptamer specific for thrombin coupled to label-free piezoelectric transduction is reported. We aimed at critically evaluating the importance of simple key steps in aptasensor development, which have significant implications on its analytical performances in terms of selectivity, linearity ($R^2$), reproducibility (coefficient of variation CV %), and stability (cycles). In particular, the influence of the aptamer immobilization procedure (chemistry, length, concentration, and pretreatment of the aptamer) as well as the binding conditions employed in the assay was studied.

The sensor is finally applied to the analysis of complex matrixes such as human serum and plasma to exploit its ability to also bind the target analyte in these complex samples.

The elucidation of critical parameters for optimal aptamer performance is of general applicability in aptasensing development, and also when other transduction principles and aptamers are employed. The final aim and the novelty of the paper is to demonstrate that simple, sometime neglected, steps are strategic for the true analytical applicability of the label-free device, having however in mind that each aptamer possess individual characteristics.

## EXPERIMENTAL SECTION

**Apparatus.** The 9.5-MHz AT-cut quartz crystals (14 mm) with gold evaporated (42.6-mm$^2$ area) on both sides were purchased from International Crystal Manufacturing. The measurements were conducted in a methacrylate cell where only one side of the crystal was in contact with the solution. Experiments were carried out using the quartz crystal analyzer Liquid Oscillator Unit with

* To whom correspondence should be addressed. E-mail: Marco.mascini@unifi.it. Fax: +39 0554573384.

(1) Ellington, A. D.; Szostak, J. W. *Nature* **1990**, *346*, 818−822.
(2) Tuerk, C.; Gold, L. *Science* **1990**, *249*, 505−510.
(3) Tombelli, S.; Minunni, M.; Mascini, M. *Biosens. Bioelectron.* **2005**, *20*, 2424−2434.
(4) Cole, J. R.; Dick, L. W., Jr.; Morgan, E. J.; McGown, L. B. *Anal. Chem.* **2007**, *79*, 273−279.
(5) O'Sullivan, C. K. *Anal. Bioanal. Chem.* **2002**, *372*, 44−48.
(6) Lai, R. Y.; Plaxco, K. W.; Heeger, A. J. *Anal. Chem.* **2007**, *79*, 229−233.
(7) Zayats, M.; Huang, Y.; Gill, R.; Ma, C.; Willner, I. *J. Am. Chem. Soc.* **2006**, *128*, 13666−13667.
(8) Pavlov, V.; Xiao, Y.; Shlyahovsky, B.; Willner, I. *J. Am. Chem. Soc.* **2004**, *126*, 11768−11769.
(9) Hansen, J. A.; Wang, J.; Kawde, A. N.; Xiang, Y.; Gothelf, K. V.; Collins, G. *J. Am. Chem. Soc.* **2006**, *128*, 2228−2229.
(10) Radi, A.-E.; Acero Sanchez, J. L.; Baldrich, E.; O'Sullivan, C. K. *J. Am. Chem. Soc.* **2006**, *128*, 117−124.
(11) Ho, H. A.; Leclerc, M. *J. Am. Chem. Soc.* **2004**, *126*, 1384−1387.
(12) Zhang, H.; Wang, Z.; Li, X.-F.; Le, X. C. *Angew. Chem., Int. Ed.* **2006**, *45*, 1576−1580.
(13) Yoshida, W.; Sode, K.; Ikebukuro, K. *Biochem. Biophys. Res. Commun.* **2006**, *348*, 245−252.
(14) Cai, H.; Ming-Hung, Lee, T.; Hsing, I.-M. *Sens. Actuators, B: Chem.* **2006**, *114*, 433−437.
(15) Liss, M.; Petersen, B.; Wolf, H.; Prohaska, E. *Anal. Chem.* **2002**, *74*, 4488−4495.
(16) Hianik, T.; Ostatná, V.; Zajacová, Z.; Stoikova, E.; Evtugyn, G. *Bioorg. Med. Chem. Lett.* **2005**, *15*, 291−295.
(17) Kawde, A.-N.; Rodriguez, M. C., Lee, T. M. H.; Wang, J. *Electrochem. Commun.* **2005**, *7*, 537−540.
(18) Maehashi, K.; Katsura, T.; Kerman, K.; Takamura, Y.; Matsumoto, K.; Tamiya, E. *Anal. Chem.* **2007**, *79*, 782−787.
(19) Baldrich, E.; Restrepo, A.; O'Sullivan, C. K. *Anal. Chem.* **2004**, *76*, 7053−7063.
(20) Xiao, Y.; Lubin, A. A.; Heeger, A. J.; Plaxco, K. W. *Angew. Chem., Int. Ed.* **2005**, *44*, 5456−5459.
(21) Heyduk, E.; Heyduk, T. *Anal. Chem.* **2005**, *77*, 1147−1156.



10.1021/ac070096g CCC: $37.00 
Published on Web 03/06/2007

the software QCMagic 0.3.1× by Elbatech (Marciana, Livorno, Italy). The resonance frequency was displayed in real time and recorded. All the measurements have been performed at room temperature ($T \approx 25$ °C).

**Reagents and Aptamers.** The DNA thrombin-binding aptamer was purchased from MWG Biotech (Milan, Italy) with two different modifications: (a) 5′-biotin-TT TTT TTT TTT TTT TTT GGT TGG TGT GGT TGG - 3′; (b) 5′-biotin-GGT TGG TGT GGT TGG - 3′; (c) 5′-SH-$(CH_2)_6$-GGTTGGTGTGGT TGG-3′.

The composition of the buffers used for the experiments is reported below: (a) immobilization buffer, 300 mM NaCl, 20 mM $Na_2HPO_4$, 0.1 mM EDTA pH 7.4; (b) binding buffer, 50 mM Tris-HCl, pH 7.4, 140 mM NaCl, 1 mM $MgCl_2$.

Human serum albumin (HSA) and all the reagents used for the buffer preparation were purchased from Sigma (Milan, Italy).

**Modification of the Sensor Surface and Biotinylated Aptamer Immobilization.** The gold surface of the quartz crystal was modified by immobilizing the thrombin-binding aptamer. The crystal was washed with a 1:1:5 solution of $H_2O_2$ (30%), $NH_3$ (30%), and MilliQ water for 10 min and then rinsed with MilliQ water. The biotinylated aptamer was immobilized via biotin−streptavidin interaction on the gold sensor surface previously modified with a layer of thiol/dextran/streptavidin as reported by Tombelli et al.[22]

**Thiolated Aptamer Immobilization.** The thiolated aptamer is anchored to the sensor surface by chemisorption based on the formation of gold−thiol bonds. Several crystals were modified with thiolated aptamer following the procedure previously reported.[23]

**Binding Measurements.** Once the receptor was immobilized on the gold surface, the binding step with thrombin in binding buffer was realized by adding 100 $\mu$L of the protein solution at different concentrations in the range 50−200 nM. The reaction was monitored for 20 min, the solution was then removed, and the surface was washed with the same binding buffer to eliminate the unbound protein. The analytical signal, reported as a frequency shift (Hz), was given by the difference between the value recorded before the binding and after the washing (baseline), once the binding has occurred; both values are taken when the crystal is in contact with the same solution (binding buffer).

After each cycle of binding, the crystal surface was regenerated by a 1-min treatment with 2 M NaCl.[19] With this treatment, the sensor-bound analyte is released at increased ionic strength, which unfolds the three-dimensional structure of the aptamer without damaging the oligomer structure, and the baseline is reached again, allowing the multiuse of the sensor.

**Spiked Samples.** Standard solutions of thrombin were added to serum or plasma to test the performance of the sensor in complex matrixes. Since serum does not contain coagulation factors, the addition of thrombin does not affect the samples. On the contrary, the addition of thrombin to plasma, which contains all the proteins involved in the coagulation cascade including fibrinogen, leads to the formation of fibrin and to rapid sample clotting. To avoid this phenomenon, fibrinogen was precipitated from plasma before the addition of thrombin in the preparation of spiked samples.

(22) Tombelli, S.; Mascini, M.; Turner, A. P. F. *Biosens. Bioelectron.* **2002**, *17*, 929−936.

(23) Tombelli, S.; Minunni, M.; Mascini, M. *Methods* **2005**, *37*, 48−56.

**Table 1. Comparison between the Results Obtained with the Sensor When Immobilizing the Biotinylated or the Thiolated Aptamer**

| immobilized aptamer | immobilization shift (Hz) and density (molecules/cm$^2$) | thrombin 100 nM (Hz) | thrombin 200 nM (Hz) |
|---|---|---|---|
| biotinylated aptamer (with tail) | $-225 \pm 36$; $2.4 \times 10^{13}$ | $-16 \pm 9$ | $-48 \pm 10$ |
| thiolated aptamer | $-138 \pm 30$; $3.4 \times 10^{13}$ | $-12 \pm 13$ | $-23 \pm 13$ |

Such selective precipitation is based on the use of ammonium sulfate as precipitant: 250 $\mu$L of plasma was treated with 1250 $\mu$L of 2 M ammonium sulfate and 1000 $\mu$L of 0.1 M sodium chloride. The solution was mixed for 3−4 min, then centrifuged, and the supernatant was eluted in a NAP column for rapid desalting and buffer exchange. The protein amount of the raw plasma and of the eluted solution was evaluated by spectrophotometric measurements at $\lambda = 280$ nm, and a loss of protein content (∼40%) was detected after precipitation of fibrinogen.

## RESULTS AND DISCUSSION

The developed aptasensor consists of the 15-mer thrombin aptamer (5′-GGTTGGTGTGGTTGG-3′) immobilized on the gold surface of 9.5-MHz piezoelectric crystals and the analyte (thrombin) added in solution. The signal is recorded in real time without the use of any label.

The binding buffer for the dilution of thrombin has been previously[24] optimized by using optical sensing with the Biacore X device and then transferred to the piezoelectric system. The best performances in terms of sensitivity and reproducibility were obtained with thrombin diluted in 50 mM Tris-HCl, pH 7.4, 140 mM NaCl, 1 mM $MgCl_2$, buffer very similar to the one used for aptamer selection.[25]

The second step was the investigation of the influence of the aptamer immobilization method on its binding with thrombin. The aptamer has been immobilized on gold when modified with a thiol group or on streptavidin when functionalized with biotin at its 5′-end with the insertion of a polyT (20-mer) tail. After the immobilization, the binding between the immobilized aptamer and 100 and 200 nM thrombin was studied with an interaction time of 20 min. The immobilization results for the biotinylated and the thiolated aptamer are reported in Table 1. From the shifts resulting from the immobilization of the two different aptamers, a similar density of immobilized molecules can be estimated considering 1 Hz = 2 ng/cm$^2$. The tested aptamers were compared in terms of signal amplitude, reproducibility, and selectivity. The results indicated that the best performances were obtained with the 15-mer biotinylated aptamer carrying the polyT(20) tail.

This aptamer showed a good reproducibility (average CV for the two concentrations, 13%) and a very good selectivity as demonstrated by the low signal ($\Delta F < 3$ Hz) obtained with a high concentration of HSA (77 $\mu$M), used as negative control. The higher sensitivity obtained with this aptamer is probably due to the presence of the spacer, which maintains the aptamer far from

(24) Centi, S.; Tombelli, S.; Minunni, M.; Mascini, M. *Anal. Chem.* **2007**, *79*, 1466−1473.

(25) Bock, L. C.; Griffin, L. C.; Latham, J. A.; Vermaas, E. H.; Toole, J. J. *Nature* **1992**, *355*, 564−566.

**Table 2. Comparison between the Analytical Characteristics of the Sensor Obtained When Immobilizing the Biotinylated Aptamer with a PolyT Tail**

| immobilized aptamer concn | binding time (min) | linear regression | $R^2$ | CV (%) | cycles[a] |
|---|---|---|---|---|---|
| 1 $\mu$M | 20 | $y = -0.22x + 1.94$ | 0.933 | 35 | 14 |
| 1 $\mu$M thermal treatment | 20 | $y = -0.23x + 0.42$ | 0.977 | 21 | 18 |
| 0.5 $\mu$M thermal treatment | 20 | $y = -0.23x + 0.68$ | 0.988 | 14 | 18 |
| 0.5 $\mu$M thermal treatment | 30 | $y = -0.22x$ | 0.998 | 10 | 22 |

[a] Binding cycles performed without loosing in sensitivity

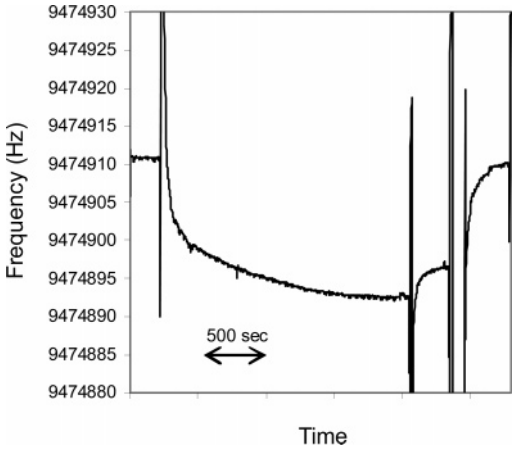


**Figure 1.** Typical binding curve (30 min) obtained with 50 nM thrombin interacting with the immobilized biotinylated aptamer.

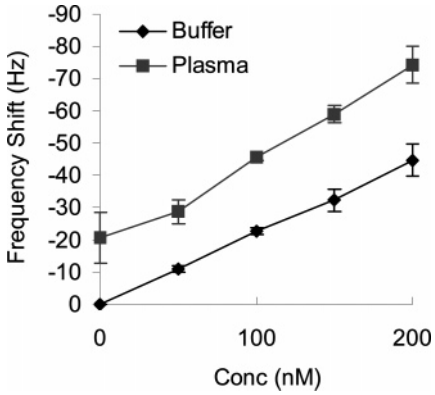


**Figure 2.** Calibration plot obtained with different concentrations of thrombin in buffer and plasma.

the sensor surface, allowing the proper conformation for molecular recognition. When the biotinylated aptamer (without polyT tail) was also immobilized, very low sensitivity ($\Delta F$ for 200 nM thrombin, <20 Hz) was found, even if comparable surface density occurred.

Further investigation has been conducted with the biotinylated aptamer with the polyT tail by studying the different parameters influencing the aptamer immobilization and consequently its binding to the protein. In particular, the influences of a thermal treatment of the aptamer (heating at 95 °C for 1 min and then cooling in ice for 10 min) and its concentration (varied from 0.1 to 1 $\mu$M) have been investigated. Moreover, in the binding conditions optimization, the interaction time has been increased from 20 to 30 min. The results are reported in Table 2, which shows the improvements in terms of sensitivity, linearity, reproducibility, and reusability, by varying these parameters.

The thermal treatment unfolds the aptamer making the biotin label at the 5′-end available for interaction with streptavidin on the crystal surface.[26] Even if the thermal treatment has no effect on the aptamer surface density ($2.5 \times 10^{13}$ molecules/cm$^2$), the linearity in the thrombin range 0−200 nM ($R^2 = 0.977$), and the reproducibility of the binding step (CV = 21%) significantly improved. This result confirms that the thermal treatment ensures correct intramolecular folding. Moreover, the results indicate that the surface capacity was not affected by the dilution from 1 to 0.5 $\mu$M of the aptamer. On the contrary, a further dilution to 0.1 $\mu$M dramatically reduced the sensor sensitivity (data not shown).

Finally, the increase in the interaction time from 20 to 30 min resulted in improved linearity and reproducibility. The sensorgram showing a typical binding curve of the aptamer and 50 nM thrombin, obtained with the optimized conditions, is displayed in Figure 1.

To check the specificity of the sensor, HSA at a concentration of 77 $\mu$M, in a 1400-fold excess with respect to thrombin, was used. The interaction did not result in a measurable frequency decrease ($\Delta F$ < 3 Hz), demonstrating the high specificity of the sensor.

Finally, the ability of the aptasensor to detect the analyte in complex matrixes was tested. Thrombin is the last enzyme protease involved in the coagulation cascade and it converts fibrinogen to insoluble fibrin that forms the fibrin gel.[27] Since the detection of thrombin in plasma or blood is clinically relevant, an aptamer-based sensor as alternative diagnostic tool for thrombin analysis or blood coagulation investigation could gain a great interest in the clinical and diagnostic area. Standard solutions of thrombin were added to serum and plasma to test the performances of the aptasensor in these complex matrixes. Since serum does not contain coagulation factors, the addition of thrombin does not affect the samples. On the contrary, the addition of thrombin to plasma, which contains all the proteins involved in the coagulation cascade including fibrinogen, leads to the formation of fibrin and to rapid sample clotting. To avoid this phenomenon, fibrinogen was precipitated from plasma before the addition of thrombin in the preparation of spiked samples. Thrombin was detected in serum diluted 1:100 spiked with thrombin in a concentration range 0−200 nM, with a blank value of −32 Hz (data not shown). The recorded signals increased with the concentration of added thrombin, demonstrating that the aptasensor was able to operate in this complex matrix. However, since serum does not contain the proteins involved in coagulation, further experiments have been carried out with plasma, which is the matrix where thrombin is normally detected. Figure 2 shows the signals obtained in spiked plasma without fibrinogen (final dilution 1:100). Reproducibility is good (CV = 13%), and the response is linear in the tested concentration range, 0−200 nM, ($R^2 = 0.990$). In this

(26) Tombelli, S.; Minunni, M.; Luzi, E.; Mascini, M. *Bioelectrochemistry* **2005**, *67*, 135−141.

(27) Holland, C. A.; Henry, A. T.; Whinna, H. C.; Church, F. C. *FEBS Lett.* **2000**, *484*, 87−91.

range, no saturation of the surface was observed. The matrix effect with a blank signal of −21 Hz is present but, despite the high complexity of the matrix, the increase in thrombin concentration could be detected. Due to the high dilution factor, the reached sensitivity is not sufficient for a direct application of the aptasensor to the detection of thrombin in real samples. This could be successfully performed by the use of amplification methods such as the use of a secondary affinity interaction or of enzymatic reactions.[24,28] The goal of this work was to critically evaluate all the parameters that can influence the sensor performances by using thrombin as the model target, and the ability to detect the analyte in complex matrixes demonstrates the potentialities of aptamer-based sensing for potential medical investigations.

Moreover, a simple 2 M NaCl treatment was applied as a sensor regeneration step (1 min), allowing its reuse up to 20 times without losing in sensitivity.

Other label-free reported aptasensors are based on the quartz crystal microbalance (QCM),[15,16] surface acoustic waves (SAW),[29,30] or electrochemical transduction such as impedance[14] or field-effect transistors.[18] In the case of QCM,[16] a detection limit for thrombin of 1 nM in buffer is reported, even if this datum is not supported by the study of other important analytical parameters such as specificity, reproducibility, or matrix effect. For SAW[29,30] devices, the reported sensitivity is in the same order of magnitude (submicromolar) of the proposed approach, but also in this case, the analysis is limited to standard solutions. By using impedance,[14] significant improvement in the sensitivity, at least in buffer, was achieved, but no evaluation of real samples is given. To date, however, a rational evaluation of the different important key steps in aptasensor development has been reported only for an ELONA assay.[19] The appealing aspect of this paper is represented exactly by the consideration of the different parameters influencing the analytical performances of this label-free, portable, and reusable sensor. Microarrays could represent an interesting tool in aptamer-based methods, improving the number of interactions that can be detected simultaneously and decreasing the amount of capture molecules immobilized on the chip with a reduction of the cost of analysis.

## CONCLUSIONS

The proposed study can be considered as reference approach in aptasensing development. In particular, it should be stressed how little variations in simple steps in the assay development could lead to much improved analytical performances. In addition, the proposed study demonstrates the ability of label-free aptasensing to operate in complex matrixes. This is of paramount importance for a real applicability of these new, interesting, and attractive devices to clinical diagnostic, environmental, and food analysis.

(28) Ikebukuro, K.; Kiyohara, C.; Sode, K. *Biosens. Bioelectron.* **2005**, *20*, 2168−2172.
(29) Schlensog, M. D.; Gronewold, T. M. A.; Tewes, M.; Famulok, M.; Quandt, E. *Sens. Actuators, B: Chem.* **2004**, *10*, 308−315.
(30) Gronewold, T. M. A.; Glass, S.; Quandt, E.; Famulok, M. *Biosens. Bioelectron.* **2005**, *20*, 2044−2052.

Received for review January 16, 2007. Accepted February 22, 2007.

AC070096G